Development and Implementation of Feed-back Controlled Drug Administration during Anesthesia and Sedation

Ontwikkeling en implementatie van feed-back gecontroleerde geneesmiddelen toediening gedurende anesthesie en sedatie

Thesis submitted to obtain the degree of Doctor in Health Sciences.

ir. Tom DE SMET

Promotor: Prof. Dr. Michel M.R.F. STRUYS

Co-Promotor: Prof. Dr. Eric P. MORTIER

Preface

Tempus fugit....

I completed the foreword of my final year's thesis on Tuesday June 16th 1995. Exactly twenty years later the sequel is ready. It took slightly more time than expected.

In these twenty years the world changed considerably. We executed our first trials on a CRT-equipped desktop PC hosting an Intel 80486 processor, taking more than three minutes to calculate the patient profile after induction. Even today's average Smartphone is more powerful.

The insight in anesthesia and its mechanisms has advanced by leaps and bounds similarly. While our initial efforts targeted control of mean arterial pressure and FEMG, today we can choose from a variety of indexes correlating to one or another aspect of anesthesia. All this progress is driven by people, a lot of whom I have met over the past twenty years. Each and every one was a specialist in his field, but they all shared the passion to uncover and share knowledge to move ahead faster together. I look back at each encounter with great pleasure and respect.

A doctoral research project, should it be said, is teamwork. Being an engineer surrounded by anesthetists is an amazing experience. Each trivial question asked was meticulously answered, which made me feel privileged every time. Although the standard procedures of anesthesia appear deceivingly straightforward after some time, I often witnessed in admiration how they manage complex situations.

I want to express my gratitude to the co-authors of our research and articles. The statement "it would not have been possible without them" is to be taken both figuratively and literally – although I can now carry the title of Doctor in Health Sciences, don't consult me for a headache yet.

A special acknowledgement goes out to my promotor, Prof. Dr. Michel Struys. Putting our heads together during a jetlagged night at congress or during long flights always brought new insight and direction, benefiting from his clear long-term view and vision. My co-promotor Prof. Dr. Eric Mortier emerged as the silent supporter providing wise counsel whenever required.

Proof reading this document must have been a challenge. I want to express my gratitude to the members of the reading committee, for their constructive additions and comments.

As it is not possible to acknowledge all other people who contributed to this work by name –please accept a warm anonymous thank you for all your efforts to make this work succeed.

Combining this thesis with my daytime occupation has been challenging sometimes, not only for me. I therefore dedicate this thesis to Isabelle, Mathijs and Korneel, for their patience, understanding and indispensable moral support.

Tom De Smet

Tuesday, June 16, 2015

Index :

Chapter 1

Introduction and aims of the thesis

The objective of any drug administration is to obtain and maintain a desired clinical and therapeutic level of drug effect as fast and accurate as possible while minimizing adverse drug effects. Optimizing drug administration during anesthesia and sedation has gained importance as essential part of higher standards in patient care and peri-operative management.

A performing and safe control of the patient's anesthetic state under varying surgical conditions and for a broad patient population demands for application of drugs providing a wide spectrum of pharmacological actions (analgesia, hypnosis, and suppression of somatic and autonomic responses to noxious stimuli) [1].

Nowadays, except for the inhaled anesthetics (for which end-tidal concentrations can be measured online), most drugs given to control anesthesia are titrated using standard dosing guidelines, without diving due consideration to their pharmacokinetics and dynamics in guiding their administration [2]. Unfortunately, for most of them, large inter-individual variability is observed when studying population pharmacology and it shows challenging to quantify the expected clinical effect.

An improved mastering of the complex dose-response relation of an administered drug will enable to optimize the efficacy and quality of anesthesia through better accuracy.

The dose-response relation of a drug can be divided into three parts: the relation between the administered dose and the plasma concentration (the pharmacokinetic phase), the relation between the effector organ concentration and the clinical effect (the pharmacodynamic phase) and the temporal relationship between pharmacokinetics and dynamics. Pharmacokinetics concerns the characterization and prediction of the time course of the concentration of a drug in the body. It describes the characteristics of drug absorption, distribution, metabolism and elimination. Pharmacodynamics describes the relation between drug concentration and effect in the biophase, defined as the direct (theoretical not anatomical!!!) environment of the receptor at the site of action of the drug. Here the first step in the process of pharmacodynamics occurs, the interaction with the receptor. This results in what is often referred to as "effectuation", which could be, for example, the formation of a second messenger, the inhibition of an enzyme, or an effect on an ion channel. This physiological process ultimately results in the response, defined as the clinical drug effect[3].

In control engineering terminology, an anesthesiologist maintaining or changing a desired target drug dose or concentration to establish or maintain a desired clinical effect may be considered as a closed-loop control system. The clinician selects the initial dose, observes the clinical effect of his/her drug administration and potentially decides to alter the drug administration. The anesthesiologist's intervention may be purely reactive if he only responds to the observed clinical effects, or proactive if he adjusts the administration rate to prepare the patient for imminent noxious stimuli provoked by the surgical intervention. In any case, the pure variability and complexity of the dose-response relationship requires constant titration of the drug administration rate.
The anesthesiologist as a closed-loop control system is, however, of a special nature: (i) it has a *human controller* in the loop, and (ii) as a consequence, the control actions are intermittent and irregular in time[4].

Autonomous "Closed-loop controllers" are computer programs designed to assist him/her in this process by maintaining a targeted effect through adaptation of the administered amount of drugs taking into account the drug effect. They measure the controlled variable (e.g. measure of the hypnotic of analgesic component of anesthesia) and apply the errors between the set point entered and the actual value to alter the input to the system. In closed-loop control, the clinician carefully selects the desired clinical-effect to be maintained based on surgical circumstances, while the controller performs all underlying calculations to maintain this desired effect.

The application of closed-loop systems for drug administration is complex and requires an optimization of all the basic components required to develop such a system: 1) an adequate control variable to measure the drug effect is obligatory; 2) an accurate set-point for this variable, which is the chosen target value specified by the user should be defined; 3) a stable and potentially model-based controller for the actuator is required; 4) the control actuator, which is, is this case, the infusion pump driving the drug, should be accurate and; 5) a system, in this case a patient, whose pharmacokinetic-dynamic characteristics should be modeled as accurate as possible when required by the controller[5].

The primary concept of studying control of "depth of anesthesia" in this thesis should be interpreted as "observing the hypnotic component of anesthesia under intravenous infusion of propofol". This

“hypnotic component” can be defined as a “continuum” between consciousness, anxiolysis, amnesia, and unconsciousness. The terms “sedation” and “anesthesia” can be referred as different clinical conditions in this spectrum.
Propofol (di-isopropylfenol) is a short-acting intravenously administered hypnotic/amnestic agent applied to induce and maintain general anesthesia and sedation.

In this thesis, we hypothesized that by developing and validating the closed-loop system for titrating the hypnotic component of anesthesia, intravenous drug administration can be optimized.

As such, the aim of this thesis was to evaluate the following issues:

1) Is it possible to develop an automatic closed-loop system for the administration of intravenous hypnotic-anesthetic drugs during sedation and anesthesia and does it offer more accurate drug administration than manual control?

2) Is it possible to apply pharmacological models in such a closed-loop system and is this a better approach than applying standard engineering control methods?

3) Is it possible to develop a technology that takes into account population variability during closed-loop infusion of intravenous anesthetic-hypnotic drugs and is this technology feasible to be used into clinical practice and during specific research conditions?

4) Can we use our closed-loop system during challenging research conditions to maintain a specific level of the hypnotic component of anesthesia?

For the less experienced reader, the theoretical chapter 2 precedes this thesis providing background in various closed-loop delivery techniques for anesthesia to serve as a basis to fully understand the choices we made during our experimental work.

Accurate drug administration requires the best available model. For propofol, various models have been published and the debate over what model provides the best drug concentration prediction is

still “very hot”. In chapter 3, we studied the differences in some of the clinically applied compartmental models describing the time course of plasma concentration and drug effect.

In chapter 4, we described the development and clinical application of our first closed-loop system. We tested the accuracy of this closed-loop control system versus “standard practice” controlled administration. In an editorial accompanying the study, Glass et al. questioned whether the controller was stressed enough to demonstrate its performance.

As it might be considered unethical to test a closed-loop system under extreme conditions in clinical practice we decided to apply simulation technology for our follow-up study. Additionally, we wanted to benchmark our closed-loop control strategy versus a classical control application using PID (proportional-integral-derivative) control. Using simulation, facilitating comparison of two closed-loop control strategies in the same patient model, we compared the performance of our closed-loop control systems with the PID control system published by Absalom[6] et al [7].(Chapter 5).

Our initial patient-individualised model-based adaptive control system suffered from some limitations precluding a more general use during sedation and anesthesia. First off all, it required initial drug-free patients to establish its patient model, proving not applicable in already anesthetized patients. Furthermore, a concentration versus response profile is likely to change over the course of anesthesia, mostly as a result of changing levels of noxious stimulation, but also because of possible pharmacodynamics (i.e., acute tolerance to opioids) or because of changes to the patient (e.g., liver transplantation). In an attempt to resolve these shortcomings, a Bayesian approach was included in our existing control algorithm.

Bayesian optimization, as proposed by Sheiner et al [8], is classically used in pharmacokinetic-dynamic modeling to individualize drug dosing regimen by combining individual information with an *a priori* probability density function containing the statistical properties of the model parameters to be estimated[9].

Elaborating the full mathematical background of applying Bayesian methods for individualization of population pharmacokinetics is outside the scope of this manuscript. For the interested reader, especially the study by Sheiner et Al [6] provides a detailed background insight in the Bayesian theory.

The Bayesian method starts from a standard, population-based response model providing the prior distribution of parameter values. These values are adjusted to reflect the patient's own parameters over time, based on the observed response of the individual patient under varying circumstances. This process makes use of specific modeling weights, called Bayesian variances, which determine how the patient-specific model can deviate from the population model. For a pharmacokinetic model the Bayesian variances are the variances of the parameters resulting from the modeling process obtained, for example, using a NONMEM analysis. For the pharmacodynamic portion of the model, such a priori population model information is not readily available from the literature. Moreover, being an essential contributing factor in the control operation, we choose to optimize these Bayesian variances for control performance in our target population. In a first study we applied simulations to select the Bayesian variances yielding the optimal controller for a Bayesian-based closed-loop system for propofol administration using the BIS as a controlled variable (chapter 6).

Chapter 7 describes the introduction of this newly developed system into clinical practice and how we compared its accuracy and clinical feasibility under direct observation of an anesthesiologist versus BIS guided, effect compartment controlled propofol administration titrated by the anesthesiologist during ambulatory gynecological procedures. The main novelty in this investigation compared to the referenced studies is that the new control system enables us to include the induction phase in the closed-loop control mode of the controller rather than only the maintenance phase.

Since our closed-loop control system is able to target a specific level of drug effect, we applied it during a specific research protocol requiring 3 different levels of hypnosis, defined as a BIS level of 70, 50 and 30. During this trial, we could study the stability of our system under various hypnotic conditions (chapter 8).

Chapter 2

Principles of drug action

Target Controlled Infusions and Closed-Loop Administration

Modified from:

Michel M.R.F. Struys, T. De Smet

Target Controlled Infusions and Closed-Loop Administration

In: A. Evers, M. Maze, E.D Kharasch. Anesthetic Pharmacology (Second Edition),

Cambridge University Press, Cambridge, UK

2011 pp 103-132

INTRODUCTION

The goal of optimal drug dosing in anesthesia is the capability to obtain and maintain a desired time course of clinical and therapeutic drug effect as accurately as possible. Accuracy of administration is essential for effective anesthesia with minimal adverse drug effects. In current clinical practice, anesthetic drugs are predominantly still administered using standard dosing guidelines and techniques, ignoring the large inter-individual variability in dose-response relationships. The application of computer-controlled continuously updated infusion rates based on mathematical models, clinical-effects feedback, or, in the absence of quantifiable effects, carefully selected surrogate measures, may yield better patient-individualized dosing. The dose-response relationship can be divided into three parts (fig. 1): the relationship between the administered dose and the plasma concentration (pharmacokinetics, PK), the relationship between blood or effect-organ concentration and clinical effect (pharmacodynamics, PD), and the coupling between pharmacokinetics and pharmacodynamics (PK/PD). If the plasma or effect-site concentration of a drug could be known, then the complexity of the dose-response relationship would be reduced to pharmacodynamics only (fig.1).

In contrast to inhalation anesthetics, for which the inspired and end-tidal concentrations can be measured continuously in real time ("on-line"), the actual plasma or effect-organ concentration of an intravenously administered drug is not immediately measurable in clinical practice. Therefore, it is impossible to steer intravenous infusion regimens manually to maintain an on-line measured plasma concentration. It becomes even more complex if one wants to target a specific effect-site concentration. Consequently, it requires a drug model and a computer continuously updating the administration rate to maintain an estimated drug concentration in plasma or at the effect-site. This technique is called **target-controlled infusion** (TCI).

Two methods for controlling drug administration can be distinguished: open-loop and closed-loop control. **Open-loop control** is considered to be any practice where the anesthesiologist administers a drug (either a dose or an infusion based on a desired or targeted drug concentration or clinical effect), assesses the patients' response, and makes a decision to revise the dosing accordingly. Decision-making may be assisted by information on the estimated (if using TCI (target-controlled infusion), or real (inhalational anesthetic) plasma or effect-site concentration. **Closed-loop control** (also called "feed-back" control) takes the anesthesiologist "out of the loop". The anesthesiologist only enters the desired clinical or surrogate effect to be maintained (depth of hypnosis, muscle twitch, etc). The

computer program-based controller will autonomously calculate the optimal drug administration rate, based on the measured actual value of the controlled variable, the set point and, potentially, internal models of the expected dose-response relationship of the (individual) patient.

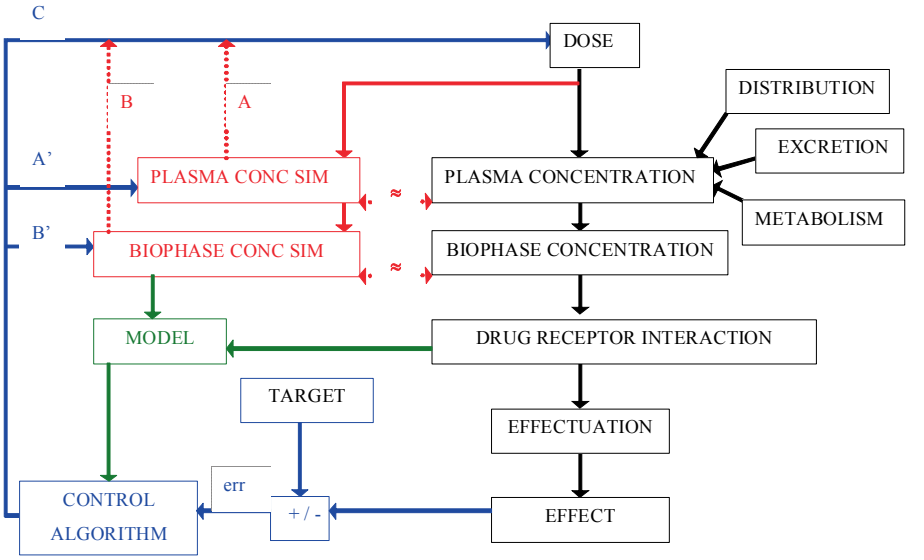

Fig. 1: *Schematic representation of the pharmacokinetic and pharmacodynamic processes determining the relationship between administered dose and resulting effect intensity of a drug (black). Pharmacokinetic factors like distribution, metabolism, and/or excretion determine the relationship between drug dose and drug concentration in the biophase. In the biophase the drug interacts with the receptor and the pharmacological effect is accomplished via transduction processes. TCI (Target-controlled infusion) will use a model to estimate the plasma or biophase drug concentration (red), and will calculate the dose needed to approach a target concentration in plasma (A) or biophase/effect-site (B). Closed-loop feedback will measure the error between the effect and the target effect to control the dose administration (blue). Better closed-loop performance can result if, rather than using the dose as a direct actuator, the simulated variable of a TCI system is used as actuated variable. (A/A', B/B'). The TCI system compensates for part of the complexity of the dose-interaction relationship. Advanced control algorithms may take into account a (continuously updated) model of the interaction (green).*

OPEN-LOOP TARGET CONTROLLED INFUSION

History and definitions

The availability of computers embedded in syringe pumps and better knowledge of drug PK/PD models, have now enabled the administration of intravenous drugs as easily as inhalation anesthetics, by applying TCI to achieve and maintain a desired plasma or effect-site concentration. The principle behind TCI techniques is to use PK/PD modeling and calculations to predict a set concentration in one of the pharmacokinetic compartments. TCI was developed to optimize the time course of drug effect by targeting a specific therapeutic drug concentration in a specific body compartment, mostly the plasma or the effect-site. Multicompartment mammillary PK/PD models, derived from pharmacological modeling studies, are used in TCI systems to calculate the infusion rates to achieve and maintain the target concentration as fast and accurately as possible without an overshoot in drug concentrations. This avoids side effects which often occur after initial bolus dosing. A microprocessor-controlled infusion pump is required to perform the complex calculations and control drug administration. It is impossible to achieve the required concentrations with the same accuracy when using manually controlled infusion systems, due to the complexity of drug PK/PD characteristics. The target concentration is set by the anesthesiologist, after having evaluated a patients' individual requirements. This technique is called open-loop controlled TCI.

TCI is based on the original theoretical approach for maintaining and achieving a steady- state blood concentration of a drug whose pharmacokinetics can be described by a two-compartment model as first published by Kruger-Thiemer[10] and clinically tested by Schwilden and coworkers[11]. The schemes developed by these pioneers for drugs conforming to a two-compartment model became known as BET (bolus, elimination, transfer) schemes, and are built on three concepts. First, the initial bolus dose of drug required to achieve the initial targeted plasma concentration (C_{pT}) is equal to $C_{pT} . V_d$ (where V_d is the volume of distribution). Second, the elimination rate (k_e) is proportional to the plasma concentration, so a constant plasma concentration in steady-state causes a fixed portion of the total drug amount to be eliminated per unit of time. To maintain a constant plasma concentration, elimination is compensated for by a constant-rate infusion. Third, the amount of drug distributed or transferred to peripheral tissues declines exponentially, as the gradient between the central compartment and the peripheral compartment decreases. This requires an infusion at an exponentially declining rate to replace drug "lost" from the central compartment by distribution until steady state.

Since BET schemes are relatively straightforward to calculate manually, they lead to standard dosing guidelines which are still being used. However, BET has two major drawbacks. First, it is only applicable in the absence of drug previously administered. Since changing the concentration target violates this requirement, it becomes very difficult to find equally straightforward rules in such situations. Second, it has been recognized over the years that the pharmacokinetics of most anesthetics conform best to a three- rather than a two-compartment model, requiring similar but more complex infusion strategies. Furthermore, it was understood that plasma is not the site of drug effect, and one needs to consider the temporal hysteresis of drug effect (*i.e.* effect lags behind blood concentration) to optimize drug delivery, making the standard infusion schemes even more complex. As a result, effect-compartment-controlled TCI was developed, targeting the effect-site[12].
Continuously calculating the required infusion rate to rapidly achieve and maintain a concentration level trajectory which accurately meets the needs of surgical patients therefore requires a computer-controlled infusion pump. It is impossible to achieve similar performance when using manual controlled infusion systems.
Several academic groups developed TCI systems to study drug optimization. Since the early 1990s the software for the systems developed in Stanford (Stanpump®), Stellenbosch (Stelpump®) and Gent (RUGLOOP®) universities has been available on request from the authors and at times freely available over the Internet. Several pharmacokinetic simulation programs have also been available (examples include IVA-SIM®, TIVATrainer®). Initially, the individual academic groups have referred to TCI technology by a variety of acronyms, including CATIA (computer-assisted total intravenous anesthesia) [13], TIAC (titration of intravenous agents by computer)[14], CACI (computer-assisted continuous infusion)[15] , and CCIP (computer-controlled infusion pump) [16]. The term has been used in this context most often [17] and has become the standard. The development of TCI introduced various new conceptual terminologies into anesthesia, which are listed in table 1 [18].
The first commercially available TCI system was the Diprifusor® (AstraZeneca, London, UK), a microprocessor module included in intravenous infusion pumps sold by several manufacturers from 1996 until 2006 (in numerous countries around the world except the USA). The development of the Diprifusor® has been described in detail [19]. Its application was limited to target-controlled infusions of Diprivan® (propofol; AstraZeneca) targeting plasma concentrations, and it imposed the use of pre-filled glass syringes of propofol tagged electronically for single use. More recently, pump companies have introduced more flexible so-called “open TCI” systems capable of administering propofol, but

also opiates, ketamine, muscle relaxants, etc in modes targeting either plasma or effect-compartment concentrations (figure 2).

Table 1. Terminology introduced by TCI. Adopted from Glass *et al.* [18]

C_{pT}	Target plasma concentration
C_{eT}	Target effect site concentration
C_{pM}	Measured plasma concentration
C_{pCALC}	Calculated plasma concentration
C_{eCALC}	Calculated effect-site concentration

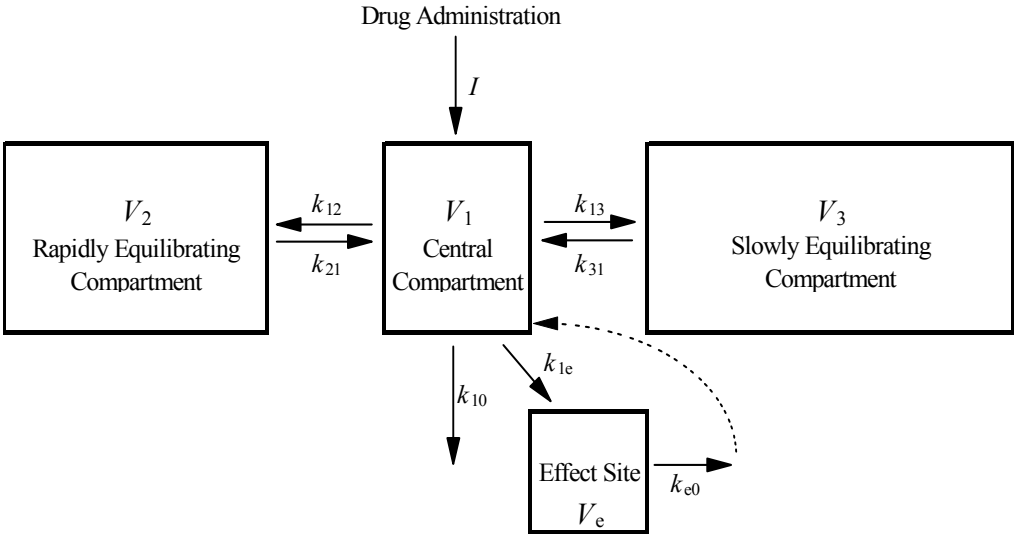

Fig. 2. *Schematic representation of a three-compartmental mammillary plus effect-site compartment model for the behavior of an intravenously administered drug in the body.*

Mathematical model

The pharmacokinetics of many intravenous drugs can be accurately described by mammillary multicompartment models. The concept of these models and the underlying mathematical representation is based on the theory of linear stationary systems [20]. Whenever these models are used, it is assumed that the represented processes of drug distribution and elimination in the body are linear and time-invariant, or that the applied amounts are small enough to be represented by such models. All TCI implementations apply, in one form or another, two essential principles resulting from this assumption: the principle of *superposition*, stating that the response to a composite input is identical to the sum of the responses of the inputs separately, and the principle of *time invariance*, stating that if a signal input *x(t)* results in an output *y(t)*, then the time-shifted input signal *x(t+T)* results in exactly the same output *y(t+T)*, shifted over the same amount of time.

A three-compartment mammillary model including the effect-site compartment is shown in figure 2. In this model structure, intravenous drugs are delivered into and eliminated from the central (plasma compartment) only. The central compartment exchanges drug with the peripheral compartments at a rate proportional to the drug concentration gradients between them. The effect-site compartment is considered as a negligibly small fourth compartment whose drug exchange rate with the central compartment is characterized by the rate constant k_{1e}. The differential equations describing this model are expressed in terms of drug amount, not concentrations, knowing that the drug concentration in a compartment equals the drug amount divided by the compartment's volume. The following differential equations describe the model as a function of time:

$$\begin{aligned} dA_1(t) &= (I(t) + k_{21}.A_2(t) + k_{31}.A_3(t) + k_{e0}.A_4(t) - (k_{10} + k_{12} + k_{13} + k_{1e}).A_1(t)).dt \\ dA_2(t) &= (k_{12}.A_1(t) - k_{21}.A_2(t)).dt \\ dA_3(t) &= (k_{13}.A_1(t) - k_{31}.A_3(t)).dt \\ dA_4(t) &= (k_{1e}.A_1(t) - k_{e0}.A_4(t)).dt \end{aligned}$$ **Equation 1**

Since the effect-site compartment is considered a negligibly small, the terms $k_{e0}.\ A_4(t)$ and $k_{1e}.A_1(t)$ can be ignored in the calculation of $dA_1(t)$, yielding the simplified differential equation:

$$dA_1(t) = (I(t) + k_{21}.A_2(t) + k_{31}.A_3(t) - (k_{10} + k_{12} + k_{13}).A_1(t)).dt$$ **Equation 2**

One particular feature in the ratio of compartment volumes and drug exchange constants must be taken into account. In equilibrium, the drug concentration in all compartments should be identical. At that time, there is no more net drug transfer between the central and the peripheral compartments:

$dA_n = 0$ or $k_{1n}.A_1(t) = k_{n1}.A_n(t)$, $\forall\ n > 1$ **Equation 3**

Since

$c_n(t) = A_n(t)/V_n$, $c_n(\infty) = c_1(\infty)$, $\forall\ n$ **Equation 4**

must necessarily

$k_{1n}\ .c_1(\infty).V_1 = k_{n1}\ .\ c_n(\infty).V_n$ or $V_n = V_1\ k_{n1}\ /\ k_{1n}.\ \forall\ n > 1$ **Equation 5**

so the volume of any peripheral compartment is known when the ratio of exchange rates with the central compartment is known.

The set of differential equations to calculate the drug concentration in the central compartment can be converted into an equivalent impulse response function. The impulse response for an *n*-compartment model, $u_n(t)$ is an *n*-exponential function of the form:

$u_1(t) = P_1e^{-\alpha_1 t} + P_2e^{-\alpha_2 t} + ... + P_ne^{-\alpha_n t}$ **Equation 6**

The impulse response can be considered as the central-compartment concentration over time in response to a unit amount of drug, infused instantaneously. A derivation of the impulse response function from the differential equations is found in the specialized literature [21].

As for any linear time-invariant system, the relationship between an arbitrary drug input $r(t)$ and the resulting central compartment drug concentration can be calculated as:

$$A_1(t) = r(t)^* \ u_1(t) \qquad \textbf{Equation 7}$$

where $u_1(t)$ is the impulse response function and * denotes the mathematical operation of convolution.

If pharmacodynamic data are also available for the drug of interest so that a value has been defined for k_{e0}, there exists a $n + 1$ exponential impulse response function, $u_e(t)$, for the effect compartment of the form :

$$u_e(t) = Q_1 e^{-\alpha_1 t} + Q_2 e^{-\alpha_2 t} + ... + Q_n e^{-\alpha_n t} + [SQ_i].e^{-k_{e0} t} \qquad \textbf{Equation 8}$$

$i = 1$

with $Q_i = -P.k_{e0} / (\alpha_i - k_{e0})$, which characterizes completely the relation between drug input into the central compartment and the resulting effect-compartment drug concentration, such that

$$A_e(t) = r(t)^* . u_e(t) \qquad \textbf{Equation 9}$$

If the time course of the central compartment drug concentration is known, an alternative method to calculate the effect-site concentration is the following convolution integral:

$$A_e(t) = k_{1e}.\exp(-k_{e0}.t)^* A_1(t) \qquad \textbf{Equation 10}$$

Since the effect-site compartment is assumed to have an arbitrarily small volume, the relationship between k_{1e} and k_{e0} is known as $k_{1e} = k_{e0} * V_e / V_1$.

In practice, the convolution method is too cumbersome for TCI systems using embedded microcontrollers with long drug infusion histories. Most TCI systems will apply a piecewise constant infusion rate rather than a continuously adjusted infusion rate to track the target concentration set by the anesthesiologist. A typical constant rate interval is 10 seconds. At each multiple of the interval

time, the concentration resulting from the infusion is calculated. For this evaluation, either an Euler approximation of the differential equations [22] or an analytical solution for a piecewise-continuous infusion profile in a recursive algorithm [12] is applied.

Control Strategy

Theoretically, the infusion regimen required over time can be calculated using a mathematical deconvolution from the desired concentration profile:

$$r(t) = u_1(t)^{*-1}.\ c_{1d} \qquad \textbf{Equation 11}$$

where $^{*-1}$ denotes deconvolution. A (piecewise constant) concentration c_{1_d}, meaning the target concentration set by the anesthesiologist, is the desired outcome. This approach is impractical for TCI implementations in the embedded microprocessors. Instead, at each multiple of the standard interval time, the superposition principle is used to calculate the appropriate administration rate for the next interval to reach the user-set target concentration as soon as possible, as shown in figures 3A and 3B for plasma and effect-compartment TCI, respectively.

Plasma targeting

The two- and three-compartmental pharmacokinetic models ignore the complex front-end kinetics of arterio-venous mixing and initial recirculation. In this simplified model, the predicted maximum plasma concentration resulting from a constant infusion rate over an infusion interval in the absence of earlier drug administration occurs at the end of the infusion interval. Let $C_{pr}(t)$ be the plasma concentration resulting from a reference amount rate $r[0,T]$ applied over the infusion interval T. The superposition principle is then applied as follows (and as graphically represented figure 3A):

$$\begin{aligned} &r_1[0,T] = C_t/C_{pr}(T).r \text{ yields } C_{p1}(t),\ C_{p1}(T) = C_t \\ &r_2[T,2T] = (C_t\text{-}C_{p1}(2T))/C_{pr}(T).r \text{ yields } C_{p2}(t), \\ &C_{p1}(2T) + C_{p2}(2T) = C_t \text{ etc.} \end{aligned} \qquad \textbf{Equation 12}$$

Effect-site targeting

Even with TCI control, the only way to decrease plasma concentration and "extract" an infused dose of drug from the body is by waiting for its elimination. Thus an overshoot in drug concentration leading to an overshoot in clinical effect or potentially adverse drug effects should be avoided. The delay between the time course of the plasma and effect-site concentrations results in a peak effect-site concentration only some time after an instantaneous bolus infusion of drug. This time to peak effect-site concentration (t_{peak}) will cause the peak effect-site concentration induced by a constant infusion rate interval to be postponed past the end of the infusion interval (t_{peak},T). Consequently, targeting for an effect-site concentration to be reached exactly at the end of the infusion interval T results in an effect-site concentration overshoot afterwards. To attain the target effect-site concentration without overshoot, the TCI algorithms reference the concentration at t_{peak},T. There is a minor caveat, however: the time of peak effect-site concentration resulting from the superposition of two successive constant–rate infusion intervals is a nonlinear function of the relative magnitude of the two infusions (Figure 3B). When targeting the effect-site concentration, TCI systems need to take an iterative approach to calculate the required infusion rate each interval instead of the straightforward approach for targeting plasma concentration [12].

Manual infusion, plasma or effect-compartment controlled TCI?

The benefits of TCI become clear when compared to manual infusion schemes. The simulations in Figure 4 demonstrate the differences between various administration modes. In this virtual patient (male, 170 cm, 70 kg, 25 years), the propofol plasma and effect-site concentrations (simulated using the model published by Schnider *et al*. [23], [24]) and the infusion rates are depicted. When administering a single bolus (part A), plasma concentration peaks high (depending on the infusion rate) and the hysteresis with the effect-site concentration is observed. A bolus achieves only a few moments of accurate concentrations. With a continuous infusion (Part B), a high peak plasma concentration is avoided, but therapeutic concentrations are only achieved after a long time.

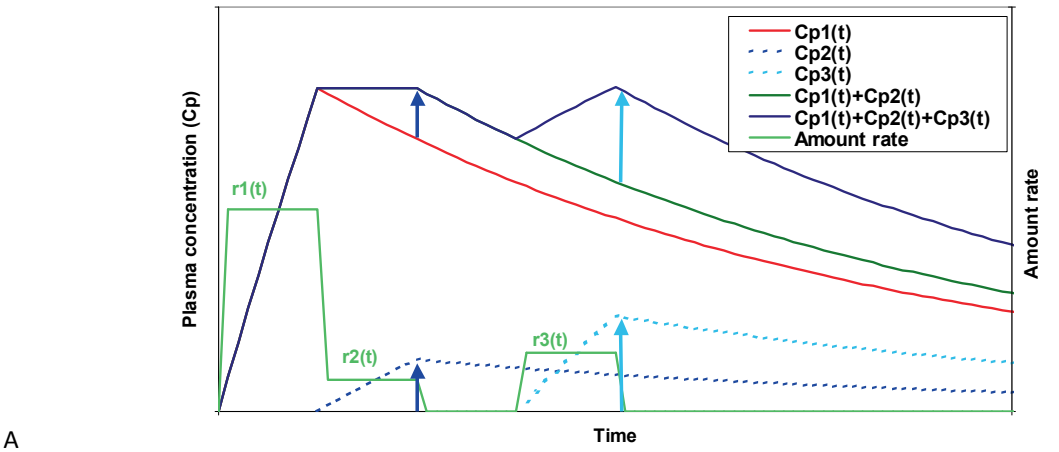

A

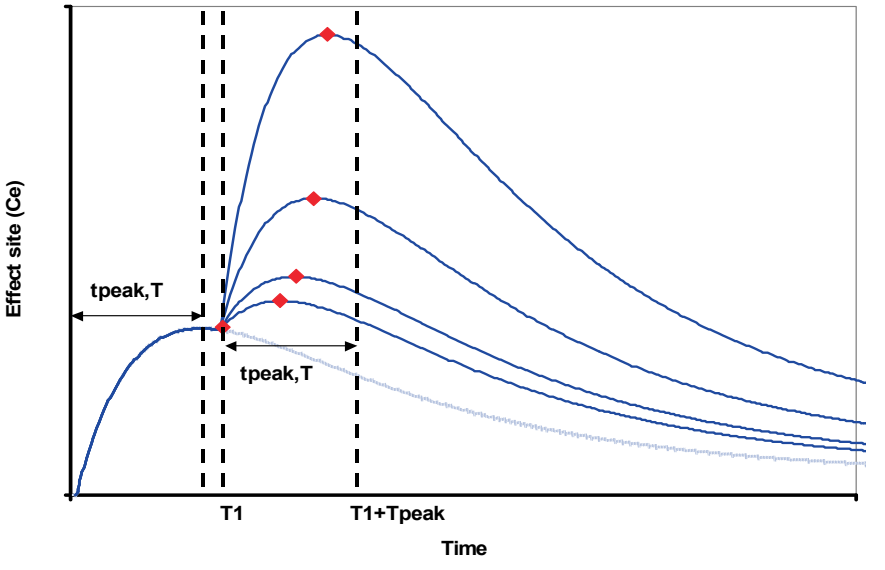

B

Fig. 3: *Superposition principle applied in (A) plasma and (B) effect-site targeting with a piecewise continuous infusion. In plasma targeting, the required infusion rate is readily calculated knowing the target concentration, zero-infusion concentration decay and the plasma concentration resulting from a unit rate infusion interval. In effect-site concentration, the maximum effect-site concentration occurs at* $t_{peak,T}$ *instead of at the end of the infusion. Subsequent infusions yield a* $t_{peak,T}$ *that is a function of both the infusion history and the infusion rate to be applied.*

Classically, propofol is administered as a bolus and a stepwise decreased infusion (*e.g.*, 10 – 8 – 6 mg /kg /h) (Part C). This enables some stable concentration trajectory, but still results in concentrations which are initially high and change slowly, with possible accumulation during long-lasting infusions. Part D shows a plasma targeted TCI infusion. The infusion profile shows the need for an initial bolus to reach the target concentration, followed by a continuously decreasing infusion to maintain a stable plasma concentration. The effect-site concentration, however, still shows a slow equilibration to the target concentration. In order to reach and maintain an accurate effect-site concentration, without overshoot at the effect-site level, effect compartment TCI is required (Part E).

Here, the initial bolus is larger, overshooting the plasma level but not the effect-site level. After the bolus, the pump stops infusing and waits for equilibration. Then, a slowly decreasing infusion rate is needed to maintain all concentrations at the target level. The simulations in figure 4 are done with propofol, but could have been done using various other intravenous drugs.

The simulations illustrate how effect-compartment TCI offers the fastest control of clinical drug effect. When using effect-compartment TCI, two potential pitfalls should be recognized. First, the accuracy of k_{e0} is especially critical in effect-site targeting, because it will determine the overshoot and undershoot in plasma concentrations during changes in targeted effect-site concentrations. Accurate simulated concentrations demand a model developed from a study combining blood sampling with frequent measurements of drug effect, resulting in an overall model for the dose-response behavior of the drug. Historically, the time constants of PK models and the k_{e0} of PD studies without accurate blood samples (hereby lacking the PK model) were sometimes naively merged, possibly resulting in inaccurate predictions of clinical drug effect [25]. However, if no integrated PK/PD model exists, the time of peak effect after a bolus injection (t_{peak}) can be used to recalculate k_{e0} using the PK of interest to yield the correct time of peak effect [12]. Second, “the” effect-site is calculated using one typical drug effect (*e.g.*, cerebral drug effect as measured by EEG). The time course of other (side) effects (*e.g.*, hemodynamic effect for hypnotics) most frequently follows another trajectory and one should therefore be careful when overshooting the plasma concentration to hasten plasma-effect-site equilibration in compromised patients to avoid the onset of side effects. Concerns about high plasma concentrations that result from targeting the effect site can be addressed by limiting the peak plasma concentration overshoot [26].

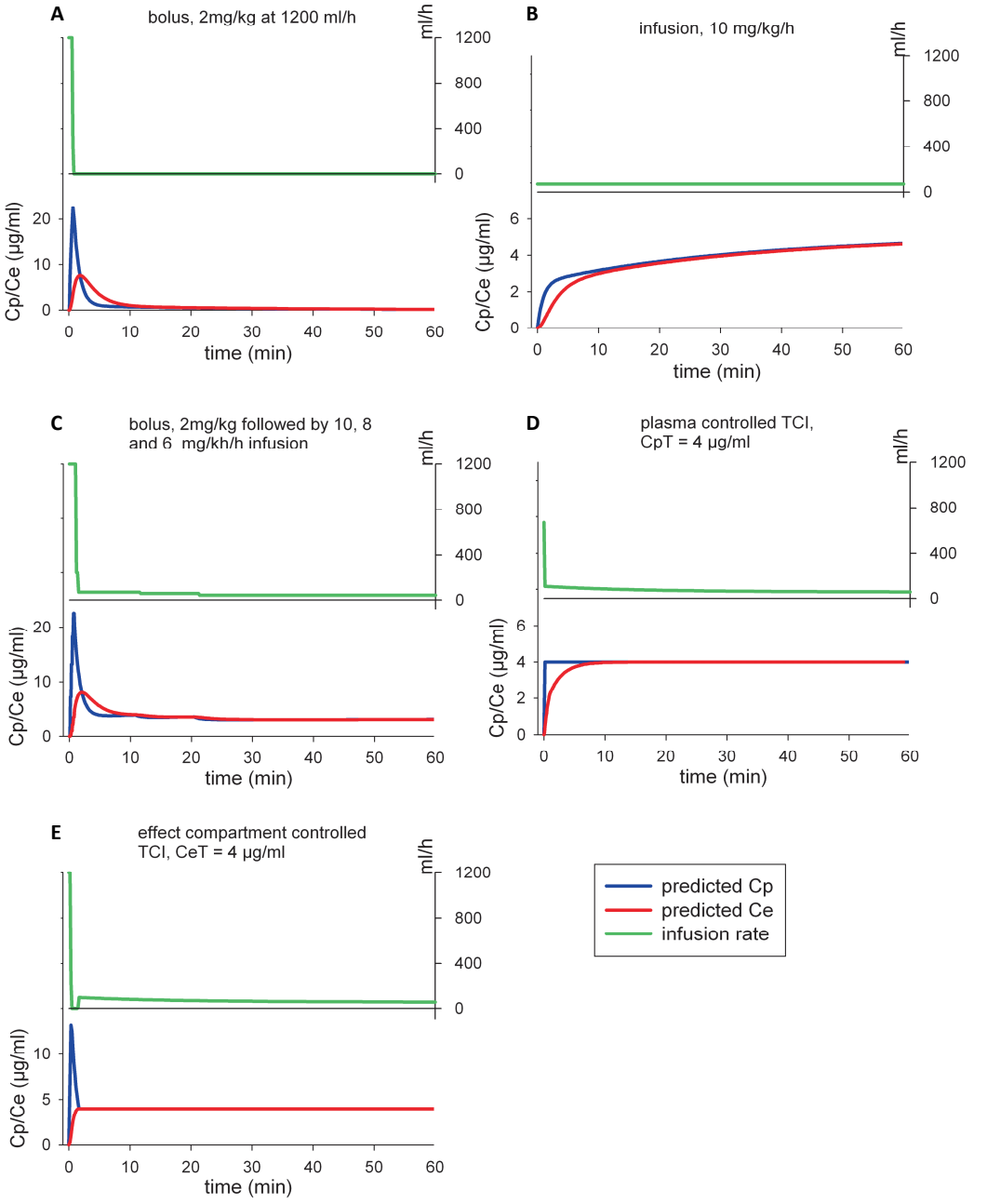

Fig. 4*. Influence of various modes of drug administration on predicted propofol plasma and effect-site concentrations. Plasma (blue) and effect-site (red) concentrations in a virtual patient (male, 170 cm, 70 kg, 25 years) were simulated using published models [23, 24]. Propofol infusion rates required to*

achieve these concentrations are depicted in green. The targeted plasma (C_p) and effect-site concentrations (C_e) are both 4 µg m^{-1}. (A) Single bolus. Plasma concentrations peak high and hysteresis with the effect site is observed. Concentrations are accurate for only a few moments. (B) Continuous infusion. A high peak plasma concentration is avoided, but therapeutic concentrations are only achieved after a long time. (C) Bolus and stepwise decreased infusion. This concentration trajectory is more stable, but still results in concentrations which are initially high and change slowly. (D) Plasma TCI. The infusion profile shows an initial bolus to reach the target concentration, followed by a continuously decreasing infusion to maintain a stable plasma concentration. The effect-site concentration however still shows a slow equilibration to the target concentration. (E) Effect compartment TCI. The initial bolus is larger, to achieve the desired effect-site concentration, but overshoots the plasma concentration. After the bolus, the pump stops infusing and waits for equilibration. Then a slowly decreasing infusion rate is needed to maintain target concentrations.

Context-sensitive half-time and decrement time

Originally, the context-sensitive half-time was defined as the time required for the plasma concentration to decrease by 50% after an infusion that maintained a constant concentration, with the context being the duration of infusion [27]. As the effect-site is most often more relevant, the original concept was enlarged towards the *context-sensitive decrement* time, in which the decrement is calculated in the compartment of interest (plasma or effect-site) [28]. TCI technology enables the user to specify an endpoint concentration, and the computer will estimate the time to reach this concentration taking into account the infusion history. This feature might help in optimizing the targets at the end of anesthesia in order to avoid delayed recovery, and it can be used for both hypnotics and analgesics. Due to the exponential decays involved in drug elimination, together with population variability, the inaccuracy on these estimates in predicting clinical endpoints is large, especially after long infusions or for low endpoint concentrations.

Performance evaluation of TCI technology

In order to select the best PK/PD model for TCI application, prospective testing is required during TCI application. For some of the drugs, research (and the controversy) is still going on. Tables 2 and 3 show the most commonly applied models and drugs in clinically available TCI devices. Investigators who have assessed the accuracy of propofol TCI report inevitable deviation of actual plasma concentrations from the targeted plasma concentrations [29]. Other than possible technical problems in both software and hardware, possible sources of variability arise during estimation of the pharmacokinetic parameters and from the TCI.

Table 2: *Commonly applied PK/PD models for TCI systems for hypnotics*

Drug	**Propofol**	**Propofol**	**Propofol**	**Propofol**	**Ketamine**
Model	Marsh [30]	Schnider [23], [24]	Paedfusor [31]	Kataria [32]	Domino [33]
Parameter					
$V1$	0.228 L /kg	4.27 L	0.458 L /kg	0.52 L /kg	0.063 L /kg
$V2$	0.363 L /kg	18.9 – 0.391 x (age - 53) L	1.34 L /kg	1.0 L /kg	0.207 L /kg
$V3$	2.893 L /kg	238 L	8.20 L /kg	8.2 L /kg	1.51 L /kg
K_{10} (min^{-1})	0.119	0.443+ 0.0107 x (weight - 77) - 0.0159 x (LBM - 59) + 0.0062 x (height - 177)	70 * ($weight^{-0.3}$) /458.3	0.066	0.4381
K_{12} (min^{-1})	0.112	0.302 - 0.0056 x (age - 53)	0.12	0.113	0.5921
K_{13} (min^{-1})	0.042	0.196	0.034	0.051	0.59
K_{21} (min^{-1})	0.055	(1.29-0.024 x (age - 53))/ (18.9 - 0.391 (age - 53))	0.041	0.059	0.247
K_{31} (min^{-1})	0.0033	0.0035	0.0019	0.0032	0.0146
K_{e0} (min^{-1})	0.26 [a]	0.456	NA	NA	NA
TPPE (min)	NA	1.69	NA	NA	NA

[a] = K_{e0} derived independently from the PK model[34]

NA, not available

For example, there is variance among the parameters of a polyexponential function fitted to a single set of concentration-time data. In addition, there is PK variation among the subjects who constituted the sample from which the averaged parameter set was derived. Often, because of cost

considerations, the number of subjects in the sample is small, casting doubt as to whether the sample can be assumed to represent the population adequately.

Furthermore, patients receiving TCI do not necessarily belong to the same population from whom the original pharmacokinetic model was derived, and the effect of the surgical procedure can result in PK variability within each patient [35]. All of these factors can lead to bias and inaccuracy of the concentrations achieved during TCI.

Table 3. *Commonly applied PK/PD models for TCI systems for analgesics*

Drug	Remifentanil	Sufentanil	Fentanyl	Alfentanil
Model	Minto [36, 37]	Gepts [38]	Shafer[16]	Maitre [39]
Parameter				
$V1$	5.1-0.0201 (age-40) + 0.072(LBM - 55) L	14.3 L	6.09 L	♂= 0.111 L /kg ♀=1.15 x 0.111 L /kg
$V2$	9.82 - 0.0811 (age - 40) + 0.108 (LBM-55) L	63.4 L	28.1 L	12.0 L
$V3$	5.42 L	251.9 L	228 L	10.5 L
K_{10} (min^{-1})	((2.6 - 0.0162 (age - 40) + 0.0191 (LBM-55))/$V1$	0.0645	0.083	< 40 yr = 0.356/$V1$ > 40 yr = 0.356 -(0.00269(age - 40))/$V1$
K_{12} (min^{-1})	((2.05-0.0301(age - 40))/$V1$	0.1086	0.4713	0.104
K_{13} (min^{-1})	(0.076-0.00113(age - 40))/$V1$	0.0229	0.22496	0.017
K_{21} (min^{-1})	K_{12} x $V1$/$V2$	0.0245	0.1021	0.067
K_{31} (min^{-1})	K_{13} x $V1$/$V2$	0.0013	0.00601	< 40 yr = 0.0126 >40 yr = 0.0126 - 0.000113(age - 40)
K_{e0} (min^{-1})	0.595-0.007(age - 40)	NA	0.147[a]	0.77[a]
TPPE (min)[b]	NA	5.6	3.6	1.4

[a] = K_{e0} is derived independently from the PK model by Scott *et al.* [40]

[b] = from Shafer and Varvel [41]

NA, not available

Several calculation and statistical methods are used to describe the accuracy of a specific parameter set [29]:

- *Prediction error (%)* of the predicted concentration in plasma:
  PE = (measured -predicted/predicted) x 100%
  PE is an indication of the bias of the achieved concentrations, and the absolute value *PE* (|PE|) is a measure of the precision (inaccuracy).
- *Median absolute prediction error* indicates the inaccuracy of TCI in the *i*-th subject:
  $MDAPE_i$ = median $\{|PE|_{ij}, j = 1,\ldots, N_i\}$
- where N_i is the number of values $|PE|$ obtained for the *i*-th subject.
- *Median prediction error* reflects the bias of TCI in the *i*-th subject:
  $MDPE_i$ = median $\{PE_{ij}, j=1,\ldots,N_i\}$
- *Divergence* is a measure of how the resulting drug concentrations in a subject are affected by time. It is defined as the slope of the linear regression equation of |PE|against time and is expressed in units of percentage divergence per hour. A positive value indicates progressive widening of the gap between predicted and measured concentrations, whereas a negative value reveals that the measured concentrations converge on the predicted values.
- *Wobble* is another index of the time-related changes in performance and measures the intrasubject variability in performance errors. In the *i*-th subject the percentage of wobble is calculated as follows:
  $wobble_i$ = median $\{|PE_{ij} - MDPE_i|, j = 1,\ldots, N_i\}$

Clinically applied models for TCI: model selection

Hypnotics

For most intravenous drugs, multiple PK/PD models have been published. Propofol is the most extensively investigated drug (table 2). A comparison of the available propofol PK models [42] found that the parameter sets provided by Marsh *et al.* [30] proved adequate with acceptable prediction errors (MDPE –7%; MDAPE 18% [30]) during TCI use. The Marsh set has been implemented into the Diprifusor ® (AstraZeneca) and has been validated clinically in plasma-controlled TCI mode for many years in different clinical situations [42-44]. It has the major drawback of using only weight as a model

covariate. More recently, age, height, weight and LBM (lean body mass) were evaluated as covariates in a new three-compartment PK model for propofol [23]. The large variability in the study population (18 to 81 years and 44 to 123 kg) provides a wide applicability of the model. Various authors rated performance of the model as better than the Marsh model, but, when administered in combination with opiates, larger MDPE and MDAPE were found [45, 46]. Furthermore, the inclusion of lean body mass as a covariate may lead to incorrect drug dosages in morbidly obese patients due to the quadratic behavior of the lean body mass function [47], which demonstrates that care should be taken when applying a model outside its study population's range. Beside the classical 1 % and 2 % propofol known as Diprivan 1 % and 2% (AstraZeneca), multiple alternative formulations have been commercialized. For some of these, kinetics are similar [23, 48, 49].

To optimize drug delivery, targeting the effect site is more appropriate. Accurate description of the drug transfer between the plasma and effect-site requires an accurate k_{e0}, characterizing a first-order process. Previously, the Diprifusor TCI system for propofol applied a naive method of combining separate pharmacokinetic and pharmacodynamic studies, which resulted in biased results. For propofol, only the model from Schnider *et al.* has studied combined kinetics and dynamics [23, 24] and has been widely used in clinical devices. Since both k_{e0} (0.456/min) and t_{peak} (1.69 min) have been published for this model, the options are to use the k_{e0} as it stands or recalculate a new k_{e0} corresponding to a t_{peak} of 1.69 minutes in a specific patient. The last approach was clinically confirmed in various studies [50-53]. This approach has also been used in combination with the Marsh kinetic, leading to a high k_{e0} value of 1.21/min [54].

Two PK models for propofol TCI in children have been used experimentally in clinical practice. A three-compartment model for propofol in a population of children between 3 and 11 years used weight as the sole significant covariate [32]. Weight-adjusting the volumes and clearances significantly improved the accuracy of the pharmacokinetics. Adjusting the pharmacokinetics for inclusion of additional patient covariates or using a mixed-effects model did not further improve the ability of the pharmacokinetic parameters to describe the observations. This model was safely used during esophagogastroduodenoscopy in children, although no blood samples were taken[55]. A more recent test of this model found a high bias with an overall underestimation of measured propofol concentration versus the target concentration [56]. An alternative system for pediatric application of propofol TCI, called the 'Paedfusor' was developed at the Glasgow University. This TCI prototype system for children, incorporating one of the preliminary models developed by Schüttler *et al.* [57], was

clinically validated and found to have an acceptable performance [31]. No effect compartment-controlled TCI has been reported in children, due to the lack of accurate models. Preliminary work shows that propofol pharmacodynamics in children differs from that in adults [58].

Opioids

Several PK/PD models for opioids are shown in table 3. The covariate independent models for sufentanil have been verified, with acceptable MDPE ranging from -2.3% to -22.3% and MDAPE ranging from 18.5% to 29%, even for obese patients [59-61].

For alfentanil, various compartmental PK models were published in the early 1980s, but did not use a true population modeling approach. The original datasets from these studies were subsequently used to develop a new model using population modeling (NONMEM) [39]. As this analysis did not evaluate effect-site concentration coupling, the authors re-used the k_{e0} naively from a previous simultaneous PK/PD model [40]. More recently, a comparison of three different alfentanil PK models [62] found that the model by Scott *et al*. [40] had poor performance (MDPE of -35 %, MDAPE of 36%) compared to the one by Maitre *et al.* [39] (MDPE of 12%, MDAPE of 28%)). In contrast, Maitre model was reported to perform worse than the Scott model two patients groups [63].

For fentanyl, a PK model was developed without covariates specifically for TCI use [16] Since the model was derived from normal-weight patients and was not scaled to body weight, its application to obese patients may cause overprediction of fentanyl plasma concentrations. The accuracy of that fentanyl PK model in lean and obese patients was evaluated [64], and a correction to the simulated plasma concentration proposed, where corrected Cp = Cp Shafer x (1 + (196.4 x $e^{-0.025kg}$ – 53.66)/100).

Remifentanil is the only opioid for which combined PK/PD models have been developed. Remifentanil PK can be described by a three-compartment model and it has been studied in healthy volunteers and patients [36, 37, 65, 66], obese patients [67], and those with hepatic or renal disease [68, 69]. Neither renal nor hepatic insufficiency clinically alters remifentanil PK. Table 3 shows the most frequently used PK/PD model for remifentanil [36, 37]. The performance of both sets for remifentanil were found to be clinically acceptable [70]. Combined PK/PD studies are not available for all opioids. However the times to peak effect after a bolus injection of alfentanil (1.4 min), fentanyl (3.6 min) and sufentanil (5.6 min) can be used to calculate the effect-site concentration using the t_{peak} algorithm [71].

Miscellaneous

For various other drugs like benzodiazepines, muscle relaxants and ketamine, multicompartment models have been created and tested. However, these drugs are not clinically available in the commercial TCI pumps.

Selecting the right target concentrations for TCI: variability

The PK/PD models cited in the previous paragraph have all been derived from population pharmacology studies where the researchers try to identify and quantify how covariates like weight, age, gender and height influence the dose-concentration relationship. The accuracy of the estimated drug concentration for any one individual is limited by inter-patient variability; hence the applicability of the model is limited to the population studied to develop the model. Thus caution is needed when applying a PK/PD model for obese, elderly, children, diabetics, alcoholics, unless similar subjects were part of the study population from which the PK/PD model was derived. Most of the commercial implementations of TCI will therefore prevent selecting weight, height, etc. outside the range of the model's study population. Other potential causes of reduced model accuracy are errors (e.g., drug spill), excessive blood loss, or PK and/or PD drug interactions.

Accuracy of PK/PD models for highly variable populations can be improved if the model is built while exploring a wide range of possible covariates using parametric modeling, optionally nonlinear mixed-effects modeling [72, 73]. An illustration of the importance of the study population range is an ongoing debate on the accuracy of the two PK/PD models for propofol, applying k_{e0} vs. t_{peak}. Since the only difference between the models is in the PD portion, only the initial moments are relevant for a difference in infused volume. After a few minutes, the plasma and effect-site compartment concentrations will have equilibrated for a constant simulated concentration, and both models will show an identical infusion pattern. The drug amount infused by both models during induction, using effect-site targeting, is illustrated in figure 5. Within the study population limits, there are small differences in infused drug amount for two parameter sets, but much greater differences for the third. Extrapolations outside the population tremendously reduce the accuracy of one, or any, of the models. An internet initiative (www.opentci.org) has been started in an attempt to build more comprehensive models including more diverse populations.

In spite of the relative model inaccuracy, application of TCI often reduces intersubject variability in drug response compared with bolus dosing [74]. Some guidance can be found in the effective concentrations at which 50 and 95% of patients have the desired clinical effect (table 4). As with all drug administration in anesthesia, clinical judgment is always required, and target concentration should be titrated according to patient clinical responses.

Table 4. *Propofol/opioid combinations estimated to be associated with the fastest recovery from anesthesia.*

Infusion duration (min)		Propofol: alfentanil (μg/ml : ng/ml)	Propofol: sufentanil (μg/ml : ng/ml)	Propofol: remifentanil (μg/ml : ng/ml)
15	$C_{OPTIMAL}$	3.25 : 99.3	3.57 : 0.17	2.57 : 4.70
	$C_{AWAKENING}$	1.69 : 65.0	1.70 : 0.10	1.83 : 1.93
	Time to awakening (min)	8.2	9.4	5.1
60	$C_{OPTIMAL}$	3.38 : 89.7	3.34 : 0.14	2.51 : 4.78
	$C_{AWAKENING}$	1.70 : 64.9	1.70 : 0.10	1.83 : 1.93
	Time to awakening (min)	12.2	11.9	6.1
300	$C_{OPTIMAL}$	3.40 : 88.9	3.37 : 0.14	2.51 : 4.78
	$C_{AWAKENING}$	1.70 : 64.9	1.70 : 0.10	1.86 : 1.88
	Time to awakening (min)	16.0	15.6	6.7

$C_{optimal}$ represents combinations associated with a 50% probability of a response to surgical stimuli; $C_{awakening}$ concentrations represent the estimated concentrations at which consciousness will be regained; time to awakening represent the estimated time from termination of the infusion to return of consciousness in 50% of patients. (From Vuyk et al [75], and modified from Absalom and Struys [3], with permission.)

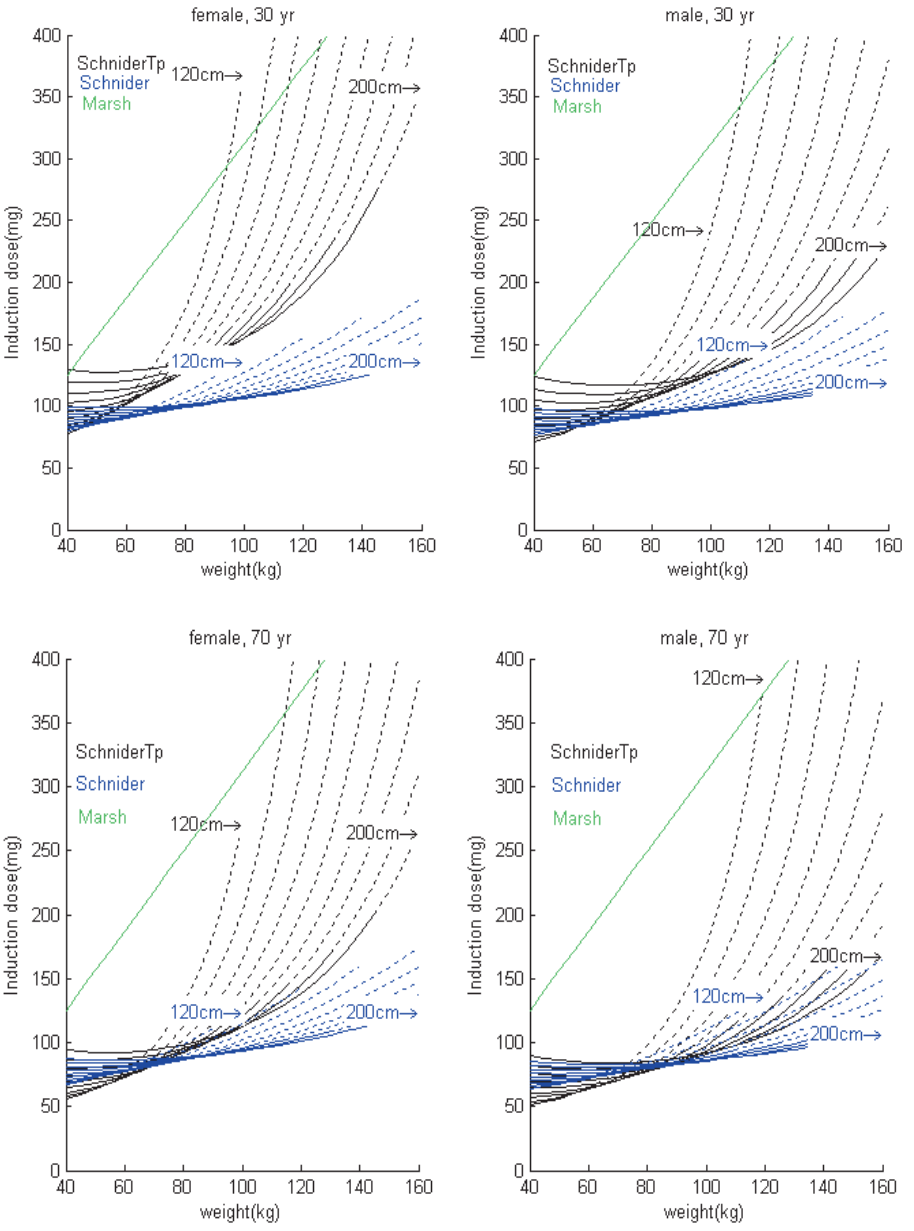

Fig. 5. *Influence of model parameters on TCI drug doses. Three propofol models (Marsh [30], Schnider with effect-site calculated using a ke0 =0.456/min [2, 3] and Schnider with effect site calculated using a* t_{peak} *= 1.6 min [2, 3] targeted an effect-site concentration of 5 µg/ml). Doses are in mg /kg, based on weight.*

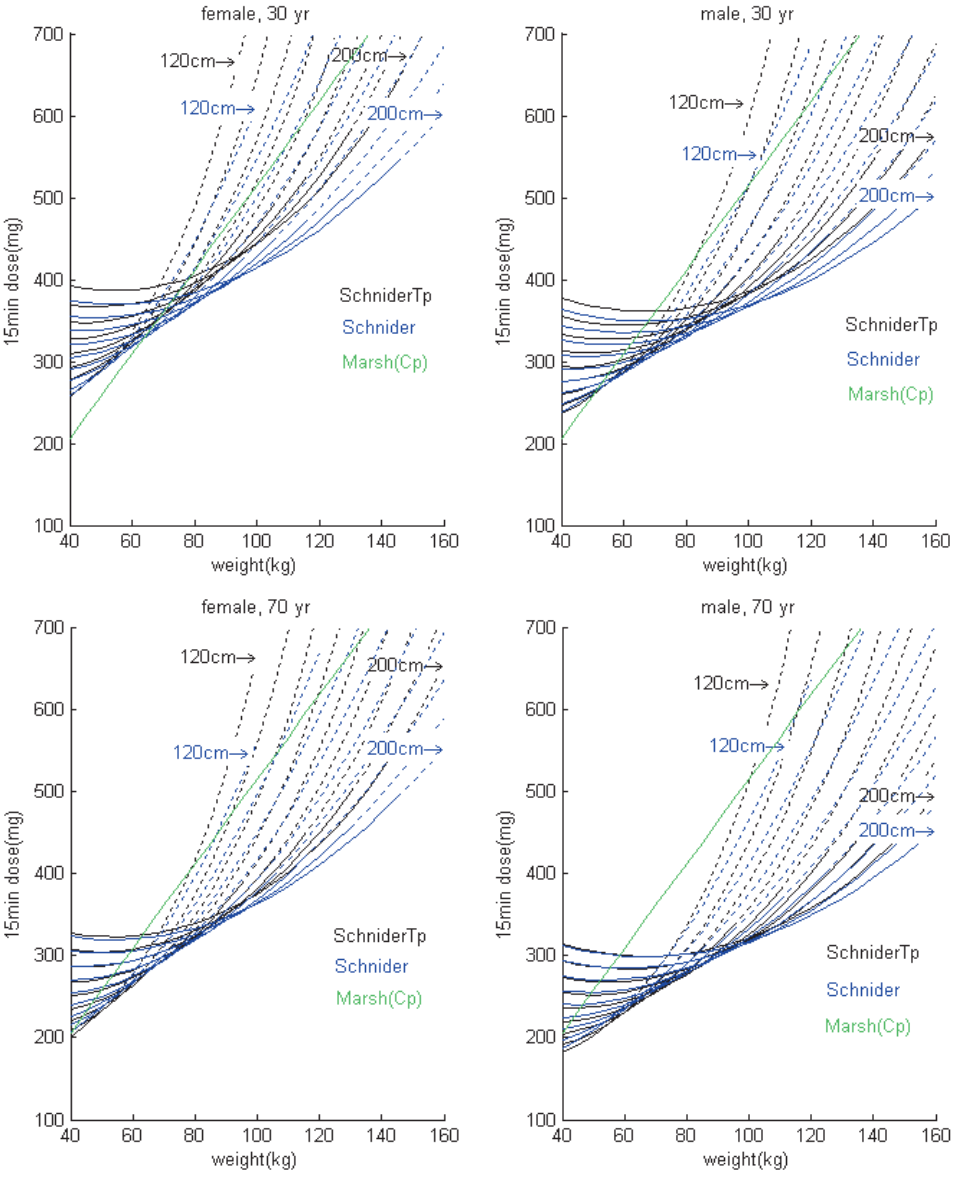

(Fig. 5.) *The induction dose is the initial bolus administered. The 15 min dose is the total amount given after 15 minutes.*

Results are given for female and male, and for 30- year-old and 70-year-old patients. Each line represents a specific patient height. The dotted line represents the extrapolation of the model outside the limit imposed by the maximum lean body mass (at the same time outside the study population).

CLOSED-LOOP DRUG ADMINISTRATION

Open-loop controlled drug administration applies PK/PD models based on the typical subject to estimate a drug concentration at certain locations in the body, without actually measuring these concentrations. The resulting inaccuracy of absolute concentration requires the clinician to manually titrate the dose regimen or target concentration based on observations of the desired therapeutic effect. The clinical benefits of a tight titration require high clinical expertise or a labor-intensive process and may divert the clinician's attention from critical actions, resulting in a suboptimal therapy or even threatening the patient's safety. Applying closed-loop drug administration techniques has the potential to optimize this process of dose titration.

The application of closed-loop systems for drug administration is complex and requires a perfect balance for all the basic components of such a system: (1) a controlled variable representative of the targeted therapeutic effect, (2) a clinically relevant set-point or target value for this variable, (3) a control actuator (in this case, the infusion pump driving the drug), (4) a system (in this case a patient), and (5) an accurate, stable control algorithm [5].

The controlled variable

Pharmacokinetic closed-loop

If drug concentrations can be measured in real time, closed-loop delivery based on pharmacokinetics is possible. The clinician can select a target drug concentration and the system will adapt its delivery to attain and maintain this concentration based on concentration measurements. On-line measuring of drug concentration is not feasible for intravenous anesthetics. In contrast, inspired and end-tidal (or end-expired) concentrations of inhaled anesthetics like isoflurane, sevoflurane and desflurane, can be measured using real-time spectroscopic methods, allowing the implementation of automated systems realizing these concentrations. The end-tidal concentration might be a reasonable surrogate for arterial blood concentration, but still shows a time lag with regard to cerebral anesthetic effects. Over the last decades, various experimental systems have been developed [76, 77], resulting in the release of a commercial closed-circuit anesthesia ventilator (Zeus; Dräger Medical, Lübeck, Germany) in 2003. This machine targets the end-tidal concentrations of inhaled anesthetics and controls the fresh gas flow and sets anesthetic concentration using closed-loop technology [78].

Pharmacokinetic-dynamic closed-loop

The effectiveness of closed-loop systems for drug administration strongly depends on the reliability, monotonicity and linearity (in contrary to on/off or saturation behavior) of the physiological signal as the indicator for the desired clinical effect. Examples of observable clinical endpoints are blood pressure [79] or neuromuscular function [80]. As "depth of hypnosis" or "level of analgesia" is not measurable, surrogate measures have to be applied as controlled variables. A clinician should be aware that a certain surrogate measure does not show 100% correlation with the desired therapeutic effect, and should backup his therapeutic decisions using secondary variables. Reliable closed-loop systems should integrate this common sense by applying the same secondary variables as boundaries to increase the efficacy and safety of the overall system.

The EEG (electroencephalogram), representing cortical activity, is widely accepted as a marker for depth of hypnosis. Several computerized EEG derivatives such as spectral edge frequency and median frequency have been used as controlled variables for closed-loop systems in the past [81]. More recently, the BIS (Bispectral Index) has been tested and validated as a measure of the hypnotic component of anesthesia and has been used as controlled variable in multiple studies. BIS has been designed using multivariate statistical analysis to combine multiple EEG features including higher-order spectra and phase correlations between spectra into a more accurate indicator. BIS values lie in the range of 0-100. BIS in the 90-100 range represents fully awake patients and ranges around 60-70 and 40-60 indicate light and moderate hypnotic states, respectively. A BIS value below 40 indicates an excessive level of hypnosis [82]. Other EEG derivatives were designed to measure the hypnotic depth of anesthesia, but have not so far been applied in closed-loop systems. Nearly all EEG-derived parameters have the drawback that the electronics used to measure the microvolt-range signals often pickup noise from electrocoagulation or disturbances like muscle activity. Furthermore, the actual EEG activity may be suppressed by other mechanisms induced by some volatile anesthetics, not directly related to the depth of hypnosis. One research group has tested auditory evoked potentials, more specifically the MLAEP as the controlled variable for closed-loop control for propofol [83].

The development of closed-loop systems for control of analgesics (mostly opioids) still lacks an optimal measurement method. Since an adequate level of analgesia balances nociception and antinociption, an automated measurement might require a noxious stimulus to be effective. Despite a complex combined effect of both hypnotic and analgesic drugs on the hemodynamic status of the patient, most anesthesiologists rely on the autonomic and somatic changes in blood pressure, heart

rate, etc. to guide their administration of perioperative opioids, supported by secondary measures such as tearing. But an automated controller for opioid control based on hemodynamic changes alone would be incapable of distinguishing between the sources of changes in blood pressure, so more complex systems are required. Recently, some preliminary reports have been published on measuring the nociception-antinociception balance by heart rate variability, variability of the pulse plethysmography, variability in the Bispectral Index (called the composite variability index) and others [84, 85].

The setpoint

The setpoint is the value for the controlled variable which the controller uses as its target. This target is specified by the anesthesiologist and will be approached as closely as possible during the maintenance of anesthesia; therefore an adequate individual target is essential for the accuracy of the closed-loop system. Two types of set-points can be used based on (1) population mean data or (2) individual data measured at the start or just before the control period. The latter type could be expected to more closely correspond to clinical needs during the course of the surgical procedure.

The control algorithm

Various closed-loop strategies have been applied for drug administration. A controller classic is the PID (proportional-integral-differential) controller commonly known from general engineering [81]. A PID controller will calculate the actuator's corrective action based on a straightforward mathematical derivative of the observed error. The general formula can be written in the time domain as:

$$dU/dt = K_P \times d(err)/dt + err/K_I + K_D \times d^2(err)/d^2t \qquad \textbf{Equation 13}$$

with *err* being the error between the target and the observed value, causing a response *U* in the actuator. The constants K_P, K_I, K_D are tuned by calculations from models of the system, by computer simulations, or derived from trials using tuning rules. For systems with a complex pharmacological behavior, a general PID controller with *U* an administration rate can be slow to establish control and dangerous to use because of possible oscillations. Fine-tuning of a PID controller is difficult in this particular setting because of the complexity of the system to control (as shown in figure 1), because of

inter-individual pharmacologic variability, and because it is not possible to directly counteract the administration of excessive drug [86].

A better approach is to incorporate information about the dose-response into the control, by using the PID controller to set a target plasma or effect-site concentration for an underlying TCI system (Figure 1, A/A'; B/B'). This approach applies the TCI system to compensate for part of the complex dose-response relationship. Even though the TCI system will only realize an approximate value for the target concentration, the dynamics of the resulting system will be of lower order [87]. PID controllers, tuned in general circumstances, may fail in situations different (*e.g.* surgical stimulation, inter-patient variability) from that for which the controller was tuned. The increasing calculation performance of computer systems may allow better control through the integration of more complex mathematical models of the overall relationship between the drug and its effect in the human body, or by reverting to other control algorithms such as model predicted control or fuzzy logic [88, 89].

The tuning of a controller does not need to be permanently fixed. In adaptive (model-based) controllers, the controller response is varied to adapt to changing circumstances. Fine-tuning of the model towards the individual patient can be done using state estimation, mixed-effects pharmacokinetic or dynamic modeling, Bayesian estimation, Kalman filtering, fuzzy logic or other engineering techniques. Bayesian optimization [8] individualizes the PD relationship by combining individual information with the knowledge of an *a priori* probability density function containing the statistical properties of the parameter to be estimated [9]. The Bayesian method starts from a standard, population-based response model providing the prior distribution of parameter values. These values are adjusted to reflect the patient's own parameters over time, based on the observed response of the individual patient under varying circumstances. Recently, this method has been used in a closed-loop system for propofol [90, 91] (figure 6). The Kalman filter will apply a recursive method to calculate numbers for a given dose-response relationship for the specific patient [92]. One investigation explored how k_{e0} can be individualized on the basis of an initial bolus and estimation of time to peak effect [93]. An alternative approach of model adaptation based on fuzzy logic has been proposed [94].

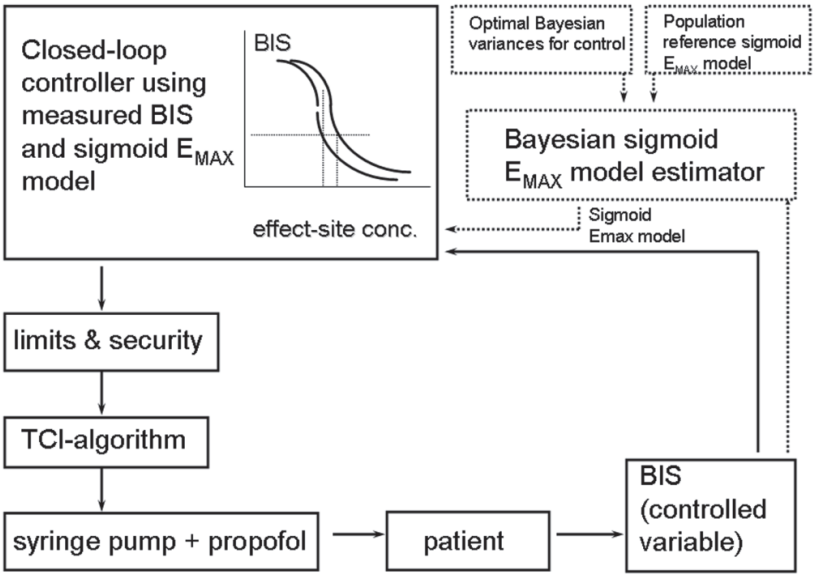

Fig. 6. *Flow chart of the closed-loop system. The straight lines represent the closed-loop control system. At each time the required effect-site concentration is calculated by the controller. This value is sent to an additional algorithm taking the safety limits into account. The result of these calculations is the required effect-site concentration sent to the TCI algorithm which steers a pump injecting propofol to the patient. The measured BIS is used as the input of the closed-loop controller. The dotted lines represent the Bayesian sigmoid E_{MAX} model estimator. The estimator receives a-priori information from the population sigmoid E_{MAX} model, the optimal Bayesian variances for control and the patient measured BIS values.*

Prototype examples of closed-loop drug delivery systems

Since 1950 various groups have investigated closed loop drug delivery during anesthesia [95]. Table 5 shows a list of prototypes for the administration of hypnotics, analgesics and muscle relaxants in humans based on changes in hemodynamic and cerebral drug effects. All systems were clinical tested.

Hypnotics

Lacking a better direct indicator, many closed-loop systems for hypnotics have been designed using hemodynamic feedback, as shown in table 5. Early studies used the MF as the controlled variable [96, 97]. A linear two-compartment model was used to describe the drug input-concentration relation in an adaptive controller. More recently, this closed-loop system was used using EEG to study the interaction of alfentanil and propofol [98]. Each patient received TCI alfentanil . Propofol was added to the alfentanil infusion by a feedback system. The set point was the range of 1.5-2.5 Hz EEG MF. Strangely, it was concluded that the interaction between alfentanil and propofol, based on the EEG in the investigated dose range, was additive [98]. After the commercialization of the Bispectral Index derived from the EEG, closed-loop systems using BIS technology were developed. Preliminary tests performed with a BIS (version 1.22)-controlled closed-loop system concluded that the system provided intra-operative hemodynamic stability and prompt recovery from sedative-hypnotic effects of propofol [99]. The performance of a closed-loop system for administration of general anesthesia, using BIS (version 3.1) as a target for control in combination with a modified PID controller for drug administration was evaluated [100]. Anesthesia was maintained by intravenous infusion of a propofol/alfentanil mixture (via an infusion pump) or an isoflurane/nitrous-oxide-based technique (inhaled anesthetics injected in the inspiratory limb of the breathing circle). Closed-loop and manually controlled administration of anesthesia resulted in similar intraoperative conditions (cardiovascular and EEG variables) and initial recovery characteristics. The closed-loop system showed no clinical advantage over conventional, manually adjusted techniques of anesthetic administration. A similar closed-loop anesthesia system using BIS as the control variable, a PID control algorithm, and a propofol plasma-controlled TCI system as the control actuator was developed [87]. Although clinical tests showed acceptable control, the authors concluded that further studies were required to determine whether control performance could be improved by changing the gain factors or by using an effect-site-targeted, TCI propofol system [101]. These researchers subsequently revised their controller algorithm, including an effect-compartment TCI in their system, which was shown to have better accuracy of control, although the PID controller might still face some stability problems [7]. Model-based adaptive control of propofol administration with BIS was previously used in a closed-loop system for sedation during spinal anesthesia and, more recently, during general anesthesia [54, 102]. The latter two reports (from the same research group) describe a closed-loop control system for propofol using the BIS as the controlled variable. The implementation applied a patient-specific PD

profile calculated during induction for control during surgery. More recently, the same authors further developed the adaptive part of the controller using Bayesian optimization [90].

Newer closed-loop systems have been evaluated. A new type of closed-loop control system using the BIS has been developed, and applied to the administration of inhaled isoflurane [103]. This controller uses a cascade structure, originally described by Gentilini *et al.* [104], which separates regulation of the PD and PK effects of isoflurane on BIS. Closed-loop control with BIS to administer isoflurane required no human intervention to maintain BIS at 50 ± 10, and performed significantly better than manual control. An indicator derived from the MLAEP, called AEPindex, has been used to investigate the synergistic interaction between propofol and remifentanil [105].

Opiates and muscle relaxants

There are relatively few closed-loop systems for anesthetic drug classes other than sedative-hypnotics. An MPC (model predictive controller) was designed for the control of mean arterial blood pressure during anesthesia, using alfentanil as the opioid. Opioid concentrations predicted by a PK model are used together with MAP by the controller algorithm to determine opioid infusion rates. Many closed-loop control systems for muscle relaxants have been explored in the past, but only a few could cope with the introduction of the latest shorter-acting neuromuscular blocking drugs. Table 5 shows a list of various prototypes.

Future closed-loop drug delivery systems

Future development of integrated closed-loop systems for total anesthesia control are only possible if multiple input/output controllers are used to control both hypnotic and analgesic components of anesthesia [106]. The ultimate goal of the closed-loop controllers is their general acceptance in clinical practice. So far, all developed closed-loop systems have been used in well-controlled scientific trial environments. Nevertheless, closed-loop delivery systems are no longer esoteric [107]. Rather, the challenge is now to establish fully the safety, efficacy, reliability and utility of closed-loop anesthesia for its adoption into clinical practice. However, regulatory challenges need to be solved [108].

Table 5. *Closed-loop systems for hypnotics, analgesics and muscle relaxants*

Reference	Drug	Controlled variable	Controller type
Bickford 1950 [95]	Thiopental	EEG	On-off
Soltero *et al.* 1951 *[109]*	Ether	EEG	P
Bellville *et al.* 1954 [110]	Cyclopropane	EEG	P
Kiersey *et al.* 1954 [86]	Thiopental	EEG	P
Bellville & Attura 1957 [111]	Cyclopropane	EEG	P
Suppan 1972 [112]	Halothane	HR	On-off/incremental
Suppan 1977 [113]	Halothane	BP	On-off/incremental
Linkens *et al.* 1982 [114]	Vecuronium	NMT	PID
Rametti *et al.* 1985 [115]	D-Tubocurare	NMT	State estim./adaptive
Ritchie *et al.* 1985 [116]	Succinylcholine	NMT	PID
Rametti & Bradlow 1983 [115]	Atracurium	NMT	State estim./adaptive
Lampard *et al.* 1986 [117]	Atracurium	NMT	On-off
de Vries *et al.* 1986 [118]	Vecuronium	NMT	On-off
Schils *et al.* 1987[119]	Halothane	BP + EEG	PI/model-based
Schwilden *et al.* 1987 [96]	Methohexital	EEG-MF	Model-based/adaptive
Webster & Cohen 1987 [120]	Atracurium	NMT	PD
Jaklitsch *et al.* 1987 [121]	Vecuronium	NMT	PID
Millard *et al.* 1988[122]	Isoflurane	MAP	Model-based/adaptive
Monk *et al.* 1989 [123]	Isoflurane	MAP	Adaptive
MacLeod *et al.* 1989 [124]	Atracurium	NMT	PI
Schwilden *et al.* 1989 [125]	Propofol	EEG-MF	Model-based/adaptive
O´Hara *et al.* 1991 [126]	Atracurium	NMT	Multiphase/PID
Olkkola & Schwilden 1991 [127]	Vecuronium	NMT	Model-based/adaptive
Olkkola *et al.* 1991 [128]	Atracurium	NMT	Model-based/adaptive
Schwilden & Stoeckel 1993 [129]	Alfentanil	EEG-MF	Model-based/adaptive
Zbinden *et al.* 1995[88]	Isoflurane	MAP	Fuzzy logic
Edwards *et al.* 1998 [130]	Atracurium	NMT	Fuzzy logic
Mortier *et al.* 1998 [102]	Propofol	EEG-BIS	Model-based/adaptive

Kenny & Mantzaridis 1999 [83]	Propofol	EEG-MLAEP	PI
Morley *et al.* 2000 [100]	Propofol-Isofl	EEG-BIS	PID + plasma TCI
Sakai *et al.* 2000 [117] [99]	Propofol	EEG-BIS	PID
Gentilini *et al.* 2001 [104]	Isoflurane	EEG-BIS	Model-based/adaptive
Allen & Smith 2001 [131]	Propofol	AEP	Neuro-fuzzy
Struys *et al.* 2001 [54]	Propofol	EEG-BIS	Model-based/adaptive
Gentilini *et al.* 2002 [132]	Alfentanil	MAP	Model-based/predictive
Absalom *et al.* 2002 [87]	Propofol	EEG-BIS	PID + plasma TCI
Absalom & Kenny 2003 [7]	Propofol	EEG-BIS	PID + effect-site TCI
Locher *et al.* 2004 [103]	Isoflurane	EEG-BIS	Model-based/adaptive
Luginbühl *et al.* 2006 [89]	Alfentanil	MAP	Model-based/predictive
Liu *et al.* 2006 [133]	Propofol	EEG-BIS	PD + effect-site TCI
Puri *et al.* 2007 [134]	Propofol	EEG-BIS	PID
De Smet *et al.* 2007 [90]	Propofol	EEG-BIS	Model-based, Bayesian
Hemmerling et Al. 2010[135]	Propofol	EEG-BIS	Rule-based

Chapter 3

Pharmacokinetic models for propofol – defining and illuminating the devil in the detail

Modified from:

A.R. Absalom, V. Mani, T. De Smet, M.M.R.F. Struys

Pharmacokinetic models for propofol- defining and illuminating the devil in the detail.

British Journal of Anesthesia, 2009; **103**: 26-37

The recently introduced open target-controlled infusion (TCI) systems can be programmed with any pharmacokinetic model, and allow either plasma- or effect-site targeting. With effect-site targeting the goal is to achieve a user-defined target effect-site concentration as rapidly as possible, by manipulating the plasma concentration around the target. Currently systems are pre-programmed with the Marsh and Schnider pharmacokinetic models for propofol. The former is an adapted version of the Gepts model, in which the rate constants are fixed, whereas compartment volumes and clearances are weight-proportional. The Schnider model was developed during combined pharmacokinetic-pharmacodynamic modelingmodeling studies. It has fixed values for V1, V3, k_{13} and k_{31}, adjusts V2, k_{12} and k_{21} for age, and adjusts k_{10} according to total weight, LBM and height. In plasma targeting mode, the small, fixed V1 results in very small initial doses on starting the system or on increasing the target concentration in comparison with the Marsh model. The Schnider model should thus always be used in effect-site targeting mode, in which larger initial doses are administered, albeit still smaller than for the Marsh model. Users of the Schnider model should be aware that in the morbidly obese the LBM equation can generate paradoxical values resulting in excessive increases in maintenance infusion rates. Finally, the two currently available open TCI systems implement different methods of effect-site targeting for the Schnider model, and in a small subset of patients the induction doses generated by the two methods can differ significantly.

When TCI devices first became commercially available in 1997, the concept was new to clinicians and regulatory authorities, many of whom feared the possible complications arising from use of a device that changed infusion rates automatically. A strong emphasis on safety was thus necessary to ensure regulatory approval and the confidence of clinicians. The systems all contained the Diprifusor® (Astra Zeneca, UK) microprocessor, programmed with the Marsh adult pharmacokinetic model for propofol[30]. The Diprifusor contained two microprocessors – one 16 bit and the other 8 bit (G.N.C. Kenny, personal communication), the former to calculate and implement the required infusion rates, and the latter to monitor the driving motor to calculate the volume of propofol actually being administered and to perform a simple calculation of the estimated plasma concentration from this. The system was designed to shut down if there was a significant discrepancy between the plasma calculations estimated by the two microprocessors.

The first generation systems only allowed the user to target the plasma concentration. At the time of their release the significance of an effect-site anatomically and temporally separate from the plasma was only just being fully appreciated. Early models only displayed the target and estimated plasma concentrations. Later on a k_{eo} value was incorporated allowing an estimate of the effect-site concentration to be made and to be displayed as additional information.

In addition to controlling the user interface, and calculating and implementing the infusion rates required to achieve the target concentration, the Diprifusor microprocessor also controlled a syringe recognition system that only allowed the use of glass pre-filled 50ml syringes of 1% or 2% propofol (Diprivan 1% ™ or Diprivan 2%™, AstraZeneca, UK).

Open TCI systems do not contain the Diprifusor microprocessor and do not have a syringe and drug recognition system. They contain a single processor that the manufacturer can program with any pharmacokinetic model for any drug, and allow the use of a wide variety of syringes of sizes between 10ml and 50ml supplied by several different manufacturers. The chief benefit of these systems is that cheaper, generic formulations of propofol can be used for TCI.

At the time of publication, there are two open TCI systems commercially available: the Alaris Asena PK™ (Carefusion, Alaris Products, Basingstoke, UK) and the Base Primea™ (Fresenius, France). These systems provide the user with a potentially confusing range of choices. Generally they are supplied with pre-loaded and activated models for remifentanil (Minto model) [36, 37], sufentanil[38], and two models for propofol. With the Base Primea system the user has a choice of the modified Marsh * and Schnider [23, 24] models, whereas with the Asena PK system, the choice is between the Marsh [30] and Schnider [23, 24] adult models and the Kataria pediatric model[32]. With all these drugs and models both plasma and effect-site targeting are possible (except with the Marsh model implemented in the Asena PK). To further add to the confusion the two systems use two different methods of implementing effect-site targeting with the Schnider model.

* Shafer S. Stanpump. Available from http://opentci.org/doku.php?id=code:code (accessed 15 may 2015)

Failure to appreciate the differences between the different propofol models and implementation methods may result in administration of excessive or inadequate doses of propofol with potentially harmful results.

PLASMA VS EFFECT-SITE TARGETING

Early TCI systems were designed to achieve a user-defined plasma 'target concentration'. It soon became apparent that there was hysteresis in the relationship between plasma concentration and clinical effect, caused by the temporal delay in equilibration between plasma concentrations and the concentration at the sites of action within the central nervous system, referred to as the 'effect–site.'

The rate of plasma/effect-site equilibration depends on factors that determine the rate of drug delivery to the effect-site (such as cardiac output and cerebral blood flow) and pharmacological properties that determine the rate of drug transfer across the blood-brain barrier (lipid solubility, degree of ionization etc). The time course of plasma/effect-site equilibration can be mathematically described by a first-order rate constant typically referred to as the k_{eo}. Strictly speaking, this term should be used to describe the rate of removal of drug from the effect-site out of the body, but the effect-site is regarded as having negligible volume, so that there is no need for separate constants describing the rate constants for movement into and out of the effect compartment (the k_{eo} defines the proportional change in each unit of time of the concentration gradient between the plasma and effect-site).

With effect-site targeting, the TCI system manipulates the plasma concentration to achieve the effect-site concentration as rapidly as possible. When the effect-site target concentration is increased, the TCI system briefly increases the plasma concentration to an optimal level above the target effect-site concentration before temporarily stopping the infusion to allow the plasma concentration to decrease to the level of the target effect-site concentration. Most systems use mathematical iterations to determine the magnitude of the optimal plasma concentration overshoot - the peak plasma concentration that generates a gradient sufficient to cause the most rapid increase in effect-site concentration but without an overshoot of the effect-site concentration above its target (figure 1).

If the target effect-site concentration is reduced the system stops the infusion, allowing the plasma concentrations to fall, thereby generating a concentration gradient out of the effect-site, until the estimated effect-site concentration has fallen to the new target. At this stage the plasma concentration will be less than the effect-site concentration, and so the system has to administer a small bolus to increase the plasma concentration to the target concentration.

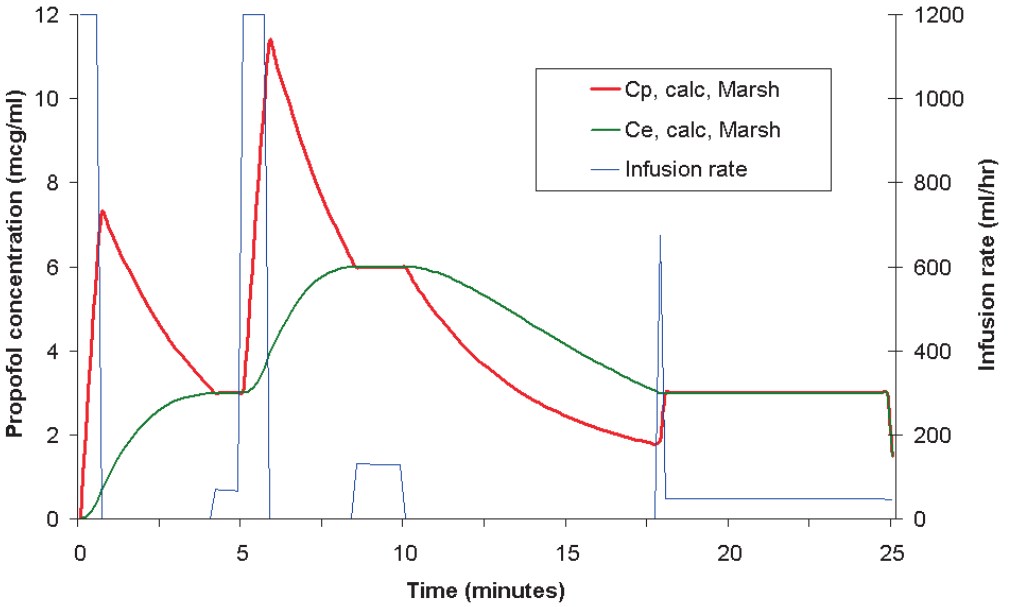

Fig. 1. *Effect-site targeted TCI. At time zero the target is set at 3 µg/ml, at 5 min it is increased to 6 µg/ml, and at 10 min it is reduced to 3 µg/ml. At each target change the system manipulates the blood concentration to rapidly achieve the target effect-site concentration*

With effect-site targeting, the magnitude of the plasma concentration overshoot estimated by the system depends critically on the k_{eo} and also on the estimated rate of decline in the plasma concentration. If a slower (smaller) k_{eo} is used, a greater overshoot in the peak plasma concentration will be required to produce a larger concentration gradient between the blood and the effect-site and thereby to hasten plasma-effect-site equilibration (figure 2).

The estimated rate of decline of the plasma concentration also has an influence on the overshoot. A system that estimates a slower decline in plasma concentrations will administer a lesser plasma

overshoot than a system estimating a faster decline, to avoid an eventual effect-site concentration overshoot. After a bolus dose, the rate of decline in plasma concentrations mostly depends on the rate of fast re-distribution, but is also influenced by the rate of drug metabolism and of slow-re-distribution. Naturally the net rate of decline caused by re-distribution depends on the concentration gradients between compartments. If a system estimates that the plasma drug concentration will fall rapidly after a bolus at a given time, then a greater overshoot is necessary to optimize the gradient driving drug into the effect-site, and the flux of drug into the effect-site, than if a slow rate of decline were estimated.

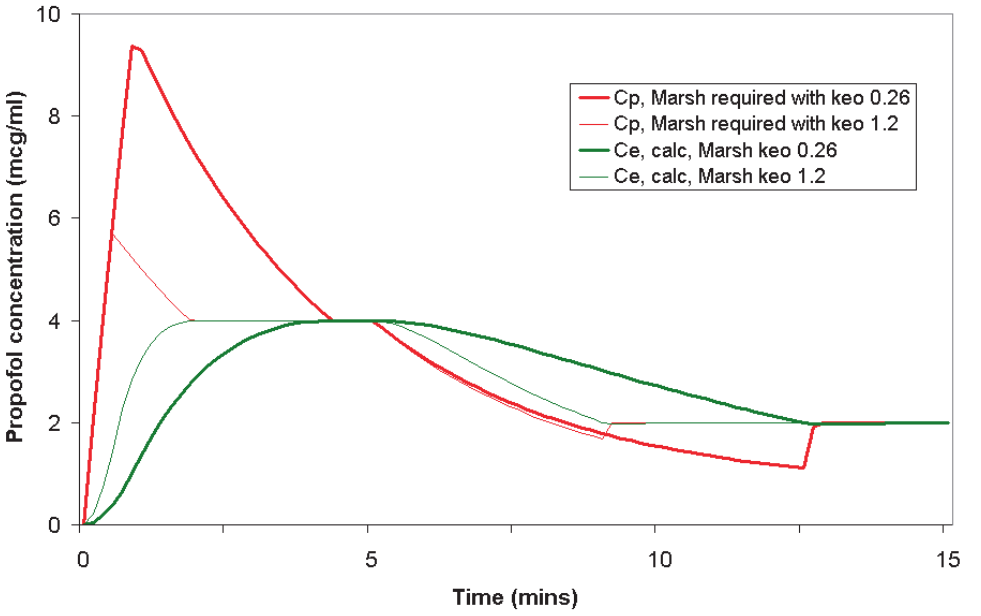

Fig. 2. *Effect-site targeted TCI for propofol (Marsh model), showing the effect of the choice of K_{e0}. If a slow K_{e0} is used, then a large overshoot in plasma concentration will result when the target concentration is increased.*

Since the accuracy of the estimated plasma concentration itself and the degree of overshoot required depend on the accuracy of several parameters and assumptions, there are multiple potential sources of error. Model errors resulting in excessively high plasma concentrations may well be tolerated by young fit patients, but in frail, elderly subjects, they may result in significant cardiovascular instability.

Methods for estimating k_{eo}

Unlike isoflurane, for which the brain concentration can be estimated with reasonable accuracy by magnetic spectroscopy [136, 137], there are currently no methods of directly estimating the effect-site concentrations of i.v. anestheanesthetic agents. The time course of changes in effect-site concentration can however be estimated by recording a measure of clinical effect and then used to generate an estimate of the k_{eo}. Ideally, a combined pharmacokinetic-pharmacodynamic (PK/PD) modelingmodeling technique should be used, in which concomitant measurements of plasma drug concentrations and clinical effect are performed in a study population during and after administration of a bolus, an infusion or a combination of the two. The result is a combined model that estimates plasma and effect-site concentrations.

When pharmacodynamic and pharmacokinetic data are not available from the same subject group, then a model-independent parameter called "Time to peak effect" (TTPE) can be used to estimate the k_{eo} for a PK model and patient group[71]. After any bolus, maximal clinical effects will occur when the effect-site concentration reaches its maximum. Since transfer of drug between blood and effect-site is gradient driven, when the plasma concentration is greater than the effect-site concentration, net transfer is from plasma to effect-site and vice versa. When depicted graphically, this peak occurs when the effect-site concentration curve crosses the plasma concentration curve, reaching a local maximum. TTPE is defined as the time delay between a bolus injection and the peak clinical effect. It is considered to be independent of the size of the bolus dose.

The effect-site compartment is assumed to have negligible volume. Hence uptake of drug into the effect-site should have negligible influence on the plasma concentration of a drug, so that the calculated plasma concentration profile following an infusion of drug is identical for any value of k_{eo}. With this assumption, determination of the k_{eo} becomes a simple one-dimensional mathematical minimization problem. This process is illustrated in figure 3, in which measured or estimated plasma concentrations (following a bolus dose) are plotted over time alongside an observed measure of clinical effect. Different k_{eo} values are then used to estimate the effect-site concentration. Smaller k_{eo} values result in the estimated peak in effect-site concentrations being smaller and occurring later than if faster (larger) k_{eo} is used. In this case, a k_{eo} of 0.38/min results in a peak effect-site concentration at 100 s which matches best with the observed maximal clinical effect.

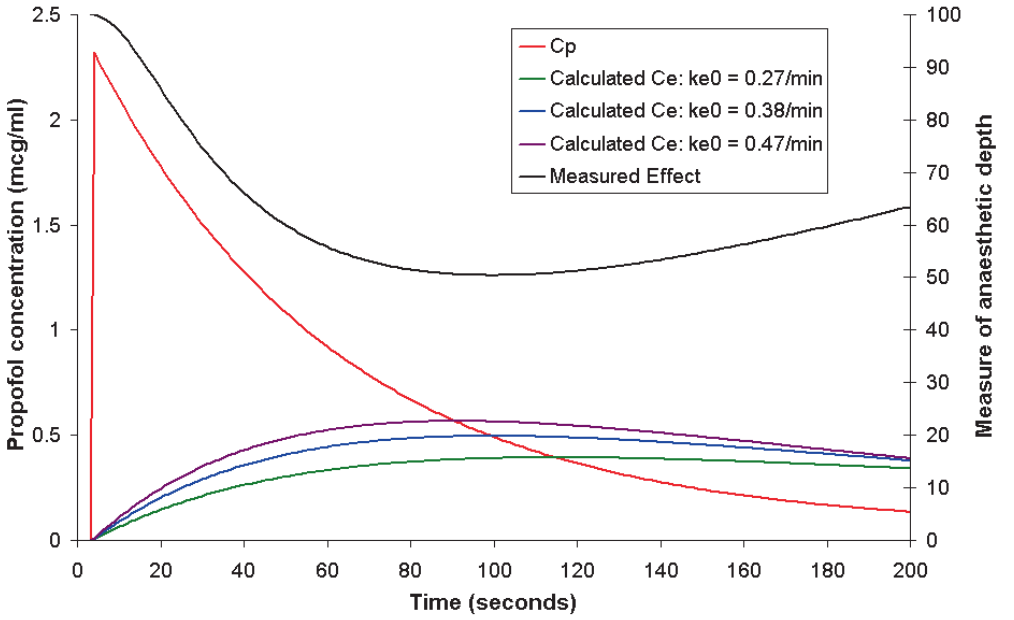

***Fig.3**. Estimation of k_{e0} using TTPE methodology. Estimated plasma concentrations and a measure of anestheanesthetic effect are plotted over time. The estimated effect-site concentrations resulting from different k_{e0} values are then calculated and plotted, to determine which k_{e0} value is associated with a peak effect-site concentration that matches the peak clinical effect.*

A disadvantage of this approach is that it requires precise observation of TTPE, whereas in real clinical situations noise and other factors make the observation of a single 'peak effect' difficult. Rather than relying mainly on one observation an alternative approach is to plot the relationship between the measure of clinical effect and the estimated effect-site concentrations arising from different k_{eo} values (figure 4). Simple mathematical techniques can then be used to determine the k_{eo} value which limits the area within the loop caused by the hysteresis effect. In this hypothetical example, a k_{eo} of 0.38/min is selected since it completely collapses the hysteresis curve. This methodology can also be applied to studies involving infusions.

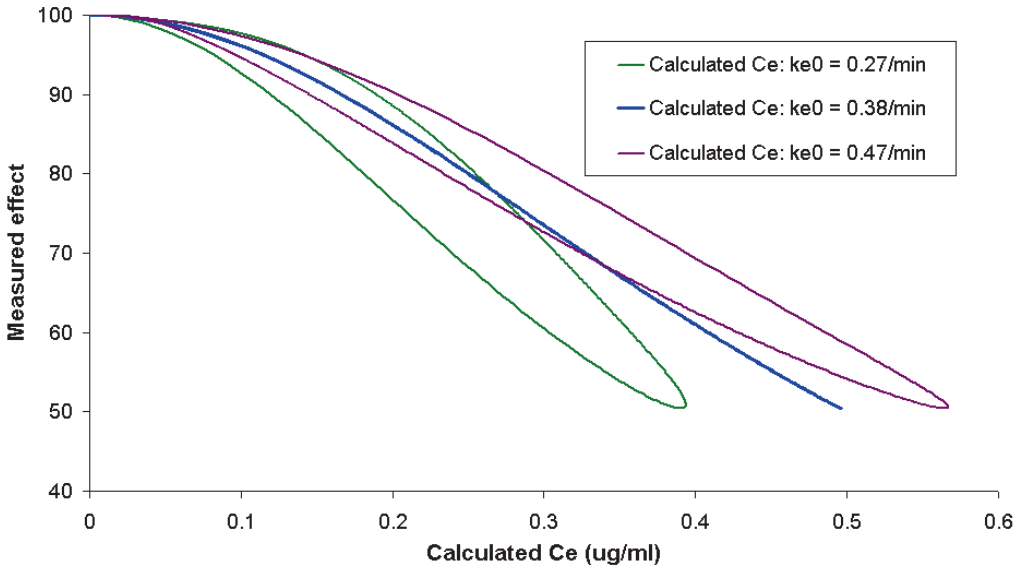

Fig. 4. *Optimization of k_{e0} value. A measure of anestheanesthetic effect is recorded continuously after a bolus dose, or during and after infusion. Estimated effect-site concentrations are calculated from the estimated plasma concentration, and different k_{e0} values. Mathematical techniques are used to determine the k_{e0} value which best collapses the hysteresis curve (i.e. most limits the aria between the two limbs of the curve).*

DIFFERENCE BETWEEN MARSH AND SCHNIDER MODELS

These models were derived in different ways, have quite different parameters, and when used to determine the infusion rates of a TCI system during effect-site TCI, can result in significantly different propofol infusion rates. In normal and mildly obese patients the differences mainly occur within the first 10 min after a target concentration increase (figure 5), whereas in more obese patients, the differences can be greater throughout the infusion.

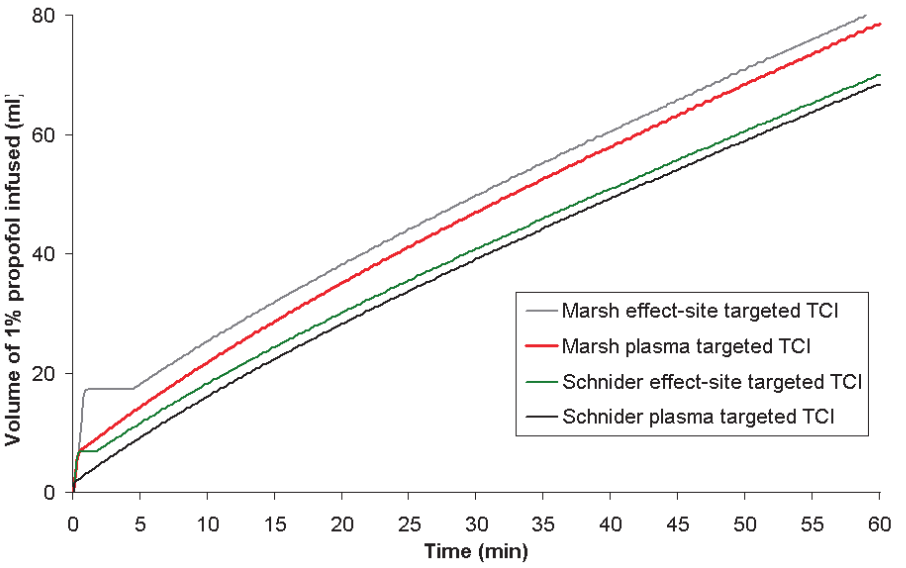

Fig. 5. *Comparison of the cumulative dose of propofol 1% infused when a TCI system uses the Marsh and Schnider models at a target blood concentration of 4 µg/ml in a 40/yr/old male patient who weighs 70 kg and is 170 cm tall.*

Marsh model

The Marsh model parameters were published with the results of a study of its predictive performance, and that of an adapted model, in children in 1991 [30]. Compartmental volumes are proportional to weight, whereas rate constants for slow and fast redistribution are fixed (table 1). It was pragmatically adapted from the Gepts three-compartmental model[138], which was developed from a study involving three groups of 6 patients who each received constant rate infusions of propofol at either 3, 6 or 9 mg/kg/h. Although full details were not published it appears that the study included few elderly or obese patients. The Marsh model is identical to the Gepts model in all respects except that the central compartmental volume was increased to 0.228 liter/kg. There is no published explanation of the rationale for this adjustment.

Later on, a k_{eo} value of 0.26/min came to be used with this model in first generation TCI pumps, to enable effect-site concentration estimations to be made. The data on which this k_{eo} value was based

were never published in the peer-reviewed literature, although it is quite similar to the value of 0.2/min found by Billard and colleagues[139].

Struys and colleagues later published evidence that a k_{eo} of 1.2/min used in conjunction with the Marsh pharmacokinetic parameters more accurately predicted the time course of clinical effect (as assessed by the Bispectral Index) than the k_{eo} of 0.26/min [25]. A k_{eo} of 1.2/min used with the Marsh model results in an estimated TTPE of approximately 1.6 min, which is consistent with the findings of other groups[23]. This combination (sometimes referred to as the "modified Marsh" model) is used in the Base Primea TCI system, and results in more gentle manipulations of the plasma concentration (above and below the target concentration) when effect-site targeting mode is used.

	Marsh [30]		Schnider [23, 24]	
	General model	70 kg	General model (LBM calculated using weight, height, gender)	70 kg, male height 170 cm
V1	0.228 liter/kg	15.9 liter	4.27 liter	4.27 liter
V2	0.463 liter/kg	32.4 liter	18.9-0.391 x (age-53) liter	24.0 liter
V3	2.893 liter/kg	202.0 liter	238 liter	238 liter
K_{10} (min^{-1})	0.119	0.119	0.443 + 0.0107 x (weight-77) -0.0159 x (LBM-59) + 0.0062 x (height-177)	0.384
K_{12} (min^{-1})	0.112	0.112	0.302-0.0056 x (age-53)	0.375
K_{13} (min^{-1})	0.042	0.042	0.196	0.196
K_{21} (min^{-1})	0.055	0.055	[1.29-0.024 x (age-53)] /[18.9-0.391 x (age-53)]	0.067
K_{31} (min^{-1})	0.0033	0.0033	0.0035	0.004
K_{e0} (min^{-1})	0.26	0.26	0.456	0.456
TTPE (min)	4.5	4.5	1.69	1.69

Table 1. *Adult propofol models*

Schnider model

This model was derived during a combined pharmacokinetic and pharmacodynamic study in a single set of 24 volunteers (11 female, 13 male; weight range 44 – 123 kg; age range 25 - 81 yr; height range 155 - 196cm)[23, 24]. The co-variates are total body weight, age, height and lean body mass calculated from total weight, gender and height) (table 1).

V1 and V3 (and thus k_{13} and k_{31}) are fixed, whereas the size of V2 (and thus k_{12} and k_{21}) is influenced only by age, being smaller with advancing age. The implications of this are that after a bolus of a given size, the Schnider model will estimate that the same peak plasma concentration is achieved for all patients, irrespective of their age, height or weight. After the peak, the initial rate of decrease in plasma concentration will depend on the age of the patient. This is in contrast to the Marsh model, where estimated plasma concentrations after a given bolus are proportional to the patient's weight, whereas the estimated rate of decline of the plasma concentration is the same for all patients.

The elimination rate constant, k_{10}, is the only parameter influenced by body mass. It varies in a complex manner with total body weight, height and lean body mass (LBM) but does not vary with age. Thus, these only influence the rate at which drug metabolism is estimated to occur, and thus the rate at which propofol is infused to replace these losses during the maintenance phase.

The Schnider model incorporates a k_{eo} of 0.456/min derived from the combined PK/PD study mentioned earlier, in which a rapidly-calculated EEG parameter was used as a measure of clinical effect. This k_{eo}, in conjunction with the PK parameters, predicts a TTPE, after a bolus dose, of 1.69 min.

LBM CALCULATION FORMULA USED IN SCHNIDER MODEL

In the Schnider model, LBM is calculated using the James formula [140], which performs satisfactorily in normal and moderately obese patients, but paradoxically in the severely obese.

The James formula calculates LBM as follows:

Males: LBM = 1.1 x weight – 128 x $(\text{weight/height})^2$

Females: LBM = 1.07 x weight – 148 x $(\text{weight/height})^2$

Figure 6 illustrates the relationship between total body weight, LBM and ideal body mass (IBM). Note that for males, the calculated LBM increases with total body mass until it reaches a maximum value slightly greater than the ideal body mass (*Males: Ideal body weight (kg) = 49.9 + 0.89 x (height in cm - 152.4) Females: Ideal body weight (kg) = 45.4 + 0.89 x (height in cm - 152.4)*[141]. Thereafter (when the BMI (body mass index) is > 42 kg m^{-2}), with increasing total body weight, the calculated LBM decreases paradoxically. A similar paradoxical situation exists with females. The calculated LBM increases with total body weight, and reaches a peak at when the BMI is approximately 37 kg m^{-2}. This maximum LBM value is slightly less than the ideal body mass (for the appropriate height) except in very short females in whom it is similar to ideal body mass.

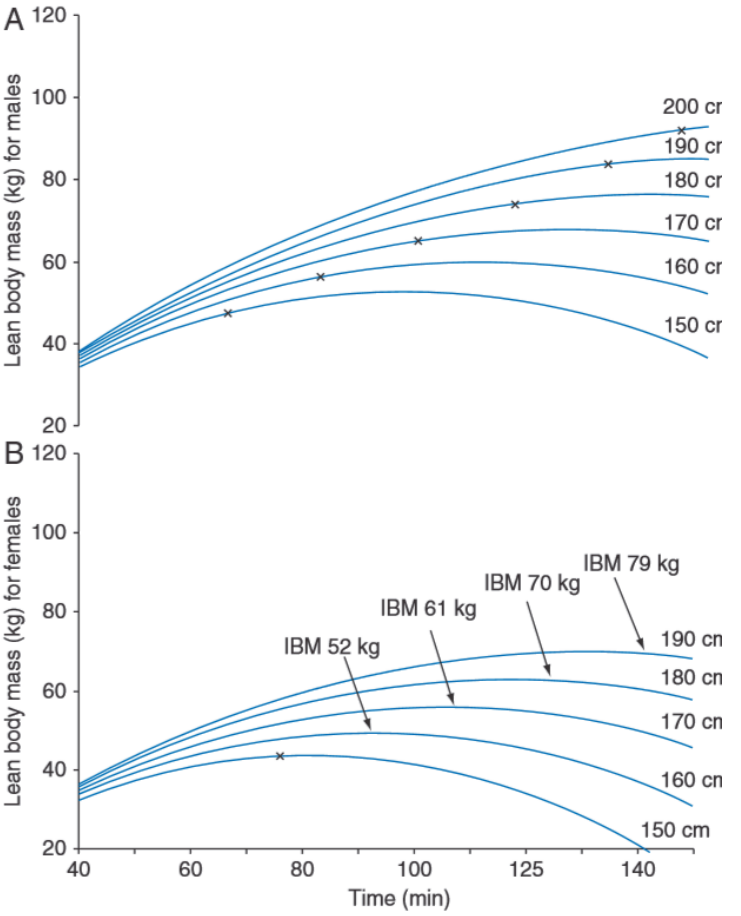

Fig. 6. *Relationship between body weight, height, and lean body mass (LBM) for males (A) and females (B), as calculated by the James formula. Each line shows the change in LBM for a given height*

(indicated on the right). Ideal body mass (IBM) for each height is indicated by a cross – read the value off the y-axis – or by text and arrows when the IBM does not fall on the LBM curve.

The effect of the calculated LBM value on the k_{10}, and hence on maintenance infusion rates, is not immediately obvious. As shown in table 1, increasing total body weight and height tend to increase the k_{10}, whereas increasing LBM will tend to decrease the k_{10}. Thus, total body weight and LBM have opposing effects on the k_{10}, with the LBM value moderating the influence of total body weight on the k_{10}. In severely obese patients, the paradoxically low calculated LBM causes a large *increase* in calculated k_{10}. As a result, as BMI increases beyond 42 kg m^{-2} in males, and 37 kg m^{-2} in females, the infusion rates required (to replace the estimated drug metabolism) increases exponentially. The relationship between total body weight and calculated k_{10} for patients of different heights is illustrated in figure 7 (solid lines).

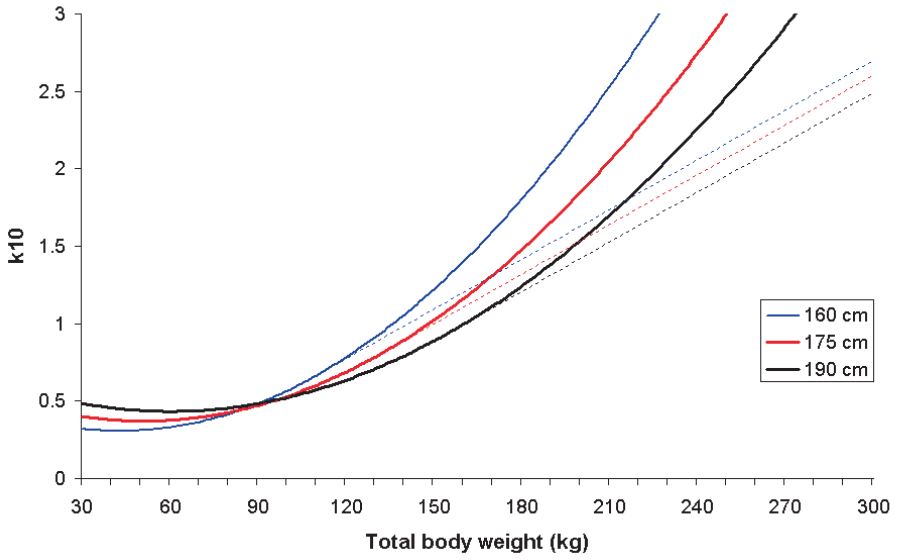

Fig. 7. *Relationship between total body weight and k_{10} for males with the Schnider model*

The manufacturers of current open TCI systems have implemented compromise solutions that may improve safety. In the the Base Primea system, if the user enters a body weight and height combination that falls on the declining portion of the total body weight (TBW) versus LBM curve, then

the maximal LBM figure for that height is used. A similar solution is implemented in the Asena PK system : for a given height, the system will not accept a TBW figure that falls on the declining portion of the curve, and the user is required to enter a total body mass at or below the value generating the maximum LBM. The influence of increasing total body weight on the calculated k_{10}, when these limits in LBM are applied in the severely obese, is illustrated in figure 7 (dashed lines).
The influence of total body weight on maintenance infusion rates in the morbidly obese are discussed in what follows.

EFFECT-SITE TARGETING IMPLEMENTATION WITH THE SCHNIDER MODEL

Schnider used semi-linear canonical correlation to calculate the 'canonical univariate parameter' from EEG data recorded from the volunteers in his study, and used this to track the time course of the pharmacodynamic effect of propofol [24]. The median TTPE of a propofol bolus, determined by this parameter, was 1.69 min. Based on visual inspection of the EEG the TTPE ranged from 1.0 to 2.4 min (median 1.6 min). When a TTPE of 1.6 min was used to calculate the k_{eo} for each of their volunteers, the median k_{eo} was 0.456/min. The authors concluded that a k_{eo} of 0.456/min used with the pharmacokinetic parameters determined in the same group of volunteers [23] provided the best description of the time course of clinical effect of propofol.

After a standard bolus dose (*e.g.* 2 mg /kg), the Marsh model estimates the same peak concentration, and the same rate of decline in plasma concentration, in all subjects, since the compartment volumes are all weight-proportional. As a result, use of a single k_{eo} value generates the same estimated TTPE in all patients. The converse is also true: if a single TTPE is used, then the calculated k_{eo} will be the same for all patients.

The situation is different with the Schnider model. A weight-adjusted dose will result in different estimated peak plasma concentrations for patients of different weight, since the volume of V1 is the same for all patients. After the peak is reached, the rate of decline in plasma concentrations will vary from patient-to-patient, depending on the age, gender, height and weight. If a fixed k_{eo} is used to calculate the TTPE in patients who differ in one or more of these parameters, then different TTPE values will result. Likewise, a single TTPE value used to calculate individual k_{eo} values will result in different values in different patients. This latter approach is illustrated in figure 8, which shows the estimated plasma and effect-site propofol concentrations arising after a 2 mg /kg propofol bolus in two different male patients, both weighing 70 kg, but one being older and taller than the other. In this example the k_{eo} has been adjusted in each case to cause the effect-site concentration to reach local maxima at 1.6 min. In the case of the elderly patient a faster (larger) k_{eo} value is required, and results in a greater estimated peak effect-site concentration.

The Asena PK open TCI system incorporates many of the software routines that are used in the RugloopII© software, developed by T.D.S. and M.M.R.F.S. Alternative implementations can be found

in Stanpump, developed by Steven L Shafer, MD at Stanford University. Thus, in common with RugloopII© and Stanpump, when implementing effect-site targeting for the Schnider model, the Asena PK uses a fixed time to peak approach to calculate a unique k_{eo} for each patient. The Base Primea system on the other hand uses a fixed k_{eo} (0.456/min), and this results in different times to peak effect for different patients.

For non-obese and mildly obese patients, fixed TTPE approach results in a k_{eo} that is in the vicinity of 0.456/min. For some severely obese patients this approach can generate a significantly faster (larger) k_{eo}. As mentioned earlier, the choice of k_{eo} will influence the degree of plasma concentration over- and under-shoot when the target concentration is changed, and thus also influences the overall dose.

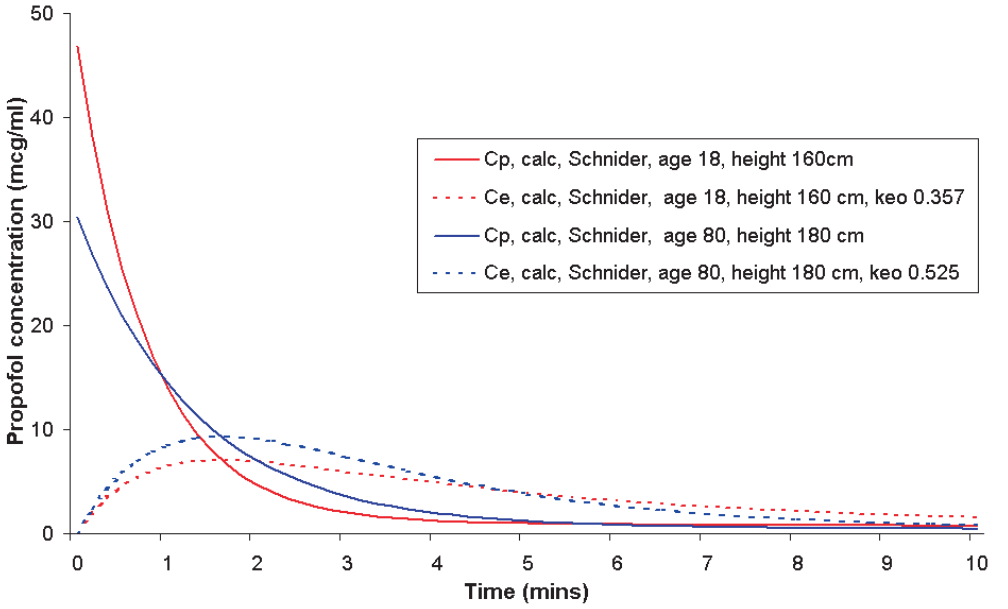

Fig. 8. *Predicted blood and effect/site concentration profiles, based on the Schnider model and TTPE of 1.6 min, for two different patients who both weigh 70 kg and who have each received a 2 mg kg $^{-1}$ i.v. bolus dose of propofol. In the older patient, plasma propofol concentrations will fall at a slower rate. To produce an estimated TTPE that is the same as in the younger patient, a faster k_{e0} value is required.*

PRACTICAL CONSEQUENCES OF DIFFERENCES BETWEEN THE MARSH AND SCHNIDER MODELS

Plasma versus effect-site targeting

In general, for non-obese or mildly obese patients, the cumulative dose administered by the two models using the two modes of operation will follow a similar pattern. The highest total dose will be given by the Marsh model in effect-site targeting mode (with a k_{eo} of 0.26/min), followed by the Marsh model in plasma targeting mode, then the Schnider model in effect-site targeting mode, and finally the lowest dose will be administered by the Schnider model in plasma targeting mode. Figure 5 shows the cumulative dose administered to a 40-yr- old man, who weighs 70 kg and is 170 cm tall, by systems implementing the Marsh and Schnider models in effect-site and plasma targeting mode (target concentration 4 μg/ml).

The important question is not, of course, which model delivers the largest or smallest dose of drug, but which one produces the most accurate predictions of plasma and effect-site concentration. Plasma concentrations can be measured directly offline using chromatography. While several studies have assessed the predictive performance of the Marsh model [42, 142-144], other than the initial study from which the Schnider model was derived, there is a paucity of published data of the ability of the latter model to predict plasma propofol concentrations accurately.

There are very few situations in which use of the Schnider model in plasma targeting mode may be recommended. When a TCI system is used in plasma targeting mode, and the target plasma concentration is increased, the size of the initial bolus dose (in mg) required to increase the plasma concentration to the new target is calculated mathematically as follows:

Bolus dose (mg) = $(C_{p,\ target,\ new} - C_{p,\ target,\ old}) \times V1 \div$ drug concentration in syringe

Thus the size of the initial bolus is directly proportional to the value of V1 in the model. In the Marsh model, V1 varies with weight of the patient (15.9 liter for a 70 kg patient), whereas in the Schnider it is fixed at 4.27 liter irrespective of the patient's weight. As a result, when plasma targeting k_{10} mode is used with the Schnider model, the small fixed V1 results in the same initial bolus being given to all

patients, for a given plasma target concentration, regardless of their age, weight or height. This is counter-intuitive and contrary to the clinical experience of anesthetists, who observe that induction requirements increase with body weight.

In effect-site targeting mode, a system implementing the Schnider model calculates a plasma concentration overshoot. The exact extent of the overshoot will depend on the age, weight and height of the patient, and will generally be of the order of 300% of the target concentration. In almost all situations where the Schnider model is used, it should be used in effect-site targeting mode.

Few would recommend the use of the Marsh model in effect-site targeting mode with a k_{eo} of 0.26/min. Although this k_{eo} value is slower (smaller) than the k_{eo} used with the Schnider model, the degree of overshoot of the estimated plasma concentration is far less than with the Schnider model. This is because the estimated rate of decline of plasma concentrations after a bolus is far slower with the Marsh model than the Schnider model, resulting in a more modest overshoot of ~150%. Nonetheless, the much larger V1 value in the Marsh model results in much greater initial doses being administered in this mode. For example, for an initial target concentration of 4 µg/ml, the initial bolus will be 172 mg for a 70 kg patient, whereas, for the Schnider model the initial dose will be 77 mg.

The Base Primea system allows effect-site targeting with the Marsh model with a faster k_{eo} value of 1.2/min, resulting in smaller overshoots (of the order of 50%). In effect-site targeting mode at an initial target of 4 µg/ml, it will administer an initial dose of 98 mg to a 70 kg man (age 40 yr, height 170 cm).

In fit, healthy, young patients, the use of the modified Marsh model in effect-site targeting mode may be safe and justifiable. With currently available evidence, in almost all other situations, the safest options, and those most commonly chosen by clinicians are either of the Marsh in plasma mode and the Schnider model in effect-site mode. Thus in the following sections we will compare the initial and subsequent doses administered with these two options.

Size of the initial dose on starting an infusion

Figure 9 illustrates the influence of choice of model and implementation, total body weight and height on the cumulative dose administered during the first 15 min of a TCI, for males and females aged 20, 40 and 80 yr. The target concentration is 5 µg/ml, and the figure illustrates the doses administered by the Marsh model in plasma targeting mode and the Schnider model in effect-site targeting mode (both fixed k_{eo} method and fixed TTPE implementation). For the Schnider implementations the dotted lines indicate the doses administered if the original LBM equations are used in the morbidly obese without the corrections mentioned earlier.

As can be seen in the figure, the dose administered by the Marsh model is unaffected by age or height. For the Schnider model increasing age decreases the dose, whereas increasing height increases the dose, except in the morbidly obese in whom shorter patients may sometimes receive larger doses than taller patients of the same weight. In shorter patients increasing total weight causes the dose administered to increase more steeply.

For the Marsh model (in plasma-targeting mode) the dose administered increases linearly with total body mass, and will be greater than the Schnider model (effect-site-targeting mode) in all patients except those adults with a very low body weight.

For the Schnider model the initial dose increases with increasing total body weight at any given height. This increase is modest in the normal and mildly obese patient, to whom far less drug would be administered than with the Marsh model. In these patients the doses resulting from the two different implementations of the Schnider model are very similar. In the severely obese the increase in total dose is much more rapid, and can be significantly different with the two different implementations of the Schnider model. In particular, in young, tall, obese patients, the fixed TTPE method will result in a greater initial propofol dose (as a result of a slower k_{eo} value, and thus a significantly higher peak plasma concentration for the same effect-site target concentration).

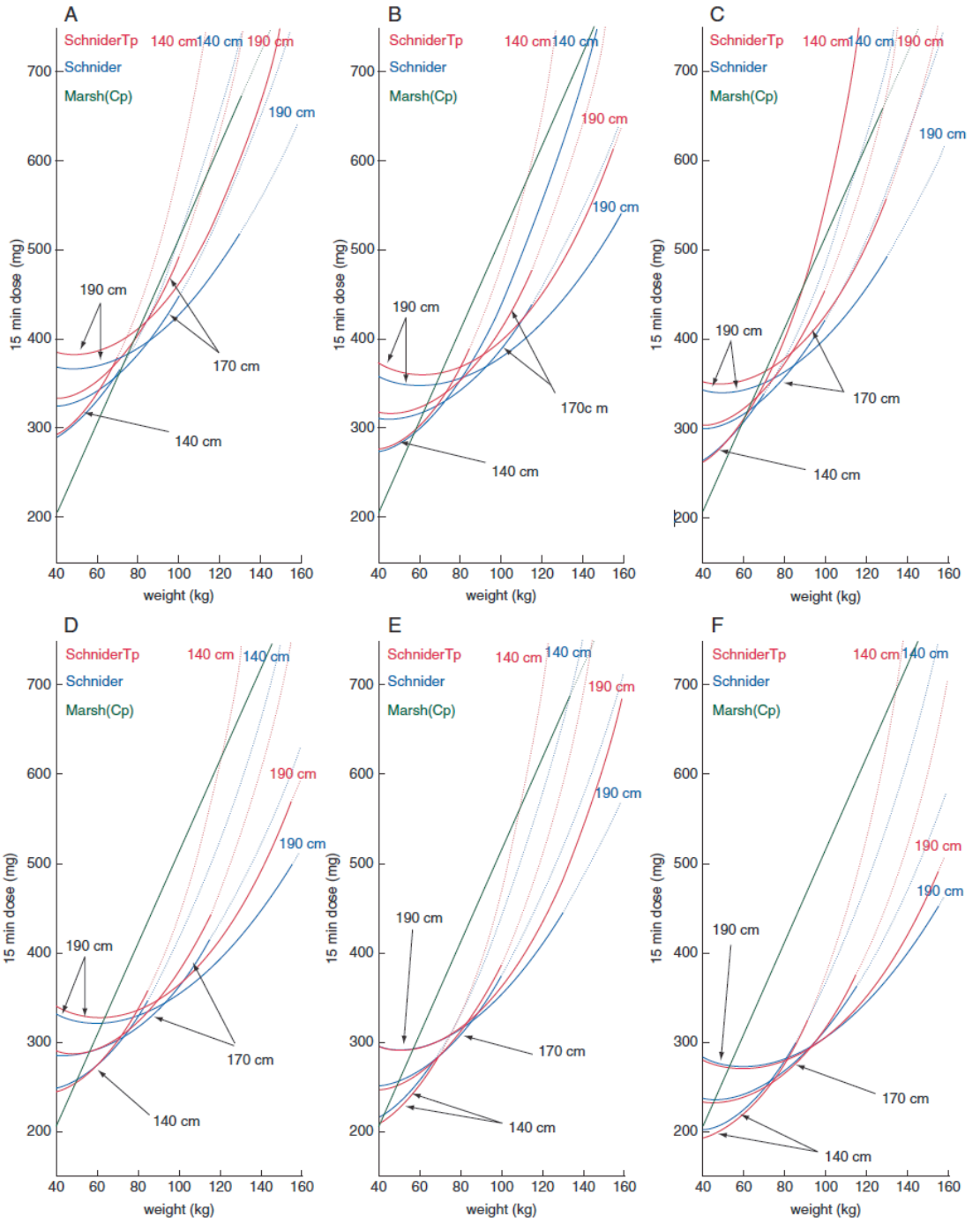

Fig. 9. *Influence of total body weight, height, age, and gender on the cumulative propofol dose administered during the first 15 min at a target concentration of 5 µg/ml. The figures illustrate the*

doses administered by the Marsh model in plasma targeting mode (green) and the Schnider model in effect-site targeting mode (fixed k_{e0} method red, fixed TTPE implementation blue). The solid lines represent the doses implemented by current infusion systems, whereas dashed lines indicate the doses that would be administered to severely obese patients if the systems did not correct for the paradoxical decrease in LBM (see text). (A) Female age 20 yr; (B) Male age 20 yr; (C) Female age 40 yr; (D) Male age 40 yr; (E) Female age 80 yr; (F) Male age 80yr.

"Maintenance" infusion rates

After the initial dose, the infusion rate administered by a TCI system depends of course on the estimated rates of redistribution and metabolism. As time passes, and the concentrations in the different compartments equilibrate, eventually the infusion rate gradually decreases to that required to replace drug lost by metabolism.

As mentioned before, for the Marsh model, the fast and slow re-distribution rate constants are proportional to the weight of the patient, whereas for the Schnider model, the fast re-distribution rate constant depends only on age, whereas the slow re-distribution rate constant is independent of age, weight or height. In the Marsh model the metabolic rate constant varies with weight only, whereas in the Schnider model it varies according to LBM and total body weight.

Figure 10 illustrates the influence of choice of model, age, gender, weight and height on the total propofol dose that would be administered to patients during the period between 15 min and 60 min after starting an infusion with a target 5 μg/ml. The dose administered by the Marsh model is unaffected by age or height, and is a linear function of body weight. For the Schnider model increasing age decreases the dose, whereas increasing height increases the dose (except in morbidly obese patients where shorted patients of the same weight will receive greater doses). Except in very thin patients, increasing weight increases the dose.

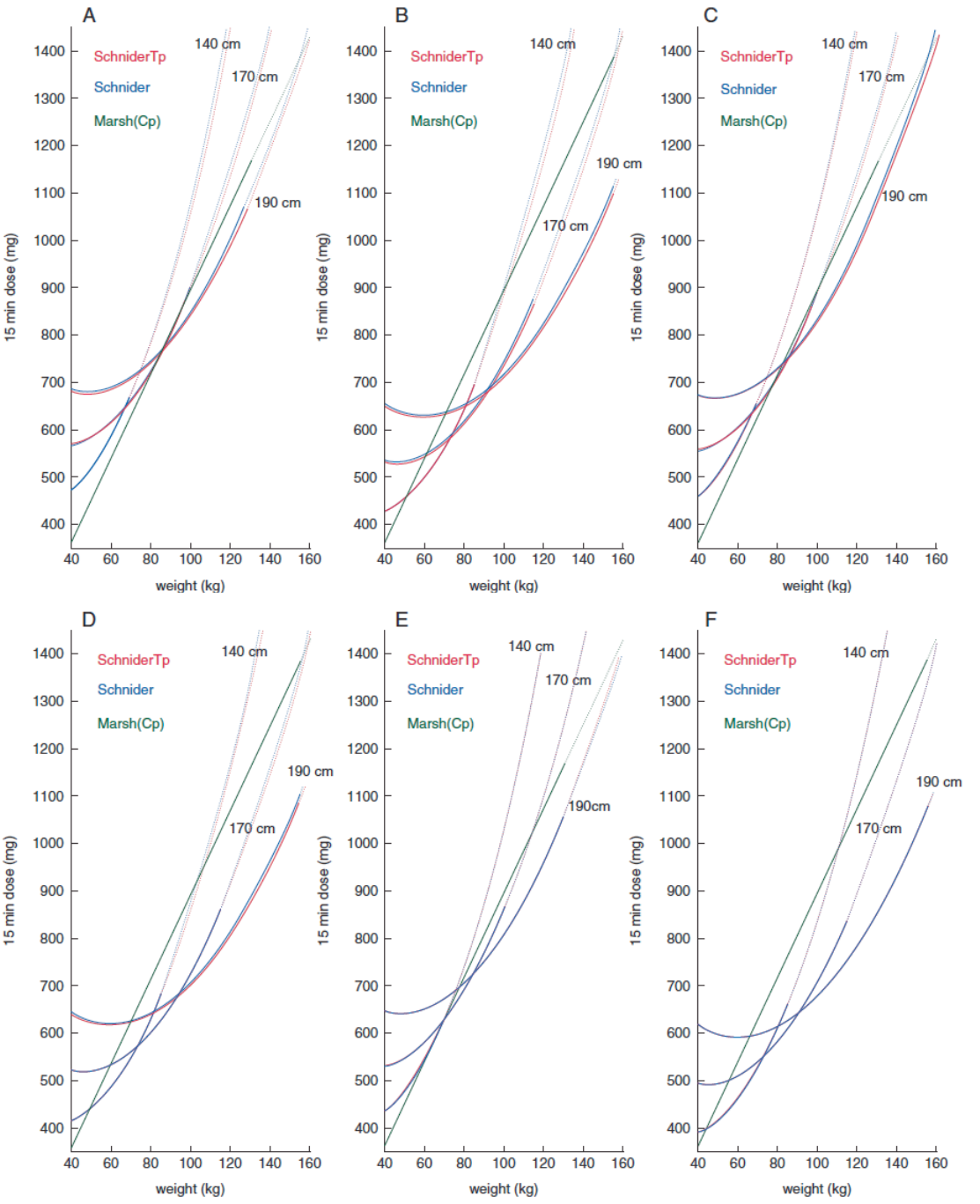

Fig. 10. *Influence of total body weight, height, age, and gender on the cumulative 'maintenance dose' administered from 15 min to 60 min after starting an infusion of propofol at a target concentration of*

5 µg/ml. The figures illustrate the doses administered by the Marsh model in plasma targeting mode (green) and the Schnider model in effect-site targeting mode (fixed k_{e0} method red, fixed TTPE method blue). The solid lines represent the doses implemented by current infusion systems, whereas dashed lines indicate the doses that would administered to severely obese patients if the systems did not correct for the paradoxical decrease in LBM (see text). (A) Female age 20 yr; (B) Male age 20 yr; (C) Female age 40 yr; (D) Male age 40 yr; (E) Female age 80 yr; (F) Male age 80 yr.

Despite these differences, for most patients the choice of model (and effect-site targeting implementation method) does not result in significantly different maintenance infusion rates.

COMMENT

With current knowledge, there is little conclusive evidence to demonstrate the superiority of any particular model or method of effect-site targeting implementation. In general it is best for anesthetists to use the model and methods with which they are most familiar, and to only use a different model or method of effect-site implementation if they understand the differences of the new model or method. Most experts would agree that if the Schnider model is used it should be used in effect-site targeting mode, whereas if the Marsh model is used it should be used in plasma targeting mode or if it is used in effect-site targeting mode, then it should be used with the faster k_{eo} for propofol recommended by Struys and colleagues (1.2/min) [25] .

Anesthetists using the Marsh model in the years after TCI systems were first available quickly learnt by experience that target concentrations appropriate for younger patients were associated with hemodynamic instability in elderly patients. This is because both pharmacokinetic and pharmacodynamic changes with age. Marsh model does not make any adjustments for age, and has been shown to under-predict plasma propofol concentrations in the elderly [144] . Advancing age is also associated with increased pharmacodynamic sensitivity to the effects of propofol.

A major benefit of the Schnider model is that it adjusts doses and infusion rates according to patient age. This provides a strong argument for using the Schnider model in elderly and unwell patients, in

whom smaller bolus doses will be given after target increases, and this may improve hemodyhemodynamic stability and safety.

The situation is less clear for morbidly obese patients. The clinical experience of anestheanesthetists using TCI systems is that if the total body mass of severely obese patients is used with the Marsh model, the resulting large doses at induction often result in adverse hemodyhemodynamic consequences. This observation probably results from the fact that the initial volume of distribution (V1) has been shown not to be significantly increased in obesity [145],and that induction dose requirements are more closely related to LBM [47].
The problem for clinicians using the Marsh model is that although induction requirements are more closely related to LBM, maintenance requirements do increase significantly with severe obesity, and are more closely related to total body mass. As a result, for the Marsh model there remains controversy over what value the user should input into the TCI system for patient weight. Most anestheanesthetists do not input the real total body weight with morbidly obese patients, when using the Marsh model. Many input a weight calculated using a formula recommended by Servin: [145] 'Input weight' = IBW + 0.4 x (TBW – IBW).

Albertin used this formula with the Marsh model during TCI propofol in obese patients, with IBM calculated using the Lemmens formula [146]. Predictive accuracy was good for the first 20 min, which is not surprising since the input weight is generally closer to the LBM than total body weight. For samples taken after 40 min, however, measured blood concentrations were significantly lower than predicted concentrations.

The problems for clinicians using the Schnider model in obese patients relate, as indicated earlier, to the problems with the LBM calculation, and the differences between the two methods of effect-site targeting implementation. The equipment manufacturers have implemented a pragmatic solution to the problem of the paradoxical decrease in LBM in the morbidly obese. In the severely obese, maintenance dose requirements do increase with increasing body weight, and the linear increase in k_{10} in the severe obese resulting from the "fixing" of LBM at the maximum value, seems to be a reasonable and logical solution. Further studies are required to provide the scientific evidence for this.

For most patients, the different methods of Schnider effect-site targeting implemented in the Asena and Base Primea systems result in clinically insignificant differences in dose administered. In a very small subset of the population the fixed TTPE method will result in significantly higher induction doses. This is because, in these patients, the system will estimate larger values for k_{10} and k_{12} than for older, shorter, thinner patients. As a result, it will estimate more rapid falls in plasma concentration after a bolus dose, which with a fixed k_{eo} results in an earlier TTPE. If the TTPE is fixed, a slower (smaller) k_{eo} is required to delay the TTPE, which results in the requirement for a greater plasma concentration overshoot and thus a much larger initial bolus size. It is not clear at present which method of effect-site targeting implementation is safest and most appropriate.

The studies from which the Marsh and Schnider pharmacokinetic models were developed did not include severely obese patients. Until there is good scientific evidence showing reasonable predictive performance of either of these, or a new pharmacokinetic model, target-controlled infusions should be used with caution in severely obese patients, regardless of which model or effect-site implementation method is used.

Chapter 4

Comparison of Closed-Loop Controlled Administration of Propofol Using Bispectral Index as the Controlled Variable versus "Standard Practice" Controlled Administration

Modified from:

M.M.R.F. Struys, T. De Smet, L.F.M. Versichelen, S. Van De Velde, R. Van Den Broecke, , E.P. Mortier. Comparison of Closed-Loop Controlled Administration of Propofol Using Bispectral Index as the Controlled Variable versus "Standard Practice" Controlled Administration

Anesthesiology 2001; **95**: 6-17

Dr. Struys, Dr. De Smet and Dr. Versichelen own propriety rights on the closed-loop algorithms. Tom De Smet is a consultant for Aspect Medical Systems, Newton, Massachusetts.

Background: This report describes a new closed-loop control system for propofol that utilizes the BIS (Bispectral Index) as the controlled variable in a patient-individualized, adaptive, model-based control system, and compares this system with manually controlled administration of propofol using hemodynamic and somatic changes to guide anesthesia.

Method: Twenty female patients, American Society of Anesthesiologists physical status I or II, who were scheduled for gynecologic laparotomy, were included to receive propofol/remifentanil anesthesia. In group I, propofol was titrated using a BIS guided model-based closed-loop system. The BIS target was set at 50. In group II, propofol was titrated using classical hemodynamic signs of (in)adequate anesthesia. Performance of control during induction and maintenance of anesthesia were compared between both groups using BIS as the controlled variable in Group I and the reference variable in Group II, and, conversely, the systolic blood pressure as the controlled variable in Group II and the reference variable in Group I. At the end of anesthesia, recovery profiles between groups were compared.

Results: Although patients undergoing manual induction of anesthesia in Group II at 300 ml/h reached a BIS level of 50 faster than patients undergoing open-loop, computer controlled induction in Group I, manual induction caused a more pronounced initial overshoot of the BIS target. This resulted in a more pronounced decrease in blood pressure in Group II. During the maintenance phase, better control of BIS and systolic blood pressure was found in Group I compared with Group II. Recovery was faster in Group I.

Conclusion: A closed-loop system for propofol administration using the BIS as a controlled variable together with a model-based controller is clinically acceptable during general anesthesia.

INTRODUCTION

The use of closed-loop systems might improve the quality of drug administration[147] . A number of basic components are required to develop a satisfactory closed-loop drug delivery system: (1) a system under control, which is the patient; (2) a controlled variable that measures the relevant drug effect; (3) a set point for this variable, which is the chosen target value specified by the user; (4) an actuator which is, in this case, the infusion pump driving the administration of drug; (5) a controller to control the actuator, which comprises an algorithm to translate a measured value of the controlled variable to a particular action for the actuator to steer the controlled variable closer to the target value [5].

Since the pioneering work of Bickford [95] , various parameters, such as the median frequency of the electroencephalogram [125] or auditory evoked potentials [83] , have been applied as controlled variables for closed-loop control of intravenous hypnotic-anesthetic drugs. More recently, the Bispectral Index (BIS; Aspect Medical Systems, Inc., Newton, MA), a single composite electroencephalogram measure, has been designed to track electroencephalographic changes associated with different anesthetic states [148, 149] .

A satisfactory controller is needed during closed-loop control [5]. In closed-loop control, the input (*i.e*., propofol infusion) at any particular time depends on the previous system output (*i.e*., BIS). When the input to the system is controlled using a behavioral model of a reference system, then the controller is said to use model-based control. For hypnotics, combined pharmacokinetic-pharmacodynamic models have been described [150] and tested [23-25, 151]. When the model-based control system uses the measured output of the system not only to determine the next input, but also to update the model describing the systems' input-output relation, then the system is defined as model-based and adaptive [152] . Adaptive, model-based control has been demonstrated by Schwilden *et al* [125] as an effective method to manage the dose-response (*i.e*., input-output) relation of propofol.

Previously described closed-loop systems for the administration of hypnotic drugs were never compared with manually controlled anesthesia (*i.e*. "standard practice"). Therefore, the purpose of this study was to describe a new closed-loop control system for propofol that uses BIS as the controlled variable in a patient-individualized, adaptive, model-based control system, and to compare its performance with manually controlled administration of propofol using hemodynamic and somatic

changes to guide anesthesia. This study complies with the recently proposed performance specifications for feedback control systems in anesthesia.*

METHODS AND MATERIAL

System specifications

Data Management, Monitored Variables, and Actuator Control.

In all patients, our setup used RUGLOOP (Ghent University, Gent, Belgium) running on a Pentium II-based computer system to steer the infusion pump and to record the BIS signal, blood pressure, and all other relevant physiologic data. All data were stored on hard disk. BIS (version 3.4) was derived from the frontal electroencephalogram (At-Fpzt) as calculated by the A-2000 BIS Monitor (Aspect Medical Systems, Inc.). Blood pressure, heart rate, end tidal carbon dioxide, and oxygen saturation were acquired using the Datex AS3 monitor (Datex, Helsinki, Finland).

RUGLOOP is a general infusion pump control and data management system, able to deliver a computer-controlled infusion, targeting either the plasma or effect-site concentrations by using a combination of compartmental pharmacokinetic and effect-site models [25] . The algorithms to target the plasma [153] and the site of drug effect [12] in RUGLOOP are adapted from STANPUMP, written by Dr. S.L Shafer.

The controlled variable.

In the closed-loop group, BIS was used as the controlled variable. The A-2000 BIS Monitor also calculates a Signal Quality Index (0-100). The suppression ratio is the percentage of isoelectric electroencephalogram within the previous minute. When detected artifacts within the electroencephalogram caused the Signal Quality Index to decrease below 15%, then the system stopped adjusting and maintained the current concentration, as further described below.

In the standard practice group, anesthesia was conducted using several criteria for inadequate anesthesia, as described below. The systolic blood pressure (SYS) was considered the main controlled variable.

---

* Glen JB, Schwilden H, Stanski DR. Workshop on Safe Feedback control of Anesthetic drug delivery. Schloss Reinharthausen, Germany. June 29, 1998. *Anesthesiology 1999;* **2**: 600-601

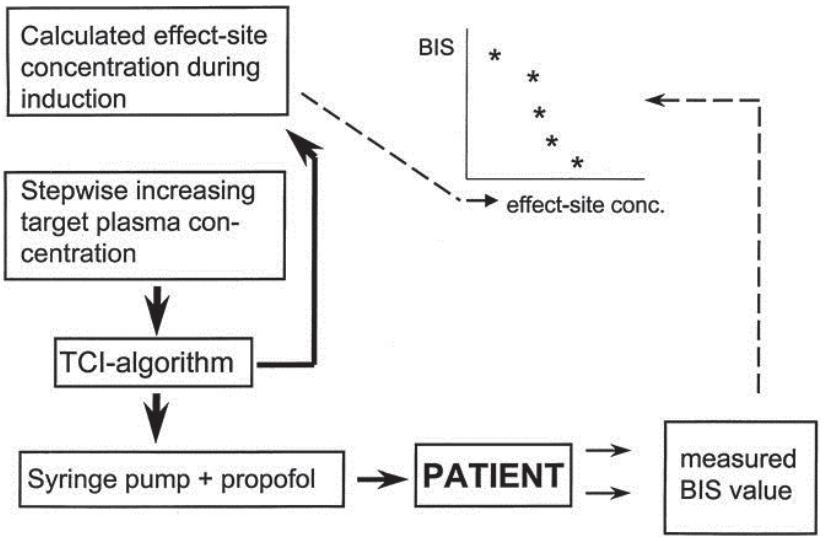

Fig. 1. *Flow chart of the steering method during induction. During induction, an automatically stepwise increasing plasma concentration is administered using a target-controlled infusion (TCI) system (RUGLOOP) for propofol (straight line). The corresponding effect-site concentration is calculated and plotted versus the effect. The effect of this effect-site concentration on the BIS (Bispectral Index) is measured and sent to the computer (dotted line). After loss of consciousness, the increase in effect-site concentration is stopped by the anesthetist, and the computer estimates the pharmacodynamic curve (effect vs. effect-site concentration). Thereafter, the loop is closed and the target set point is entered in the controller.*

The closed-loop controller

In the closed-loop group, RUGLOOP was used to manage the control algorithms as well. The measured BIS was transferred to the control algorithm that attempts to minimize the error between the measured BIS value and the target BIS value selected by the anesthesiologist. The algorithm calculated an adequate propofol effect-site concentration from the measured BIS using a specific patient-individualized, model-based, adaptive control method. This effect-site concentration was used as input to the RUGLOOP internal computer-controlled infusion system. The effect-site concentration was computed to yield a time to peak effect of 1.6 min after bolus injection, as published by Schnider *et al.* [24].

The controller was based on a pharmacodynamic model represented by a sigmoidal E_{max} model, called the "Hill curve"[154].

The initial, patient-specific pharmacodynamic profile was calculated automatically during induction by correlating all predicted propofol effect-site concentrations with the corresponding BIS values. To obtain this information, the patient received a propofol infusion using open-loop, plasma target controlled infusion. RUGLOOP calculated the corresponding effect-site concentration concurrently. Every 50 s, the target concentration was increased automatically with 0.5 μg/ml. Once the target BIS level was achieved, the induction sequence was terminated, the pharmacodynamic model was calculated from paired assessments of BIS and predicted effect-site concentrations, and the feedback loop was closed. During maintenance, RUGLOOP switched the target-controlled infusion from targeting the plasma compartment to the effect compartment. The methods are plotted in figure 1 and described in Appendix A, which is available on the ANESTHESIOLOGY Web site*.

The closed loop controller used this patient-individualized pharmacodynamic relation calculated during induction to manage the control action and to generate the target value for the internal computer-controlled infusion system.

During closed-loop control, the controller minimized the difference between measured and desired effect. Small adjustments in the infusion rate occur while the patient state remains near the set point. Larger changes in patient state (*e.g*. acute drug tolerance or arousal caused by perceived stimulation) are modeled by the controller as changes in the patient's dose-effect characteristics. As a remedy, "Hill curve" calculated during induction is adjusted to reflect the change in patient dynamics. The approach taken here is to shift the induction "Hill curve" [154]; figure 2A shows this curve calculated during induction. The specific chosen target BIS value is shown as E_I with the corresponding effect-site concentration, C_1. With small changes in effect-site concentration, corresponding changes in BIS can be noticed, moving along the operating curve in figure 2A. However, if, while operating at C_I (corresponding to the target BIS) a perceived stimulation would elevate BIS to E_s, this results in a mismatch between the current effect-site concentration and the measured effect according to the curve. The mismatch is resolved by sliding the pharmacodynamic relation to the right until the curve aligns with the measured effect, E_s, as shown in figure 2B. The new, increased target effect-site concentration is derived from the translated curve as the concentration corresponding to the target

* ANESTHESIOLOGY website available at : http://www.anesthesiology.org

effect, $E_{I,}$ *i.e.*, the desired effect can be reached by increasing the effect-site concentration by the same value as would be necessary to go from the measured effect to the desired effect during induction.

$$Ceffect_{T1} = Ceffect_{T0} + H^{-1}(\text{Desired effect}) - H^{-1}(\text{Measured effect}_{T0}) \qquad \textbf{Equation 1}$$

where H^{-1} stands for the inverse "Hill-curve" relation. Mathematically, the surgical manipulations are regarded as pushing the induction Hill curve to the right such that the current effect-site concentration equals the one for the measured effect during induction. Figure 3 shows the complete closed-loop feedback controller mechanism during maintenance.

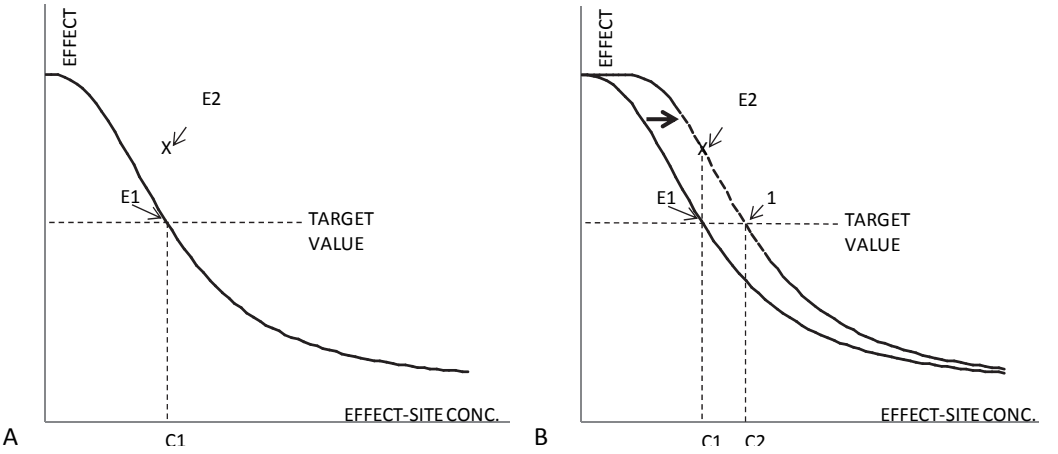

Fig.2. *(A) Theoretical example of a pharmacodynamic curve (effect vs. effect-site concentration) calculated during induction. A target value for the controlled variable is shown as the desired set point. E_1 indicates the crossing point between the original curve and the target at a specific time. C_1 is the effect-site concentration actually required to equal the effect and the target value without stimulus. If, because of surgical stimulus, the measured effect increases (i.e. , E_s), there will be a mismatch between the measured effect and the target effect value. (B) The originals curve (straight line) is moved horizontally to cross the newly measured effect E_s. The projection of the crossing point (1) of the new curve (dotted line) and the target value onto the x-axis gives the new desired effect-site concentration (C_2) to theoretically reach again the target value.*

A disadvantage of this approach is that the controller works independently from the increasing or decreasing trend in the controlled variable, as well as independent from the rate of change of the trend. This may produce overshoot in the correction of the effect-site concentration, causing oscillations and instability during anesthesia. These effects were observed using mathematical simulations of the controller[♦].

Therefore, an extra control action is implemented, using the difference between two consecutive measured BIS values multiplied by a differential factor

$$(BIS_{T1} - BIS_{T0})_{X} \text{ differential factor} \qquad \textbf{Equation 2}$$

A differential factor of 0.05 was applied based on the results of our simulations[†♦].

The Control of the Standard Practice Group:

In the standard practice group, propofol was titrated using standard practice guidelines, as described below. The criteria for inadequate anesthesia, described by Ausems *et. al*. [155] were used: (1) increase in SYS to more than 15 mmHg above the baseline for that patient (measured the evening before surgery); (2) tachycardia higher than 90 beats/min in the absence of hypovolemia; (3) other autonomic signs such as sweating or flushing; (4) and somatic responses such as movement or swallowing. Signs of an excessive level of anesthesia were defined as: (1) a decrease in SYS to more than 15 mmHg below the baseline for that patient (measured the evening before surgery); and (2) bradycardia lower than 40 beats/min.

♦ Tom De Smet, "Design of a computer-controlled closed-loop anesthesia system", Thesis to obtain the degree of Civil Engineer : University of Ghent, Faculty of applied sciences, department of Electronics and information systems, 1995.

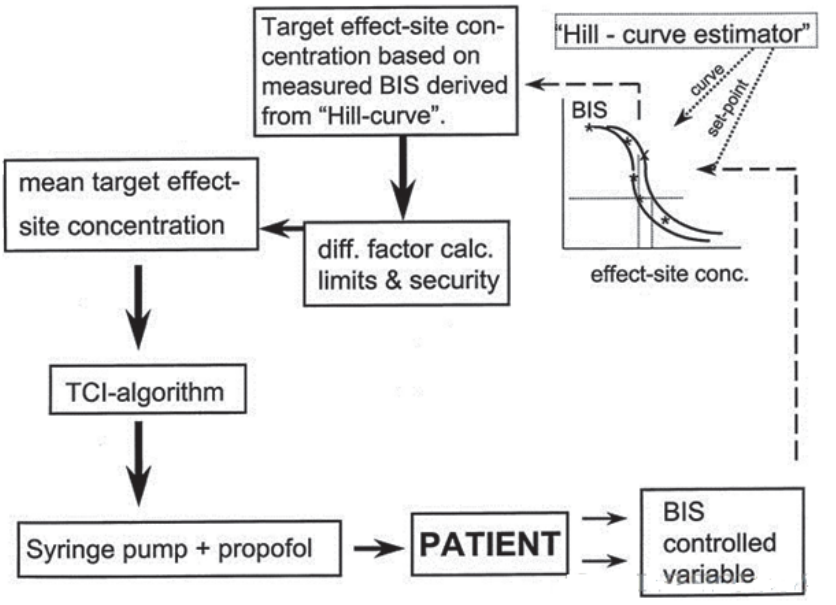

Fig. 3. *Flow chart of the controller during maintenance. At each time the required effect-site concentration is calculated by the controller. This value is sent to an additional algorithm taking the differential factor and the safety limits into account. The result of these calculations is the required effect-site concentration sent to the RUGLOOP TCI algorithm.*

The actuator

The actuator in a closed-loop system for the administration of intravenous drugs is a syringe pump. The Fresenius Modular DPS Infusion Pump connected to a Fresenius Base A (Fresenius Vial Infusion Systems, Brézins, France) was selected because of its high accuracy in both infused volume and infusion rate. A computer can monitor and drive the pump at infusion rates between 0 and 1,200 ml/hr *via* an RS-232 interface.

Clinical study

After obtaining approval from the Institutional Ethics Committee of the Ghent University Hospital (Gent, Belgium), informed consent was obtained from 20 female patients, American Society of Anesthesiologists physical status I and II, aged 18-60 years, who were scheduled for gynecologic laparotomy. Exclusion criteria included weight less than 70% or more than 130% of ideal body weight, neurologic disorder, and use of psychoactive medication including alcohol. Patients were randomly

allocated to one of the two groups. All patients received diazepam 10 mg orally 1 h before surgery as premedication. Two minutes before induction, a continuous infusion of remifentanil (0.50μg/kg/min before intubation, 0.25 μg/kg/min thereafter) was started in all patients. In the closed-loop controlled group (group I), propofol was administered using the previously described closed-loop system. Initial target concentration of propofol was set to a plasma concentration of 3 μg/ml. This target was automatically increased in a stepwise manner by 0.5-μg/ml increment concentration, every 50 s until the target BIS was reached. Thereafter, the loop was closed automatically, and the target-controlled infusion system reverted to delivering to a target effect-site concentration as dedicated by the targeted effect (BIS) value. The target BIS was fixed at 50. In the standard practice group (group II), manually controlled administration of propofol was used. Propofol was administered at 300 ml/h [156] until loss of consciousness, defined as failure to respond to verbal command, and was evaluated every 5 s. Thereafter, a continuous infusion of propofol was started at an initial rate of 10 mg/kg/h. Propofol administration was increased or decreased by 2 mg/kg/h after one of the signs of inadequate anesthetic depth, as previously described. After loss of consciousness, all patients received a bolus dose of rocuronium (0.5 mg/kg) to facilitate intubation.

The time and BIS were recorded at the moment of loss of consciousness. We also calculated the propofol induction dose as the amount of propofol delivered to the patients up to the time of loss of consciousness and the total dose used for the entire procedure.

Heart rate, end tidal carbon dioxide, oxygen saturation, and BIS were acquired every 10 s. Artifacts in the BIS caused by poor signal quality were automatically detected and excluded from further analysis. Blood pressure was acquired every 1 min.

At the end of surgery (*i.e.*, end of skin closure), all infusions were stopped and recovery parameters (time until spontaneous respiration, opening eyes, extubation and saying name and date of birth) were recorded.

Evaluation of the controller performance

Controller performance metrics are usually calculated on the measured values of the controlled variable *versus* its target value and compared with control performance data in a reference group. Because the controlled variable was different between groups, we decided to use the controlled variable of each group as a reference variable for the other group. BIS was defined as the controlled

variable in group I and as a reference variable in group II, using 50 as the target value in both groups. SYS was considered as the main controlled variable in group II and as a reference variable in group I, using the baseline pressure as the target value in both groups.

The performance of the controllers was evaluated during three periods: induction, the period surrounding initial skin incision, and during recovery. The initial performance for BIS at induction was studied by using the following parameters: (1) BIS_{LOC} = BIS at the moment of loss of consciousness; (2) $T_{BIS\ TARGET}$ = observed time required for reaching the target BIS value;

(3) $t_{PEAK,\ BIS}$ = observed time required for reaching maximal drug effect (lowest BIS value);

(4) BIS_{PEAK} = observed BIS value at $t_{PEAK,\ BIS}$; and (5) t_{EQ} = observed time required for reaching the target value after the initial overshoot, also called time to steady-state.

For SYS, three initial performance parameters were calculated, taken within the first 10 min of the anesthesia: (1) SYS_{LOC} = SYS at the moment of loss of consciousness; (2) $t_{PEAK,\ SYS}$ = observed time required for reaching maximal drug effect (lowest SYS value); and (3) SYS_{PEAK} = observed SYS value at $t_{PEAK,\ SYS}$.

The ability of the controllers to react to a perturbation after achieving the target level was evaluated using the period surrounding skin incision. The average BIS and SYS over the minute preceding incision was defined as the baseline values. The maximum and minimum BIS and SYS values measured until 5 min after skin incision were considered to be the extreme responses to this noxious stimulus. Acceptable control of BIS was defined as maintaining BIS between 40 and 60. Acceptable control of SYS was defined as maintaining SYS within15 mmHg of baseline. The percent of time of acceptable BIS control and acceptable SYS control was calculated for each patient. Based on the method of Varvel, *et al*. [29], the overall performance of both control and reference variables was characterized on the basis of following parameters for the period when the variable was being controlled (*i.e.*, after BIS reached 50 in group I [or after the patient lost consciousness in group II] until drug administration was stopped).

First, using all observations within the period, the performance error (PE) was calculated according to the following formula

$$PE = \frac{(measuredvalue - target value)}{target value} * 100$$ Equation 3

Subsequently, bias (median performance error [MDPE]), inaccuracy (median absolute PE [MDAPE]), divergence and wobble were calculated. MDPE is a measure of bias and describes whether the measured values are systematically either above or below the target value. MDPE was calculated from the following equation:

$$MDPE_i = median\{PE_{ij}, j-1,...,N_i\}$$ Equation 4

where N_i is the number of values PE obtained for the i^{th} subject.

Median absolute PE reflects the inaccuracy of the control method in the i^{th} subject:

$$MDAPE_i = median\{|PE|_{ij}, j-1,...,N_i\}$$ **Equation 5**

where N_i is the number of values | PE | obtained for the i^{th} subject.

Divergence describes the possible time-related trend of the measured effects in relation to the targeted values. It is defined as the slope of the linear regression equation of | PE | against time and is expressed in units of percentage divergence per minute. A positive value indicates progressive widening of the gap between targeted and measured values, whereas a negative value reveals that the measured values converge on the predicted values.

Wobble is another index of the time-related changes in performance and measures the intrasubject variability in PEs. In the i^{th} subject, the percentage of wobble is calculated as follows:

$$wobble_i = median\ \{|PE_{ij} - MDPE_i|, j = 1,..., N_i\}$$ **Equation 6**

Table 1. Demographic data, mean ± SD

	Group I (*n* = 10)	Group II (*n* = 10)
Age (years)	42 ± 8	46 ± 4
Weight (kg)	67 ± 10	59 ± 9
Height (cm)	166 ± 6	163 ± 5

Data are shown as mean ±SD.

Statistical analysis

Data were presented as mean ± SD, or as median (range). Differences between the groups were determined using a Mann-Whitney U test. Continuous data were analyzed using analyses of variance for repeated measures. If significant, a *post hoc* test (Tukey) was applied for paired data. Kaplan-Meier survival analysis was applied to compare recovery parameters (time until spontaneous breathing, time until opening eyes, time until extubation and time until orientation) between groups. Significance level was set at 5%.

RESULTS

Population demographics for both groups are shown in table 1. There were no significant differences between both groups. No patients were excluded from the analysis. All data captured by the recording system were included in the analysis.

Table 2. Clinical data

	Group I (n = 10)	Group II (n = 10)
Induction time (s)	120 ± 55	128 ± 44
Propofol induction dose (mg)	87 ± 16	79 ± 18
BIS at LOC	81 ± 8	82 ± 8
Intubation time (s)	285 ± 84	297 ± 77
Incision time (s)	1497 ± 315	1232 ± 293
Duration of Anesthesia (s)	6798 ± 2085	6896 ± 2018
Recovery time until spontaneous respiration (s)	281 (257)	547 (2285)
Recovery time until opening of the eyes (s)	336 (250) *	567 (2285) *
Recovery time until extubation (s)	415 (240) *	580 (2296) *
Recovery time until orientation (s)	461 (372)	592 (2291)

** = P < 0.05 between groups*

BIS = Bispectral Index; LOC = loss of consciousness

The observations made at the time of loss of consciousness are shown in table 2. Induction times, BIS values at loss of consciousness and induction doses of propofol were similar in both groups. Other clinical parameters during the maintenance of anesthesia, such as time to intubation and incision were not significantly different in both groups. In addition, the duration of anesthesia did not differ statistically between groups. The performance during the induction phase is shown in table 3. Manually controlled induction in group II reached the target level of BIS (50) faster than open-loop computer-controlled induction in group I. However, the duration and magnitude of the initial overshoot in BIS was more pronounced in the standard practice than in the closed-loop group. For

SYS, the baseline values were 122 ± 15 mmHg in group I versus 121 ± 14 mmHg in group II. A more pronounced decrease in blood pressure was observed in group II (table 3).

Table 3. Control quality during induction

	Group I (n = 10)	Group II (n = 10)
$T_{BIS\ TARGET}$ (s)	241 ± 94 *	176 ± 36 *
BIS_{PEAK}	42 ± 4 *	36 ± 4 *
$T_{PEAK,\ BIS}$ (s)	290 ± 96 *	516 ± 271 *
T_{EQ}	336 ± 114 *	1410 ± 1050 *
SYS_{LOC} (mmHg)	122 ± 17	115 ± 26
SYS_{PEAK} (mmHg)	93 ± 8 *	81 ± 8 *
$T_{PEAK,\ SYS}$ (s)	402 ± 69 *	672 ± 260 *

** = p < 0.05 between groups*

$T_{BIS\ TARGET}$ = observed time required for reaching the target BIS (Bispectral Index) value; BIS_{PEAK} = observed BIS value at $T_{PEAK,\ BIS}$; $T_{PEAK,\ BIS}$ = observed time required for reaching maximal drug effect (lowest BIS value); T_{EQ} = observed time required for reaching the target value after the initial overshoot; SYS_{LOC} = systolic blood pressure (SYS) at the moment of loss of consciousness; SYS_{PEAK} = observed SYS value at $T_{PEAK,\ SYS}$; $T_{PEAK\ ,\ SYS}$ = observed time required for reaching maximal drug effect (lowest SYS value)

The relative behavior of the controlled variables at incision, BIS in group I and SYS in group II, in relation to their target value are shown in figures 4A and 4B respectively. In group I, a significant initial increase in BIS is observed after incision, followed by a significant decrease in BIS values. In group II, only a significant increase after incision was observed, however with a large variability in results.

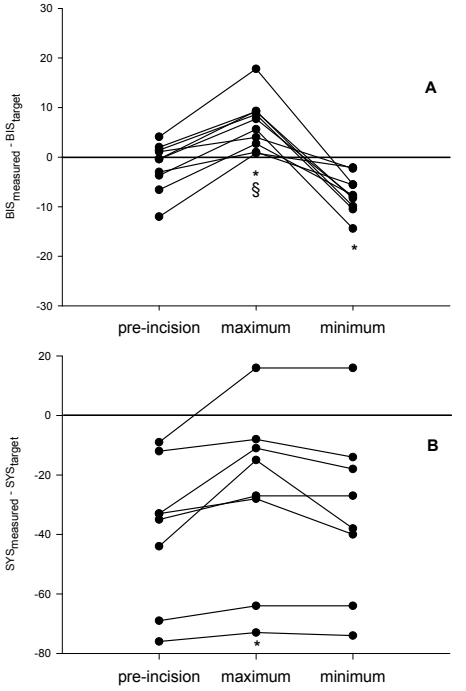

Fig. 4. *Individual behavior of the controlled variable for each patient ((A) Bispectral Index [BIS] in group I and (B) systolic blood pressure [SYS] in group II) in relation to their target value. * = P < 0.05 compared to pre-incision baseline; §= P < 0.05 between maximum and minimum post-incision values.*

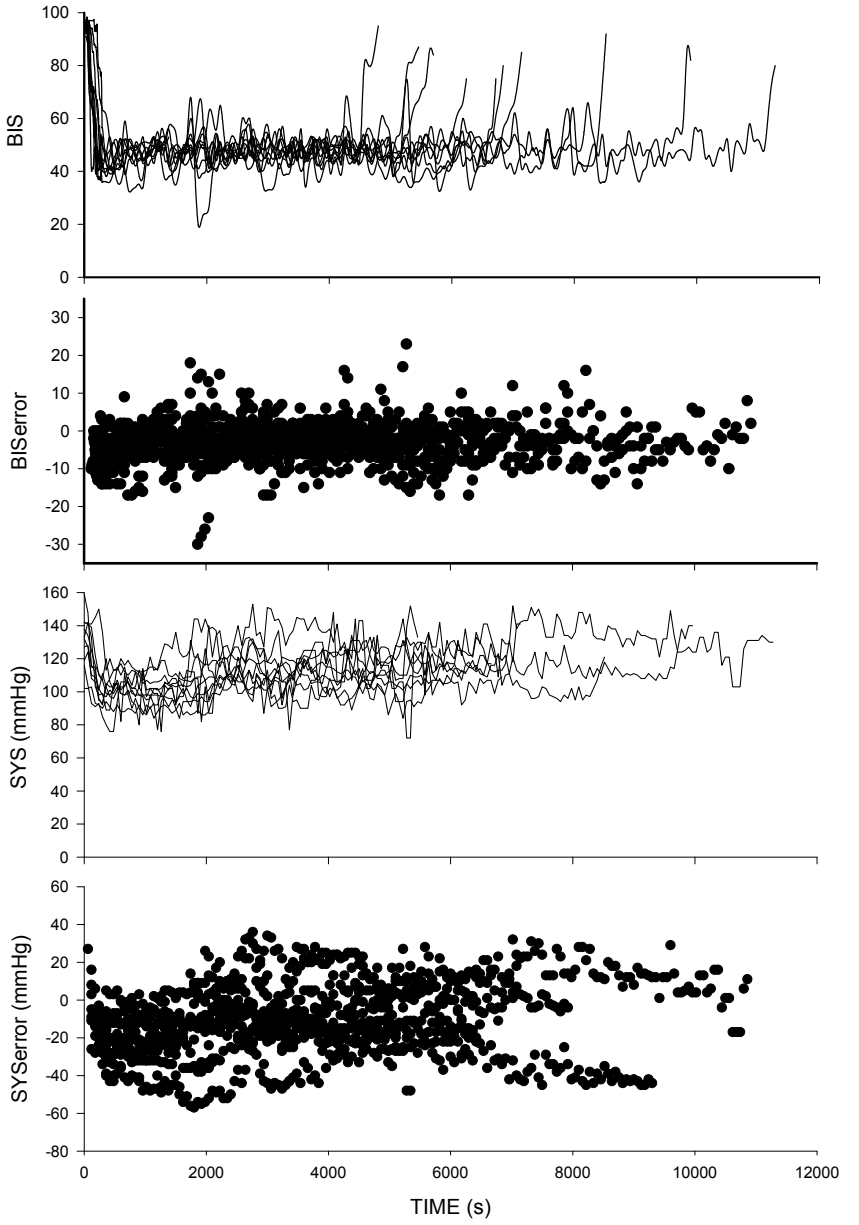

Fig. 5. *Individual data from the closed-loop controlled group (group I) during anesthesia. (A) Individual BIS (Bispectral Index) data; (B) individual BIS error calculated as the difference between BIS targeted and BIS measured (averaged every minute for the figure); (C) Individual systolic blood pressure (SYS; acquired every minute); (D) individual SYS error calculated as the difference between SYS baseline and SYS measured (averaged every minute for the figure).*

The trends of BIS, BIS error, SYS and SYS error are shown in figures 5 and 6 for groups I and II, respectively. Individual BIS data during induction, maintenance and recovery are shown in figures 5A and 6A for all patients from groups I and II, respectively. For group I, the individual errors between target and measured BIS during the period of control are plotted in figure 5B. For group II, the individual errors between the reference BIS of 50 and the measured BIS are plotted in figure 5B. When defining an adequate level of anesthesia as having a BIS between 40 and 60 [157], the incidence of accurate BIS level was significantly higher when BIS was used as controlled variable in group I (89 ± 10%) compared with the reference BIS levels in group II (49 ± 29%). Significantly higher incidences of too low BIS levels (BIS < 40) were recorded in group II (44 ± 31%) than in group I (9 ± 10%). BIS levels higher than 60 were less frequent in group I (2 ± 2%) than in group II (7 ± 16%).

Trends of SYS during induction, maintenance and recovery are shown in figures 5C and 6C for groups I and II, respectively. Likewise, errors between measured and target SYS during the period of control are plotted in figures 5D and 6D for groups I and II, respectively. Although SYS was the controlled variable in group II, adequate hemodynamic stability (within the 15-mmHg range around baseline) occurred more frequently in group I (51 ± 27%) compared with group II (34 ± 31%; $P<0.05$). The incidence of too low SYS (group I: 41 ± 33%; group II: 64 ± 31%) and the incidence of too high SYS (group I: 7 ± 11%; group II: 1 ± 2%) were both significantly different between groups ($P<0.05$).
Individual patient trends of propofol effect-site concentrations are shown in figures 7A and 7B for groups I and II, respectively. The total amount of propofol used in both groups was 6.39 ± 1.13 mg/kg/h for group I and 6.48 ± 1.59 mg/kg/h for group II, without statistical difference between groups.

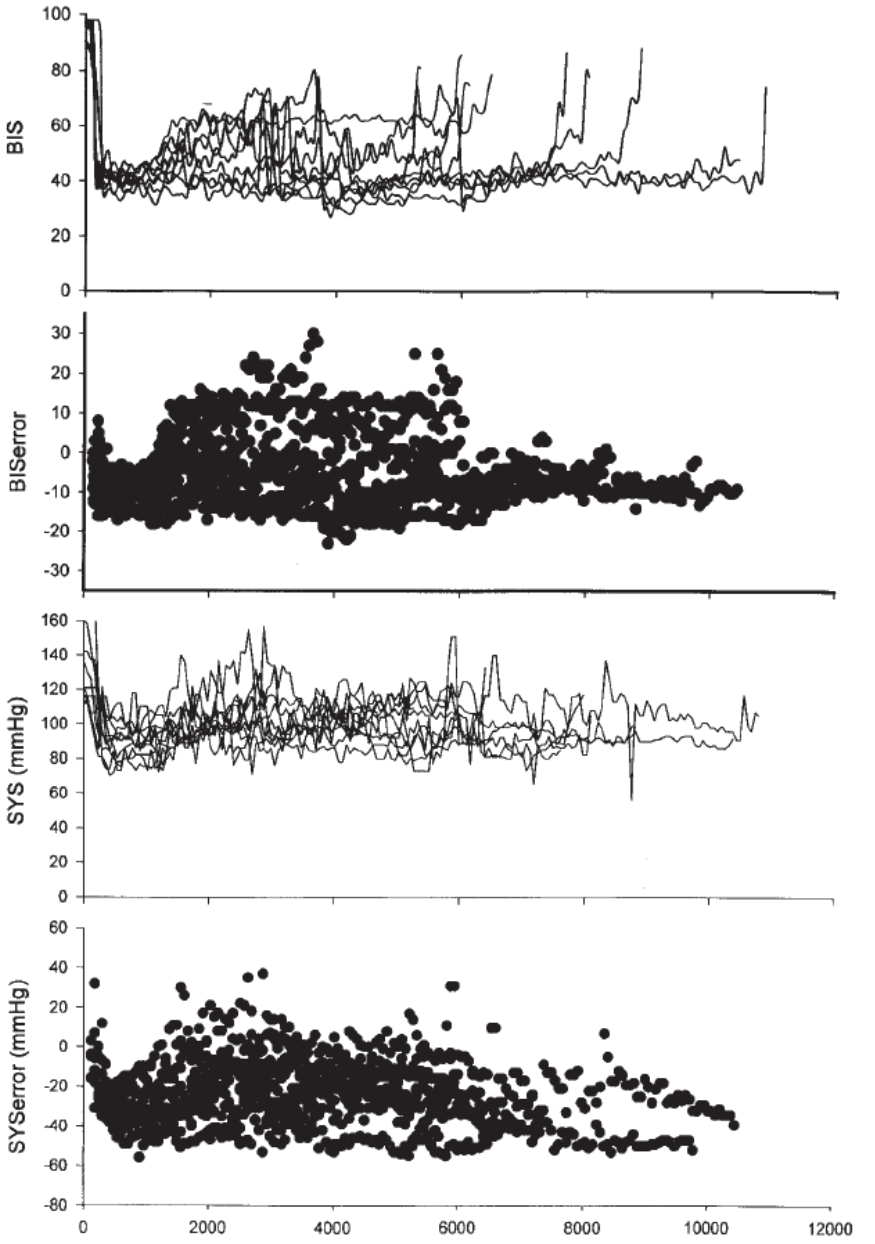

Fig. 6. *Individual data from the manual control group (group II) during anesthesia. (A) Individual Bispectral Index (BIS) data; (B) individual BIS error calculated as the difference between BIS targeted and BIS measured (averaged every minute); (C) individual systolic blood pressure (SYS; acquired every minute); (D) individual SYS error calculated as the difference between SYS baseline and SYS measured (averaged every minute for the figure).*

At the end of surgery, all infusions were stopped and recovery parameters were recorded. As shown in table 2, significantly faster median recovery times were observed for time until opening of the eyes and extubation in the closed-loop group I than in the standard-practice group II. In addition, the variability (range) for all recovery parameters in group II was much higher than in group I. Figures 8A-D show the percent of subjects within a group that had not yet met the endpoint at a certain time point for the four endpoints of recovery, return of spontaneous respiration, opening eyes, extubation and recovery, respectively. The data show that, with the exception of one fast responder in group II, subjects in the standard-practice group (group II) take longer to respond than the subjects in the closed-loop group (group I).

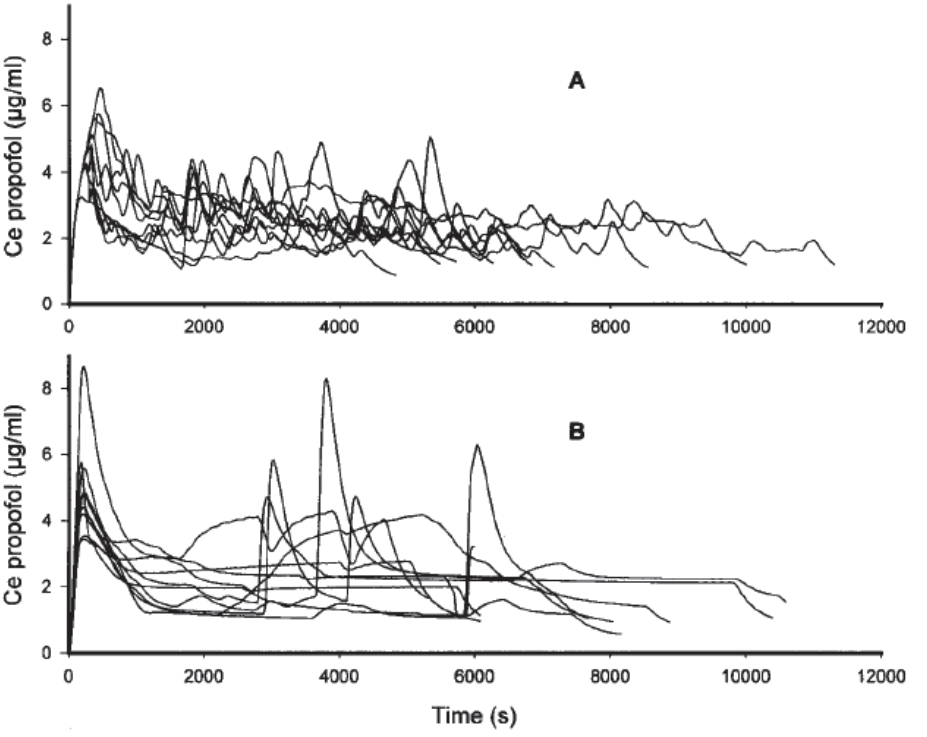

Fig. 7. *Individual propofol effect-site concentrations during induction, maintenance, and recovery in group I (A) and group II (B).*

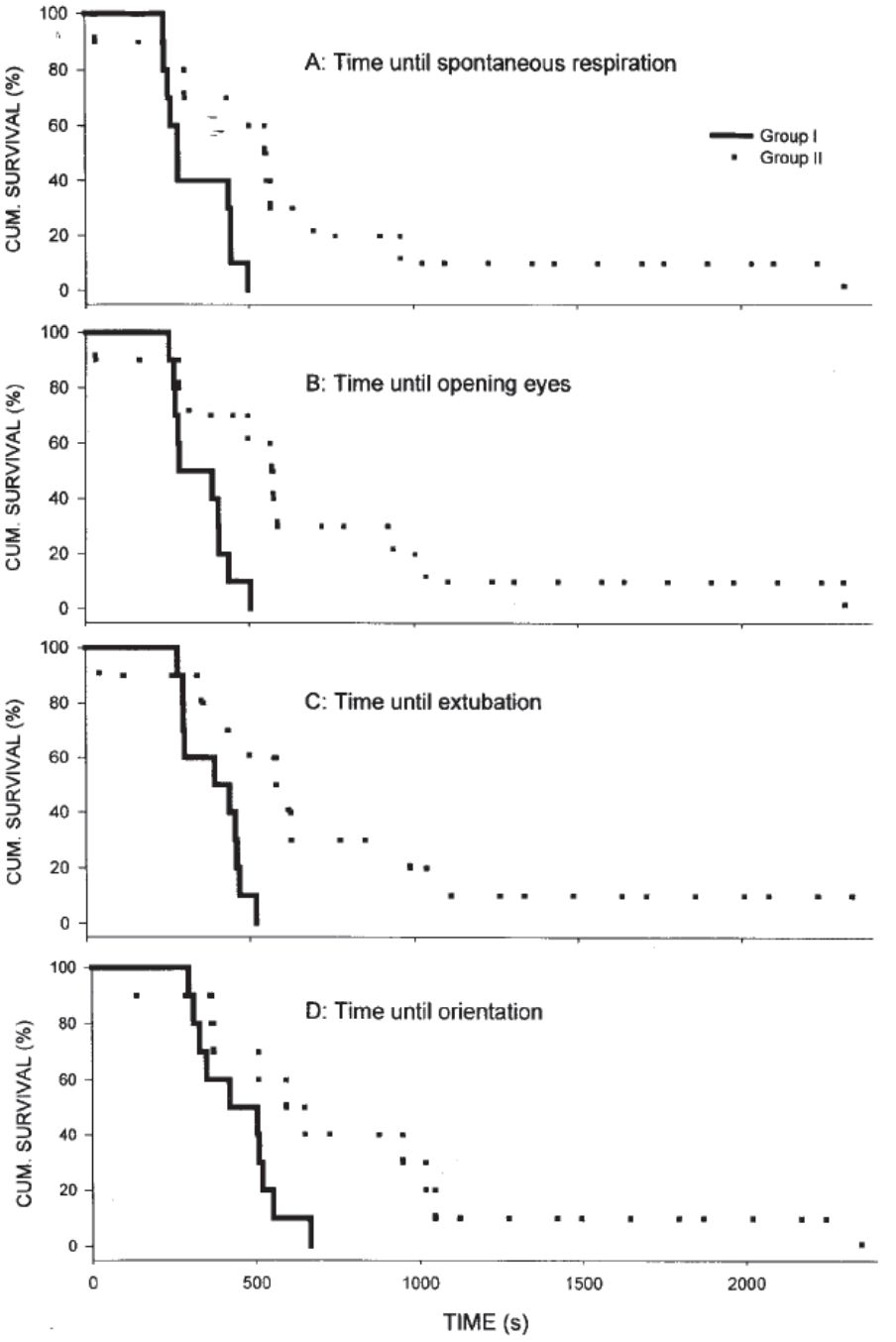

Fig. 8. *(A–D) The percent of subjects within a group that have not yet met the end point at a certain time point (in seconds) for the four end points of recovery: return of spontaneous respiration, opening eyes, extubation, and recovery, respectively.*

DISCUSSION

The purpose of the current study was to describe a new closed-loop feedback control system for propofol administration using the BIS as the controlled variable together with a patient-individualized, adaptive, model-based controller and to compare this closed-loop system with a manually controlled administration of propofol using standard practice guidelines.

One can argue about the methodology for our standard practice group. Given the nature of the procedures in the anesthetics, one could probably design a comparison group to show almost anything wanted. When designing an "effect-control" versus an "effect-site-control" study, one might choose an effect compartment target controlled versus closed-loop controlled infusion study, as this compares the ability of the clinician to titrate to a predicted effect, versus the best available measured effect. If one desired to see whether the automated system is better than the trained, vigilant human, then it would have been better to allow the standard-practice group to attempt to control the BIS. However, our aim was to compare effect-guided closed-loop control, as a unitary new method for drug administration with present-day practice and, therefore, propofol administration in the standard-practice group was titrated as previously described.

Closed-loop systems are aimed at reaching and maintaining the desired drug effect. Therefore, the drug effect should be measured adequately. Many different quantitative electroencephalographic measures have been developed to estimate the drug effect of propofol. Billard, *et al*. [139] studied the performance of delta power, spectral edge 95%, and BIS (version 1.1) and found a good performance of the BIS in modeling propofol drug effect. More recently, Leslie, *et al.*[158] found a good correlation between BIS (version 3.0) and the hypnotic effect of propofol. Other investigators have confirmed these findings [159-161]. Unfortunately, the BIS is calculated using a 30-s rolling window and thus lags behind the current status of the patient by approximately 15 s. This delay in BIS is one of the elements, among others, that contribute to global controller instability. The additional control algorithm, described in equation 2, was implemented to improve the controller stability.

In our study, a model-based adaptive controller was used. There are many examples of automatically controlled drug administration, based on different levels of control and different control methods [5]. A general PID controller is sometimes proposed. This control method calculates the infusion rate by a

straightforward mathematical formula based on the difference between the measured effect value and the chosen target effect value set by the user. PID controllers are essentially "ignorant" in that they lack knowledge of the complicated drug metabolism and the resulting time course between dosing and effect. In addition, tuning the values for the three terms (P, I and D) when the physiologic response of the subject is unknown, is very difficult[152]. Model-based adaptive control may help to refine the administration of intravenous hypnotics, as proposed by Schwilden *et al.*[125, 162]. Model-based control of drugs in response to a clinical effect (*i.e.*, surgical manipulations) is based on knowledge of the fate of the drug and its effect in the human body. Due to the large interindividual pharmacological variability, it is better to have an adaptive controller to adapt the controller towards the individual patient. A model-based, adaptive controller compares the predicted values of the control signal (*e.g.*, BIS) against the actual values of the control signal, and modifies the model parameters accordingly.

In the current study, a model-based adaptive control system integrating a previously published method for effect-compartment-controlled target controlled infusion was used to model the pharmacokinetic-pharmacodynamic relation[25]. Effect-compartment modeling is motivated by the observed hysteresis between measured blood drug concentrations and any currently measured index of drug effect. The hysteresis between pharmacokinetics and pharmacodynamics can be quantified by a rate constant, k_{e0}. The time course of drug effect parallels the time course of the effect-site concentration. Therefore, it becomes appealing to be able to quantitatively control the drug concentration in the effect compartment rather than the central compartment [163, 164] .

For correlating the effect-site concentration with the clinical effect (BIS), a patient individualized curve was defined during the initial phase. This was also done to minimize the problem of the large pharmacodynamic variability among patients. This variability might cause a problem when these combined pharmacokinetic-pharmacodynamic models, using mean population pharmacokinetic as well as mean population pharmacodynamic values, are applied for a particular dosage regimen in an individual patient [165]. Few data are found in the literature [166] concerning the use of patient-individualized pharmacodynamics in control strategies, and we therefore proposed a specific control method in this study. Previously, Schwilden *et al.* described a closed-loop feedback control system for methohexital [96] and propofol [125] anesthesia applying an online change in pharmacokinetic parameters. The difference with our controller is that we initially attempt to adapt all pharmacodynamic parameters to our patient. During the case, we shift the pharmacodynamic curve

horizontally, which is a different way of calculating the new model parameters compared with the methodology used by Schwilden *et al.* , who tried to fit the current effect on the curve by modifying the pharmacokinetic parameters. Our controller maintains the original pharmacokinetic model of drug but imposes a new target concentration. The difference in the adaptive methods is that, during the absence of variable values because of poor signal quality, we are still using the original pharmacokinetic model, whereas Schwilden *et al.* used a modified model at that time.

Differences in performance of this closed-loop system were found compared with the manually controlled administration. When comparing BIS or SYS as a control variable in one group relative to itself as a reference variable in the other group, more accurate control time was found in the closed-loop group for both variables. When comparing BIS with SYS as a controlled variable, clearly better performance time was found for BIS (figures 5 and 6). Various reports are found in the literature supporting the concept that hemodynamic parameters are poor measures of anesthetic [167].

The onset of clinical effect as measured by BIS was similar in both groups. Both groups lost consciousness at a similar time and BIS value using similar doses of propofol. However, the initial overshoot (BIS_{PEAK}) and time to steady-state (t_{EQ}) were clearly more pronounced in the manually controlled group than in the closed-loop controlled group. During the first 10 min of anesthesia, a more pronounced decrease in blood pressure was observed in group II. One can argue that these differences may not be a result of any issue of control, but rather dictated by the rate of drug administration. However, Kazama *et al.* [168] recently concluded that an infusion rate of less than 80 mg/kg/h did not reveal significant blood pressure changes during induction. In our study, the selected infusion rate of 300 ml/h in group II, as recently stated by Ludbrook *et al* [156] to be hemodynamically stable, resulted for all patients in an induction rate of less than 80 mg/kg/h.

As shown in figure 4A, surgical incision caused an initial increase in BIS level in all group I patients slightly above the target BIS. This increase was corrected by the closed-loop controller without a large overshoot. In group II, a large variability in results at incision was observed (figure 4B). The behavior of control in both groups can be illustrated by depicting the time course of propofol effect-site concentration, as plotted in figures 7A and 7B for groups I and II, respectively. In group I, the continuous adaptation of the effect-site concentration reveals that closed-loop controller provided

continuous control action. It can be observed in figure 7B that fewer control actions were seen in group II patients. Of course, it must be stated that the control behavior has to be correlated to the clinical setting like the applied remifentanil concentration and the selected targets of the respective control variables. Because this is the first study comparing closed-loop with manual control for hypnotics, it was impossible to solve all issues in a single study. Therefore, the closed–loop controller was always targeted to the same BIS level and no stress-tests were performed on the controller to evaluate, for example, changes in the performance of the controller with changes in target BIS level. More research is required to study the behavior of this closed-loop algorithm during "extreme" conditions.

Table 4. Performance of Control

	Performance of BIS		Performance of SYS	
	as Controlled Variable Group I (n = 10)	as Reference Variable Group II (n = 10)	as Reference Variable Group I (n = 10)	as Controlled Variable Group II (n = 10)
PE (%)	-6.23 ± 10.44*†	-13.49 ± 21.74*	-7.40 ± 14.5*	-18.9 ± 13.06*†
MDPE (%)	-6.6 ± 2.63†	-6.1 ± 17	-7.36 ± 3.28*	-18.93 ± 2.92*†
MDAPE (%)	7.7 ± 2.49*†	18 ± 4.5*	10.49 ± 2.14*	18.93 ± 2.92*†
Divergence (%/min)	0.024 ± 0.029*†	-0.129 ± 0.177*	0.0007 ± 0.0009*	0.00001 ± 0.001*†
Wobble (%)	5.90 ± 2.33†	7.10 ± 5.74	6.51 ± 2.97	5.12 ± 1.38†

** P < 0.05 between groups for BIS (Bispectral Index) and for systolic blood pressure (SYS). † P < 0.05 between controlled parameters (i.e., BIS in group I versus SYS in group II).*

PE = prediction error; MDPE = median prediction error; MDAPE = median absolute performance error.

The characteristics of the closed-loop controller were compared with the manual control techniques by using the performance parameters proposed by Varvel *et al.* [29]. These parameters were originally developed for describing the performance of target controlled infusion systems but are readily applied for studying the performance of a closed-loop system. As shown in table 4, the performance error (PE) was calculated for each BIS and SYS measurement. First, both controlled variables (BIS and SYS) were compared with their own reference. For BIS, an overall smaller PE was found during closed-loop control. Subsequently, the values of PE were used for intersubject data analysis. The $MDPE_i$ was similar in both groups; however, the $MDAPE_i$ was clearly larger in the standard practice group (group II). Note that $MDPE_i$ is a signed value and thus represents the direction (overprediction or underprediction) of the PE rather than the size of the errors, which is represented by $MDAPE_i$ [29]. Finally, performance characteristics were also described by $divergence_i$ and $wobble_i$. $Divergence_i$ reflects the gradual worsening of performance of control over time. $Wobble_i$ represents the variability of the PE in a specific individual. It should be clear that the definitions of $wobble_i$ and $divergence_i$ overlap somewhat. Some of the variability in PEs measured by $wobble_i$ is caused by time-related trends in those errors, which is measured by $divergence_i$. $Wobble_i$ measures the total intraindividual variability in PEs, which is directly related to the ability to achieve a stable controlled variable value during control, while $divergence_i$ measures the expected systematic time-related changes in performance [29]. However statistical differences were found between groups and between variables (table 4), we believe that the similarities between the two groups in terms of $wobble_i$ and $divergence_i$ are far more interesting than the very small and subtle differences.

A potential advantage of this model-based controller compared with PID controllers is its stability with respect to artifacts. In case of sensor failure, PID or “on-off” controllers cannot predict the future dose requirements. Our model-based controller can, however, open the loop when the input signal is biased and steer on effect compartment controlled infusion until the artifact is solved. Therefore, no instability was observed in the BIS when long, sustained periods of electrosurgery eliminated the controlled variable.

Significantly better recovery profiles were observed in the closed-loop controlled group for time until opening of the eyes and extubation. In addition, a large variability (range) in recovery times was observed in the standard-practice group. When looking to the survival curves plotted in figure 8, we observed that, with the exception of the fast responder in the control group, subjects in the control group take longer to respond. This is powerful when concerned about quick and predictable operating room scheduling. For example, using the time-until-orientation curve, we see that at 10 min, 90% of the patients in the closed-loop group are oriented, whereas only 50% are oriented in the standard-practice group.

In conclusion, we have demonstrated that the proposed closed-loop system for propofol administration using the BIS as the controlled variable together with a model-based controller is clinically acceptable during general anesthesia when compared to classical manually controlled titration of propofol using standard practice guidelines. More research is required to observe the behavior of the controller during various clinical situations.

Chapter 5

Performance evaluation of two published closed-loop control systems using Bispectral Index monitoring

A simulation study

Modified from:

M.M.R.F. Struys, T. De Smet, S. Greenwald, A.R. Absalom, S. Bingé, E.P. Mortier

Performance evaluation of two published closed-loop control systems using Bispectral Index monitoring

A simulation study

Anesthesiology *2004*; **100**: 640-7

Dr. Struys and ir. De Smet are patent holders of the model-based closed-loop system (US Patents 6,599,281 and 6,605,072). Dr. Greenwald is an employee of Aspect Medical Systems, Inc., Newton, Massachusetts, developers of the BIS® monitor.

Background: Although automated closed-loop control systems may improve quality of care, their safety must be proved under extreme control conditions. This study describes a simulation methodology to test automated controllers, and its application in a comparison of two published controllers for BIS guided propofol administration.

Methods: A patient simulator was developed to compare controllers. Using input scripts to dictate patient characteristics, target BIS values, and the time course of surgical events, the simulator continuously monitors the infusion pump under control and generates BIS values as a composite of modeled response to drug, perceived stimulation, and random noise. The simulator formats the output stream of BIS data as input to the controller under test to emulate the serial output of the actual BIS monitor. A published model-based controller and a classical proportional integral derivative controller were compared when using BIS as controlled variable. Each controller was tested using a set of 10 virtual patients undergoing a fixed surgical profile that was repeated with BIS targets set at 30, 50 and 70. Controller performance was assessed using median (absolute) prediction error, divergence, wobble, and percentage time within BIS target range metrics.

Results: Median prediction error was significantly smaller for the proportional integral derivative controller than for the model-based controller. The median absolute prediction error was smaller for the model-based controller than for the proportional integral derivative controller for each BIS target, reaching statistical significance for targets 30 and 50.

Conclusions: When simulating closed-loop control of BIS using propofol, the use of a patient-individualized, model-based adaptive closed-loop system with effect-site control resulted in better control of BIS compared to a standard proportional integral derivative controller with plasma site control. Even under extreme conditions, the modeled-based controller exhibited no behavioral problems.

One proposed benefit of automated, closed-loop anesthesia delivery systems is that continuous, responsive control of anesthesia may improve quality of care compared to intermittent control (*i.e.*, standard practice)[147]. However, one concern is that unsupervised, automated controllers may be unsafe. This article describes a simulation methodology to test automated controllers and presents the results of applying this methodology in a comparison of two published controllers.

Two different closed-loop algorithms using the BIS value as the controlled variable to steer propofol administration have been published recently. Absalom *et al*. [7] developed a closed-loop system using a PID controller and tested it during orthopedic surgery. Struys *et al*. developed a patient-individualized, model-based controller and tested it during sedation [102] and during major surgery (laparotomy) [54] .Anesthesia was administered in three phases during clinical trials of both systems. First, propofol was administered in open-loop mode during induction (*i.e.*, the initial set point was a target concentration rather than a target effect). Second, the loop was closed for the surgical phase once BIS reached its set point. Finally, the automated controller was interrupted when surgery was completed, and the anesthesiologist guided the recovery phase using standard practice. In the model-based approach, the relation between predicted propofol effect site concentration and BIS value was determined during the induction phase and was used to construct a patient-specific pharmacodynamic Emax model (or Hill-curve) as a component of the controller during the surgical phase.

In an editorial that accompanied the clinical results of the model-based controller, Glass *et al* [107] questioned whether the controller was safe for a broader range of surgery or clinical interventions because all subsequent adjustments in drug administration were based upon a static Hill curve derived during induction, and only a single target BIS value of 50 during adequate analgesia (*i.e.*, spinal blockade [102] or a continuous infusion of remifentanil) [54]) had been studied. Therefore, the editorial stated that the closed-loop system had to be tested under extreme circumstances to establish fully the safety, efficacy, reliability and utility of closed-loop anesthesia before adoption into the clinical setting. It might be considered inappropriate to stress human subjects under target effect settings and surgical stimuli beyond those accepted as good clinical practice. Although animal studies could be used to test extreme or uncommon circumstances, we believed that computer simulation of patients and intraoperative events would enable a more thorough characterization of controller responses to variation in patient types and interventions. Computer simulations are frequently used in various disciplines to evaluate control systems. For example, simulations using real human data are often used in pharmaceutical research and regulatory decision making [169]. Risk calculations using realistic computer simulations are considered state of the art in aerospace engineering and testing [170].

A number of basic components are required to develop a satisfactory patient simulator for closed-loop testing: (1) It should calculate (simulate) an appropriate effect in response to drug administration, based on an internal combined pharmacokinetic-pharmacodynamic model. Ideally, this model is based on the relation between drug and effect determined from previous clinical studies. (2) It should provide a means to simulate noxious stimuli to trigger closed-loop control actions. (3) It should provide a means to simulate monitoring delay, because each monitoring device introduces some delay between drug effect and the monitor's updated estimate of the effect parameter. Any delay in a controlled-loop system may severely influence the behavior and stability of a closed-loop controller. (4) It should provide a means to vary patient model parameters (*e.g.*, to vary the relation between drug and effect) to simulate a patient population for the controller under test. (5) It should be able to simulate effect responses to interventions/events unrelated to drug changes (*e.g.*, add a bias and/or random variation to the expected drug effect to simulate patient movement, responses to minor random stimuli, and others) to verify controller stability in pseudo-steady state situations. (6) It should enable ease of use by integrating these features into standard input configurations to enhance reproducibility and standardization. (7) Finally, it should interface with existing closed-loop control systems without requiring modifications to the systems.

The aims of this study were (1) to develop a simulation methodology to stress closed-loop anesthesia control systems and (2) to apply this methodology to compare the performance of two previously published control systems.

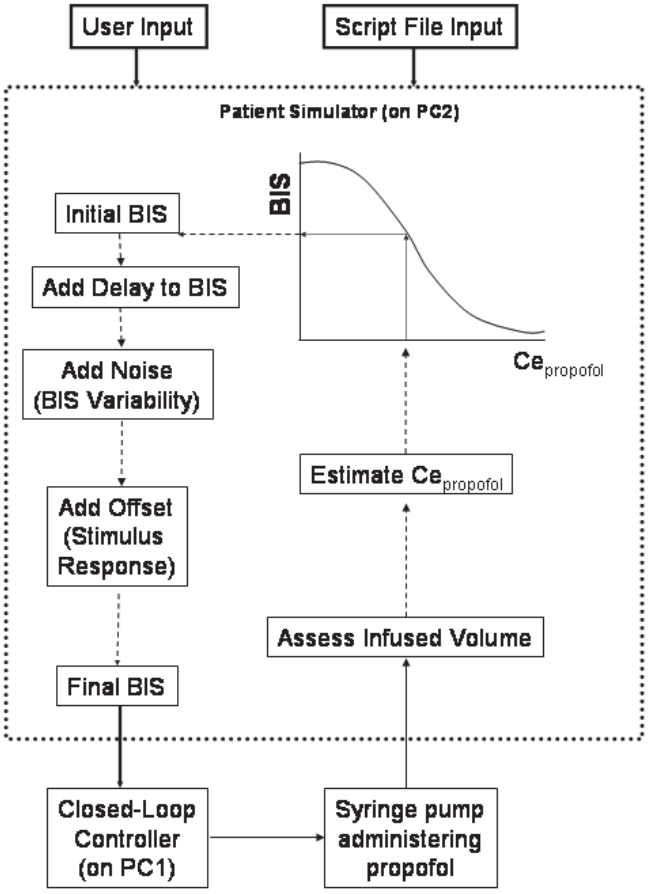

Fig. 1. *Simulator setup. On the first personal computer, the closed-loop system is running. The patient simulator is running on the second computer. First, it monitors changes in patient or surgical characteristics as input by the user or read in a script file. Second, it monitors the pump to assess the volume of drug infused in the virtual patient. Third, it estimates the resultant Bispectral Index value as a composite of response to drug, perceived stimulation, and random noise. Finally, it formats the output as input to the controller to emulate the serial output of the actual monitor (e.g. an A2000 BIS® monitor).* $Ce_{propofol}$ *= propofol effect-site concentration.*

MATERIALS AND METHODS

Software and hardware configuration

As shown in figure 1, the complete simulation trial system consists of two computers and an infusion device. The closed-loop system operates on the first computer, whereas the patient simulator operates on the second computer. Incoming BIS data from the patient simulator are used as the controlled variable by the controller to calculate an accurate propofol infusion regimen to maintain a preset target BIS value. The infusion commands are continuously sent from the controller to the infusion pump to infuse propofol. They are captured as well by the patient simulator to adjust the simulated effect. The details of operation are explained below.

First Computer: Closed-loop System

In this study, two different closed-loop systems were compared. For both systems, the RUGLOOPII© application framework was used, as developed by two of the co-authors (T.D.S. and M.S.). This program is a modular application frame with a means of standardized data exchange between modules.

In the model-based group, the closed-loop system was equipped with the controller developed and described in detail by Struys *et al.* [54]. It uses incoming BIS data as the controlled variable and is equipped with a patient-individualized model-based controller to steer the propofol administration. In the PID group, the closed-loop system was equipped with the controller developed and described in detail by Absalom *et al.* [7] . This control system also uses the BIS as the controlled variable but has a PID algorithm. Both controllers acted at least every 5 s.

Second computer: Patient Simulator

As shown in figure 1, the patient simulator executes four functions.

First, it monitors changes in patient or surgical characteristics as input by the user or a script file. Second, it monitors the pump to assess the volume of drug infused in the virtual patient. Third, it estimates the resultant BIS value as a composite of response to drug, perceived stimulation, and random noise. Finally, it formats the output as input to the controller to emulate the serial output of the actual monitor (*e.g.*, an A2000 BIS® monitor).

The following steps are required for derivation of the final BIS value: (1) estimate the propofol plasma and effect site drug concentrations from the history of drug administration using the pharmacokinetic-pharmacodynamic model of Schnider *et al.* [23, 24]; (2) produce an initial (drug-specific) BIS estimate by converting the effect-site concentration into a BIS value using an E-max pharmacodynamic model; (3) delay the initial BIS estimate over a number of seconds to simulate monitoring delay; (4) add a random, normally distributed noise value (with a mean value of 0 and a SD of 3) to simulate inherent BIS variability; (5) offset the calculated BIS value with an error signal (*i.e.*, a bias shift in the average BIS value) when simulating response to stimuli or changes in surgical circumstances.

The delay time, Emax model, error signal and noise amplitude can be dynamically altered through the user interface of the simulator or *via* a file containing a script of time-stamped changes in parameter values. Dynamic interaction allows the user to experiment with the simulation to identify conditions that stress the controller. Simulations run *via* script control ensure that various virtual patients and controllers are tested in a reproducible fashion.

Simulation protocol

We composed a simulation protocol to evaluate controller performance by adjusting parameters within the three components that comprised a study: the virtual patient, a stimulus profile, and the BIS target level.

To generate the virtual patient population, the patient simulator was fed with 10 different pharmacodynamic profiles. We defined a pharmacodynamic profile for a virtual patient as a certain drug effect site concentration-*versus*-effect relation (*i.e.*, an Emax model) combined with a certain additional delay that could be imposed by certain monitor types. To obtain realistic values, we used the Emax models derived from our previous clinical work as calculated at the end of the induction phase using data points measured during the induction phase [54]. The delay in BIS was taken from previous work by Schnider *et al.* [23, 24]; This resulted in the set of virtual patients used in our study (table 1).

Table 1. *Pharmacodynamic Profiles of 'Virtual Patients'*

Patient No	E0	Emax	C0, µg/ml	γ	Effect Delay s
1	96.9	80.95	3.9	5.17	9
2	97.66	72.23	4.27	2.41	24
3	93.8	83.49	3.91	3.09	3
4	95.66	92.94	4.42	2.65	15
5	97.25	81.31	3.79	2.16	17
6	88.89	78.29	3.73	8.09	5
7	97.59	83.13	4.57	6.02	7
8	95.82	79.8	5.77	4.43	0
9	97.7	81.79	5.11	13.11	4
10	95.79	79.75	2.7	11.05	8

We also required a standard theoretical stimulus profile to apply to a virtual patient during the controller evaluation to emulate the patient arousal reflexes during surgical procedures. Several methods of simulating arousal reflexes were considered. We selected the most straightforward way by translating the stimulus level into an offset imposed on the simulated BIS value. A BIS offset time profile was composed to emulate a typical stimulus trajectory of a surgical case. The total case time is exactly one h, including induction and time after skin closure. The BIS offset profile used for all simulations is shown in figure 2.

The simulation trial for each virtual patient was run at 3 different control targets: target BIS values of 30, 50 and 70.

Evaluation of the controller performance and statistics

To compute the percent of time BIS value was under acceptable control during maintenance (*i.e.*, starting 10 min after the start of induction), acceptable BIS control was defined as maintaining the BIS value within +/- 10 BIS units of the target value. The percent of time of acceptable BIS control, as well as percentages of time when the BIS value was above or below the range, were calculated at each target. Significance between controllers was tested using the paired *t* test (SPSS 10.0; SPSS Inc., Chicago, IL).

According to the method of Varvel et al. [29], the overall performance of both controllers was characterized on the basis of following parameters for the period when the variable was being controlled. First, using all observations within the period, the performance error (PE) was calculated according to the formula

$$PE = \frac{(measuredvalue - t\arg etvalue)}{t\arg etvalue} * 100$$

Equation 1

Subsequently, bias (MDPE), inaccuracy (MDAPE), divergence and wobble were calculated as follows. The MDPE is a measure of bias and describes whether the measured values are systematically either above or below the target value. MDPE was calculated from the measured samples j:

$$MDPE_i = median\{PE_{ij}, j = 1,..., N_i\}$$

Equation 2

where N_i is the number of values PE obtained for the ith subject.

The MDAPE reflects the inaccuracy of the control method in the ith subject:

$$MDAPE_i = median\{\left|PE\right|_{ij}, j = 1,..., N_i\}$$

Equation 3

where N_i is the number of values PE obtained for the ith subject.

Divergence describes the possible time-related trend of the measured effects in relation to the targeted values. It is defined as the slope of the linear regression equation of PE against time and is expressed in units of percentage divergence per minute. A positive value indicates progressive widening of the gap between targeted and measured values, whereas a negative value reveals that the measured values converge on the targeted values.

Wobble is another index of the time-related changes in performance and measures the intrasubject variability in PEs. In the ith subject, the percentage of wobble is calculated as follows:

wobble $_i$ = median {| PE $_{ij}$ - MDPE $_i$ | , j = 1,..., N $_i$ } **Equation 4**

For PE, MDPE, MDAPE, divergence and wobble, the SE was calculated using the two-stage approach as described by Varvel et al. [29]. Differences between groups were calculated using the paired t test.
We also calculated the amount of propofol theoretically used for both controllers at each target level.

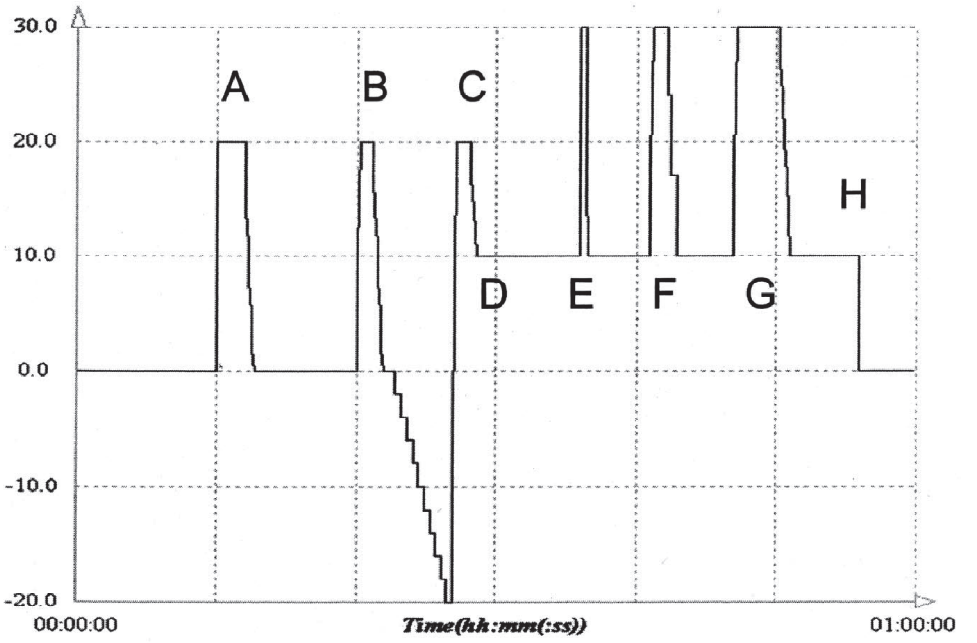

Fig. 2. *Bispectral Index offset time profile composed to emulate a typical stimulus trajectory of a surgical case. The total case time is exactly one h, including a virtual induction and time after skin closure. Stimulus A simulates the arousal due to laryngoscopy/intubation; B represents surgical incision followed by a period of no surgical stimulation (e.g., waiting for a pathology result); C represents an abrupt stimulus after a period of low-level of stimulation; D shows to onset of a continuous normal surgical stimulation; E, F and G simulates short-lasting larger stimulation within the surgical period; and H simulates the withdrawal of stimulation during the closing period.*

RESULTS

All sixty virtual operations (*i.e.*, 10 patients x 3 target BIS values x 2 controllers) were simulated. However, because the PID controller had no means to control the induction phase, and neither controller could control the recovery phase, we analyzed the controller performance only during the maintenance phase to obtain an equivalent base for comparison.

Table 2 shows the percentage of time during accurate BIS control (*i.e.*, BIS value within +/- 10 BIS units of the target value) and the percentages of time when BIS was outside of this range (*i.e.*, too high or too low), indicating less accurate control. Results for a typical case (using patient 1) for each controller and for each BIS target is shown in figure 3 for the PID and model-based controllers, respectively. In each plot, the *top* trend displays the results for a target BIS value of 70, the *middle* one is the target 50 trend, and the *bottom* trend shows the results for a target BIS value of 30. This example shows that the model-based controller provided tighter control of BIS values near each of the BIS targets, and was more responsive to changes in BIS values due to an increase or withdrawal of perceived stimulation.
The simulation results are shown in table 3. A significantly smaller mean MDPE value was observed for the PID controller compared with the model-based controller. In contrast, the model-based controller showed better MDAPE results than the PID controller for each BIS target, reaching statistical significance for targets 30 and 50.

The PID controller produced better divergence results than the model-based controller, whereas the model-based controller showed an improved wobble. Interpretation in context together with the MDAPE results shows that the relative improvement over time was greater for the PID controller because its performance was much worse initially, therefore, it had a greater opportunity to improve over time.

The intracontroller performance difference over the three targets showed a globally improving behavior at higher BIS values for both controllers, as shown in table 3. This might be caused by the division by the target value within the PE calculations, yielding lower relative errors for higher targets for a given difference between measured and targeted BIS values.

Figure 4 shows the volume of propofol used for both controllers at each target. No significant differences were found between control systems.

Table 2. *Percentage of Maintenance Time during Accurate and Inaccurate Control of BIS*

Performance	BIS Target level	PID control (%)	Model-based control (%)
Percentage time of accurate BIS control	30	58 ± 4 *	67 ± 4 *
(between ± 10 around target)	50	47 ± 10 *	63 ± 12 *
	70	44 ± 9	47 ± 18
Percentage time of too low BIS values	30	17 ± 6	17 ± 7
(more than 10 below target)	50	27 ± 7	31 ± 13
	70	30 ± 5 *	48 ± 20 *
Percentage time of too high BIS values	30	24 ± 4 *	16 ± 8 *
(more than 10 above target)	50	26 ± 3 *	6 ± 3 *
	70	26 ± 5 *	4 ± 3 *

** = p < 0.05 between both controllers*

BIS = Bispectral Index; PID = proportional integral derivative

DISCUSSION

The purpose of this study was to test the previously described patient-individualized model-based adaptive closed-loop system under several usual and extreme circumstances and to compare it with the PID-based control system. Because it was impossible to create these conditions in clinical practice, a patient simulator was developed to simulate virtual patients. The use of a set of 10 virtual patients in our patient simulator enabled a comparison of the overall performance of both controllers. Because a controller monitors recent BIS values to influence subsequent BIS values, it is not possible to directly use, for example, a set of previously recorded BIS trends to evaluate a controller. The only way to use historical data is to craft a model to describe the relation between drug concentration, stimulation profiles, and resultant BIS values.

To create realistic simulation trials, real patient pharmacodynamic profiles from our previous closed-loop work were used [54].

The clinical performance goal of any closed-loop system is to provide tight control. When defining an adequate level of control as having BIS value within +/- 10 BIS units of the target value, table 2 shows

that the percent of time during adequate BIS control was significantly higher when using a model-based controller than a PID controller, reaching significance at targets 30 and 50. BIS was not always controlled within 10 points of the target BIS because the surgical profile in this study was designed to test controllers during a number of rapid and extreme changes in patient state. The model-based controller was able to adapt more quickly to these events, thus providing a larger percent of time near the BIS target. For each targeted BIS level, significantly longer periods of BIS levels above the target were recorded using the PID controller compared with the model-based controller. This might lead to a higher risk of awareness when targeting BIS at deeper levels of anesthesia. At target 70, when subjects are expected to be aware, longer periods of BIS values below the target of 70 were observed when using model-based control. There were no significant difference between controllers in the duration of BIS value being too low when targeting BIS levels of 30 and 50.

Previously, O' Hara et al. [5] proposed the goals of automated control in anesthesia. These goals were defined as (1) keeping the average value of the controlled variable within defined limits; (2) minimizing oscillations in the controlled variable within these limits; and (3) guaranteeing stability so that over time the size of the oscillations either becomes smaller or remains constant at an acceptable level, rather than increasing, which would allow the controlled variable to swing wildly. A mathematical interpretation of these criteria can be found in Varvel et al. [29],for computer-controlled infusion pumps. These criteria can be applied on closed-loop controller performance after minor modifications.

As stated above, MDPE indicates the bias of the controller. It reveals information neither on dynamic or higher-frequency behavior nor on the amplitude of possible oscillations in control. The MDPE is a signed value and thus represents the direction (overprediction or underprediction) of the PEs rather than the size of the PEs, which is represented by MDAPE [29]. Even though MDAPE does not indicate the sign of a possible bias, it describes both the amplitude of possible bias and all other errors that prevent the controller from approaching the control target. In our study, it was observed that MDPE for both controllers is negative, which indicates that both controllers tend to overdose, leading to BIS levels below target. This can be attributed to the fact that both controllers perform, in essence, an asymmetric control operation. They only govern the infusion, not the elimination of drug from the body, which is a slower process. This phenomenon has been observed in our earlier studies as well [54]. The overdose could be solved relatively easily, without modifying the control operation or dynamics,

by setting an increased virtual target that equals the current target plus the average absolute value of the MDPE currently observed. Because shifting the target would most probably increase the MDAPE, this solution was not retained.

Table 3 shows a better MDAPE at target 30 and 50 for the model-based controller compared with the PID controller, demonstrating a better performance in approaching the target value and elimination of control errors. As a clinician, one could expect tighter control to the target BIS value from a system with a smaller MDAPE. This may reduce periods of excessive anesthesia at the deep end or reduce risk of awareness at the lighter end. This tighter control can be clearly observed in figure 3, where the model-based system's faster responsiveness and tighter control result in an overall better stability of the anesthetic depth, even under extreme circumstances. This is also demonstrated by the data shown in table 2. Divergence and wobble can be related to the oscillation of the controller behavior (wobble) and the tendency of the controller to converge on the target over a longer time (divergence).

A negative divergence number indicates convergence to the target, a positive one indicates divergence. The absolute value indicates the speed of convergence or divergence. The values of divergence obtained using the two controllers at the three different targets are shown in table 3. This shows that the PID controller produced more negative values for the divergence than the model-based controller. These negative values for divergence mean that the size of the PEs decreased appreciably with time when the PID controller was used. In the early course of control, the errors were larger and as the controller continues to operate, these errors became smaller. This time-dependent change in PEs was much less when the model-based controller was used. Comparing the wobble for both controllers shows that the model-based controller has much less overall oscillations than does the PID controller. Combining the information on wobble and divergence for the two controllers indicates that the PID controller initially performs worse than the model-based controller. This can be verified in figure 3, in which one can observe the initially large oscillations of control. These oscillations may introduce alternating periods of excessively deep and excessively light anesthesia with the risk of hemodynamic instability and awareness and are thus undesirable in clinical applications of closed-loop systems.

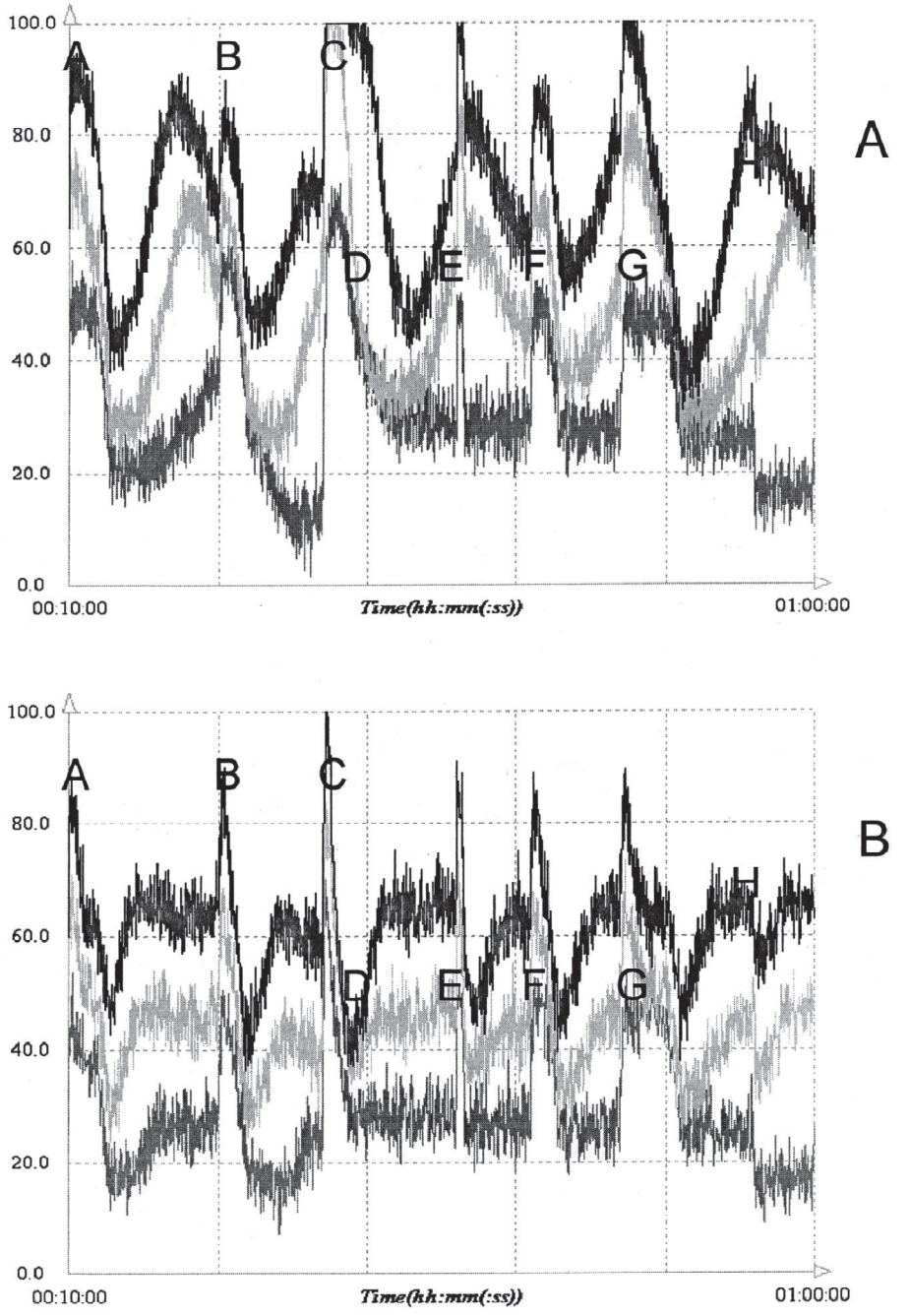

Fig. 3. *Example Bispectral Index trends for virtual patient 1 controlled by the proportional integral derivative (PID) controller (A) and model-based controller (B). Black line = target 70; light gray line = target 50; dark gray line = target 30. Stimulation events A-H are described in the legend for figure 2.*

Tighter control was achieved with the model-based controller as Bispectral Index values were more frequently near their respective target levels.

Table 3. *Performance Results*

Target	Performance	PID controller	Model-based	Sign. Level between controllers (*P* Value)
30	MDPE	-4.1974 (0.6760)†	-8.4147 (0.5247)*†	<0.0001
50	MDPE	-4.2394 (0.4664)‡	-13.3200 (0.2858)*‡	<0.0001
70	MDPE	-1.1595 (0.3578) †‡	-15.0500 (0.2468) †‡	<0.0001
30	MDAPE	25.7448 (0.4453)*†	22.6333 (0.3311) *†	<0.0001
50	MDAPE	21.7220 (0.2611)*‡	15.9100 (0.1911)*	<0.0001
70	MDAPE	16.6217 (0.1995)†‡	16.3285 (0.1976)†	0.3102
30	Divergence/s	-0.0040 (0.0004)*†	0.0013 (0.00029)*†	<0.0001
50	Divergence/s	-0.0025 (0.0002)*	-0.00024 (0.00017)*‡	<0.0001
70	Divergence/s	-0.0017 (0.00018)†	-0.0011 (0.00017)†‡	<0.0261
30	WOBBLE	22.8787 (0.4895)*†	16.3333 (0.3631)*†	<0.0001
50	WOBBLE	20.7708 (0.2772)*‡	8.8400 (0.1988)*‡	<0.0001
70	WOBBLE	16.5288 (0.2007) †‡	7.7929 (0.1644)†‡	<0.0001

** = P < 0.05 between targets 30 and 50. † = P < 0.05 between targets 30 and 70. ‡ = P < 0.05 between targets 50 and 70.*

MDAPE = median absolute performance error; MDPE = median performance error; PID = proportional integral derivative

To search for the underlying reasons resulting in the observed controller performance, we might start with the differences in the controllers. First, the PID controller uses constants that were previously tuned for auditory evoked response-guided closed-loop control (target auditory evoked potential index of 35)[83]. Therefore, it is interesting to note (fig. 3) that when the target BIS value was 30, although there were large deviations from the target, the actual BIS value spent a greater proportion of time closer to the target than it did when the target was 50 or 70. Thus, re-tuning the constants for the different control variable (BIS value) and set points, might result in improved control. Second, the PID controller uses the plasma concentration as an intermediate controller, whereas the model-based controller uses the effect-site concentration. Because we preferred to evaluate published controllers, we applied plasma concentration control for the PID controller as previously reported, even though the authors of the PID controller commented that the control performance could be improved by alterations to the gain factors in the PID controller or by using an effect-site targeted, target-controlled infusion propofol system[87].

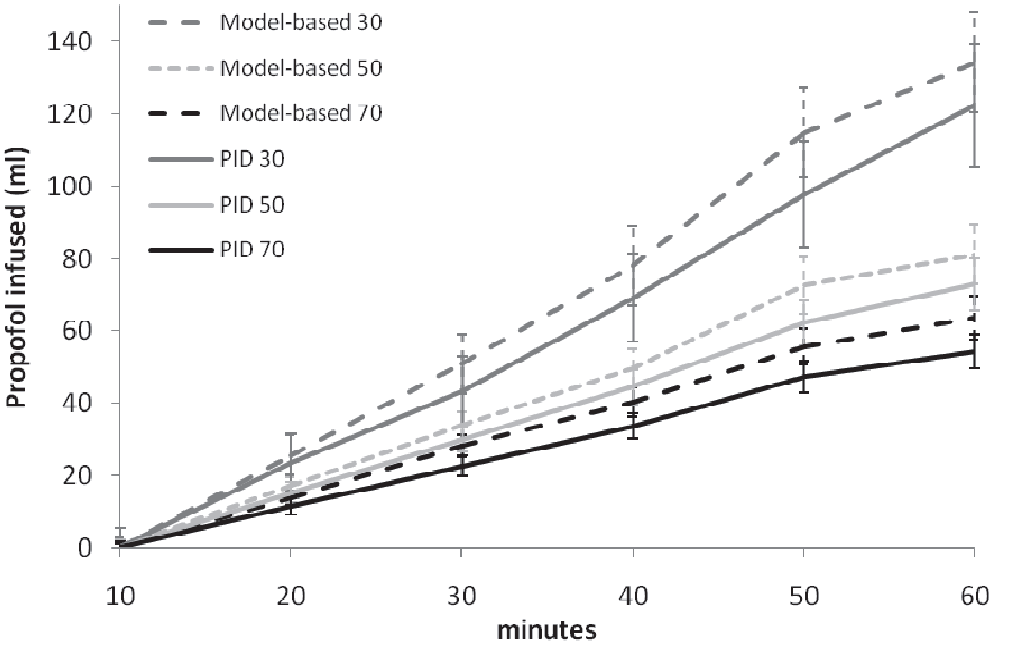

Fig.4. *Cumulative amount of propofol used for both controllers at each target value.*

The PID controller will be updated towards effect-site steering in further research by one of the coauthors (A.R.A.). One must realize that using effect site instead of plasma concentration control

without other modifications creates a faster controller but results in more overshoot. This overshoot can be compensated by using other gain factors in the PID control or, as is our belief, by applying an adaptive, model-based, individualized controller. The results of this study show that combining effect site concentration control with model-based operation can actually result in better control. This effort did not result in more propofol used, as seen in figure 4. Overall, similar amounts of propofol were used by both controllers.

One might question whether a pure feedback controller always results in worse performance than a human controller because it cannot anticipate future stimulating events, as can an anesthesiologist. One might expect to observe more sudden increases in BIS values in response to surgical stimulation (which may relate to possible arousal events) with an automated controller than with a human anesthesiologist. It is known that many anesthesiologists in clinical practice tend to bring their patient to a (too) deep level in order to avoid any risks of arousal, thus causing possible side-effects, which could be considered as poor performance as well. To the best of our knowledge, it is currently not known which of the two anestheanesthetic techniques results in the best postoperative outcome and patient satisfaction.

Furthermore, one could wonder whether a simulation study as presented here would in any way be able to predict the results in clinical practice because a simulated patient model can never be as complicated as a real patient. We have tried to simulate real patients by crafting historical data into a model and by introducing population variability through a 'set' of patients. We realize that the result of this simulation study is limited by the selected set of patients. For further research, we might consider using alternate simulated patients, increased random noise, randomized target levels, and offset.

It is generally accepted in literature that the Emax model can be used to accurately describe patient pharmacodynamics. When designing the patient simulator, we decided to use the best- described and best-validated type of pharmacodynamic model for propofol (*i.e.*, Emax model) in both the simulator and controller. We admit that using the same type of model (albeit with different parameter values) could generate a study bias in favor of the model-based controller. However, the wide variety of simulated patients, combined with the random noise and the delay, should partially compensate for

this. Moreover, we reasoned that using an inferior model may produce poor patient simulations, possibly resulting in worse accuracy of simulating actual, clinical performance of the controllers.

When evaluating the performance of two previously published closed-loop control systems for propofol administration using the BIS value as the controlled variable, it can be concluded that the additional mathematical effort imposed by using a patient-individualized model-based adaptive closed-loop system with effect site control can result in a better controller compared with a standard PID controller with plasma control. Even under extreme conditions, the model-based controller exhibited no behavioral problems.

Chapter 6

Estimation of optimal modeling weights for a Bayesian-based closed loop system for propofol administration using the BIS as a controlled variable: A simulation study

Modified from:

T. De Smet, M.M.R.F. Struys, S. Greenwald, E.P. Mortier, S.L. Shafer

Estimation of optimal modeling weights for a Bayesian-based closed loop system for propofol administration using the BIS as a controlled variable: A simulation study

Anesthesia & Analgesia *2007*; **105**: 1629-38

Disclosure: Michel M.R.F. Struys, MD, PhD; Tom De Smet, MSc; and Steven L. Shafer, MD are patent holders of the "model-based" closed-loop system. Scott Greenwald, PhD is an employee of Aspect Medical, the developers of BIS®. The new controller framework has been published in detail in the patent application WO 2005/072792 A1 (see http://www.wipo.int/pctdb/en/search-adv.jsp).

Background: Implementing Bayesian methods in a model-based closed-loop system requires the integration of a standard response model with a patient-specific response model. This process makes use of specific modeling weights, called Bayesian variances, which determine how the specific model can deviate from the standard model. In this study we applied simulations to select the Bayesian variances yielding the optimal controller for a Bayesian-based closed-loop system for propofol administration using the BIS as a controlled variable.

Methods: the relevant Bayesian variances determining the modeling process were identified. Each set of such Bayesian variances represents a potential controller. The set, which will result in optimal control, was estimated using calculations on a simulated population. We selected 625 candidate sets. Similar to our previous closed-loop performance study, we applied a simulation protocol to evaluate controller performance. Our population consisted of 416 virtual patients, generated using population characteristics from previous work. A BIS offset trajectory similar to a surgical case was used.

Results: We were able to develop, describe and optimize the parameter setting for a patient-individualized model-based closed-loop controller using Bayesian optimization. Selection of the optimal set yields a controller performing with the following median absolute prediction errors at BIS targets 30, 50 and 70 : 12.9 ± 2.87, 7.59 ± 0.74 and ; 5.76 ± 1.03 respectively.

Conclusions: We believe this system can be introduced safely into clinical testing for both induction and maintenance of anesthesia under direct observation of an anesthesiologist.

Automated control of anesthesia using continuous feedback of a patient's clinical state might improve the quality of anesthetic drug administration, resulting in a better control of anesthesia and faster recovery [54, 147]. Various closed-loop systems have been proposed to guide IV drug administration using spontaneous electroencephalographic [7, 54, 100, 102, 103, 125, 171] or auditory evoked-potential indices [83] as controlled variables. However, limitations of these control systems have precluded their adoption into clinical practice. Most controllers are designed to maintain the anesthetic only during stable periods of anesthesia, and thus exclude induction. Model-based controllers reported in the literature may be used during induction; however, these controllers typically assume an initial drug-free patient, and thus cannot be used in already anesthetized patients [54, 102, 171]. Finally, the concentration versus response profile is likely to change over the course of anesthesia, mostly as a result of changing levels of noxious stimulation, but also because of possible pharmacodynamics (*i.e.*, acute tolerance to opioids) or because of changes to the patient (*e.g.*, liver transplantation).

In an attempt to resolve these shortcomings, the Bayesian approach was included in our existing control algorithm [54, 102, 171]. Bayesian optimization, as proposed by Sheiner *et al.* [8] is classically used in pharmacokinetic-dynamic modeling to individualize drug dosing regimen by combining individual information with the knowledge of an *a priori* probability density function containing the statistical properties of the parameter to be estimated [9].
Elaborating the full mathematical background of applying Bayesian methods for individualization of population pharmacokinetics is outside the scope of this manuscript. For the interested reader, especially the study by Sheiner et Al [6] provides a detailed background insight in the Bayesian theory.

The Bayesian method starts from a standard, population-based response model providing the previous distribution of parameter values. These values are adjusted to reflect the patient's own parameters over time, based on the observed response of the individual patient under varying circumstances. This process makes use of specific modeling weights, called Bayesian variances, which determine how the patient-specific model can deviate from the population model. These Bayesian variances need to be optimized for control performance in a target population.

The aim of this study was to apply simulations to select the Bayesian variances yielding the optimal controller for a Bayesian-based closed loop system for propofol administration using the BIS (Bispectral Index) as a controlled variable.

Methods

We have previously described a closed-loop controller applying a patient-individualized sigmoid E_{max} model as controller input [54] . This controller estimated the patient-specific pharmacodynamic relationship (sigmoid E_{max} model) using the measured BIS from the induction phase. The modified controller developed and evaluated in this study uses a patient-specific sigmoid E_{max} model continuously adjusted to the observed responses over the entire course of the anesthetic using a Bayesian technique. The steps in this process are described below.

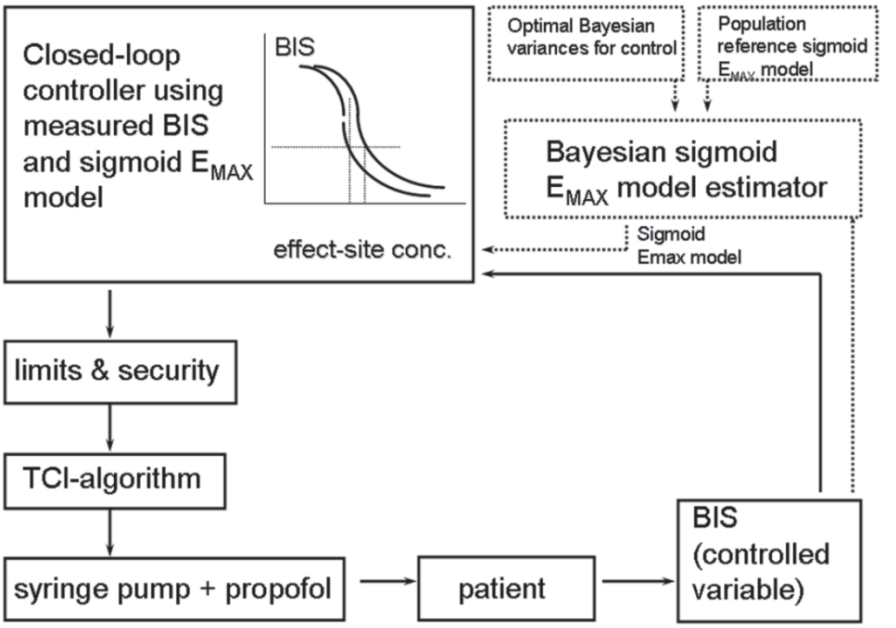

Fig. 1. *Flow chart of the closed-loop system. The straight lines represent the closed-loop control system. At each time the required effect-site concentration is calculated by the controller. This value is sent to an additional algorithm considering the safety limits. The result of these calculations is the required effect-site concentration sent to the TCI algorithm which steers a pump injecting propofol to*

the patient. The measured BIS is used as the input of the closed-loop controller. The dotted lines represent the Bayesian sigmoid E_{MAX} model estimator. The estimator receives a priori information from the population sigmoid E_{MAX} model, the optimal Bayesian variances for control and the patient measured BIS values.

Closed-loop system structure

Figure 1 shows the schematic representation of the system.

Overall controller action

The closed-loop controller applies a sigmoid E_{max} model describing the relation between BIS and propofol effect-site concentration, and characterized by four parameters: E_0 equals the BIS value at no drug effect; E_{max} equals the change in BIS between no drug effect and maximum drug effect); c_{50} represents the propofol effect-site concentration at 50% of effect and γ represents the steepness of drug effect around 50%. The model can be presented as:

$$BIS = E_0 - E_{MAX}\left(\frac{c^{\gamma}}{c^{\gamma} + c_{50}{}^{\gamma}}\right) \qquad \textbf{Equation 1}$$

The controller always uses the latest available sigmoid E_{MAX} model calculated by the Bayesian model estimator, as described below. The output of the controller is a predicted propofol effect-site concentration, which will be used as the input parameter of an effect-compartment controlled infusion system. This computer-assisted continuous infusion device targets an effect-site concentration using a three-compartment model completed with an effect-site compartment (RUGLOOP). For propofol, the pharmacokinetic-dynamic model previously published by Schnider *et al.* was used [23, 172]. Propofol effect-site concentration was computed to yield a time to peak effect of 1.6 min after bolus injection, as published by Schnider *et al* [24, 71], and clinically confirmed by Struys *et al.*[25].

Sigmoid E_{MAX} Model Estimator Integrating Bayesian Approach

The model estimator will continuously calculate a sigmoid E_{MAX} model based on the patient's drug response. A standard approach to fit a model to a set of measured samples is using a least-squares technique by minimizing

$$\sum (BIS_{sample} - BIS_{estimated})^2 \qquad \textbf{Equation 2}$$

over a set of measured points. In Eq. 2, BIS_{sample} is the observed value and $BIS_{estimated}$ is the estimated value based on the model to be fitted. The sum is called the objective function.

For applying the Bayesian technique in the estimator, a reference sigmoid E_{max} model is used as *a priori* information, while the patient-specific propofol effect site-concentration versus measured BIS data pairs are used to tune this reference or population model towards the sigmoid E_{max} model in the individual patient.

To incorporate the *a priori* knowledge while using the least-squares technique, we introduced additional terms in the objective function, representing a penalty for the difference between the reference model (the *a priori* knowledge) and the resulting sigmoid E_{max} model. This yields the following objective function

$$\begin{aligned}&\sum (BIS_{sample} - BIS_{estimated})^2 + (E_{0,Population} - E_{0,Estimated})^2 \\ &+ (E_{\max,Population} - E_{\max,Estimated})^2 + (c_{50,Population} - c_{50,Estimated})^2 \\ &+ (\gamma_{Population} - \gamma_{Estimated})^2\end{aligned} \qquad \textbf{Equation 3}$$

The second to fifth terms account for the covariates that determine the sigmoid E_{max} model to be estimated. "Population" is the original population reference model parameter (= *a priori* information), and "Estimated" is the estimated value of parameter for the individual.

The minimization of Eq. 3 without any measured samples will yield the reference model only. As observations are made over the course of a procedure, the model in the individual will gradually diverge from the original population model. With many samples, the optimal solution becomes

primarily one that minimizes the difference between the measured and predicted observations, and the reliance on the original population model diminishes. This is the nature of Bayesian inference.

Both the observations and the model parameters may vary in magnitude over several orders of magnitude. When this is the case, the model primarily works to minimize the error in the large observations, and minimizes the deviation in the large parameters from the initial population estimate, as the larger numbers typically have much larger squared errors. This behavior is undesirable, and is most appropriately handled by weighting the squared error by the expected variance. In the case of the model parameters, the expected variance represents the Bayesian uncertainty about the parameter estimate. As a consequence, the variance used to weight the squared difference between parameter estimate and population estimate will be defined as the Bayesian variances.

The patient-specific sigmoid E_{max} model's characteristics as calculated continuously by the estimator will depend on the population model, the patient's drug response as well as the applied Bayesian variances (Fig. 1).

The optimal values for the Bayesian variances depend on the specific terms to which they are applied. For the observations, they typically reflect the variance in the measurements themselves. For the parameters they reflect the interindividual variability in the reference model parameters. Or they could be selected empirically using simulations to obtain the best controller behavior according to a predefined criterion in a closed-loop application. This is the intent of the present investigation.

As the patient response during induction might not be representative for the response during surgery, and because the concentration versus response relationship may change over time, it may be undesirable to calculate the current patient-specific drug-response model using the full history of patient-specific samples. Therefore, the samples considered for the modeling are time-limited using a forgetting factor: as samples get older, their contribution in the modeling is reduced, until it vanishes completely.
The resulting objective function incorporating these effects is shown in Eq. 4.

$$\sum \frac{(BIS_{sample} - BIS_{estimated})^2 * MAX\left[\left(1 - \left[\frac{(t - t_{sample})}{sample_{TO}}\right]^2\right); 0\right]}{VAR^2_{samples}} + \frac{(E_{0,Population} - E_{0,Estimated})^2}{VAR^2_{E_0}}$$
$$+ \frac{(E_{\max,Population} - E_{\max,Estimated})^2}{VAR^2_{E_{\max}}} + \frac{(c_{50,Population} - c_{50,Estimated})^2}{VAR^2_{c_{50}}}$$
$$+ \frac{(\gamma_{Population} - \gamma_{Estimated})^2}{VAR^2_{\gamma}}$$

Equation 4

In this equation, the VARs are the Bayesian variances for each covariate, $sample_{TO}$ represents the sample time out, which can also be defined as the forgetting factor, *t* is the current time and t_{sample} is the time when each sample was captured. MAX means that the contribution of a specific sample in the objective function is only appreciated while it is larger than zero.

The actual minimization of the objective function uses the Levenberg-Marquardt method for fitting using non-linear models [173, 174].

Applied Estimator Parameters Shortlist

The BIS values, which we used as the controlled variable, can have any value between 100 and 0. Therefore, both E_0 and E_{max} are fixed at 100 to simplify the identification of the patient's own sigmoid E_{max} model. This leaves only two parameters to estimate using the Bayesian technique: c_{50} and γ.

As learned from pilot trials (data not shown), the overall delay or timing mismatch of the controlled system was important in our estimator. This total delay of the system is an overall estimate that includes misspecification of plasma-effect site equilibration, IV line flow delay and monitoring delay. The initial trials showed a vast improvement in the modeling (not yet control) when an attempt was made to estimate the overall delay as well.

$$\sum \frac{(BIS_{sample} - BIS_{estimated})^2 * MAX\left[\left(1 - \left[\frac{(t - t_{sample})}{sample_{TO}}\right]^2\right);0\right]}{VAR^2_{samples}} + \frac{(c_{50,Population} - c_{50,Estimated})^2}{VAR^2_{c_{50}}}$$

$$+ \frac{(\gamma_{Population} - \gamma_{Estimated})^2}{VAR^2_{\gamma}} + \frac{(D_{Population} - D_{Estimated})^2}{VAR^2_{D}}$$

Whereby D is the delay to be estimated. **Equation 5**

The patient-specific sigmoid E_{max} model resulting from the objective function shown in Eq. 5 is used in the control algorithm as shown in figure 1.

Table 1. *Original and Modified Reference Sigmoid E_{MAX} Model*

Original model				
	c_{50} (*μg/ml*)	E_0	E_{max}	γ
Typical Value	4.92	95.9	87.5	2.69
CV	34%	4%	11%	32%
SD	4.5			
OBJ	5016.448			
Modified Model				
Typical Value	4.98	100	100	2.62
CV	35%	6%	17%	33%
SD	4,5			
OBJ	5029			

CV = coefficient of variation; SD = standard deviation; OBJ = value of the objective function in NONMEM V; E_0 = Bispectral Index value at no drug effect; E_{max} = change in BIS between no drug effect and maximum drug effect; C_{50} = concentration at 50% of drug effect as measured by the Bispectral Index; γ = steepness of drug effect around C_{50}.

Population Reference Model Selection

The controller uses the reference sigmoid E_{max} model whenever the model estimator does not obtain a valid model. (*e.g.* at start of case when no patient-specific information is available). A good selection of the reference model should result in safe, effective control in the absence of patient-specific data samples. The reference model was calculated from previous work regarding propofol and BIS[50] as shown in table 1. As our closed-loop controller uses a fixed E_0 and E_{max} (Eq. 4) both at 100, new c_{50} and γ typical values were modeled on the raw data using NONMEM whereby the values for E_0 and E_{max} were fixed. This yields the modified reference model as applied in our controller.

The reference value for the total delay in the system, $D_{population}$, was set at 10 s which represents the cumulative delay generated from the delay from the A 2000 BIS-XP monitor, infusion delay, plus a possible mismatch in the pharmacokinetic-dynamic link model (represent by a population ke0).

Table 2. *Values for Bayesian Variances Used in Simulations*

Bayesian Variances	Values	Units
Variability C_{50} = VAR C_{50}	0,5,10,15,20	(μg/ml)
Variability $\gamma = VAR_{\gamma}$	0,2.5,5,7.5,10	—
Variability Delay = VAR_{Delay}	0,30,60,90,120	S
Sample Time Out = $Sample_{TO}$	120,315,510,705,900	S

Bayesian Variances Optimization for Closed-Loop

Identification of the Bayesian Variances to be Optimized

The aim of this study was to apply simulations to select the Bayesian variances, represented by the various VAR^2 terms in Eq. 5, yielding the optimal controller for a Bayesian-based closed loop system for propofol administration using the BIS as a controlled variable.

As indicated earlier, we use the Bayesian technique to tune two parameters of the sigmoid E_{max} model to be used in closed-loop: C_{50} and γ. The following terms from Eq. 5 are retained in the optimization:
Bayesian variance for squared deviation in C_{50}, called "VAR_{C50}"
Bayesian variance for squared deviation in γ, called "VAR_{γ}"
Bayesian variance for the squared deviation in delay, called "VAR_{Delay}"
the optimal number of samples to consider for model estimation, represented by "$Sample_{TO}$"
Bayesian variance for the squared deviation in samples, called "VAR_{Sample}". The sum of the variances is only a scaling factor for the objective function, so we can arbitrarily choose the Bayesian variance for the samples equal to 1. We only need to optimize for the three others and $Sample_{TO}$.

Each set of Bayesian variances and $Sample_{TO}$ as defined above represents a potential controller. The set that will result in optimal control for a Bayesian-based, closed-loop system for propofol administration using the BIS as the controlled variable, was estimated using calculations on a simulated population (defined below).
To limit the number of evaluations to be done, we selected 625 candidate sets, assuming continuous performance in-between. The candidate sets were chosen after preliminary simulations (data not shown), which indicated good starting points, while still broad enough to cover all useful values. The evaluated sets are shown in table 2.

Simulation Population
Similar to our previous closed-loop performance study[171], we applied a simulation protocol to evaluate controller performance by adjusting parameters within the three components that comprised a study: (1) the virtual patient, (2) a stimulus profile, and (3) the BIS target level. Our population consisted of 416 virtual patients, generated using population characteristics from previous work not connected to the closed-loop controller algorithms (independent dataset) [175]. This study provided the pharmacological characteristics for 13 patients. Of these 13 patients, we created the

simulation population of 416 virtual patients by varying the C_{50}, γ, k_{e0} and clearance parameters considering the coefficient of variation numbers.

Case Simulation

As shown in figure 2, a BIS offset was composed to emulate a typical stimulus trajectory similar to a surgical case and was already found to be accurate in previous work [171]. The total case time is exactly three h. The simulation trial for each virtual patient was run at three different control targets: target BIS values of 30, 50 and 70.

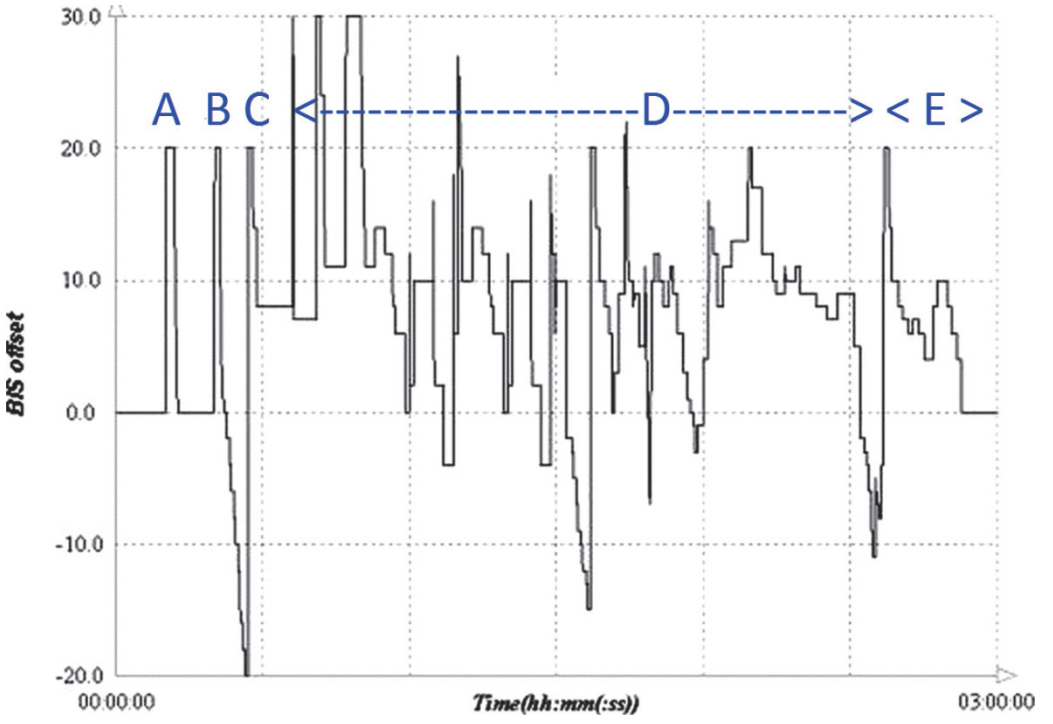

Fig. 2: *BIS (Bispectral Index) offset over time emulating a typical stimulus trajectory of surgical case. The total case time is exactly 3 h, including a virtual induction, maintenance and skin closure. Stimulus A simulates the arousal due to laryngoscopy/intubation; B represents surgical incision followed by a period of no surgical stimulation; C represents an abrupt stimulus after a period of low level stimulation; D shows on- and offset of normal surgical stimulation and; E simulates the withdrawal of stimulation during the closing period.*

Processing of Simulation Results

A total of 625 different controllers were simulated, each against all patients. Each controller was tested at three different target values for BIS: 70, 50 and 30, representing the target levels for sedation, anesthesia and deep anesthesia, respectively.

Based on the method of Varvel et al.[29], previously applied for the performance of a closed-loop system for hypnotics [7, 54, 87] , the overall performance of all controllers was characterized on the basis of the following parameters. First, using all observations within the period, the PE (performance error) was calculated according to the formula

$$PE = \frac{(\text{measuredvalue-targetvalue})}{\text{targetvalue}} * 100$$

Equation 6

Subsequently, the inaccuracy (MDAPE) was calculated as follows:

$$MDAPE_i = median\{|PE|_{ij}, j = 1,..., N_i\}$$

Equation 7

where N_i is the number of values PE obtained for the *i*-th subject. Standard errors (SE) were calculated using the two-stage approach as described by Varvel *et al.*[29].

Additionally, as shown in figure 3, the induction phase parameters average first time to target (AVGFTTT) and worst time to target (MAXFTTT), required to reach lowest BIS (from start of induction), average overshoot (AVGOVS) and worst overshoot, (MINOVS) respectively, were used to compare both the speed and stability of induction between the controllers. The overshoot was used as a negative value.

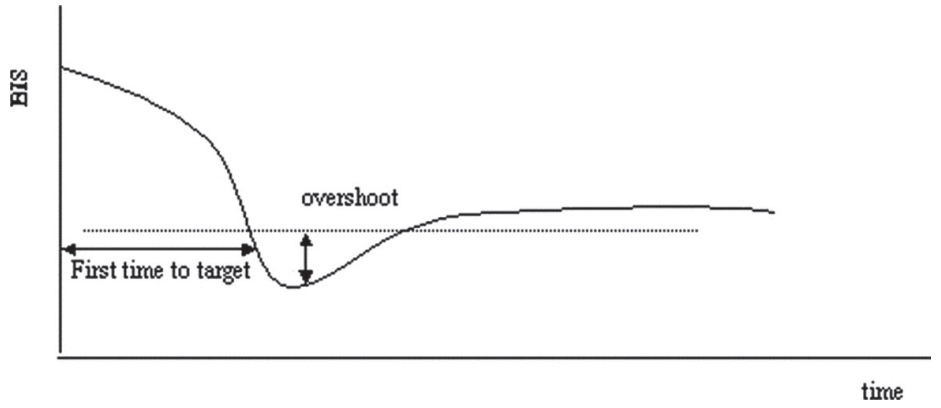

Fig. 3. *Schematic representation of the induction characteristics "first time to target" and "overshoot".*

With larger values for the Bayesian variances, the freedom of the model to be calculated for the patient is increased, but the chances to get an "off" model is increased as well. Therefore, we introduced a cost function (COST) which penalized a higher degree of freedom (larger Bayesian variance values).

To ease the search for the best controller, we grouped all criteria in an overall quality number. This one metric combined all the performance parameters in a balanced way by normalizing the parameters for each controller versus the minimum (Min) and maximum (Max) of those in the group of controllers, and by multiplying with a power factor afterwards. The weight of each term in the sum is chosen to obtain an equal importance of the overall MDAPE versus all other parameters (induction characteristics and overall cost).

$$Q = [\ -5\frac{(MDAPE - MDAPE_{Min})}{(MDAPE_{Max} - MDAPE_{Min})} - \frac{(AVGFTTT - AVGFTTT_{Min})}{(AVGFTTT_{Max} - AVGFTTT_{Min})}$$
$$- \frac{(MAXFTTT_{Max} - MAXFTTT)}{(MAXFTTT_{Max} - MAXFTTT_{Min})} - \frac{(AVGOVS - AVGOVS_{Min})}{(AVGOVS_{Max} - AVGOVS_{Min})}$$
$$- \frac{(T\arg etBIS + MINOVS)}{(MINOVS_{Max} - MINOVS_{Min})} - \frac{(COST - COST_{Min})}{(COST_{Max} - COST_{Min})}\ ]*100$$

Equation 8

This formula results in a Q value between 0 and -1000, with 0 the best performing controller. Still, to avoid that controllers performing out of range for a criterion would show up in an acceptable range,

they were discriminated with a large value (-1000) for the corresponding criterion, widening the scale from 0 to –6000.

The controller with the best Q factor was found using Excel (Microsoft, Redmond,WA) by listing all controllers and their Q factors. As it might be undesirable to use a different controller at every different target, an overall best controller will be suggested. To asses a systematical evolution of the Q factor versus the separate variables "$VARc_{50}$", "VAR_{γ}", "VAR_{Delay}" and "$Sample_{TO}$" , the Q factors were clustered in bins for each value of a single "VAR" parameter, whereas Q is ranked within those bins. In the figures (see below), the leftmost peak in every bin represents the best controller within each bin.

Finally, the overall MDAPE for best and the worst controller and the final selected controller (called "overall best controller") at each target was studied.

RESULTS

All 780,000 simulation cases (*i.e.*, 416 patients x 625 controllers x 3 target BIS values) were included in the analysis. We investigated the controller performance during both the induction phase and the maintenance phase.

Table 3 shows the Q factors and the Bayesian variance values for the best and worst behaving controllers for the three targets. It can be observed that only VAR_{Delay} and $VARc_{50}$ differ between the best controllers for the three targets.

Table 3. Q Factor as Influenced by the most Optimal and Worst Controller Behavior Resulting from the Bayesian variances' Selection

Target	Bayesian variance	Best controller	Worst controller
30	SampleTO	120 s	120 s
	$VARc_{50}$	5 µg/ml	0 µg/ml
	VAR_{γ}	0	10
	VAR_{Delay}	60 s	120 s
	Q factor	-118	-1547
50	SampleTO	120 s	120 s
	$VARc_{50}$	5 µg/ml	0 µg/ml
	VAR_{γ}	0	10
	VAR_{Delay}	30 s	90 s
	Q factor	-8	-1577
70	Sample Time Out	120 s	120 s
	$VARc_{50}$	0 µg/ml	0 µg/ml
	VAR_{γ}	0	7.5
	VAR_{Delay}	0 s	90 s
	Q factor	-31	-2310

To further explore these differences, figures 4, 5 and 6 plot a pooled ranking of the controllers at each target. The four charts within a figure each represent a ranking of all the Q factors for the BIS target versus one of the Bayesian variances ("$Sample_{TO}$", "$VARc_{50}$", "VAR_{γ}", "VAR_{Delay}"). Within a chart, the Q factor values are grouped for each single value of the Bayesian variance and sorted within this group from best to worst. The influence of this Bayesian variance on the Q factor shows best from the sequence of the peaks as a function of this variable. The best controller (highest Q factor) is marked with an arrow.
As a secondary measurement, one could observe the sequence of the rightmost peaks indicating the worst controller for each group, but we are little interested in the evolution of the worst controller. For target BIS of 30, the evolution of the best controllers is most marked as a function of VAR_{γ}, even though the other variables still show a clear trend. For target BIS of 50, the most express dependency is in both VAR_{γ} and $VARc_{50.}$ Minimal dependency is observed for $SAMPLE_{TO}$. Lastly, target 70 displays a clear downgrade in performance of the best controller with increasing value for all variables.

To select the overall best performing controller, we considered the three BIS targets simultaneously, and weighed the performance of each BIS target's best controller at the other BIS targets. It showed that the best controller for BIS target 50 was ranked 2^{nd} best performing at BIS target 70 and 3^{rd} best performing at BIS target 30. However, the best controller at BIS target 30 was ranked 7^{th} and 23^{rd} at BIS targets 50 and 70 respectively. Finally, the optimal controller for BIS target 70 performed as 32^{nd} and 31^{st} best at the BIS targets 30 and 50. As such overall preferred controller clearly was the one which performed best at BIS target 50. The resulting controller Bayesian Variances are shown in table 4.

Finally, the behavior of the best, the worst, and the final selected controller (called "overall best controller") at each target is detailed. Table 5 shows MDAPE for each specific controller.

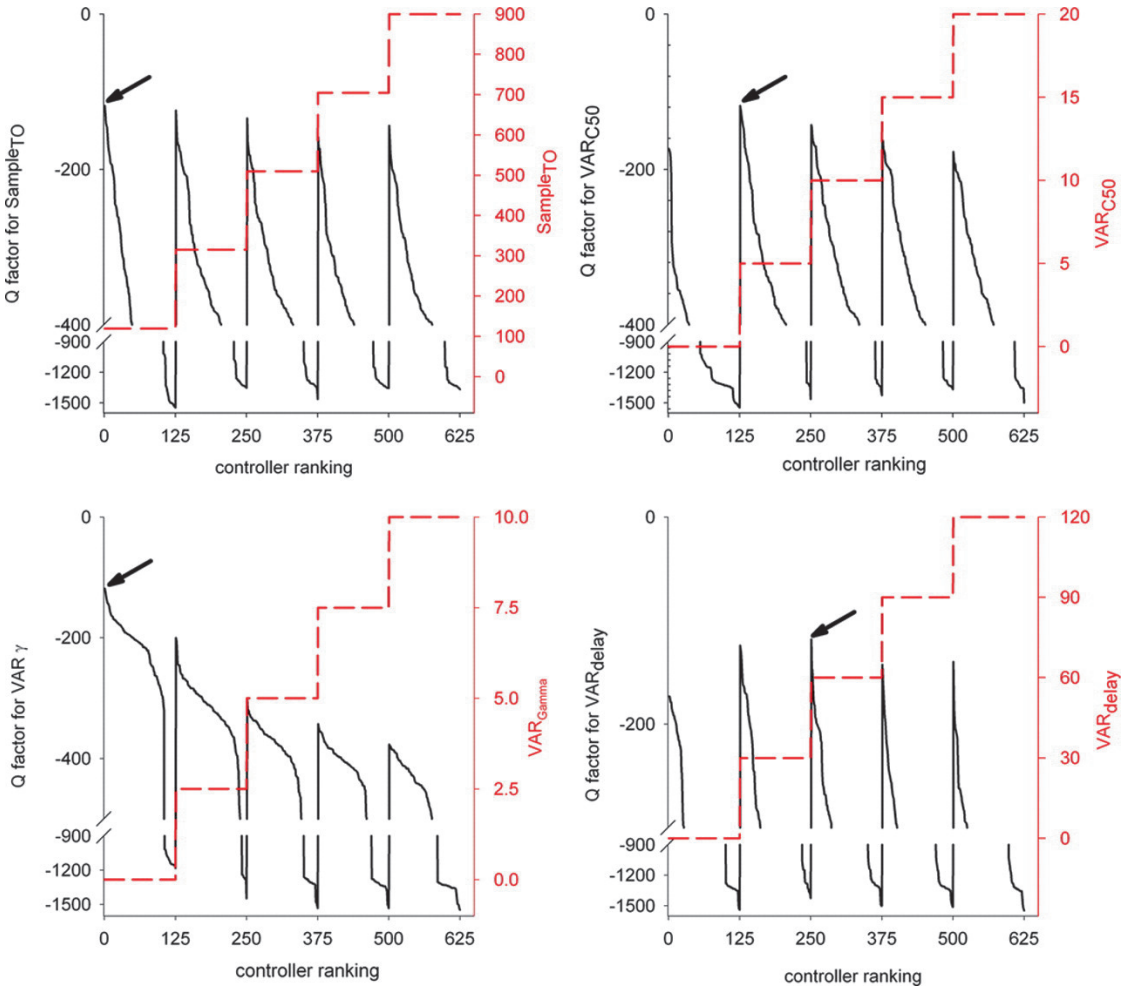

Fig. 4. *Pooled ranking of the controllers at BIS (Bispectral Index) target 30. The four charts each represent a ranking of all the Q factors for BIS target 30 versus one of the Bayesian variances ("Sample$_{TO}$", "VARc$_{50}$", "VAR$_{\gamma}$", "VAR$_{Delay}$"). Within a chart, the Q factor values are grouped for each single value of the Bayesian variance and sorted within this group from best to worst. The influence of this Bayesian variance on the Q factor shows best from the sequence of the peaks as a function of this variable. The best controller (highest Q factor) is marked with an arrow.*

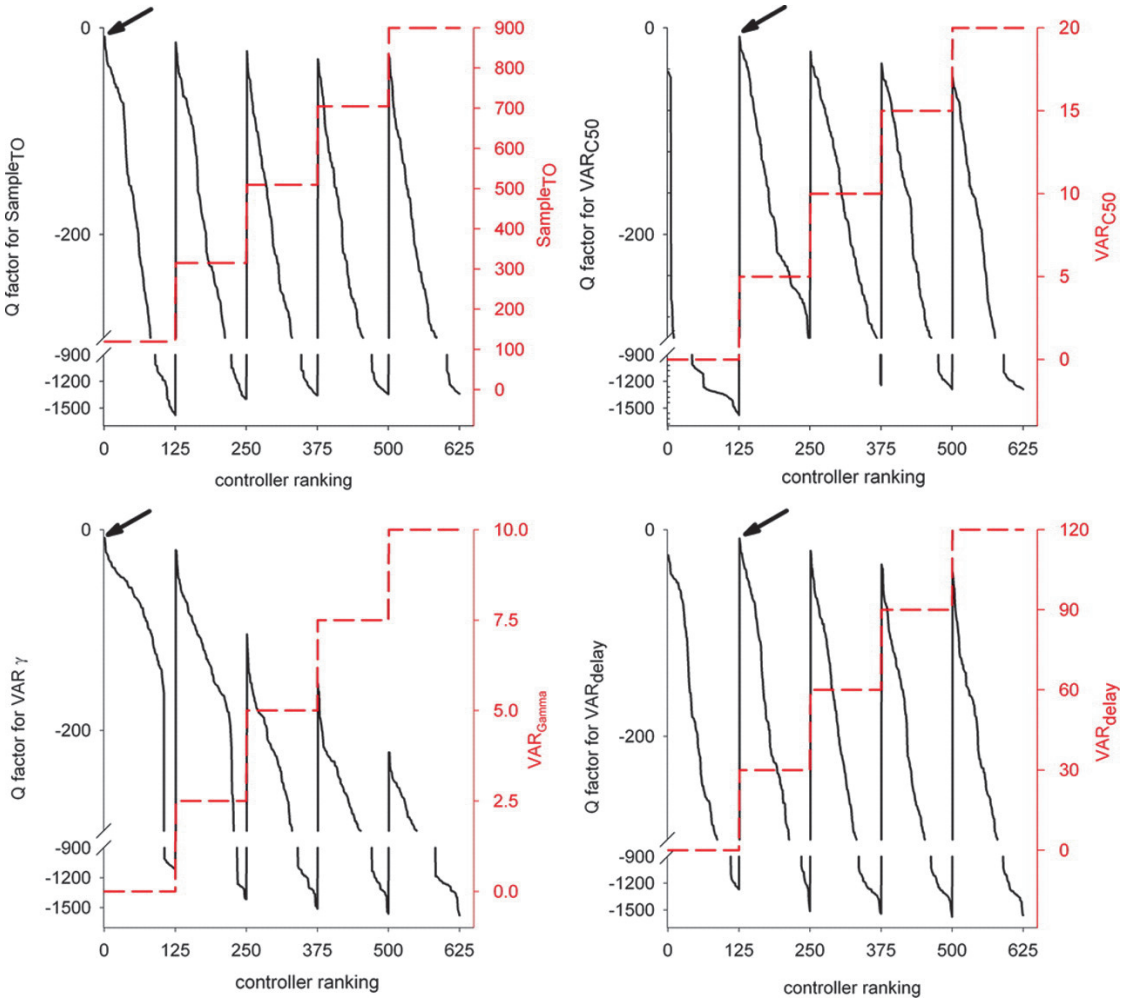

Fig. 5. *Pooled ranking of the controllers at BIS target 50. The four charts each represent a ranking of all the Q factors for BIS target 50 versus one of the Bayesian variances ("Sample$_{TO}$", "VARc$_{50}$", "VAR$_{\gamma}$", "VAR$_{Delay}$"). Within a chart, the Q factor values are grouped for each single value of the Bayesian variance and sorted within this group from best to worst. The influence of this Bayesian variance on the Q factor shows best from the sequence of the peaks as a function of this variable. The best controller (highest Q factor) is marked with an arrow.*

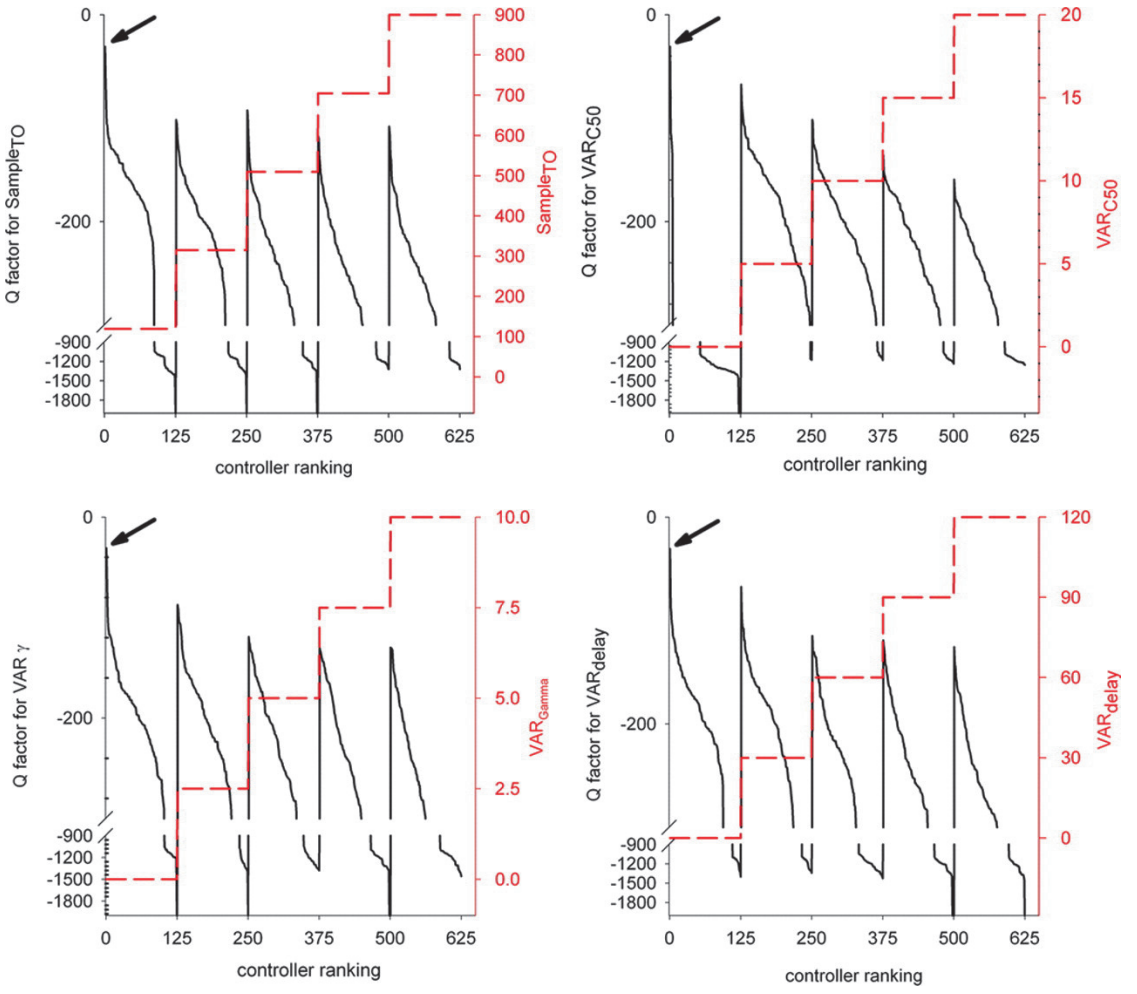

Fig. 6. *Pooled ranking of the controllers at BIS (Bispectral Index) target 70. The four charts each represent a ranking of all the Q factors for BIS target 70 versus one of the Bayesian variances ("Sample$_{TO}$", "VARc$_{50}$", "VAR$_{\gamma}$", "VAR$_{Delay}$"). Within a chart, the Q factor values are grouped for each single value of the Bayesian variance and sorted within this group from best to worst. The influence of this Bayesian variance on the Q factor shows best from the sequence of the peaks as a function of this variable. The best controller (highest Q factor) is marked with an arrow.*

Table 4. Bayesian variances yielding the best results in the current trials.

$Sample_{TO}$	120 s
$VARc_{50}$	5 *μg/ml*
VAR_{γ}	0
VAR_{Delay}	30 s

Table 5. Overall MDAPE for the Best, the Worst, and the Final Selected Controller (called "Overall Best Controller") at Each Target.

	MDAPE (%)
Best controller at target 30	12.56 ± 2.87
Overall best controller at target 30	12.90 ± 2.87
Worst controller at target 30	14.75 ± 2.60
Best controller at target 50	7.59 ±0.74
Overall best controller at target 50	7.59 ±0.74
Worst controller at target 50	11.53 ± 2.73
Best controller at target 70	5.98 ± 1.27
Overall best controller at target 70	5.76 ± 1.03
Worst controller at target 70	7.75 ± 3.00

DISCUSSION

We applied simulations to estimate the optimal Bayesian variances for a Bayesian-based closed-loop system for propofol administration using the BIS as a controlled variable. Our final goal was to develop a practical patient-individualized model-based closed loop controller using Bayesian optimization that can be introduced safely into clinical testing.

The introduction of Bayesian methods in our previously published [54] model-based adaptive control strategy will allow the use of the controller in a more universal way. The use of *a priori* information will permit the use of the controller during anesthesia induction, a distinct advantage compared to previously reported control algorithms [5]. It can be used on an already anesthetized patient, where the controller will keep the total anesthetic state at a steady level, whereas the patients' drug history (even unknown) is gradually washing out. The mismatch between, the controller-perceived required drug concentration and the total patient drug concentration is actually irrelevant and compensated for by the Bayesian modeling.

Similar to other control algorithms [5], a Bayesian controller's performance is influenced by multiple parameters, called Bayesian variances, which are constant numbers requiring fine tuning to guarantee optimal behavior. This fine-tuning implies testing under extreme clinical circumstances to establish fully the safety, efficacy, and reliability of closed-loop anesthesia before introduction into clinical testing. As it might be considered morally irresponsible to stress human subjects under target effect settings and surgical stimuli beyond those accepted as good clinical practice, we felt that computer simulation of patients and intraoperative events would enable a more thorough characterization of controller responses to variation in patient types and interventions. The applied simulation methods were previously used to compare different closed-loop control algorithms [171].

As we use the sigmoid E_{max} model obtained using Bayesian approach for our closed-loop algorithm, we need to optimize the Bayesian variances towards this application. The optimal selection should result in a Bayesian sigmoid E_{max} model estimator providing the best model for accurate closed-loop control for all BIS targets. After optimization to three clinically significant BIS targets (30, 50, 70), we selected a single overall optimal controller for future testing. Even though part of the selection criteria was

based on overshoot, undershoot and avoiding oscillations, we do not intend to imply that this study tested robustness of a particular controller, which must be done in further research.

The optimal values for the Bayesian variances resulting from our simulations were 5 for $VARc_{50}$, 0 for VAR_{γ}, 30 for VAR_{Delay} and 120 for $Sample_{TO}$. Compared to the proposed universe of Bayesian variances sets, as shown in table 2, this set, providing optimal control, allows relatively little amount of intersubject variability. This means that the improvement in control performance resulting from the larger degree of freedom did not compensate for the drawback introduced by the cost function.

Verification of the dependency of the Q factor on $VARc_{50}$ in figures 5 and 6 for targets 50 and 70 shows that the controller performance decreases when $VARc_{50}$ is zero. An underlying explanation is that the modeling algorithm cannot properly model incoming data centered on a different c_{50} by varying γ only. This leads to absurd models and, accordingly, absurd control behavior resulting from it. It can be concluded that the model does best when it can differentiate between sensitive patients and resistant patients.

As for the VAR_{Delay}, one might wonder why a delay to be estimated was introduced. As the total delay is an overall estimate that groups pharmacokinetic-dynamic modeling mismatch or “ke0 mismatch”, IV line flow delay, and artifact-dependent monitoring delay, several uncertainties contribute to an overall mismatch between the expected time behavior versus the actual time behavior. One could try to separately model the ke0 and the delay, but this only leads to more difficult identification of the various model parameters from the measured data in the modeling procedure. Moreover, using a varying ke0 would lead to difficult interpretation of effect-site concentration by the anesthesiologist in future clinical applications.

The value of 120 for $Sample_{TO}$ means that only the last 2 min of patient data are considered to build the model. One can wonder whether the patient history of 15 min ago reflects the current patient state better than the population model. The simulation results seem to reveal that this is not the case. Most probably, the population model has the advantage of being a considered starting value providing a good basic control.

Selection of accurate *a priori* information is the foundation of good Bayesian control. All Bayesian methods start from relevant measured data [8]. The population model, which was used by the controller when no patient-specific measurements were acquired, determines the control behavior during induction. We selected our *a priori* information based on previous work as shown in table 1. Although this selection resulted in satisfying results in the current simulations, a (relatively) high c_{50} could mean a possible threat to people not tolerating high propofol concentrations due to hemodynamic instability. One might make the initial population models' c_{50} dependent on patient covariates including age, ASA classification and concurrent disease. The possible benefit of this might be the subject of further research.

To introduce the final selected controller into clinical testing, its safety performance needs to be stressed. As shown in table 5, MDAPE of the final selected controller are close to the best at each target and are better than the worst controller at each target. Even more, the MDAPE results from this simulation study shows better results than the MDAPE's from our own previous work using similar simulations but a model-based controller without Bayesian approach [171].
The MDAPE's are also better or comparable with various clinically applied closed-loop systems [54, 103, 176] but this Bayesian based controller offers much more freedom during clinical applications as stated above.

In conclusion, we were able to develop, describe and optimize the parameter setting for a patient-individualized model-based closed-loop controller using Bayesian optimization. We believe this system can be introduced safely into clinical testing under direct observation of an anesthesiologist.

Chapter 7

The Accuracy and Clinical Feasibility of a New Bayesian-Based Closed-Loop Control System for Propofol Administration Using the Bispectral Index as a Controlled Variable

Modified from:

T. De Smet, M.M.R.F. Struys, M.M. Neckebroek, K. Van Den Hauwe, S. Bonte, E.P. Mortier

The Accuracy and Clinical Feasibility of a New Bayesian-Based Closed-Loop Control System for Propofol Administration Using the Bispectral Index as a Controlled Variable

Anesthesia & Analgesia *2008*; **107**: 1200-1210

The first two authors contributed equally to this work.

M.M.R.F. Struys, MD, PhD, Tom De Smet, MSc and Steven L. Shafer, MD, are patent holders of the "model-based" closed-loop system. The new controller framework has been published in detail in the patent application WO 2005/072792 A1 (see http://www.wipo.int/pctdb/en/search-adv.jsp). Aspect Medical Systems (Norwood, MA, USA) is the applicant in all countries except United States.

Background: Closed-loop control of the hypnotic component of anesthesia has been proposed in an attempt to optimize drug delivery. Here, we introduce a newly developed Bayesian-based, patient-individualized, model-based, adaptive control method for BIS guided propofol infusion into clinical practice and compare its accuracy and clinical feasibility under direct observation of an anesthesiologist versus BIS guided, effect compartment controlled propofol administration titrated by the anesthesiologist during ambulatory gynecological procedures.
Methods: Forty ASA patients were randomly allocated to the closed-loop or manual control group. All patients received midazolam 1 mg IV and alfentanil 0.5 mg IV before induction. In the closed-loop control group, propofol was administered using the previously described closed-loop control system to reach and maintain a target BIS of 50. In the manual control group, the propofol effect-site concentration was adapted at the discretion of the anesthesiologist to reach and maintain a BIS as close as possible to 50. Induction characteristics, performance and robustness during maintenance and recovery times were compared. Hemodynamic and respiratory stability were calculated as clinical feasibility parameters.
Results: The closed-loop control system titrated propofol administration accurately resulting in BIS values close to the set point. The closed-loop control system was able to induce the patients within clinically accepted time limits and with less overshoot than the manual control group. Automated control resulted in beneficial recovery times. Our closed-loop control group showed similar acceptable clinical performance specified by similar hemodynamic, respiratory stability, comparable movement rates and quality scores than the manual control group.
Conclusions: The Bayesian-based-closed loop control system for propofol administration using the BIS as a controlled variable performed accurate during anesthesia for ambulatory gynecological procedures. This control system shows clinical feasibility and can be further validated in clinical practice.

Closed-loop control of the hypnotic component of anesthesia has been proposed in an attempt to optimize drug delivery [95]. Various automated drug delivery systems have been described in the literature using spontaneous electroencephalogram [7, 54, 87, 101, 103, 104, 106, 133, 171] or auditory evoked potential indices [83] as controlled variables. However, several limitations such as lack of control during induction, exclusion of already anesthetized patients when applying model-based controllers and problems dealing with patient variability during control have been encountered in previous work.

Outside anesthesia, adaptive control has been well used in medicine for decades, for example, to control nitroprusside infusions [177].

Our group has developed a new model-based patient-individualized closed loop control system for propofol administration using the BIS as a controlled variable taking care of these limitations by implementing Bayesian methodology. Recently, we have applied simulations to select these Bayesian variances yielding the optimal controller for this Bayesian-based control system [178]. Bayesian optimization, as proposed by Sheiner and coworkers [8] , individualizes the pharmacodynamic relationship by combining individual information with the knowledge of an *a priori* probability density function containing the statistical properties of the parameter to be estimated [9]. The Bayesian method starts from a standard, population-based response model providing the prior distribution of parameter values. These values are adjusted to reflect the patient's own parameters over time, based on the observed response of the individual patient under varying circumstances. This process makes use of specific modeling weights, called Bayesian variances, which determine how the patient-specific model can deviate from the population model. These Bayesian variances need to be optimized for control performance in a target population, which was done for this controller and described in previous work [178].

The aim of this study was to introduce this newly developed system into clinical practice and compare its accuracy and clinical feasibility under direct observation of an anesthesiologist versus BIS guided, effect compartment controlled propofol administration titrated by the anesthesiologist during ambulatory gynecological procedures. The main novelty in this investigation compared to the referenced studies is that the new control system enables us to include the induction phase in the closed-loop control mode of the controller rather than only the maintenance phase.

METHODS

System specifications

Controlled Variable, Data Management and Actuator Control

The BIS was applied as controlled variable to titrate propofol administration. BIS (BIS-XP®, version 4) is derived from the frontal electroencephalogram as calculated by the A-2000 BIS® Monitor using four BIS-Sensor electrodes.

In all patients, our setup used a laptop running RugloopII© to calculate the TCI algorithms to steer the infusion pump, and to record all relevant physiologic data including the BIS signal. The target controlled infusion system used a three compartment model with an effect compartment, previously published by Schnider *et al*. [23, 24]. As in a previous study of Struys *et al.*[174], for the calculation of the CePROP (propofol effect-site concentration) a fixed time-to-peak effect site concentration [71] of 1.6 min was used, as also published by Schnider *et al*.[24].

In the closed-loop control group, the RugloopII© platform also executed the closed-loop control, calculating an adequate propofol effect-site concentration from the measured BIS, to serve as the input to the effect compartment controlled TCI system. In the control group the anesthetist applied the TCI system directly to titrate the propofol administration.

Blood pressure, heart rate, end-tidal CO_2, and SpO_2 were acquired using the S5-monitor (GE Healthcare, Helsinki, Finland). All data were stored on hard disk at a 5-s interval.

Closed-Loop Controller

The closed-loop control algorithm attempts to minimize the error between the measured BIS value and the target BIS value selected by the anesthesiologist by calculating an adequate propofol effect-site concentration using a patient-individualized, model-based, adaptive control method. The applied model-based adaptive control system with Bayesian model optimization is described extensively in our previous work [90].

The controller is based on a pharmacodynamic model represented by a patient-individualized sigmoid E_{max} model, describing the relation between BIS and CePROP, and characterized by four parameters:

E_0 equals the BIS value at no drug effect; E_{max} equals the change in BIS between no drug effect and maximum drug effect; EC_{50} represents the CePROP at 50% of effect; and γ represents the steepness of drug effect around 50%. The model can be presented as:

$$BIS = E_0 - (E_0 - E_{MAX}) * \left(\frac{CePROP^{\gamma}}{CePROP^{\gamma} + EC_{50}{}^{\gamma}} \right)$$

Equation 1

The controller estimates the target propofol effect-site concentration that will minimize the difference between measured and target value for the controlled variable (BIS) by shifting the sigmoid E_{max} model along the propofol effect-site concentration axis. A detailed explanation of this "moving curve controller" can be found in our previous work [54].

Originally, the patient-specific sigmoid E_{max} curve was estimated during induction and used unchanged throughout the case. Recently, the model estimator was improved by implementing a Bayesian technique to continuously calculate a patient-individualized sigmoid E_{max} combining an initial population mean model with the observed responses over the entire course of the anesthetic. The development of and the estimation of the optimal modelingmodeling weights for this Bayesian-based closed loop control system were reported previously [90]. Generally, the Bayesian objective function looks like:

$$\sum \frac{(BIS_{sample} - BIS_{estimated})^2 * MAX\left[\left(1 - \left[\frac{(t - t_{sample})}{sample_{TO}}\right]^2\right); 0\right]}{VAR^2_{samples}} + \frac{(EC_{50,Population} - EC_{50,Estimated})^2}{VAR^2_{EC_{50}}}$$
$$+ \frac{(\gamma_{Population} - \gamma_{Estimated})^2}{VAR^2_{\gamma}} + \frac{(D_{Population} - D_{Estimated})^2}{VAR^2_{D}}$$

Equation 2

Whereby BIS_{sample} is the observed value and $BIS_{estimated}$ is the estimated value based on the model to be fitted. EC_{50} and γ are the nonfixed terms of the sigmoid E_{max} model, "Population" is the original population reference model parameter (= *a priori* information), and "Estimated" is the estimated value of parameter for the individual. SampleTO is a forgetting factor representing the samples taken

into account for the modelingmodeling on a time-limited base, and D is the systems delay to be estimated.

Clinical study

After Institutional Ethics Committee (Ethics Committee of the Ghent University Hospital, Gent, Belgium) approval, informed consent was obtained from 40 ASA I and II female patients, aged 18-45 years, scheduled for ovum retrieval whereby ovocytes are collected from the follicles in the ovaries by aspiration using ultrasonic-guided needle puncture through the vaginal wall. They were randomly (permuted block randomization, blocks of 4, 20 patients per group) allocated to the closed-loop or manual control group. Exclusion criteria included weight <70% or more than 130% of ideal body weight, neurological disorder, and use of psychoactive medication including alcohol. All patients received midazolam 1 mg IV 7 min and alfentanil 0.5 mg IV 2 min before induction with propofol. All drugs were administered via a large left forearm vein. Every patient received about 300 ml of crystalloid fluid during the study period. No fluid load was given before induction. No other drugs were given, except paracetamol 1g IV at the end of the procedure to provide post-operative pain relief. All patients maintained spontaneous ventilation via a facemask delivering oxygen 6 L/min.

In the closed-loop control group, propofol was administered using the previously described closed-loop control system. To start and maintain propofol administration, the requested BIS target was fixed at 50 for the complete duration of the case. In the manual group, propofol was administered using the effect compartment controlled TCI system (RugloopII©). The initial target propofol effect-site concentration was set at 5.0 µg/ml, which was exactly similar to the initial EC_{50} in the initial population model in the closed-loop controller. The propofol target concentration was adapted at the discretion of the anesthesiologist (the same person in all cases) in order to maintain a BIS as close as possible to 50.

The time and BIS were recorded at the moment of LOC. We also calculated the propofol dose used for the entire procedure. Heart rate, end tidal CO_2, SpO_2, and BIS were acquired every 5 s. Artifacts in the BIS due to poor signal quality were automatically detected and excluded from further analysis. Blood pressure was acquired every 1 minute. RUGLOOPII digitally recorded all vital signs and infusion data. During the case, incidents of spontaneous movement were documented.

At the end of surgery (*i.e.* end of surgical stimulus), propofol administration was stopped and recovery parameters (time until opening eyes, and time until saying name and date of birth) were recorded.

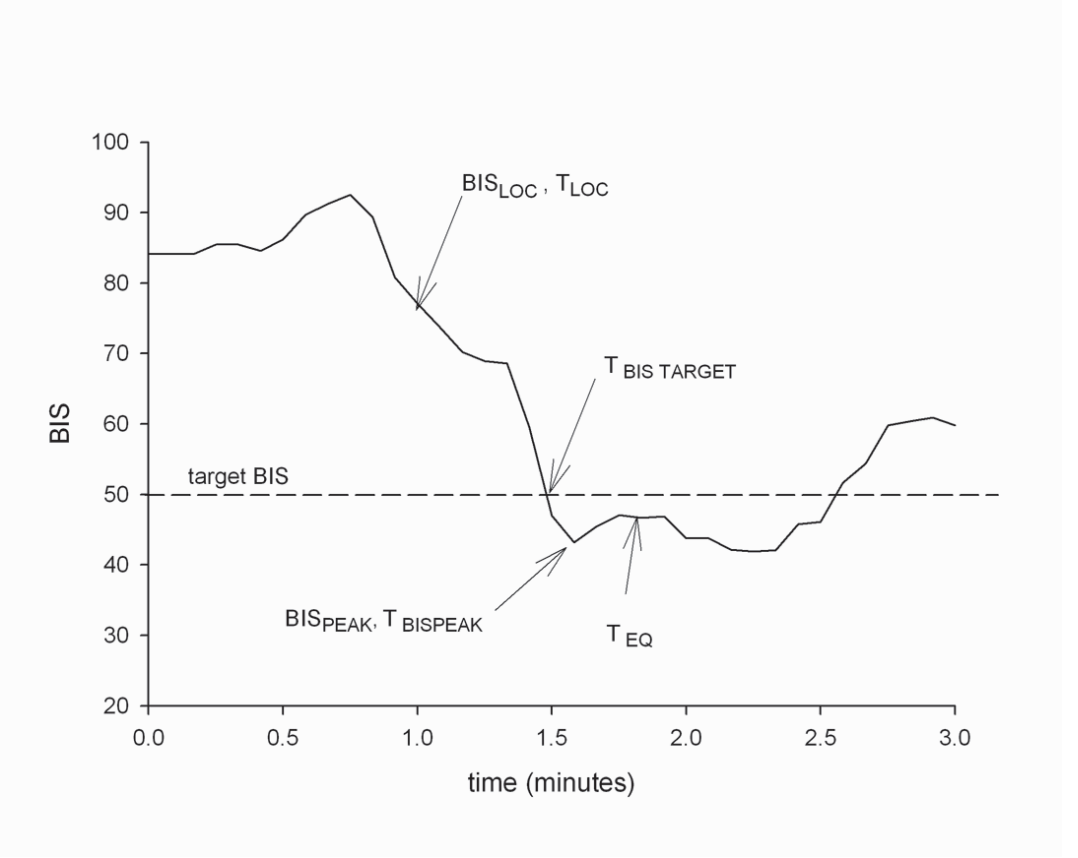

Fig. 1. *Schematic representation of performance during induction. T_{LOC} = moment of loss of consciousness, BIS_{LOC} = BIS at the moment of loss of consciousness, $T_{BIS\ TARGET}$ = observed time required for reaching the target BIS value, $T_{PEAK,\ BIS}$ = observed time required for reaching maximal drug effect (lowest BIS value), BIS_{PEAK} = observed BIS value at $T_{PEAK,\ BIS}$, T_{EQ} = observed time required for reaching the target value after the initial overshoot, also called time to steady-state.*

Evaluation of the control performance

The evaluation methods of the control performance were described and applied previously [54]. BIS was defined as the controlled variable in both groups and the BIS target value was set at 50 in both groups. Controller performance metrics are calculated on the measured values of the controlled variable versus its target value. The performance metrics of the closed-loop and manual control group was evaluated and compared during induction, maintenance and recovery.

We recorded time until LOC from the start of propofol infusion and the amount of propofol used during induction. The control performance during induction was studied taking into account the following parameters (Fig. 1):

BIS_{LOC} = BIS at the moment of loss of consciousness.

$T_{BIS\ TARGET}$ = observed time required for reaching the target BIS value.

$T_{PEAK,\ BIS}$ = observed time required for reaching maximal drug effect (lowest BIS value).

BIS_{PEAK} = observed BIS value at $T_{PEAK,\ BIS}$.

T_{EQ} = observed time required for finally reaching the target value with or without overshoot, also called time to steady-state.

The control performance on the controlled variable (BIS) was calculated for each patient from the start until termination of propofol administration using the following performance metrics.

First, we evaluated the percentage of case time the BIS remained between 40-60 and 45-55. An important derivative metric is the percentage of time with too low BIS (lower than 40 or 45, respectively) or too high BIS (higher than 60 or 55, respectively).

Additionally, the performance-error based method of Varvel *et al*. [29] was applied. Using all observations within the period, the performance error (PE) was calculated according to Equation 2.

$$PE = \frac{(measuredvalue - t\arg etvalue)}{t\arg etvalue} * 100$$

Equation 3

Subsequently, for each patient bias (MDPE), inaccuracy (MDAPE), divergence and wobble were calculated:

MDPE is a measure of bias and describes whether the measured values are systematically either above or below the target value. MDPE was calculated from

$$MDPE_i = median\{PE_{ij}, j = 1,..., N_i\}$$ **Equation 4**

where N_i is the number of values PE obtained for the *i*-th subject.

MDAPE reflects the inaccuracy of the control method in the *i*-th subject:

$$MDAPE_i = median\{|PE|_{ij}, j = 1,..., N_i\}$$ **Equation 5**

where N_i is the number of values PE obtained for the *i*-th subject.

Divergence describes the possible time-related trend of the measured effects in relationship to the targeted values. It is defined as the slope of the linear regression equation of PE against time and is expressed in units of percentage divergence per minute. A positive value indicates progressive widening of the gap between targeted and measured values, whereas a negative value reveals that the measured values converge on the predicted values.
Wobble is another index of the time-related changes in performance and measures the intrasubject variability in performance errors. In the *i*-th subject the percentage of wobble is calculated as follows :

$$wobble_i = median\{|PE_{ij} - MDPE_i|, j = 1,..., N_i\}$$ **Equation 6**

Additionally, we compared hemodynamic (heart rate and mean arterial blood pressure) and respiratory (oxygen saturation) stability from start until termination of the propofol administration between groups. For heart rate, we evaluated the percentage of case time heart rate remained between 50 and 90 bpm. As such the percentage of time with bradycardia (lower than 50 bpm) or tachycardia (higher than 90 bpm) was calculated too. For mean arterial blood pressure, we evaluated moderate and severe hypotension indicated by the percentage of case time the blood pressure went

below 60 and 50 mm Hg respectively, and hypertension defined by a blood pressure values above 135 mm Hg [179].

During recovery, we compared the time from stop propofol infusion until opening of the eyes on command and orientation. Hereby, orientation was defined as saying name and date of birth on request. The commands for opening of the eyes and orientation were repeated every 10 s until positive.

In these clinical procedures, patients are allowed to move smoothly with feet or hands, however, no movement of the upper legs nor pelvis is allowed as this might result in dangerous malpositioning of the needle during the retrieval procedure. Therefore, incidence (number of patients) of allowed and not allowed movements was recorded. Additionally, we asked the gynecologist at the end of the procedure to score the overall patients' anesthetic condition between 0 and 100%, whereby 0 means very unsafe to work and 100 means perfect.

Statistical Analysis Used

Power calculations were based on previous studies [54]. For control, overshoot at induction and MDAPE are important endpoints. For overshoot at induction, Struys *et al*. [54] found a difference in BIS_{PEAK} of 6 BIS units with a standard deviation of 4. Based on this, 12 patients would be required to show a difference between groups with a type I and II error of 5 %. For MDAPE, a 30 % better result for closed-loop control versus manual control with a standard deviation of 25 % in both groups would be revealed with a type I and II error of 5 % when studying 18 patients per group. As such, we included 20 patients per group to reveal accurate power.

Statistical analysis was performed using SPSS version 12.0 (SPSS Inc, Chicago, IL). Data are presented as mean ± SD or as median (range). All data were checked for Gaussian distribution by the method of Kolmogorov and Smirnov. Differences between groups were analyzed by a Student's *t*-test or Mann-Withney test, depending on their distribution. Categorical data (movement) were analyzed by a X^2 test.

Evaluation of Bayesian Functionality

The addition of the Bayesian optimization adds complexity to the control system. This added complexity can only be justified if, at least, the parameters calculated by the Bayesian optimization for the individual patient deviate from the typical values. This comparison was realized by comparing graphically the difference in model EC_{50} and delay, target effect site concentration change calculated by the controller using the Bayesian-optimized model versus a hypothetical controller using the unchanged typical values, as well as the time integration of the latter one.

Table 1. Demographic data:

	Closed-loop control (*n* = 20)	Manual control (*n* = 20)
Age (yr)	31.6 ± 5.3	32.5 ± 5.0
Height (cm)	165.0 ± 5.9	168.8 ± 5.5
Weight (kg)	62.2 ± 9.0	65.4 ± 8.0

Table 2. Clinical data:

	Closed-loop control	Manual control (n = 20)
Induction time (s)	66 ± 25 *	49 ± 9 *
Propofol dose until LOC (mg)	91 ± 22 *	106 ± 10 *
BIS_{LOC}	73 ± 11 *	82 ± 7 *
Duration of anesthesia from start until Stop propofol infusion (s)	1013 ± 191	1031 ± 239
Total propofol used (mg)	261 ± 68	292 ± 67
BIS at stop propofol administration	46 ± 5	43 ± 11
CePROP at stop propofol administration	3.1 ± 0.8	3.5 ± 0.9
Recovery time until opening of the eyes (s)	215 ± 133 *	316 ± 125 *
Recovery times until orientation (s)	259 ± 128 *	343 ± 112 *

BIS = bispectral index; LOC = loss of consciousness, CePROP = propofol effect-site concentration * = P < 0.05 between groups

Table 3. Control Quality and Safety During Induction and Maintenance

	Closed-loop control	Manual-control
$T_{BIS\ TARGET}$ (s)	93 ± 34	89 ± 64
BIS_{peak}	40 ± 7 *	33 ± 10 *
$T_{PEAK,\ BIS}$ (s)	125 ± 61	148 ± 112
T_{EQ} (s)	176 ± 101	204 ± 124[a]
% of time BIS between 40 and 60	75 ± 13 *	43 ± 17 *
% of time BIS between 45 and 55	47 ± 13 *	20 ± 16 *
% of time BIS lower than 40	15 ± 12 *	48 ± 17 *
% of time BIS lower than 45	39 ± 12 *	69 ± 17 *
% of time BIS higher than 60	9 ± 3	9 ± 4
% of time BIS higher than 55	13 ± 3	11 ± 6
% of time HR between 50 and 90 beats/min	100 (6) [b]	100 (10) [b]
% of time HR lower than 50 beats/min	0 (0) [b]	0 (0) [b]
% of time HR higher than 90 beats/min	0 (6) [b]	0 (10) [b]
% of time MAP lower than 60 mm Hg	6 (78) [b]	6 (87) [b]
% of time MAP lower than 50 mm Hg	0 (0) [b]	0 (3)*
% of time MAP higher than 135 mm Hg	0 (0) [b]	0 (0) [b]

$T_{BIS\ TARGET}$ = observed time required for reaching the target BIS (Bispectral Index) value; BIS_{PEAK} = observed BIS value at $T_{PEAK,\ BIS}$; $T_{PEAK,\ BIS}$ = observed time required for reaching maximal drug effect (lowest BIS value); T_{EQ} = observed time required for reaching the target value after the initial overshoot; HR = heart rate; MAP = mean arterial blood pressure.

[a] = only 16 out of the 20 patients returned to BIS target during the entire case.

[b] = these data are presented as median (range).

* = P<0.05 between groups

RESULTS

Similar population demographics were found between groups for age, weight and height (Table 1). No patients were excluded and all data captured by the recording system were included in the analysis. The observations made at LOC are listed in Table 2. Some longer induction times are noticed in the closed-loop control group. Other clinical parameters during induction revealed some statistical differences without clinical relevance.

Times until first surgical stimulus (not shown), duration of anesthesia and total amount of propofol used were similar in both groups. The performance of the hypnotic control using BIS during the induction phase is shown in Table 3. Although slower induction time was observed, similar times to reach the target BIS were found in the closed-loop control group than the manual control group. However, the duration and magnitude of the initial overshoot in BIS below target was less pronounced in the closed-loop control group than the manual control group. The trajectory of BIS between start and termination of propofol (= the real duration of control) for all individual patients accompanied by the average value for the group versus time is plotted in Figure 2. As observed in parts A and B, significant lower BIS values and more interindividual variability were found in the manual control group, leading to a significant worse prediction error over time (parts C and D). Figures 3E and F show the individual and averaged CePROP between start and termination of propofol administration. It can be noticed that during and shortly after induction, the CePROP was lower in the closed-loop control group than manual control group. Additionally, Table 3 proves that the percentages of case time with accurate BIS control was

Significant differences were due to more too low BIS values in the manual control group. The overall performance of control for BIS is shown in Table 4. Performances are calculated from start to stop of the propofol infusion, except for divergence, which was analyzed from the moment of $T_{\text{BIS TARGET}}$ until stop of the propofol administration. It was chosen to use $T_{\text{BIS TARGET}}$ rather than T_{EQ} as, in the manual control group, not all patients reached the target BIS again. The overall better performance of BIS control in the closed-loop control group is also proven by analyzing the PE, MDPE, MDAPE, divergence and wobble which revealed all more advantageous results for the closed-loop control group compared to the manual control group.

significantly better in the closed-loop control group compared with the manual group.

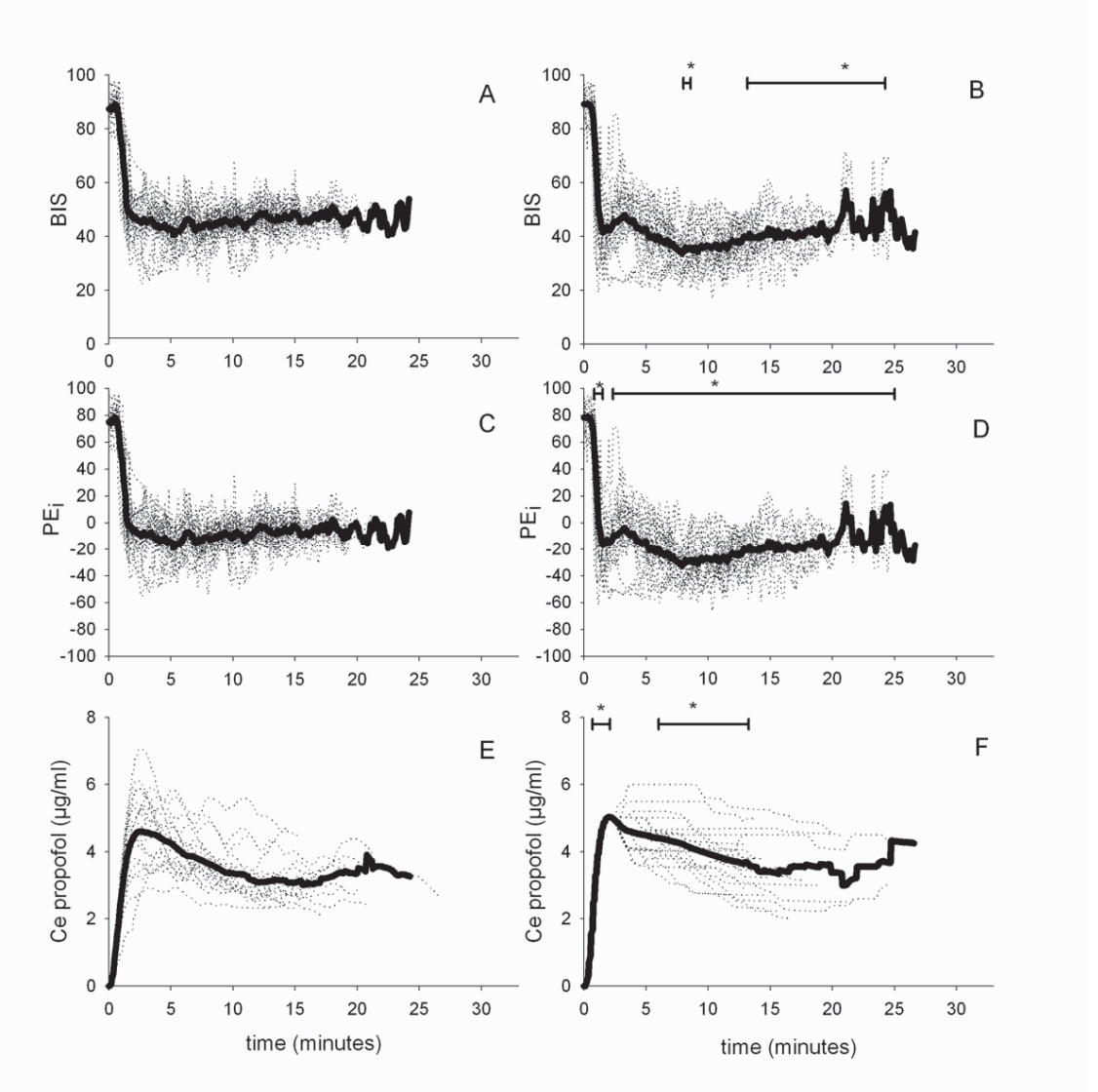

Fig. 2. *Individual (dotted line) and average (fat line) BIS (Bispectral Index), performance error (PE) and propofol effect-site concentration (CePROP) for closed-loop control (parts A, C and E) and manual control (parts B, D and F) group. For each patient, data are represented from start (time = 0) until stop of the propofol administration. - and * indicates the time period during the case that showed significance (P < 0.05) between groups*

Hemodynamic stability was similar in both groups without dangerous alterations due to inaccurate control. Similar trends in heart rate were found during the cases in both groups (Figs. 3A and B). No long-lasting incidences of brady- or tachycardia were noticed (Table 3). As shown in figure 3 (C and D), lower blood pressures were observed in the closed-loop control group compared to the manual control group between 300 and 600 s from the start of the propofol administration. However, this didn't result in a higher incidence of moderate nor severe hypotension (Table 3). No episodes of hypertension were observed in both groups (Table 3). No patients had respiratory depression leading to a drop in saturation (data not shown).

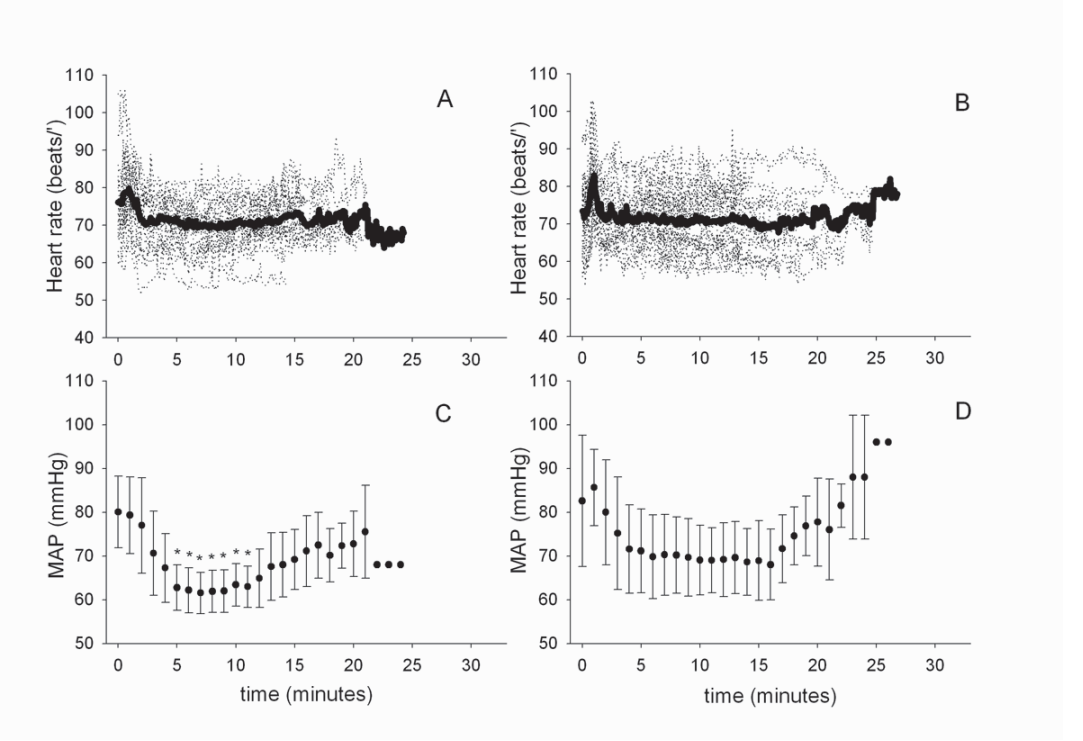

Fig. 3. *Individual (dotted line) and average (fat line) heart rate from start until stop of the propofol administration for the closed-loop control (A) and manual control (B) group. MAP (mean ± SD) for closed-loop control (C) and manual control (D) group. * P < 0.05 between groups.*

Table 4. *Performance of Control for BIS From Start Until Termination of Propofol Administration*

	Closed-loop control	Manual-control
Average PE (%)	-2.91 ± 24.49*	-14.17 ± 28.88*
MDPE (%)	-7.78 ± 3.46*	-19.96 ± 8.38*
MDAP (%)	11.51 ± 4.0*	24.06 ± 8.01*
Divergence (% min)	-0.009 ± 0.012[a]	0.004 ± 0.025[a]
Wobble (%)	8.44 ± 2.84*	11.48 ± 4.19*

PE = prediction error; MDPE = median prediction error, MDAPE = median absolute performance.

[a] Divergence was calculated from the moment of $T_{BIS\ TARGET}$ until termination of the propofol infusion

** = P < 0.05 between groups.*

At the end of the procedure, propofol administration was stopped. BIS and CePROP were similar between groups at the end of the propofol administration. Recovery times were recorded. As shown in Table 2, times until opening of the eyes and orientation were significantly shorter in the closed-loop control group than the manual control group.

Movements were recorded. In the closed-loop control group, 7 patients showed allowed and 4 not allowed movements. In the manual control group, 3 patients showed allowed and 5 showed not allowed movements. None of these events leaded to complications other than short lasting interruption of the retrieval procedure. In the closed-loop control group, overall quality of anesthesia received a 94 % (11 %) score compared to a 89 % (17 %) score in the manual control group.

Figure 4 demonstrates the functionality of the Bayesian modeling. Parts (A) and (B) show a clear change over time of the calculated EC_{50} and estimated delay. As γ is not estimated, it has a constant value, as well as E_0 and E_{MAX} (not shown).

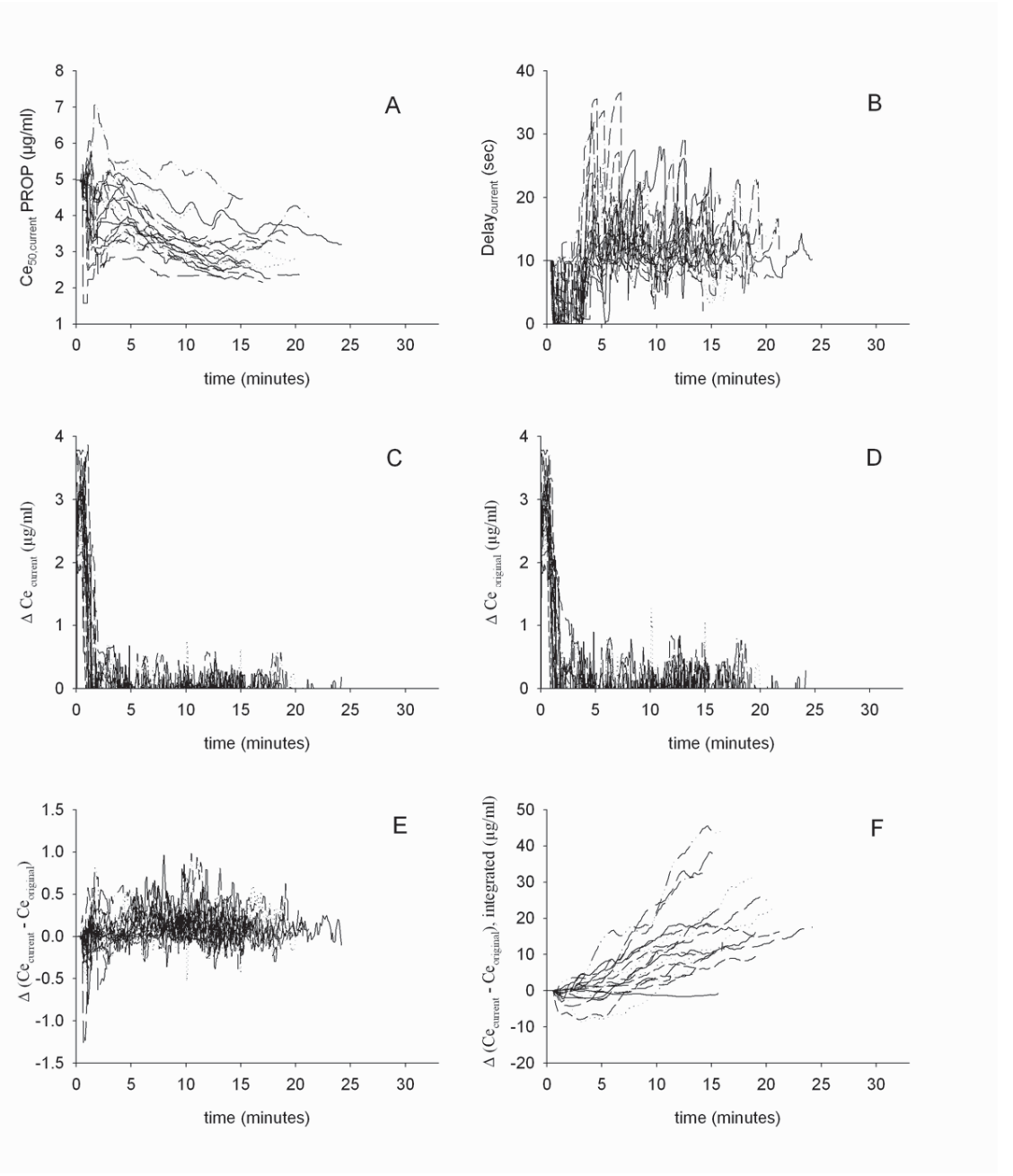

Fig. 4. *Functionality of the Bayesian modeling. Parts (A) and (B) show the change over time of the calculated EC_{50} and estimated delay. Part C demonstrates the control action that was executed by the controller using the Bayesian-optimized curve, compared to a hypothetical controller that would use the unchanged typical values (Part D). Part E plots the difference between these control actions to*

enlarge the scale. Part F shows the integration over time (F) to demonstrate the cumulative difference of the data points shown in part E.

More illustrative than the covariate values is the difference in control behavior, represented in Figures 4C and D. Part C demonstrates the control action that was executed by the controller using the Bayesian-optimized curve, compared to a hypothetical controller that would use the unchanged typical values (Part D). Unlike pharmacokinetic datasets, a closed-loop control dataset cannot be compared against multiple control algorithms since the *post hoc* calculated control actions cannot have a real effect on the patient. Each sample point in Figure 4D therefore should be regarded as an instantaneous hypothetical control to be applied on the patient's state realized by the control history of the original controller. Consequently, all controllers with identical steady-state behavior will show an average control difference close to zero most of the time. Part E plots the difference between these control actions to enlarge the scale. To verify the net effect of the control difference, the control differences were integrated over time (Part F) demonstrating the cumulative control difference.

DISCUSSION

It was hypothesized that the implementation of Bayesian technology into our previously described and validated [171] patient-individualized, adaptive, model-based closed-loop control system would allow us to overcome previous limitations of existing systems hereby guaranteeing clinical feasibility and accuracy. We found that our closed-loop control system titrated propofol administration accurately resulting in BIS values close to the set point. The closed-loop control system was able to induce the patients within clinically accepted time limits and with less overshoot than the manual control group. Automated control resulted in beneficial recovery times. Our closed-loop control group showed acceptable performance compared to the manual control group specified by similar hemodynamic, respiratory stability, comparable movement and quality scores.

The design of this investigation was carefully considered. In previous work from our group [54], some of our methodology was criticized as propofol was titrated manually in our control group to achieve set points that are commonly used during anesthesia, *i.e*., blood pressure, heart rate, and sympathetic tone while using BIS in the closed-loop control group [107]. Therefore, in this study we allowed the clinician to see and use the BIS online and to use similar TCI algorithm and titration limits as the closed-loop control system in order to approach the closed-loop control group methodology as close as possible. Although our closed-loop control system would have been able to compensate for interindividual variability, we aimed at studying a very homogenous patient population. As a result, the only real difference between the two study populations was the automated or manual control of the hypnotic component of anesthesia. As stated in an editorial by Glass and Rampil [107], it is important to underline the critical role of analgesia in the performance of hypnotic control. High dosages of opiates will dampen the arousal effects caused by a noxious stimulus [180] hereby requiring much smaller adjustments in propofol concentration. As the ovum retrieval procedure only requires a small dose of opiates, the performance of control was not influenced by high opiate concentrations. The noxious stimuli during this procedure are very homogeneous in all patients. Additionally, as all patients were aimed at breathing spontaneously and could move during the procedure, this introduced a lot or performance challenges for both human and automated control. This closed-loop controller is able to manage both induction of anesthesia and pharmacodynamic changes during the case. This is due to the application of the Bayesian optimization technology. For the induction, we showed that our closed-loop control system performed better compared to the manually induced

patients with similar times to reach the set point but with less overshoot and faster return to the set point after the initial overshoot, even though both the closed-loop controller and the clinician in the manual control group started with a same CePROP target of 5 μg/ml. The beneficial results for closed-loop control are due to the fact that the closed-loop controller will correct faster (even during the bolus) when individual patient drug response (BIS change) becomes available while a human operator will "wait and see" before he/she corrects.

During maintenance, the clinical performance goal of any control system, both human and automated, is to provide tight control. For BIS, adequate levels of control were defined as having a BIS value within ± 10 BIS units of the set point [171]. Table 3 demonstrates that closed-loop control offered accurate control during significantly more percentages of case time. Hereby, it is important to state that the analyzed time period starts and stops at start and termination of propofol administration, so includes the induction phase. In this study, induction is an integral part of the control period and included in the analysis. In the manual control, it can be observed that a too deep level of anesthesia caused worse control.

Additionally, robustness of the controller should be proven. O' Hara and colleagues [5] proposed the goals of control in anesthesia as (1) keeping the average value of the controlled variable within defined limits; (2) minimizing oscillations in the controlled variable within these limits, and (3) guaranteeing stability so that over time the size of the oscillations either becomes smaller or remains constant at an acceptable level, rather than increasing. A mathematical interpretation of these criteria can be found in Varvel and co-workers [29] for computer-controlled infusion pumps, which can be applied on closed-loop controller performance after minor modifications [171]. As observed in Table 4 and Figure 2, overall and time specific PE's were significantly better in the closed-loop than manual control group. All derived performance parameters (MDPE, MDAPE, divergence, and wobble) were significantly better in our closed-loop control group compared to the manual control group.

Hereby, it is important to underline that the results of the closed-loop controller are clinically acceptable alone, even without comparing it with a manually controlled group. The performance results from the manual control group can be used to have an idea of the performance of the trained clinician and as such, to compare absolute performance values. MDPE indicates the bias of the

controller without revealing any information neither on dynamic or higher-frequency behavior nor on the amplitude of possible oscillations in control. Note that MDPE is a signed value and thus represents the direction (over- or underprediction) of the performance errors rather than the size of the errors, which is represented by MDAPE. Even though MDAPE does not indicate the sign of a possible bias, it describes both the amplitude of possible bias as well as all other errors that prevent the controller from approaching the control target. Note that MDPE is negative when applying our closed-loop control system, which indicates that the system tends to overdose, leading to BIS levels below target. This can be attributed to the fact that closed-loop control for drug delivery performs, in essence, an asymmetric control operation. They only govern the infusion, not the elimination of drug from the body, which is a slower process. This phenomenon has been observed in our earlier studies as well[54]. Divergence and wobble indicates to the oscillation of the controller behavior (wobble) and the tendency of the controller to converge on the target over a longer time (divergence). A negative divergence number indicates convergence to the target. The absolute value indicates the speed of convergence or divergence. As shown in Table 4, the divergence in the closed-loop control group shows an average negative number in contrast to the manual control group. A careful interpretation of Figure 2D shows that, after initially reaching the target, the manual control group drifts to significantly lower BIS values needing more time to correct. This episode might remain dominant in the divergence number, falsely suggesting that control in the manual control group will keep on diverging. This, obviously, does not reduce the significance of the negative divergence in the control group.

Whereas model based adaptive control is not new, the integration of Bayesian methods for model estimation is a new method. The Bayesian approach individualizes population based parameter values according to patient-specific knowledge acquired during treatment. As a clear deviation is seen between the controller based on the Bayesian-estimated curve and a hypothetical controller using the unchanged typical values, the added complexity is justified.
The net positive sum in Figure 4F demonstrates that, on average, the Bayesian controller causes a faster response for drug increase than the original controller, except for one patient where the accumulated difference remains close to zero. The change in typical value is apparent for the ce50 and delay, which are estimated in the Bayesian approach. In spite of γ being held constant, the slope of the

curve will still change during the case. This is illustrated by plotting the concentration changes proposed by the two controllers.

A significantly better recovery profile was observed in the closed-loop control group than the manual control group, both for time until opening of the eyes and saying name and birth date. Because of the short duration and homogenous characteristics of the procedure, the differences in recovery times are perhaps clinically less important than found in previous work with longer cases [54]. As neither BIS nor CePROP were different at the end of the propofol infusion although we found a longer recovery times in the manual control group and more propofol given, the dosing history and its related context sensitive decrement times might be responsible for the differences in recovery profiles.

Before being able to introduce automated control into clinical practice, it has to be proven that it is as clinically feasible as manual control[107]. Therefore, the presence of a control group where a human operator is in charge of controlling a similar system under similar circumstances is essential, as neither well-described criteria nor guidelines are available in the literature. We found that our closed-loop control system resulted in similar hemodynamic and respiratory stability than manual control. Even though some lower MAP was found just after induction, no episodes of severe hypotension or hypertension were found. Heart rate and saturation remained as stable as in the manual control group. It is important to state that patients remained breathing spontaneously which is challenging for whatever control system. During these procedures, patients were allowed to move their feet, hands or head. However the upper legs and pelvis should remain steady as this might result in a short lasting interruption of the retrieval and will upset the gynecologist. Similar results for movement and overall score were found. These results indicate the stability of control under difficult conditions for the operator. It has to be noted that movement response was not and cannot be controlled with a closed-loop control system, as it depends on the given dose of antinociceptive drugs. At its best, control of the hypnotic component of anesthesia can manage possible arousal reflexes caused by nociceptive stimuli.

It has to be stressed that one should be careful not to extrapolate these results for other patient groups. This was a first feasibility study and as such, we cannot claim full clinical safety, accuracy or utility. To reach this goal, a large multicenter study is required to investigate the behavior of the system in various populations and specific surgical situations. Additionally, the design and implementation of intelligent alarm systems have to be considered. Although the anesthesiologist in

charge of the manual control group has been never involved in the development of this closed-loop system, we accept the possible limitations and bias.

This study has demonstrated our closed-loop control system accurately administers propofol. The realized BIS values are close to the set point, the induction is completed within clinically acceptable time limits but less overshoot than the manual control group, and patients in the closed-loop group wake up faster. This performance is combined with an acceptable robustness. Benchmarking our closed-loop group to a manual control group showed similar hemodynamic and respiratory stability, as well as comparable movement and quality scores.

Chapter 8

Accuracy of the Composite Variability Index as a measure of the balance between nociception and antinociception during anesthesia.

Modified from : Sahinovic MM, Eleveld DJ, Kalmar AF, Heeremans EH, De Smet T, Seshagiri CV, Absalom AR, Vereecke HE, Struys MM: Accuracy of the Composite Variability Index as a Measure of the Balance Between Nociception and Antinociception During Anesthesia. Anesth Analg 2014; 119: 288-301

Background: The CVI (Composite Variability Index), derived from the electroencephalogram, was developed to assess the antinociception-nociception balance whereas the BIS (Bispectral Index) was developed to assess the hypnotic state during anesthesia. We studied the relationships between these indices, level of hypnosis (BIS level) and anti-nociception (predicted remifentanil effect-site concentrations, CeREMI) before and after simulation. Also, we measured their association with movement in response to a noxious stimulus.

Methods: We randomized 120 patients to one of 12 groups targeting different hypnotic levels (BIS 70, 50 and 30) and various CeREMI (0, 2, 4 or 6 ng/ml). At pseudo-steady state, baseline values were observed and a series of stimuli were applied. Changes in BIS, CVI, heart rate (HR) and mean arterial blood pressure (MAP) between baseline and response period were analyzed in relation to level of hypnosis, anti-nociception, and somatic response to the stimuli.

Results: CVI and BIS more accurately correlate with somatic response to an Observer Assessment of Alertness and Sedation-noxious stimulation than HR, MAP, CeREMI and propofol effect-site concentration (Tukey post-hoc tests $P < 0.01$). Change in CVI is more adequate to monitor response to stimulation than changes in BIS, HR or MAP (as described by the Mathews Correlation Coefficient with significance level set at $P < 0.001$). In contrast, none of the candidate analgesic state indices was uniquely related to a specific opioid concentration and is extensively influenced by the hypnotic state as measured by BIS.

Conclusions: CVI appears to correlate with somatic responses to noxious stimuli. However, unstimulated CVI depends more on hypnotic drug effect than on opioid concentration. (*Anesth Analg 2014*; **119**: 288-301)

INTRODUCTION

The cerebral effect of hypnotic drugs can be monitored by means of validated monitors that analyze and condense information derived from the EEG into a single value in order to simplify interpretation [82]. Less progress has been made with development of objective indices of the analgesic state. The development and validation of such indices is important since optimal analgesic titration during anesthesia might reduce total drug consumption and ultimately improve clinical outcomes [181-183].

The analgesic state is the net physiological result of the simultaneously opposing effects of nociceptive stimulation (e.g., surgery) and antinociceptive (analgesic) medication [184].

An imbalance between nociception and antinociception may result in somatic (movement), autonomic (cardiovascular) and/or arousal (an apparent decrease in the hypnotic component of anesthesia) reactions. Nociception-induced arousal responses during anesthesia result from the activation of brainstem arousal systems [185] by ascending sensory signals, which lead to cortical activation. These arousal reactions can be blunted by administering antinociceptive medication such as opioids that attenuate ascending sensory traffic and inhibit activation of sub-cortical arousal systems [186]. Very high concentrations of hypnotics can also blunt arousal reactions, even in the absence of analgesics; in the case of propofol this is predominantly achieved by suppression of cortical activity and responsiveness [187]. Interestingly, in the absence of hypnotics, even high doses of opioids are unable to fully attenuate these arousal responses. These phenomena illustrate the complex interaction between hypnotics and analgesics [188].

Recently, an EEG-derived index of the analgesic state has been introduced, described as the CVI[189]. CVI was developed as an index of the combined variability of the BIS and electromyographic power (EMG) measured by frontal electroencephalographic electrodes and increases in CVI have been associated with intraoperative somatic responses [189]. Recently, Ellerkmann et al. [190] studied the influence of remifentanil on CVI and tested the ability of CVI to predict patient movement, following a noxious stimulus. In all patients, CePROP was titrated to maintain a BIS between 35 and 65. However, they did not study the effect of the hypnotic level on CVI. They concluded that changes in CVI following a noxious stimulus were dependent on the CeREMI and change in CVI correlated with movement significantly better than changes in HR and noninvasively measured MAP. However, since some indices of the analgesic state such as movement and autonomic reactions might be influenced by the level of hypnosis, the performance and use of CVI may not be equal at all levels of hypnotic drug effect (as titrated using BIS) nor at all levels of antinociception (using CeREMI as a surrogate).

The aim of this study was to investigate the relationship among CVI, BIS, and CeREMI across a wide range of hypnotic and antinociceptive levels, both with and without nociceptive stimulation. We also assessed the correlation of different thresholds for each measure with the probability of responsiveness and tolerance to stimulation. We considered HR and MAP as measures because they are still clinically used to titrate hypnotic and analgesic administration.

METHODS

After institutional ethics committee (University Medical Hospital Groningen, The Netherlands) approval and registration at ClinicalTrials.gov (NCT01053611), written informed consent was obtained from 147 ASA physical status I and II patients, aged 18 – 65 years, scheduled for surgery requiring general anesthesia. Complete group allocation is reported in Figure 1. Exclusion criteria were: weight < 70% or > 30% of ideal body weight, use of loco-regional anesthetic techniques, neurological disorder or any condition or treatment that could potentially interfere with cardiovascular status or level of consciousness during the induction. After exclusion, 120 patients were randomly allocated to 1 of 12 study groups (3 x 4 groups of 10 patients) to receive propofol with or without remifentanil infusions. Cohorts of 10 patients per group were used as a convenience sample based on previous drug interaction studies [180, 191, 192].

On arrival in the operating room, an IV cannula was inserted in the nondominant hand or forearm. All patients received an IV infusion of crystalloid solution, at a rate of 500 cc/h, to deliver the required drugs and fluids during the study period. The study was performed before any surgical intervention in a quiet operating room. Standard vital signs monitoring was used, including EEG, hemodynamic and respiratory monitoring. Frontal EEG activity was recorded using a Vista BIS monitor with 4 electrodes (BIS™ Quatro Sensor). The cerebral drug effect was monitored using the BIS, derived from the raw frontal EEG. BIS electrodes were placed as recommended by the manufacturer. HR, 3-lead electrocardiogram, capnography and pulse oximetry were recorded continuously, and noninvasive MAP was recorded every minute using a Philips IntelliVue MP50 (Philips, Eindhoven, The Netherlands) monitor. Numerical and waveform data were recorded electronically using RugloopII© software. The raw EEG was recorded at a rate of 128 Hz and stored for post hoc analysis.

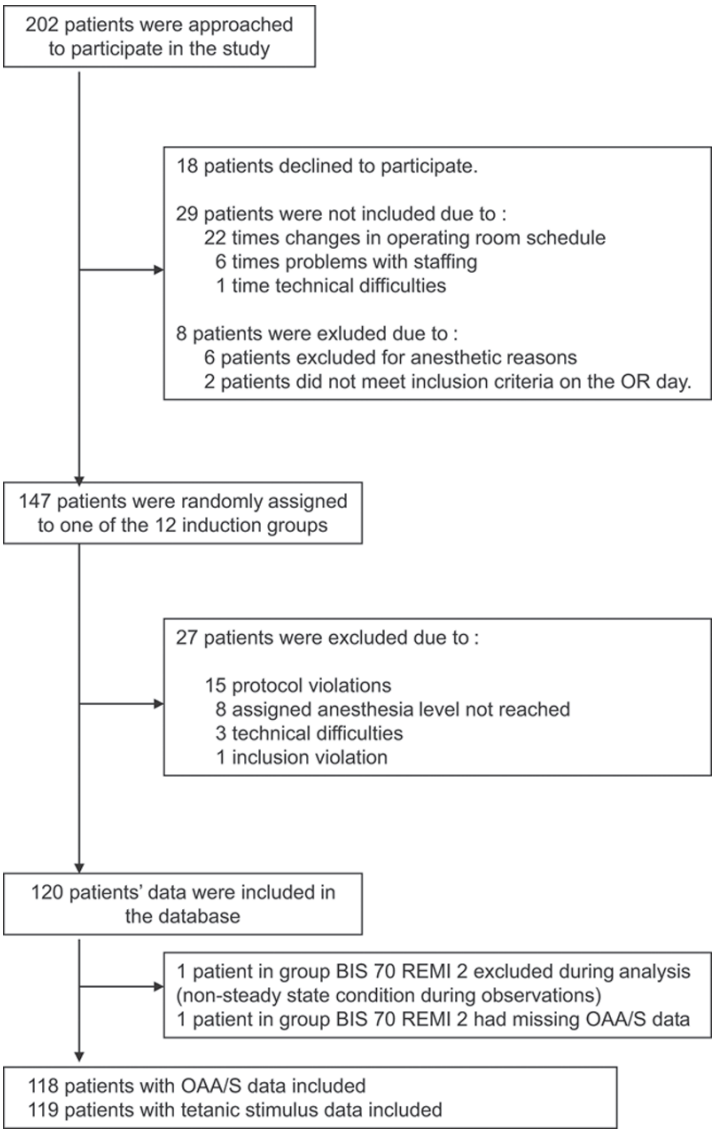

Fig. 1. Consort guideline inclusion strategy

Patients were allocated to one of the 12 groups by stratified randomization. Three different hypnotic levels, "light" "intermediate" and "deep" were allocated to BIS targets of 70, 50 and 30, respectively. Within each of the hypnotic levels, patients were randomized into 4 groups receiving predicted CeREMI of 0, 2, 4 or 6 ng/ml. To ensure that the intended hypnotic level was achieved, a previously published and validated BIS-guided closed-loop system [91] was used for propofol administration. Propofol and

remifentanil predicted concentrations were calculated using the Schnider and Minto model, respectively [23, 24, 36, 37]. The specific remifentanil concentrations were selected to cover a clinically relevant spectrum of antinociception.

The timeline of the study is shown in Figure 2. All event times are reported in seconds relative to the start of the Modified Observer Assessment of Alertness and Sedation (OAA/S) evaluation. For each patient, a target-controlled infusion system for remifentanil infusion was started at the beginning of each study, targeting the allocated predicted remifentanil effect-compartment concentration. The start of the remifentanil infusion was defined as -1080 seconds. Three minutes later (900 seconds before the start of the OAA/S scale evaluation), the closed-loop controlled propofol infusion was started, targeting the allocated BIS level. Immediately after loss of consciousness, a laryngeal mask airway was inserted to maintain a patent airway (in patients who remained responsive to verbal commands a tight-fitting facemask was used to administer oxygen). If required, manually assisted ventilation was performed to maintain oxygenation and normocapnia. At 30 seconds before the start of the OAA/S scale evaluation, CePROP and CeREMI were assumed to be sufficiently close to steady-state equilibrium. At this time, the propofol closed-loop infusion was switched to an open-loop target-controlled administration, and the effect-site target concentration was fixed at the “steady-state” CePROP last achieved by the closed-loop infusion system. This approach ensured that CePROP remained stable during the response period (Fig. 2) and that arousal in the BIS signal, if present, could be attributed to the stimulus.

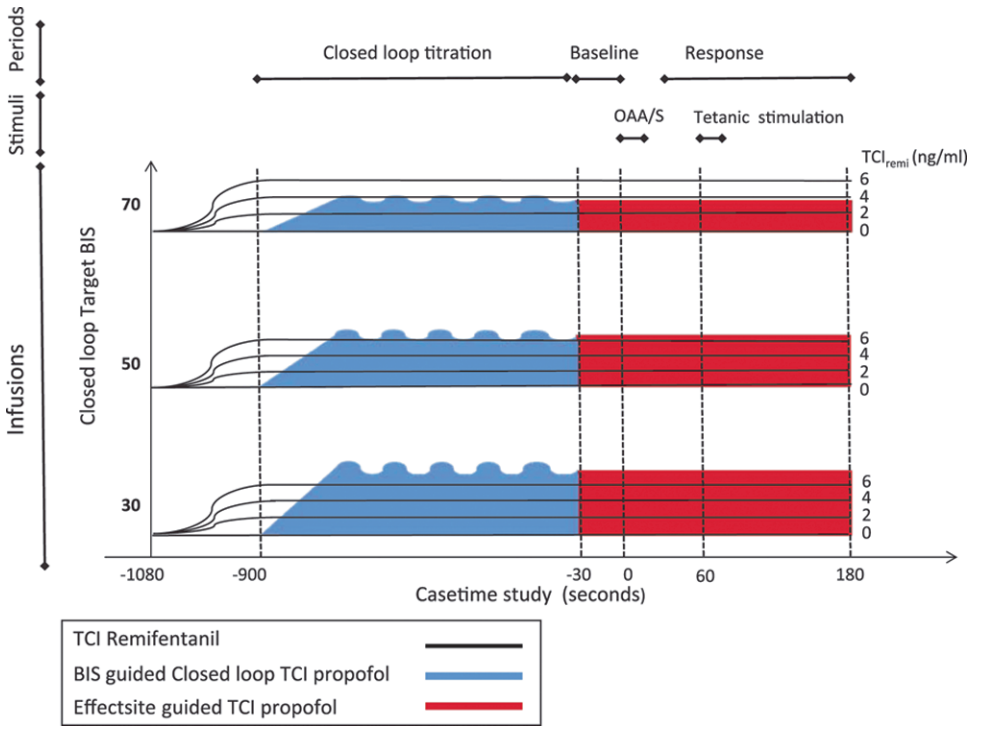

Fig. 2. *Study timeline*

Table 1. *The Distribution of the OAA/S Scale Registered During the Study and Patients Classified as Responders to Tetanic Stimulation, Shown as Number of Patients*

	OAA/S scale 0/1/2/3/4/5			
	REMI 0	**REMI 2**	**REMI 4**	**REMI 6**
BIS 70	2/0/0/1/2/5	4/0/2/2/0/0	6/3/1/0/0/0	6/2/1/0/0/1
BIS 50	3/7/0/0/0/0	10/0/0/0/0/0	10/0/0/0/0/0	10/0/0/0/0/0
BIS 30	10/0/0/0/0/0	10/0/0/0/0/0	10/0/0/0/0/0	10/0/0/0/0/0
	Tolerant/responsive to the combined OAAS/tetanic stimulus*			
	REMI 0	**REMI 2**	**REMI 4**	**REMI 6**
BIS 70	1/9	5/4	8/2	9/1
BIS 50	3/7	10/0	10/0	10/0
BIS 30	9/1	10/0	10/0	10/0

Applied OAA/S scale: 5 = Responds readily to name spoken in normal tone; 4 = Lethargic response to name spoken in normal tone; 3 = Responds only after name is called loudly and/or repeatedly; 2 = Responds only after mild prodding or shaking; 1 = Responds only after painful trapezius squeeze; 0 =

No response after painful trapezius squeeze. OAA/S = Modified Observer Assessment of Alertness and Sedation; BIS = Bispecral Index; REMI = Remifentanil

**= For ethical reasons, patients who scored an OAA/S of 5 didn't receive a tetanic stimulus and were considered responsive.*

At timepoint "0 seconds", we applied the sequence of stepwise, graded stimuli of the OAA/S scale [193] (Table 1). Stimuli for OAA/S values between 5 and 3 focus on the hypnotic component of anesthesia while those for 2 or lower contain a nociceptive component. Sixty seconds after the start of the OAA/S scale evaluation, defined as "60 seconds", patients received a 30-second long (100 Hz, 60 mA) electrical stimulus [194, 195]. The stimulation electrodes were placed over the ulnar nerve on the volar side of the wrist. The presence or absence of purposeful movement in response to tetanic stimulation was noted by the observer. For ethical reasons, patients who scored an OAA/S of 5 didn't receive a tetanic stimulus and were considered responders. All observations were continued until 180 seconds after the start of the OAA/S scale evaluation.

We used CeREMI as a measure of the level of antinociception, a standardized stimulus as nociception and the observed BIS as the measure of the degree of hypnosis. Individuals with an OAA/S score of 0 and no movement in response to tetanic stimulation were considered tolerant (=non-responders) while individuals with an OAA/S greater than 0 and/or purposeful movement in response to tetanic stimulus were considered responsive (=responders). The systematic application of OAA/S and tetanic stimulation as performed in this study was treated as 1 stimulation sequence.

Offline analysis of the recorded raw electroencephalogram was later performed to calculate CVI (v2.1). CVI, which has previously been described [189] is a weighted combination of BIS, sBIS and sEMG, where sBIS is the standard deviation (SD) of the BIS signal over the previous 3 minutes, and sEMG is the SD EMG over the previous 3 minutes. BIS is derived from the electroencephalogram power in the frequency band from 0 to 47 Hz using a proprietary algorithm based on the fixed, weighted combination of several subparameters, including β-ratio, SynchFastSlow, QUAZI, and burst suppression ratio. EMG is a measure of the power of the signal in the frequency band between 70 and 110 Hz recorded using the frontal electrodes of the BIS monitor. The fixed-weighted combination of BIS, sBIS, and sEMG results in CVI, which is a dimensionless index that ranges between 0 and 10 with lower values indicating an ideal balance between nociception and antinociception. The applied weights for BIS, sBIS and sEMG into the CVI calculation and specific artifact filters are proprietary.

STATISTICAL ANALYSIS

The measures considered during the analysis were BIS, CePROP, CeREMI, CVI, HR and MAP. We defined 2 analysis periods relative to timing of the application of OAA/S: (1) the baseline period, from -30 to 0 seconds and (2) the response period, from 45 to 180 seconds after the start of the OAA/S scale evaluation. The tetanic stimulus was applied during the response period (always given at 60 seconds until 90 seconds after the start of the OAA/S scale evaluation). The value of a measure for an individual was defined as its median value over the relevant time period. For example, the baseline BIS for an individual was the median BIS observation over the period 30 seconds before until 0 second, the start of the OAA/S scale evaluation.

In addition, we calculated for each individual patient (i) the change in measure as a result of stimulation as the difference between baseline and response value, defined as below:

$$\Delta parameter_i = median(parameter_{response,i}) - median(parameter_{baseline,i})$$

Median values are used to reduce the possibility of imbalanced noise and outlier observations unduly influencing the estimate of the typical value of a signal during the period.

To explore relationships between the measures and Baseline BIS or CeREMI, we performed a linear regression analysis between each measure (CVI, HR and MAP) and Baseline BIS or CeREMI and determined the coefficient of determination (R^2) for each pair. In addition, a Pearson product-moment correlation coefficient (ρ) between CVI, HR and MAP versus Baseline BIS or CeREMI was calculated. Significance of this correlation, defined as a 95% confidence interval excluding 0, was determined.

For all the measures, descriptive statistics were investigated for each group. Two-way analysis of variance with Tukey post hoc test was done to analyze differences between various CeREMI levels or various BIS levels. Significance level was set at 5 %.

The ability of the measures (BIS, CVI, CePROP, CeREMI, HR and MAP) to correlate with the observed tolerance or responsiveness to the combined OAA/S-noxious stimulus was evaluated using the prediction probability (P_K), which compares the performance of the measures having different units, as developed by Smith et al. [196, 197] and described previously in anesthetic research [53, 198]. Briefly, consider a variable such as BIS, CVI, etc… and a "gold standard" such as the observed tolerance or response to the combined OAA/S-noxious stimulus. Then, a P_K of 1 for the measure would mean that that measure always shows higher values when the patient responded to the combined OAA/S-

noxious stimulus. Alternatively, a P_K value of 0.5 would mean that the specific variable is useless for measuring the clinical response. For CePROP and CeREMI, this relationship was inverted. The jack-knife method was used to compute the standard error (SE) of the estimate, based on the assumption that all assessments were independent. Prediction probability was calculated using a custom spreadsheet macro, P_KMACRO, developed by Smith et al. [196, 197].

For the clinician, it is important to know the cutoff (threshold) values at which the measure can maximally discriminate responders and nonresponders, and also the sensitivity and specificity of this value [199]. Practically, this is the answer to the question: "which number should I put as alarm limit for BIS, CVI, … on my vital signs monitor to detect responsiveness and how accurate is this value?" As P_K calculations only offer a general impression of accuracy, this question should be answered by using sensitivity/specificity analysis. As such, the number of false positives (FP), false negatives (FN), true positives (TP), and true negatives (TN) were determined at each threshold. From these values, we calculated the positive and negative predictive values (PPV=TP/(TP+FP) and NPV=TN/(TN+FN)). PPV is the proportion of individuals with a measure value higher than the threshold (claiming somatic responsiveness) that are observed as responders. NPV is the proportion of individuals with a measure value lower than the threshold (claiming somatic tolerance) that is observed as nonresponders. We considered an appropriate range of threshold values for each measure and determined whether the observed value for each individual was greater (or less) than the threshold. For CePROP and CeREMI, this relationship was inverted. Good classifiers have some threshold where both PPV and NPV are close to 1.

To determine which threshold value offers the best discrimination and accuracy, we determined an optimal threshold by the maximum of the Matthews Correlation Coefficient (MCC) with respect to the threshold, defined as below:

$$MCC = \frac{TP \cdot TN - FP \cdot FN}{\sqrt{(TP + FP)(TP + FN)(TN + FP)(TN + FN)}}$$

The MCC is a useful indicator of binary classifier performance, unaffected by differences in the sizes of the classes. It returns a value between −1 and +1, where +1 indicates perfect prediction, 0 no better than random prediction and −1 total disagreement between prediction and observation [200].

Significance level was determined by using the (2-sided) *t* test for correlation coefficients. We calculated the MCC value corresponding to a *P* value of 0.001.
Comparison between BIS, CVI, CePROP, CeREMI, HR and MAP for responders versus nonresponders was done using a *t* test.

RESULTS

All included patients completed the study. As described in Figure 1, data from 120 patients were analyzed. Characteristics of analyzed patients were similar between groups (data not shown). One individual from the BIS 70 REMI 2 group was not analyzed due to unstable predicted plasma propofol concentrations during the response period due to a user error when opening the closed-loop system. For another individual from the BIS 70 REMI 2 group the OAA/S response was not recorded. Table 1 shows the OAA/S scores registered during the study and the number of patients classified as responders to the OAA/S and/or tetanic stimulation.
For all groups combined, the individual measures (BIS, CePROP, CeREMI, CVI, HR and MAP) at baseline and during the response period are plotted for tolerant and responsive patients separately in Figure 3. It can be observed that the closed-loop control system for BIS performed well, showing peaks in density around the BIS targets of 30, 50 and 70 at baseline. As BIS closed-loop control was stopped before baseline measure, changes in BIS were observed during the stimulation period. Per protocol, both CePROP and CeREMI were stable at baseline and during the response period. De visu differences (especially in the inter-individual variability range) can be observed between tolerant and responsive patients for most of the measures.

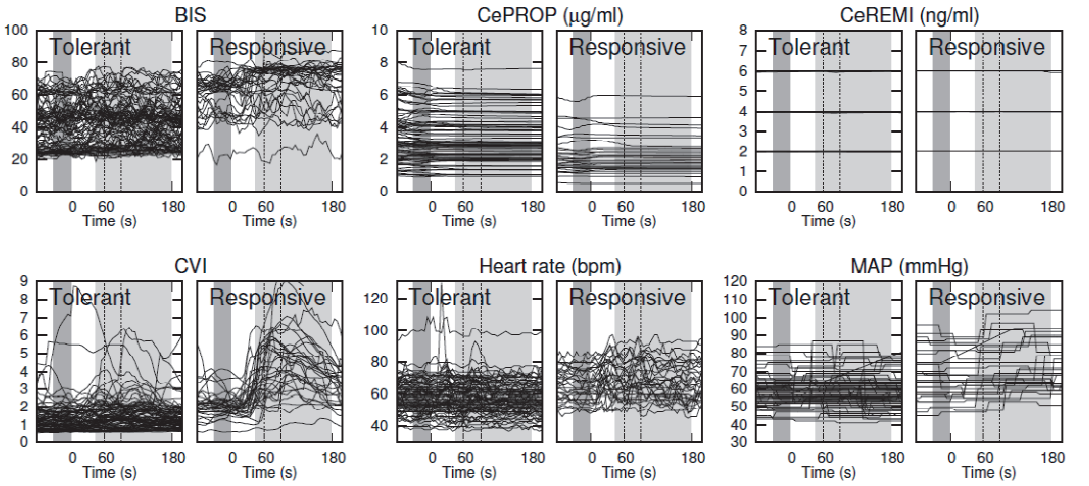

Fig. 3. R*aw data. Individual BIS, CePROP, CeREMI, CVI, HR and MAP for tolerant and responsive patients to a noxious stimulus. Time 0 is the moment of performance of OAA/S. Dark shaded area is the baseline period (0-30 s before OAA/S) and light-shaded area is the response period (45-180 s after OAA/S). Vertical dotted lines indicate the period of tetanic stimulation (60-90 s after OAA/S).*

Figure 4 displays the relationship between the individual median baseline, response CVI and ΔCVI versus Baseline BIS and CeREMI using 2-dimensional regressions. A significant correlation is shown between Baseline CVI and Response CVI versus Baseline BIS. More scatter is seen in the Response CVI versus Baseline BIS plot, resulting in a lower R^2. Although significant, ΔCVI shows a weak correlation and a lot of scatter versus Baseline BIS. No significant correlation is seen between CVI and CeREMI. We also detailed the mean (SD) CVI values for all groups separately. Table 2 shows the average of individual median CVI values during baseline and response period for all groups separately. Table 3 shows the data for ΔCVI. When the BIS target was 50, CVI values during both the baseline and response periods were higher when no remifentanil was given. For the BIS 70 and BIS 30 target levels, similar CVI values were found between various CeREMI. As stated before, for a given CeREMI, lower CVI values are seen at lower BIS targets for both baseline and response periods. Table 3 reveals very few significant differences in ΔCVI versus various BIS and CeREMI levels. As higher ΔCVI values were observed for all groups at targeted BIS of 70 and for the group BIS 50 – CeREMI 0 versus all more extensive drug levels, it seems there is a clear differentiation between these 2 cohorts of groups.

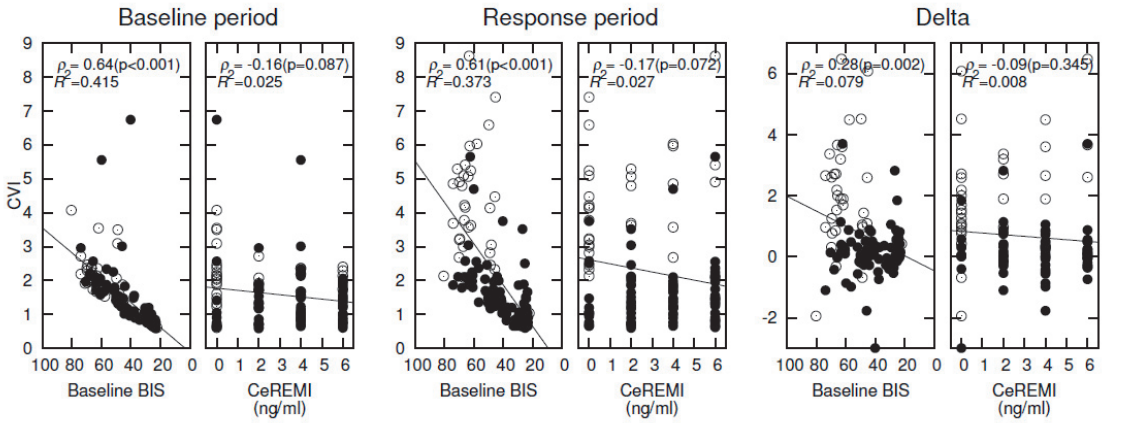

Fig. 4. *Linear regression analysis between baseline CVI, response CVI and ΔCVI versus Baseline BIS or CeREMI. R^2 = coefficient of determination for each pair. P = Pearson product-moment correlation coefficient. * = significance of the correlation, defined as a 95% confidence interval excluding 0. Each point is the median response for an individual over the indicated time-period. Filled circles represent individuals classified as tolerant, empty circles responsive individuals to the combined OAA/S-noxious stimulus.*

Figure 5 shows the relationship between the individual median baseline, response HR and ΔHR versus baseline BIS and CeREMI using 2-dimensional regressions, where only a weak correlation between ΔHR and Baseline BIS is observed. The relationship between Baseline and Response HR versus CeREMI is moderate, however, not resulting in a significant relation between ΔHR and CeREMI. For Baseline and Response HR, Table 2 shows a significant decrease when remifentanil is given at BIS levels 50 and 70. No overall differences in ΔHR are observed (Table 3). Figure 6 shows the relationship between the individual median baseline, response MAP and ΔMAP versus BIS and CeREMI. Similar to HR, MAP only reveals a significant relationship with CeREMI at Baseline and Response level, not resulting in significance for ΔMAP. No relationship with Baseline BIS is observed. These findings are confirmed in the detailed values shown in Tables 2 and 3.

For CVI, HR and MAP, the individual data for subjects who were tolerant (nonresponders) versus responsive (responders) to stimulation are plotted in figures 4-6. For CVI, de visu observation of Figure 4 shows a clear differentiation of responders and nonresponders in both baseline and response conditions. For HR and MAP, this is less clear. Table 4 shows the significantly different average values (with SD) of each metric between tolerant and responsive subjects. As differences in the mean are not

sensitive enough to observe the accuracy of differentiation, we tested the ability of the measures to differentiate responders versus nonresponders using the P_K assessment and the results are shown in Table 4.

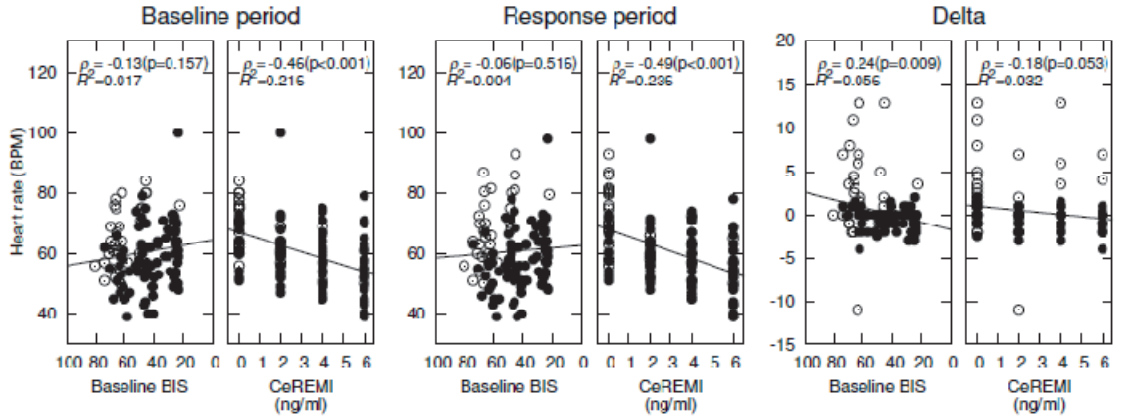

Fig.5. *Linear regression analysis between HR and ΔHR versus Baseline BIS or CeREMI. R^2 = coefficient of determination for each pair. P = Pearson product-moment correlation coefficient. * = significance of the correlation, defined as a 95% confidence interval excluding 0. Each point is the median response for an individual over the indicated time-period. Filled circles represent individuals classified as tolerant, empty circles responsive individuals to the combined OAA/S-noxious stimulus.*

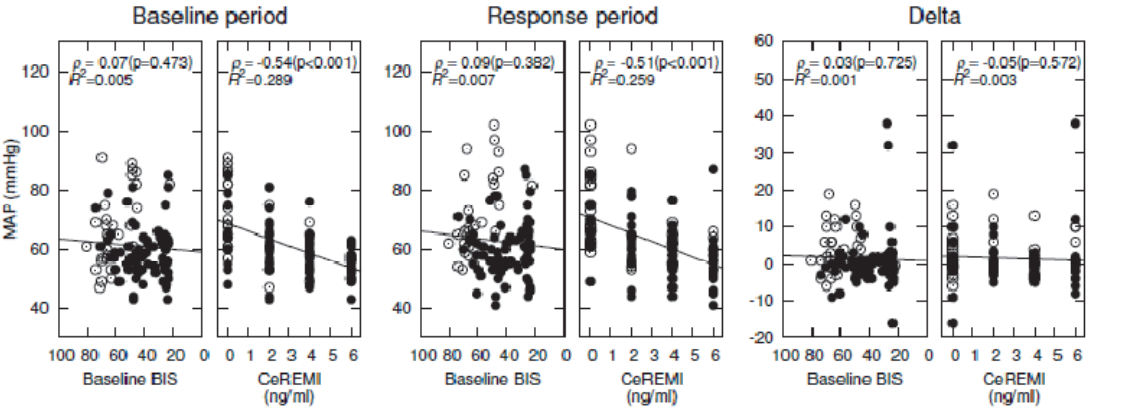

Fig. 6. *Linear regression analysis between MAP and ΔMAP versus Baseline BIS or CeREMI. R^2 = coefficient of determination for each pair. P = Pearson product-moment correlation coefficient. * = significance of the correlation, defined as a 95% confidence interval excluding 0. Each point is the median response for an individual over the indicated time-period. Filled circles represent individuals classified as tolerant, empty circles responsive individuals to the combined OAA/S-noxious stimulus.*

P_K values for BIS and CVI at baseline showed a similar and acceptable prediction probability. Other measures performed poorly. During the response period, CVI and BIS showed a good association with the response to the combined OAA/S-noxious stimulus. Other measures performed significantly less accurate. ΔCVI is a significantly better measure to monitor the response to stimulation than ΔBIS, ΔHR or ΔMAP, as depicted by a significant higher P_K value.

Figures 7-9 show the PPV and NPV for a range of thresholds (being specific measure values) for each measure to classify individuals as tolerant or responsive to the applied stimuli for the baseline, stimulation period and the change or "Δ" between baseline and response, respectively. In addition, the MCC is shown for each specific threshold, to indicate the binary classifier performance. Only the MCC values outside the shaded range are statistically significant. The highest (or lowest) MCC value indicates the best threshold value for discrimination. During baseline (Figure 7), similar performance was seen for BIS and CVI. The overall MCC values are only showing moderate performance (all values around 0.5). The highest MCC for BIS and CVI is found around a BIS of 60, and a CVI of 1.8. For the other measures, no meaningful thresholds can be defined indicating overall low performance. During the stimulation period (Figure 8), CVI performed the best followed by BIS. Maximum MCC values for BIS and CVI were 0.55 and 0.8, at BIS and CVI thresholds of 66 and 2.5 respectively. Thus, CVI shows better performance than BIS at their most accurate threshold values. Other measures showed poor performance without meaningful threshold values.

Figure 9 shows the accuracy of the change in values between baseline and stimulation period for each measure in relation to tolerance or response to stimulation. For ΔCVI, the highest combined PPV and NPV for a range of thresholds to detect tolerance/responsiveness to stimulation (being the value where the lines cross) is seen at a difference in value of 0.8 between tolerant and responsive subjects with an accuracy, defined by the MCC, of around 0.9. In contrast, ΔBIS was not useful to classify tolerance versus response, achieving an MCC of 0.4 at the value of highest combined PPV and NPV.

Table 2: *The average of individual median BIS, CePROP, CVI, heart rate and non-invasive median blood pressure values during the baseline and response periods.*

Baseline period		CeREMI 0 ng/ml	CeREMI 2 ng/ml	CeREMI 4 ng/ml	CeREMI 6 ng/ml
BIS 70	Measured BIS	68 (5)	67 (5)	64 (5)	64 (5)
	CePROP‡‡ (µg/ml)	1.87 (0.49)	2.00 (0.90)	1.49 (0.45)	1.23 (0.37)§
	CVI	2.55 (0.70)	2.07 (0.46)	2.33 (1.18)	2.01 (0.23)
	Heart rate (bpm)	67 (10)	59 (6)	55 (8)†	52 (6)†
	Non-invasive median blood pressure (mmHg)	68 (10)	61 (10)	59 (6)	54 (4)£
BIS 50	Measured BIS	47 (3)‡‡	48 (3)‡‡	44 (7)‡‡	46 (3)‡‡
	CePROP‡‡ (µg/ml)	3.40 (0.86)‡‡	2.81 (0.51)	3.28 (1.36)§§	2.60 (0.75)‡‡
	CVI	2.44 (1.70)	1.45 (0.22)‡‡	1.48 (0.76)	1.29 (0.18)‡, ‡‡
	Heart rate (bpm)	72 (10)	58 (6)¶	58 (11)#	56 (12)**
	Non-invasive median blood pressure (mmHg)	77 (11)	61 (11)	58 (8)	54 (5)
BIS 30	Measured BIS	26 (3)‡‡	26 (2)‡‡	29 (6)‡‡	29 (7)‡‡
	CePROP‡‡ (µg/ml)	4.68 (0.98)‡‡	4.43 (0.97)¶¶	4.06 (1.94)££	4.41 (1.57)‡‡
	CVI	0.73 (0.14)¶¶	0.80 (0.22)‡‡	0.91 (0.25)££	0.97 (0.40)‡‡
	Heart rate (bpm)	66 (7)	65 (14)	62 (7)	56 (10)
	Non-invasive median blood pressure (mmHg)	65 (13)	61 (10)	58 (6)	55 (5)
Response period					
BIS 70	Measured BIS	73 (5)	69 (8)	68 (7)	71 (8)
	CVI	3.67 (1.03)	3.49 (1.36)	3.55 (1.72)	3.81 (2.24)
	Heart rate (bpm)	70 (11)	59 (5)††	57 (9)*	52 (7)*
	Non-invasive median blood pressure (mmHg)	67 (8)	65 (13)	61 (5)	58 (6)
BIS 50	Measured BIS	52 (10)‡‡	49 (4)‡‡	45 (4)‡‡	48 (4)‡‡
	CVI	3.85 (1.89)	1.67 (0.46)*	1.37 (0.19)*	1.46 (0.25)*
	Heart rate (bpm)	73 (13)	58 (6)*	58 (11)*	55 (12)*
	Non-invasive median blood pressure (mmHg)	83 (14)§§	62 (11)*	57 (8)*	54 (5)*
BIS 30	Measured BIS	29 (5)‡‡	29 (6)‡‡	33 (6)‡‡	28 (5)‡‡
	CVI	1.06 (0.54)	1.12 (0.88)	1.24 (0.45)	0.89 (0.31)
	Heart rate (bpm)	66 (8)	64 (13)	61 (7)	56 (9)
	Non-invasive median blood pressure (mmHg)	69 (11)¶¶	61 (9)	58 (8)	58 (12)

CeREMI = predicted remifentanil effect-site concentrations; CVI = Composite Variability Index; BIS = Bispectral Index.

**P < 0.01 between R0 and R2, R4 and R6 (within same BIS level).*

†P < 1.01 between R0 and R4, R6 (within same BIS level).

‡P = 0.0464 between R0 and R6 (within same BIS level).

§P = 0.0307 between R2 and R6 (within same BIS level).

£P < 0.01 between R0 and R9 (within same BIS level).

¶P = 0.0278 between R0 and R2 (within same BIS level).

#P = 0.02755 between R0 and R4 (within same BIS level).

***P < 0.01 between R0 and R6 (within same BIS level).*

††P = 0.03 between R0 and R2 (within same BIS level).

‡‡P < 0.01 between BIS 70. BIS 50 and BIS 30 (within same CeREMI category).

§§P = 0.02 between BIS 70 and BIS 50 (within same CeREMI category).

££P < 0.01 between BIS 70 and BIS 30 (within same CeREMI category).

¶¶P < 1.01 between BIS 50 and BIS 30 (within same CeREMI category).

Table 3. *The average (Standard Deviation) of Individual Median ΔMeasured BIS, ΔCVI, ΔHeart Rate and ΔNoninvasive Median Blood Pressure Values.*

Response		REMI 0	REMI 2	REMI 4	REMI 6
BIS 70 target	ΔMeasured BIS	4.71 (3.92)	2.24 (9.45)	3.85 (4.82)	7.29 (6.94)
	ΔCVI	1.11 (1.32)	1.42 (1.51)	1.22 (1.83)	1.80 (2.23)
	ΔHeart rate (bpm)	3.20 (3.72)	-0.44 (4.77)	2.45 (4.23)	0.10 (3.18)
	ΔNon-invasive median blood pressure (mm-Hg)	-0.90 (4.43)	3.88 (7.92)	1.86 (5.70)	3.67 (6.42)
BIS 50 target	ΔMeasured BIS	5.25 (10.30)	0.84 (3.25)	1.28 (4.68)	1.32 (3.46)
	ΔCVI	1.41 (2.56)	0.21 (0.45)‡	-0.11 (0.75)	0.17 (0.22)§
	ΔHeart rate (bpm)	1.25(4.71)	-0.45(0.69)	-0.45(1.26)	-0.75(0.72)
	ΔNon-invasive median blood pressure (mm-Hg)	5.67 (6.52)	1.22 (4.99)	-0.65 (1.92)*	-0.56 (1.74)*
BIS 30 target	ΔMeasured BIS	3.64 (5.93)†	3.22 (5.73)	4.65 (7.91)	-1.11 (5.28)†
	ΔCVI	0.32 (0.60)	0.32 (0.95)	0.33 (0.54)	-0.08 (0.34)†
	ΔHeart rate (bpm)	0.25 (1.64)	-0.70 (1.25)	-1.05 (1.17)†	-0.15 (0.82)
	ΔNon-invasive median blood pressure (mm-Hg)	3.61 (12.79)	-0.20 (2.06)	-0.50 (2.85)	2.94 (13.34)

CeREMI = predicted remifentanil effect-site concentrations; BIS = Bispectral Index; CVI = Composite Variability Index.

**P = 0.02 for R0 versus R4 and R0 versus R6.*

†P < 0.01 between BIS 70 and BIS 30 (within same CeREMI category).

‡P = 0.0465 between BIS 70 and BIS 50 (within same CeREMI category).

§P = 0.0254 between BIS 70 and BIS 50 (within same CeREMI category).

DISCUSSION

In a patient undergoing anesthesia, adequate suppression of consciousness and an optimal nociception-antinociception balance should ensure somatic tolerance to subsequent painful stimuli. We found that values of 2 indices, BIS and CVI, derived from the EEG detected this optimal state more accurately than hemodynamic measures. However, the interpretation of these indices in clinical practice may be challenging as the cerebrally derived information of analgesic state is strongly influenced by the hypnotic drug effect and does not differentiate well between opioid levels in the unstimulated condition. The performance seems to be improved in conditions where noxious stimulation is present.

No significant relation was observed between CVI and CeREMI in the absence of a noxious stimulus, except between no remifentanil and a very high dose of remifentanil (6 ng/ml) at a target BIS of 50 (decrease in CVI). During stimulation at a target BIS level of 50, a significantly lower CVI was found when remifentanil was given, although without a concentration-effect relation. As a result, ΔCVI was not different at various CeREMI levels. Our findings are partially in agreement with those from Ellerkman et al.[190], who also did not find a significant decrease in CVI at increasing CeREMI without stimulation, but found significant changes during stimulations, resulting in a better relationship between ΔCVI and CeREMI. Their study only included a lower range of CeREMI concentrations (0 - 3 ng/ml).

Relating analgesic state indices to specific opioid concentrations in the absence of a noxious stimulus remains challenging as published previously for other measures derived from the autonomic nervous system[84, 184, 195, 201-203]. In the presence of a noxious stimulus, we and others found an influence of remifentanil on the performance of the surgical pleth index, an analgesic state index derived from the plethysmographic wave. However, as in the current study, only differences between no- and low-dose remifentanil were revealed, and no relationship was seen with further increases in CeREMI[195, 202]. Although Rantanen et al.[194] demonstrated that a 30-second tetanic stimulus emulates the noxious stimulus generated at skin incision, use of other noxious stimuli might result in more significant relations between CVI and CeREMI. This has to be clarified in further studies.

Some authors claim that an ideal index of the analgesic state should be independent from the hypnotic level of anesthesia. Using this reasoning, indices of the analgesic state should correlate

directly with the level of antinociception (e.g., an opioid concentration) in the absence of a noxious stimulus. Without noxious stimulus, these indices should ideally not be influenced by the level of hypnosis[84, 184, 195, 201, 202]. In our study, CVI values both before and during the noxious stimulation were influenced by the hypnotic level. Lower BIS levels were associated with lower CVI levels, both in the absence and presence of a noxious stimulus. As seen in Figure 4, at very deep levels of hypnosis, the influence of remifentanil on CVI is overwhelmed by the high concentration of propofol. Previous studies[190] did not include a determination of the influence of various hypnotic levels on CVI. As such, our study demonstrates that one should examine various hypnotic levels before making conclusions on the accuracy of analgesic state monitors in the presence or absence of a noxious stimulus. The primary site of action for analgesic drugs such as opioids is in the spinal cord and brainstem. Due to the challenges and limitation of currently available technology to adequately monitor these areas noninvasively, all current analgesic state monitors assess some physiological signal at more accessible sites to try and calculate the modulation on the observed signal by the noxious stimuli[204].

The results of this study confirm that CVI, an index of the variability of BIS and frontal EMG activity, is not independent of the hypnotic state and is not purely related to CeREMI. We also realize that BIS and CVI are not measuring the effect on the spinal cord but reveal secondary information from the noxious stimulus when reaching the cerebral cortex via ascending pathways. As such, we would rather define CVI as an arousability index and not as a measure of the balance between nociception and antinociception, similar to the suggestion by Glass in his mental model stating that "opioids attenuate the noxious stimulus that activates the neural response circuitry, whereas hypnotics directly suppress the neural response circuitry"[188, 205]. Interestingly, we also observed (Table 3) that ΔCVI depends on both hypnotic and antinociceptive levels, and see this as concordant with the abovementioned suggestion of Glass. In all BIS 70 groups and the BIS 50 CeREMI 0 group, higher ΔCVI values occurred in response to nociception. At other combinations, no ΔCVIs were observed. As such, ΔCVI as a result of a noxious stimulus could be an interesting indicator of overall arousal caused by inadequate hypnosis, inadequate antinociception or the combination of both.

Table 4. *The Average (Standard Deviation) of Individual Median Measure Values During the Baseline and Response Periods and Changes for Responders versus NonResponders.*

Baseline period		Responders	Non-responders	P_K
	BIS	61 (12)	41 (14)*	0.85 (0.04)
	CePROP	2.24 (1.20)	3.32 (1.54)*	0.72 (0.05)†§
	CeREMI	1.69 (2.22)	3.49 (2.07)*	0.73 (0.06)†§
	CVI	2.15 (0.69)	1.37 (0.92)*	0.84 (0.04)
	Heart rate (bpm)	66 (10)	59 (10)*	0.69 (0.06)†‡
	Non-invasive median blood pressure (mmHg)	67 (13)	59 (8)*	0.69 (0.06)†‡
Response period				
	BIS	68 (13)	43 (14)*	0.89 (0.04)
	CVI	4.22 (1.65)	1.53 (0.86)*	0.94 (0.03)
	Heart rate (bpm)	68 (11)	58 (10)*	0.75 (0.05)†‡
	Non-invasive median blood pressure (mmHg)	71 (14)	60 (9)*	0.77 (0.05)†‡
Delta				
	BIS	7 (7)	2 (6)*	0.72 (0.05)‡
	CVI	2.07 (1.81)	0.16 (0.78)*	0.87 (0.05)
	Heart rate (bpm)	2 (5)	-1 (1)*	0.73 (0.06)‡
	Non-invasive median blood pressure (mmHg)	4 (6)	1 (7)*	0.70 (0.06)‡

The prediction probabilities (P_K) results (jack-knife estimates and SE) are also shown.

CeREMI = predicted remifentanil effect-site concentrations; CVI = Composite Variability Index; BIS = Bispectral Index; CePROP = propofol effect-site concentration.

**P < 0.01 between responders and nonresponders*

†P < 0.01 with BIS

‡P < 0.01 with CVI

§P_K for these measures are shown as "1 value".

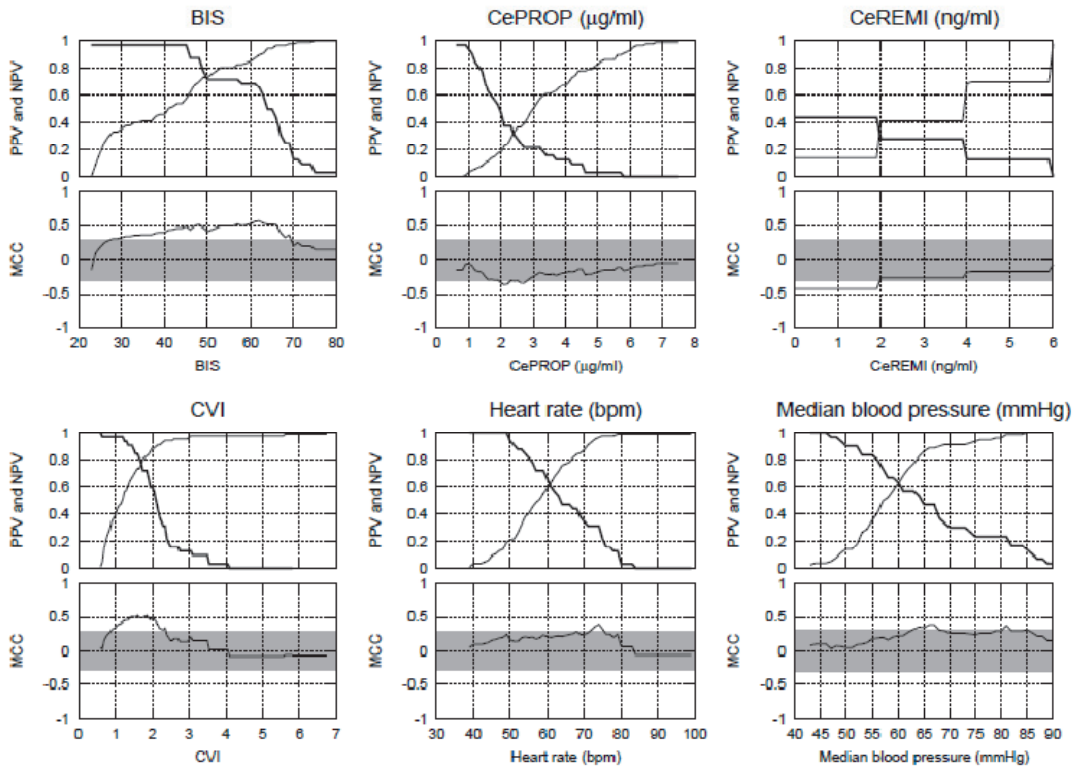

Fig. 7. *Performance of Baseline Values. Positive and Negative Predictive Value (PPV and NPV, thick and thin line respectively) for a range of thresholds to predict tolerance/responsiveness to stimulation. Data was from the baseline time period, i.e. 0-30 s before application of the stimulation sequence. Also shown is the Matthews Correlation Coefficient (MCC), a measure of binary classifier performance. The shaded area corresponds to non-significant values (at a level of p=0.001).*

We successfully controlled the hypnotic component of anesthesia by titrating CePROP to a specified BIS target using a previously validated closed-loop system[91]. Our aim was to standardize cerebral drug effect to minimize inter-individual variability and to automatically consider the pharmacodynamic synergy between propofol and remifentanil at a specific hypnotic level. Although BIS is a surrogate measure of the hypnotic component of anesthesia and has its limitations[82], we contend that standardization of cerebral effect would not have been possible with a fixed CePROP and CeREMI approach.

Because HR and MAP are still used in clinical practice to titrate administration of both hypnotics and analgesics, we investigated their relationship with CeREMI and BIS. Similar to previous publications[53, 198], we found neither useful relationships for both HR and MAP, nor for ΔHR and ΔMAP. Only the known hemodynamic side effects (bradycardia and hypotension) were identifiable when remifentanil was given.

Somatic response such as movement in response to a noxious stimulus can also be considered as a mixed clinical phenomenon. Immobility is recognized as a cardinal feature of general anesthesia and can be achieved by high concentration of hypnotics or opiates or by optimal combinations of different drugs[206, 207]. As such, movement after a tetanic stimulus can be caused by inadequate hypnosis or a mismatch in the analgesic state or a combination of both. The ability to identify individuals likely to respond to stimulation is useful because it gives the anesthesiologist the opportunity to increase 1 or both of the components of anesthesia before stimulation/response occurs. BIS, CVI, HR and MAP were significantly different between responders and nonresponders to an OAA/S-noxious stimulus, both at baseline and during the stimulation period. The changes in these measures were also significantly larger in the response group. This is in agreement with previous studies[189, 190]. Because differences in the mean values do not have to result in high sensitivity and specificity for a specific measure per se, we also searched for an objective accuracy evaluation (using P_K) and an identifiable threshold significantly discriminating the presence or absence of responses to an OAA/S-noxious stimulation. We first assessed the ability of the baseline measures to accurately predict movement responses. Using the P_K and the MCC, we found that BIS and CVI were the most accurate predictors of somatic responses among those tested. CePROP, CeREMI, HR and MAP were not found to be reliable predictors. As movement in response to a noxious stimulus is a spinal cord and not brain-based function, we could question whether CVI and BIS can predict movement at all. The spinal-cerebral relationship might be too complex to call cerebrally derived indices “predictors of movement”. Whereas there are some anesthetics that are classified as immobilizers (can achieve minimum alveolar concentration [MAC]), there are others that, while providing unconsciousness, will not immobilize the subject at any concentration (nonimmobilizers). Movement or an assessment of MAC still has a spinal cord origin. The concentration-effect relation for hypnotics versus MAC is well-defined for the volatile anesthetics that is fairly steep[208]. Because we used a combination of propofol and opioids, the concentration-effect relationship between interacting drugs and immobility becomes rather complex. Although clinically applicable, we should realize we are not measuring the spinal cord,

but we are just revealing information from an epiphenomenon. Although the definition of P_K could be interpreted in a predictive way, we rather would be careful and agree with the conclusion of Mathews et al.[189] stating that "CVI might detect periods of somatic response". This was certainly revealed by the more accurate performance during the stimulus period.

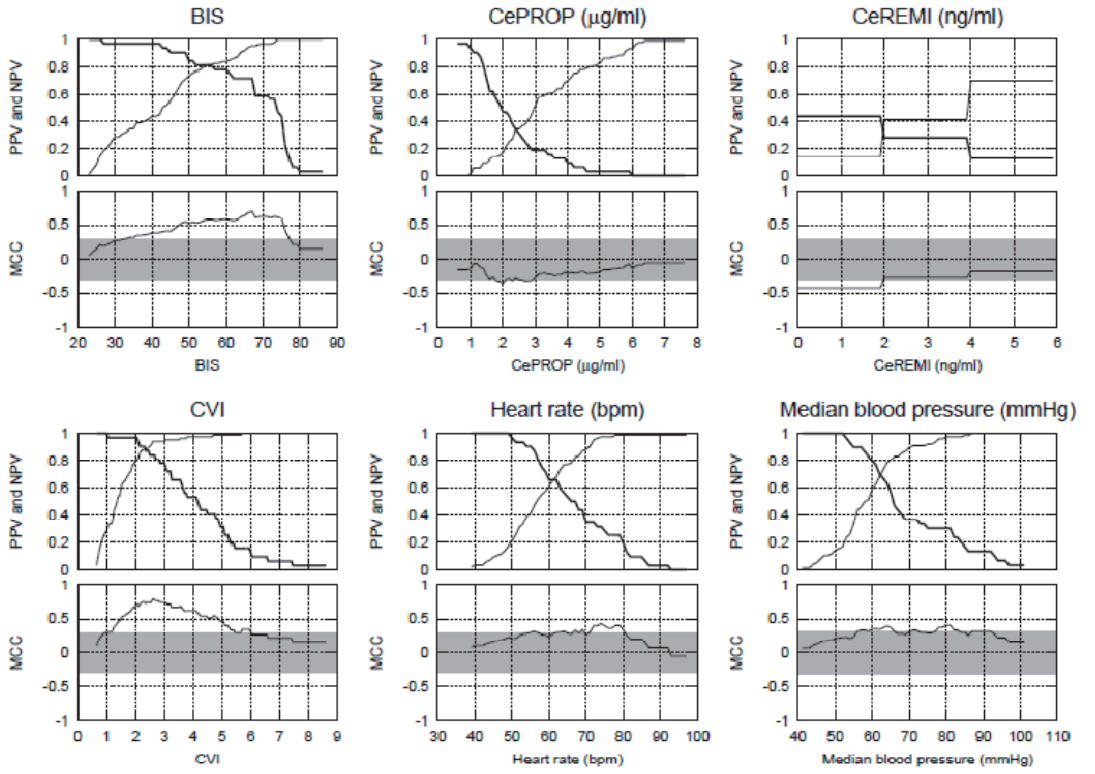

Fig. 8. *Performance of Response Values. Positive and Negative Predictive Value (PPV and NPV, thick and thin line respectively) for a range of thresholds to detect tolerance/responsiveness to stimulation. Data was from the response time period, i.e. 45-180 s after the start of the application of the stimulation sequence. Also shown is the Matthews Correlation Coefficient (MCC), a measure of binary classifier performance. The shaded area corresponds to non-significant values (at a level of p=0.001).*

Here, we clearly found that BIS and CVI correlated with the probability of somatic responses. The other measures provided no clear predictions or indications of somatic response.

The detailed sensitivity/specificity analysis showed that only BIS and CVI are meaningful measures to detect somatic responsiveness. At baseline, a threshold value for BIS and CVI indicating that an individual would be responsive to an upcoming OAA/S-noxious stimulus was revealed, however, with only moderate accuracy (MCC values approximately 0.55). During stimulation, CVI showed a higher MCC than BIS, indicating a better performance at the best discriminating threshold value. During periods of stimulation, a CVI value higher than 2.5 can be associated with periods of somatic responsiveness. For BIS and CVI, our findings are in agreement with a recent publication by Mathews et al.[189] who found that increases in EEG and EMG variability were associated with an increased incidence of intraoperative somatic responses. Different findings are observed for the changes in the indices ("Δ") between baseline and stimulation. The ΔBIS is not accurate for monitoring response to stimulation compared to BIS during the Baseline and Response period. Although derived partially from BIS, ΔCVI is a much better measure than BIS for this purpose. This suggests that changes in frontal EMG activity (a component of CVI[189, 209]) provide useful information. Although the frontal muscles are rather resistant to neuromuscular blockade, the performance of CVI during profound neuromuscular blockade might be compromised. This has to be investigated in future studies. All other measures performed poorly as binary classifiers for tolerance or response to noxious stimulus.

One could question if CVI offers more clinical benefits than BIS in detecting response to a noxious stimulus. CVI offers a value of arousability that is derived from changes in BIS and frontal EMG over time. We are convinced that clinicians cannot focus enough on the fast temporary changes in BIS and EMG measures to detect arousability online, so a derived measure might be of clinical value. In addition, our group has proven that static views of small changes in displayed vital signs information are not always accurately diagnosed by the clinician[210].

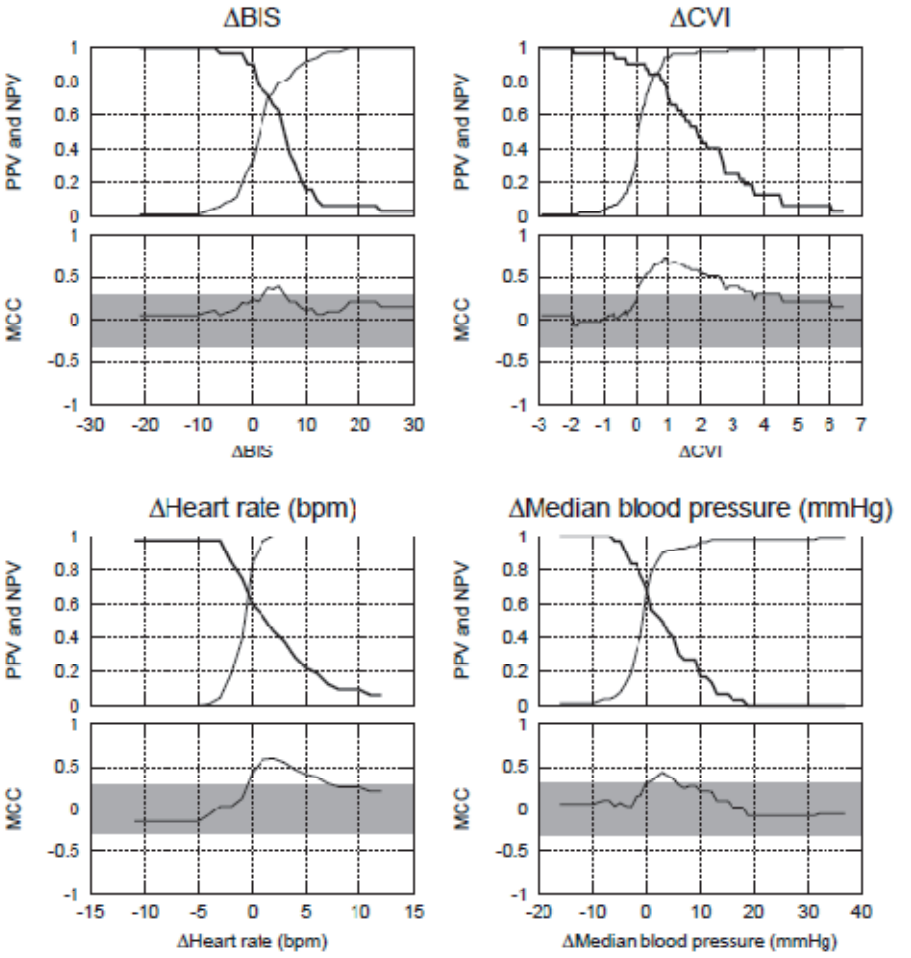

Fig. 9. *Performance of Δ Values. Positive and Negative Predictive Value (PPV and NPV, thick and thin line respectively) for a range of thresholds to predict tolerance/responsiveness to stimulation. Data show the "Δ" values as a result of stimulation. Also shown is the Matthews Correlation Coefficient (MCC), a measure of binary classifier performance. The shaded area corresponds to non-significant values (at a level of p=0.001).*

In conclusion, CVI and BIS more accurately detect somatic responses to an OAA/S-noxious stimulation than HR, MAP or CeREMI and CePROP. ΔCVI is a better measure to monitor the time course of the response to stimulation than ΔBIS, ΔHR or ΔMAP. We cannot conclude that CVI is an independent index of the balance between nociception and antinociception; however, we can state that CVI and ΔCVI offer information on arousability. None of the candidate analgesic state measures were uniquely related to a specific opioid concentration and is extensively influenced by the hypnotic state as measured by BIS. More research is required to investigate if combined drug concentration information from both hypnotic and analgesic drugs resulting in accurate clinical anesthesia would be better correlated to measures of the balance between nociception and antinociception.

DISCLOSURES

Name: Marco M. Sahinovic, MD

Contribution: This author helped design and conduct the study, analyze the data, and write the manuscript.

Attestation: Marco M. Sahinovic has seen the original study data, reviewed the analysis of the data, approved the final manuscript, and is the author responsible for archiving the study files.

Conflicts of Interest: The author has no conflicts of interest to declare.

Name: Douglas J. Eleveld, PhD

Contribution: This author helped analyze the data and write the manuscript.

Attestation: Douglas J. Eleveld has seen the original study data, reviewed the analysis of the data, and approved the final manuscript.

Conflicts of Interest: The author has no conflicts of interest to declare.

Name: Alain F. Kalmar MD, PhD

Contribution: This author helped design and conduct the study and write the manuscript.

Attestation: Alain F. Kalmar has seen the original study data and approved the final manuscript.

Conflicts of Interest: The author has no conflicts of interest to declare.

Name: Eleonora H. Heeremans, MD

Contribution: This author helped design and conduct the study

Attestation: Eleonora H. Heeremans has seen the original study data and approved the final manuscript.

Conflicts of Interest: The author has no conflicts of interest to declare.

Name: Tom De Smet, ir., MSc

Contribution: This author helped design the study and developed the closed-loop system applied in this study.

Attestation: Tom De Smet approved the final manuscript.

Conflicts of Interest: Tom De Smet is the co inventor of the applied closed-loop system. In the past, he received honorarium as a consultant for Covidien (Boulder, CO).

Name: Chandran V. Seshagiri, PhD

Contribution: This author helped analyze the data and write the manuscript.

Attestation: Chandran V. Seshagiri has seen the original study data and approved the final manuscript.

Conflicts of Interest: Chandran V. Seshagiri was a full time employee of Covidien, Boulder, CO.

Name: Anthony R. Absalom, MBChB, FRCA, MD

Contribution: This author helped design and conduct the study and wrote the manuscript.

Attestation: Anthony R. Absalom has seen the original study data and approved the final manuscript.

Conflicts of Interest: The author has no conflicts of interest to declare.

Name: Hugo E.M. Vereecke, MD, PhD

Contribution: This author helped design and conduct the study and write the manuscript.

Attestation: Hugo E.M. Vereecke approved the final manuscript.

Conflicts of Interest: The author has no conflicts of interest to declare.

Name: Michel M.R.F. Struys, MD, PhD

Contribution: This author helped design and conduct the study, analyze the data, and write the manuscript.

Attestation: Michel M.R.F. Struys helped design the study, has seen the original study data, reviewed the analysis of the data, approved the final manuscript, coauthored the writing of the manuscript, and is the author responsible for archiving the study files.

Conflicts of Interest: During the last 5 years, Michel M.R.F. Struys served twice as a member of an advisory panel organized by Covidien (Boulder, CO). He received speakers' honoraria from Covidien. He is also co inventor of the applied closed-loop system in the study.

Chapter 9

Discussion and future perspectives

Feedback based control systems are a part of nature itself, and regulatory mechanisms are applied by most biological systems controlling lifesaving homeostasis.
To accomplish their function we can identify three main properties of such systems, combined together to form a robust control system: adaptation, which is the ability to cope with changes; parameter insensitivity, signified as the insensitivity to specific parameters; and graceful degradation, reflecting the slow degradation after damage rather than catastrophic failure [211].

Artificial closed-loop applications are the building blocks of all industrial processes. They may enhance operator performance, provide tighter control when operated standalone, or overall improve the process control. One may expect them to provide similar advantages when trying to optimize drug administration.
Automated control of anesthesia for patients under surgery has been investigated with variable success. The complexity of the pharmacokinetic and pharmacodynamic processes, their nonlinearity and variability within patient populations and the multi-variability of the observed characteristics poses a multitude of challenges [212].

This thesis tried to find some answers on how to realize a model-based predictive controller to implement a robust controller. Although challenging, control of the hypnotic component of anesthesia was selected as a prototype to prove this theory.

As remarked in the introduction, our closed-loop system could only become accurate if all basic requirements were optimized. Hereby, an adequate control variable to measure the drug effect was obligatory. As hypnotic drugs express their clinical effect at the cerebral level, we decided to apply the drug induced chances in the electrical activity of the brain as the control variable. Although still controversial [82, 213, 214], we selected the BIS, a numerical representation of some characteristics of the electro-encephalogram, as the control variable. This decision was made using evidence in the literature. From all clinically available EEG parameters used in anesthesia to measure hypnotic drug

effect, BIS is still the most extensively validated [215]. Additionally, reasonable set-points relating hypnotic levels induced by propofol with specific BIS values are available in the literature [51, 53, 175, 198].

To compensate for the complex pharmacokinetic and pharmacodynamic drug-response relationship, our controller should integrate a proper model for the process of drug distribution and drug action in the patient. As we applied the anesthetic drug propofol to effectuate hypnotic drug effect, rational propofol model selection was required. In our system, the pharmacokinetic-dynamic model published by Schnider et al. was selected. In chapter 3, we studied the literature and found evidence for our decision. More research from our group has confirmed this choice [216].

In chapter 4 [54], we describe the development of our initial closed-loop system for propofol utilizing the BIS as the controlled variable in a patient-individualized, adaptive, model-based control system. This system is the first applying adaptive model-based control on the pharmacodynamic part of the model, hereby shifting the "Hill-curve" in order to optimize control. Model-based adaptive control of the pharmacokinetic parameters was already successfully used by Schwilden and Schüttler in the 80's [125]. A patent was filed on this "moving Hill-curve" approach (see appendix). As described in this study, compared to manually titrated propofol administration, patients in the closed loop group reached the target BIS at a somewhat slower rate, but this resulted in less BIS overshoot and better hemodynamics after induction. During the maintenance phase, better control of BIS and systolic blood pressure was found in the closed loop group. Recovery in the closed-loop group was faster with less unpredictable outliers.

After publication, our result was commented by others claiming that classical engineering approach such as PID control of the administration rate would result in a more predictable and better control. Whereas PID control is still the workhorse of industrial controllers, it poses some particular drawbacks in our specific setup. First, since it is impossible to directly counteract the administration of excessive drug, fine-tuning PID control parameters through excessive control actions potentially results in safety hazards. Second, the inter-individual pharmacological variability requires tuning of the controller to each specific patient. A more appropriate approach could be to use a PID control system governing a TCI system to lower the order of complexity between dose and response as done by Absalom and coworkers [7], however, we were still convinced that our approach offered better control. Yet, in an

accompanying editorial to our work, Glass questioned whether our controller was stressed enough to be called performing and challenged us to test the boundaries of our controller [107].

Challenged by these comments, we decided to apply simulation technology to compare the performance of our closed-loop control systems with the PID control system, published by Absalom et al. [7] and to test both systems under extreme conditions (chapter 5)[171]. We applied this in silicon approach as it is clinically impossible to compare two closed-loop control strategies in the same patient and as it might be considered unethical to test a closed-loop system under extreme conditions in clinical practice. We found that, during these simulations, the use of a patient-individualized, model-based adaptive control system during BIS-guided propofol administration resulted in a better control of BIS compared to a PID approach. The model-based controller outperformed without behavioral problems, even under extreme control conditions such as low and high BIS levels and abrupt changes in BIS levels.

Our original control algorithm was based on a patient-specific pharmacodynamic profile estimated during induction, which caused some limitations precluding a more general use during sedation and anesthesia. The requirement of an initial drug-free patient to model the drug-response relationship excluded the controller's application in already anesthetized patients. In addition, the concentration versus response profile is likely to change over the course of anesthesia, mostly as a result of changing levels of noxious stimulation, but also because of possible pharmacodynamics (i.e., acute tolerance to opioids) or because of changes to the patient (e.g., liver transplantation). In an attempt to resolve these shortcomings, a Bayesian approach was included in our existing control algorithm [8].

The Bayesian method starts from a standard, population-based response model providing the prior distribution of parameter values. These values are tuned to the patient's own parameters based on the observed response of the individual patient. This process makes use of specific modeling weights, called Bayesian variances, which determine how the patient-specific model can deviate from the population model. For a pharmacokinetic model the Bayesian variances are the variances of the parameters resulting from the modeling process obtained, for example, using a NONMEM analysis. For the pharmacodynamic portion of the model, such a priori population model information is not readily available from the literature. Moreover, being an essential contributing factor in the control

operation, we choose to optimize these Bayesian variances for control performance in our target population. In a first study we applied simulations to select the Bayesian variances yielding the optimal controller for a Bayesian-based closed-loop system for propofol administration using the BIS as a controlled variable (chapter 6).

The Bayesian approach applies a population-based or otherwise applicable reference model providing the prior distribution of parameter values, which is tuned towards a specific patient based on the observed response of the individual patient under varying circumstances. The freedom of the specific model to differ from the reference model is determined by the Bayesian variances. These variances are the parameter variances resulting from the modeling process, or, as they are equally influential on the control actions as the model itself, are carefully selected for optimal control. We realized this selection yielding the optimal controller for a Bayesian-based closed-loop system for propofol administration using the BIS as a controlled variable through computer simulations. A total simulated control time of 2340000 hours (416 virtual patients x 625 proposed controllers x 3 target BIS values x 3 hours/case) resulted in the selection of the optimal set yielding to an acceptable control. (see chapter 6) [90]. The Bayesian control system has been patented by our team (see appendix).

In chapter 7 [91], we describe how we compared the feasibility and accuracy of the new Bayesian-Based closed loop system versus manually controlled BIS guided effect compartment controlled propofol TCI during ambulatory gynecological procedures. We especially selected this population as the use of only limited amount of opioids during the procedure resulting in a nearly propofol based deep sedation, is very challenging for the control system. We found that the closed-loop control system titrated propofol administration accurately resulting in BIS values close to the set point. The closed-loop control system was able to induce anesthesia in the patients within clinically accepted time limits and with less overshoot than the manual control group. Automated control resulted in beneficial recovery times. This closed-loop control group showed similar acceptable clinical performance specified by similar hemodynamic, respiratory stability, comparable movement rates, and quality scores than the manual control group.

Some specific research protocols require a tight control of a specific depth of the hypnotic component of anesthesia in patients. Accurate control of such specific levels, especially in the sedation range, is

very challenging for any human or automated controller. Since closed-loop control is designed to target a specific level of drug effect, we applied our closed-loop system described in chapter 8 during a specific research protocol requiring 3 different levels of hypnosis, defined as a BIS level of 70, 50 and 30. During this trial, we could study the stability of our system under various hypnotic conditions and found that the system performed well in a larger study of 120 patients.

In this thesis, we were able to answer the 4 questions raised in the introduction. We have successfully realized an automatic closed-loop system for the administration of intravenous hypnotic-anesthetic drugs during sedation and anesthesia offering more accurate drug administration than manual control under the studied conditions.
Our closed-loop system successfully combines population pharmacological drug models and Bayesian methods to compensate for population variability into a technology offering accurate control.
We proved this technology is able to maintain a specific level of the hypnotic component of anesthesia even under extreme conditions, both in clinical practice and during specific research conditions.

But can we be satisfied now? Is a hypnotic-only closed loop control using BIS as controlled variable the target and endpoint?

A state-of-the art anesthetic procedure introduces sedation or unconsciousness in the patient by administration of a hypnotic, accompanied with the infusion of an opioid to prevent noxious stimuli from reaching the consciousness centre. [217] MIMO controllers administering the two drugs simultaneously require representative controlled variables as well as concise pharmacological modeling, not only for the drugs individually but, in case of synergetic or additive drugs, for the interaction of these drugs. Experimental feedback systems controlling multiple drugs based on a single index have been described but are unlikely in clinical circumstances as they necessarily only indicatively titrate the unmeasured analgesic component [232].

In the past ten years research brought major improvements in the building blocks for a true MIMO controller.

First of all, the exploration for indices accurately describing hypnosis and antinociception is ongoing. Indices will evolve and become more accurate as the insight in the anesthesia syndrome grows. Indeed, we cannot actually measure sleep today, even the phenomenon of anesthesia related unconsciousness is not very well understood [227]. Consequently, BIS monitoring, although considered by many as the golden standard for depth of anesthesia monitoring, was criticized [225, 226] and, in time, may be replaced with newer indices. The research for an accurate prediction of response to painful stimulus continues as well.

New indices were proposed and investigated [175, 190, 224, 228-230]. Recently, Schneider and colleagues found that a multimodal integration of both standard monitoring and electroencephalographic parameters may more precisely reflect the level of anesthesia compared with monitoring based on one of these aspects alone [231].

But the knowledge of drug action and the interaction between drugs has grown too. Since no drug has an exclusively hypnotic or analgesic effect, its dose-response relationship may be subject to simultaneously administered drugs. Drug interaction models were launched with promising result.[218-224]

All these findings offer a framework for a true multimodal closed-loop system using multiple-input-multiple-output strategies. More importantly, the evolution shows that such implementation will require flexibility to adapt to new insights readily. Our research successfully combined population pharmacological drug models and Bayesian methods to compensate for population variability into a technology offering accurate control. Whereas our research has focused on control of the hypnotic component alone, the applied principle is universally applicable. A Bayesian approach to control both hypnotics and analgesics using a carefully selected set of indices seems a viable option for a second generation controller.

Our first generation controller has been implemented and used under strict experimental conditions. To convert this into a commercial system, the first challenge is to prove fully the safety and utility for its adaption into clinical practice and to find industrial partners willing to take all required regulatory steps when developing a marketable system [108]. As we have witnessed personally, the worldwide financial crisis has directed the monitoring equipment industry to merely focus on consolidation

rather than investing into new technology. But now the dust is settling, a new promising momentum can be observed.

Ultimately, clinicians will determine whether or not computer systems facilitate better control and improve outcome in their daily clinical practice [4]. Whereas our approach has proven to be clinically feasible and efficient, closed-loop systems only serve to support the clinical decisions of the anesthesiologist. They provide the anesthesiologist an automated pilot function executing the basic tasks of the anesthetic practice, offering him the opportunity to stay vigilant and focused and to retain a better overall view of the patient's wellbeing. This should ensure better care at critical times where it really matters.

References

1. Kissin, I., *General anesthetic action: an obsolete notion? [editorial].* Anesth Analg, 1993. **76**(2): p. 215-8.
2. Struys, M.M., T. De Smet, and E.P. Mortier, *Simulated drug administration: an emerging tool for teaching clinical pharmacology during anesthesiology training.* Clin Pharmacol Ther, 2008. **84**(1): p. 170-4.
3. Absalom, A. and M.M.R.F. Struys, *An overview of TCI&TIVA (second edition)*. 2007, Gent: Academia Press.
4. Absalom, A.R., R. De Keyser, and M.M. Struys, *Closed loop anesthesia: are we getting close to finding the holy grail?* Anesth Analg, 2011. **112**(3): p. 516-8.
5. O'Hara, D.A., D.K. Bogen, and A. Noordergraaf, *The use of computers for controlling the delivery of anesthesia.* Anesthesiology, 1992. **77**(3): p. 563-81.
6. Sheiner, L.B. and S.L. Beal, *Bayesian individualization of pharmacokinetics: simple implementation and comparison with non-Bayesian methods.* J Pharm Sci, 1982. **71**(12): p. 1344-8.
7. Absalom, A.R. and G.N. Kenny, *Closed-loop control of propofol anaesthesia using bispectral index: performance assessment in patients receiving computer-controlled propofol and manually controlled remifentanil infusions for minor surgery.* Br J Anaesth, 2003. **90**(6): p. 737-41.
8. Sheiner, L.B., et al., *Forecasting individual pharmacokinetics.* Clin Pharmacol Ther, 1979. **26**(3): p. 294-305.
9. Garraffo, R., et al., *Application of Bayesian estimation for the prediction of an appropriate dosage regimen of amikacin.* J Pharm Sci, 1989. **78**(9): p. 753-7.
10. Kruger-Theimer, E., *Continuous intravenous infusion and multicompartment accumulation.* Eur J Pharmacol, 1968. **4**: p. 317-324.
11. Schwilden, H., *A general method for calculating the dosage scheme in linear pharmacokinetics.* Eur J Clin Pharmacol, 1981. **20**(5): p. 379-86.
12. Shafer, S.L. and K.M. Gregg, *Algorithms to rapidly achieve and maintain stable drug concentrations at the site of drug effect with a computer-controlled infusion pump.* J Pharmacokinet Biopharm, 1992. **20**(2): p. 147-69.
13. Schuttler, J., H. Schwilden, and H. Stoekel, *Pharmacokinetics as applied to total intravenous anaesthesia. Practical implications.* Anaesthesia, 1983. **38 Suppl**: p. 53-6.
14. Ausems, M.E., D.R. Stanski, and C.C. Hug, *An evaluation of the accuracy of pharmacokinetic data for the computer assisted infusion of alfentanil.* Br J Anaesth, 1985. **57**(12): p. 1217-25.
15. Glass, P.S., et al., *Pharmacokinetic model-driven infusion of fentanyl: assessment of accuracy.* Anesthesiology, 1990. **73**(6): p. 1082-90.
16. Shafer, S.L., et al., *Pharmacokinetics of fentanyl administered by computer-controlled infusion pump.* Anesthesiology, 1990. **73**(6): p. 1091-102.
17. Chaudhri, S., M. White, and G.N. Kenny, *Induction of anaesthesia with propofol using a target-controlled infusion system [see comments].* Anaesthesia, 1992. **47**(7): p. 551-3.
18. Glass, P.S., et al., *Nomenclature for computer-assisted infusion devices [letter].* Anesthesiology, 1997. **86**(6): p. 1430-1.
19. Glen, J.B., *The development of 'Diprifusor': a TCI system for propofol.* Anaesthesia, 1998. **53 Suppl 1**: p. 13-21.

20. Cutler, D.J., *Linear systems analysis in the kinetics of anaesthetic agents.* Anaesth Pharm Rev, 1994. **2**: p. 243-249.
21. Jacobs, J.R., *Analytical solution to the three-compartment pharmacokinetic model.* IEEE Trans Biomed Eng, 1988. **35**(9): p. 763-5.
22. Shafer, S.L., et al., *Testing computer-controlled infusion pumps by simulation.* Anesthesiology, 1988. **68**(2): p. 261-6.
23. Schnider, T.W., et al., *The influence of method of administration and covariates on the pharmacokinetics of propofol in adult volunteers [In Process Citation].* Anesthesiology, 1998. **88**(5): p. 1170-82.
24. Schnider, T.W., et al., *The influence of age on propofol pharmacodynamics.* Anesthesiology, 1999. **90**(6): p. 1502-16.
25. Struys, M.M., et al., *Comparison of plasma compartment versus two methods for effect compartment--controlled target-controlled infusion for propofol.* Anesthesiology, 2000. **92**(2): p. 399-406.
26. Van Poucke, G.E., L.J.B. Bravo, and S.L. Shafer, *target controlled infusions: targeting the effect site while limiting peak plasma concentration.* IEEE Trans Biomed Eng, 2004. **51**: p. 1869-1875.
27. Hughes, M.A., P.S. Glass, and J.R. Jacobs, *Context-sensitive half-time in multicompartment pharmacokinetic models for intravenous anesthetic drugs [see comments].* Anesthesiology, 1992. **76**(3): p. 334-41.
28. Youngs, E.J. and S.L. Shafer, *Pharmacokinetic parameters relevant to recovery from opioids.* Anesthesiology, 1994. **81**(4): p. 833-42.
29. Varvel, J.R., D.L. Donoho, and S.L. Shafer, *Measuring the predictive performance of computer-controlled infusion pumps.* J Pharmacokinet Biopharm, 1992. **20**(1): p. 63-94.
30. Marsh, B., et al., *Pharmacokinetic model driven infusion of propofol in children.* Br J Anaesth, 1991. **67**(1): p. 41-8.
31. Absalom, A., et al., *Accuracy of the 'Paedfusor' in children undergoing cardiac surgery or catheterization.* Br J Anaesth, 2003. **91**(4): p. 507-13.
32. Kataria, B.K., et al., *The pharmacokinetics of propofol in children using three different data analysis approaches.* Anesthesiology, 1994. **80**(1): p. 104-22.
33. Domino, E.F., et al., *Ketamine kinetics in unmedicated and diazepam-premedicated subjects.* Clin Pharmacol Ther, 1984. **36**(5): p. 645-53.
34. Schuttler, J., H. Stoeckel, and H. Schwilden, *Pharmacokinetic and pharmacodynamic modelling of propofol ('Diprivan') in volunteers and surgical patients.* Postgrad Med J, 1985. **61**(Suppl 3): p. 53-4.
35. Shafer, A., et al., *Pharmacokinetics and pharmacodynamics of propofol infusions during general anesthesia.* Anesthesiology, 1988. **69**(3): p. 348-56.
36. Minto, C.F., et al., *Influence of age and gender on the pharmacokinetics and pharmacodynamics of remifentanil. I. Model development.* Anesthesiology, 1997. **86**(1): p. 10-23.
37. Minto, C.F., T.W. Schnider, and S.L. Shafer, *Pharmacokinetics and pharmacodynamics of remifentanil. II. Model application.* Anesthesiology, 1997. **86**(1): p. 24-33.
38. Gepts, E., et al., *Linearity of pharmacokinetics and model estimation of sufentanil.* Anesthesiology, 1995. **83**(6): p. 1194-204.

39. Maitre, P.O., et al., *Population pharmacokinetics of alfentanil: the average dose-plasma concentration relationship and interindividual variability in patients.* Anesthesiology, 1987. **66**(1): p. 3-12.
40. Scott, J.C., K.V. Ponganis, and D.R. Stanski, *EEG quantitation of narcotic effect: the comparative pharmacodynamics of fentanyl and alfentanil.* Anesthesiology, 1985. **62**(3): p. 234-41.
41. Shafer, S.L. and J.R. Varvel, *Pharmacokinetics, pharmacodynamics, and rational opioid selection.* Anesthesiology, 1991. **74**(1): p. 53-63.
42. Coetzee, J.F., et al., *Pharmacokinetic model selection for target controlled infusions of propofol. Assessment of three parameter sets.* Anesthesiology, 1995. **82**(6): p. 1328-45.
43. Fabregas, N., et al., *Modeling of the sedative and airway obstruction effects of propofol in patients with Parkinson disease undergoing stereotactic surgery.* Anesthesiology, 2002. **97**(6): p. 1378-86.
44. Hoymork, S.C., et al., *Bispectral index, predicted and measured drug levels of target-controlled infusions of remifentanil and propofol during laparoscopic cholecystectomy and emergence.* Acta Anaesthesiol Scand, 2000. **44**(9): p. 1138-44.
45. Struys, M.M., et al., *Influence of Administration Rate on Propofol Plasma-Effect Site Equilibration.* Anesthesiology, 2007. **107**(3): p. 386-396.
46. Wietasch, J.K., et al., *The performance of a target-controlled infusion of propofol in combination with remifentanil: a clinical investigation with two propofol formulations.* Anesth Analg, 2006. **102**(2): p. 430-7.
47. Bouillon, T. and S.L. Shafer, *Does size matter?* Anesthesiology, 1998. **89**(3): p. 557-60.
48. Doenicke, A.W., et al., *Pharmacokinetics and pharmacodynamics of propofol in a new solvent.* Anesth Analg, 1997. **85**(6): p. 1399-403.
49. Ward, D.S., et al., *Pharmacodynamics and pharmacokinetics of propofol in a medium-chain triglyceride emulsion.* Anesthesiology, 2002. **97**(6): p. 1401-8.
50. Vanluchene, A.L., et al., *Spectral entropy as an electroencephalographic measure of anesthetic drug effect: a comparison with bispectral index and processed midlatency auditory evoked response.* Anesthesiology, 2004. **101**(1): p. 34-42.
51. Vanluchene, A.L., et al., *Spectral entropy measurement of patient responsiveness during propofol and remifentanil. A comparison with the bispectral index.* Br J Anaesth, 2004. **93**(5): p. 645-54.
52. Vereecke, H.E., M.M. Struys, and E.P. Mortier, *A comparison of bispectral index and ARX-derived auditory evoked potential index in measuring the clinical interaction between ketamine and propofol anaesthesia.* Anaesthesia, 2003. **58**(10): p. 957-61.
53. Struys, M.M., et al., *Ability of the bispectral index, autoregressive modelling with exogenous input-derived auditory evoked potentials, and predicted propofol concentrations to measure patient responsiveness during anesthesia with propofol and remifentanil.* Anesthesiology, 2003. **99**(4): p. 802-12.
54. Struys, M.M., et al., *Comparison of closed-loop controlled administration of propofol using Bispectral Index as the controlled variable versus "standard practice" controlled administration.* Anesthesiology, 2001. **95**(1): p. 6-17.
55. Drover, D.R., et al., *Determination of the pharmacodynamic interaction of propofol and remifentanil during esophagogastroduodenoscopy in children.* Anesthesiology, 2004. **100**(6): p. 1382-6.

56. Rigouzzo, A., et al., *The relationship between bispectral index and propofol during target-controlled infusion anesthesia: a comparative study between children and young adults.* Anesth Analg, 2008. **106**(4): p. 1109-16, table of contents.
57. Schuttler, J. and H. Ihmsen, *Population pharmacokinetics of propofol: a multicenter study.* Anesthesiology, 2000. **92**(3): p. 727-38.
58. Cortinez, L.I., et al., *Performance of the cerebral state index during increasing levels of propofol anesthesia: a comparison with the bispectral index.* Anesth Analg, 2007. **104**(3): p. 605-10.
59. Slepchenko, G., et al., *Performance of target-controlled sufentanil infusion in obese patients.* Anesthesiology, 2003. **98**(1): p. 65-73.
60. Barvais, L., et al., *Pharmacokinetic model-driven infusion of sufentanil and midazolam during cardiac surgery: assessment of the prospective predictive accuracy and the quality of anesthesia.* J Cardiothorac Vasc Anesth, 2000. **14**(4): p. 402-8.
61. Hudson, R.J., et al., *Pharmacokinetics of sufentanil in patients undergoing coronary artery bypass graft surgery.* J Cardiothorac Vasc Anesth, 2001. **15**(6): p. 693-9.
62. van den Nieuwenhuyzen, M.C., et al., *Computer-controlled infusion of alfentanil for postoperative analgesia. A pharmacokinetic and pharmacodynamic evaluation.* Anesthesiology, 1993. **79**(3): p. 481-92; discussion 27A.
63. Raemer, D.B., et al., *The prospective use of population pharmacokinetics in a computer-driven infusion system for alfentanil [published erratum appears in Anesthesiology 1990 Oct;73(4):798].* Anesthesiology, 1990. **73**(1): p. 66-72.
64. Shibutani, K., et al., *Pharmacokinetic mass of fentanyl for postoperative analgesia in lean and obese patients.* Br J Anaesth, 2005. **95**(3): p. 377-83.
65. Egan, T.D., et al., *Remifentanil versus alfentanil: comparative pharmacokinetics and pharmacodynamics in healthy adult male volunteers [published erratum appears in Anesthesiology 1996 Sep;85(3):695].* Anesthesiology, 1996. **84**(4): p. 821-33.
66. Drover, D.R. and H.J. Lemmens, *Population pharmacodynamics and pharmacokinetics of remifentanil as a supplement to nitrous oxide anesthesia for elective abdominal surgery.* Anesthesiology, 1998. **89**(4): p. 869-77.
67. Egan, T.D., et al., *Remifentanil pharmacokinetics in obese versus lean patients.* Anesthesiology, 1998. **89**(3): p. 562-73.
68. Dershwitz, M., et al., *Pharmacokinetics and pharmacodynamics of remifentanil in volunteer subjects with severe liver disease.* Anesthesiology, 1996. **84**(4): p. 812-20.
69. Hoke, J.F., et al., *Pharmacokinetics and pharmacodynamics of remifentanil in persons with renal failure compared with healthy volunteers.* Anesthesiology, 1997. **87**(3): p. 533-41.
70. Mertens, M.J., et al., *Predictive performance of computer-controlled infusion of remifentanil during propofol/remifentanil anaesthesia.* Br J Anaesth, 2003. **90**(2): p. 132-41.
71. Minto, C.F., et al., *Using the Time of Maximum Effect Site Concentration to Combine Pharmacokinetics and Pharmacodynamics.* Anesthesiology, 2003. **99**(2): p. 324-333.
72. Egan, T.D., *Remifentanil pharmacokinetics and pharmacodynamics. A preliminary appraisal.* Clin Pharmacokinet, 1995. **29**(2): p. 80-94.
73. Somma, J., et al., *Population pharmacodynamics of midazolam administered by target controlled infusion in SICU patients after CABG surgery.* Anesthesiology, 1998. **89**(6): p. 1430-43.
74. Hu, C., D.J. Horstman, and S.L. Shafer, *Variability of target-controlled infusion is less than the variability after bolus injection.* Anesthesiology, 2005. **102**(3): p. 639-45.

75. Vuyk, J., et al., *Propofol anesthesia and rational opioid selection: determination of optimal EC50-EC95 propofol-opioid concentrations that assure adequate anesthesia and a rapid return of consciousness.* Anesthesiology, 1997. **87**(6): p. 1549-62.
76. Verkaaik, A.P. and G. Van Dijk, *High flow closed circuit anaesthesia.* Anaesth Intensive Care, 1994. **22**(4): p. 426-34.
77. el-Attar, A.M., *Guided isoflurane injection in a totally closed circuit.* Anaesthesia, 1991. **46**(12): p. 1059-63.
78. Struys, M.M., et al., *Time course of inhaled anaesthetic drug delivery using a new multifunctional closed-circuit anaesthesia ventilator. In vitro comparison with a classical anaesthesia machine.* Br J Anaesth, 2005. **94**(3): p. 306-17.
79. Chaudhri, S., et al., *Evaluation of closed loop control of arterial pressure during hypotensive anaesthesia for local resection of intraocular melanoma [see comments].* Br J Anaesth, 1992. **69**(6): p. 607-10.
80. Claudius, C. and J. Viby-Mogensen, *Acceleromyography for use in scientific and clinical practice: a systematic review of the evidence.* Anesthesiology, 2008. **108**(6): p. 1117-40.
81. Schüttler, J. and H. Schwilden, *Closed-loop systems in clinical practice.* Current Opinion in Anesthesiology, 1997. **9**: p. 457-461.
82. Bruhn, J., et al., *Depth of anaesthesia monitoring: what's available, what's validated and what's next?* Br J Anaesth, 2006. **97**(1): p. 85-94.
83. Kenny, G.N. and H. Mantzaridis, *Closed-loop control of propofol anaesthesia.* Br J Anaesth, 1999. **83**(2): p. 223-8.
84. Luginbuhl, M., et al., *Heart rate variability does not discriminate between different levels of haemodynamic responsiveness during surgical anaesthesia.* Br J Anaesth, 2007. **98**(6): p. 728-36.
85. Huiku, M., et al., *Assessment of surgical stress during general anaesthesia.* British Journal of Anaesthesia., 2006. **submitted**.
86. Kiersey, D.K., A. Faulconer, Jr., and R.G. Bickford, *Automatic electroencephalographic control of thiopental anesthesia.* Anesthesiology, 1954. **15**(4): p. 356-64.
87. Absalom, A.R., N. Sutcliffe, and G.N. Kenny, *Closed-loop control of anesthesia using Bispectral index: performance assessment in patients undergoing major orthopedic surgery under combined general and regional anesthesia.* Anesthesiology, 2002. **96**(1): p. 67-73.
88. Zbinden, A.M., et al., *Arterial pressure control with isoflurane using fuzzy logic.* Br J Anaesth, 1995. **74**(1): p. 66-72.
89. Luginbuhl, M., et al., *Closed-loop control of mean arterial blood pressure during surgery with alfentanil: clinical evaluation of a novel model-based predictive controller.* Anesthesiology, 2006. **105**(3): p. 462-70.
90. De Smet, T., et al., *Estimation of optimal modeling weights for a Bayesian-based closed-loop system for propofol administration using the bispectral index as a controlled variable: a simulation study.* Anesth Analg, 2007. **105**(6): p. 1629-38, table of contents.
91. De Smet, T., et al., *The accuracy and clinical feasibility of a new bayesian-based closed-loop control system for propofol administration using the bispectral index as a controlled variable.* Anesth Analg, 2008. **107**(4): p. 1200-10.
92. Sartori, V., et al. *On-line estimation of propofol pharmacodynamic parameters*. in *27th IEEE EMBS Conference*. 2005. Shangai.
93. Gentilini, A., et al., *Identification and targeting ploicies for computer-controlled infusion pumps.* Crit.Rev.Biomed.Eng., 2000. **28**: p. 179-185.

94. Kern, S.E., J.O. Johnson, and D.R. Westenskow, *Fuzzy logic for model adaptation of a pharmacokinetic-based closed loop delivery system for pancuronium.* Artif Intell Med, 1997. **11**(1): p. 9-31.
95. Bickford, R., *Automatic EEEG control of general anesthesia.* Electroencephalography and Clinical Neurophysiology, 1950. **2**: p. 93-96.
96. Schwilden, H., J. Schuttler, and H. Stoeckel, *Closed-loop feedback control of methohexital anesthesia by quantitative EEG analysis in humans.* Anesthesiology, 1987. **67**(3): p. 341-7.
97. Schwilden, H., H. Stoeckel, and J. Schuttler, *Closed-loop feedback control of propofol anaesthesia by quantitative EEG analysis in humans [see comments].* Br J Anaesth, 1989. **62**(3): p. 290-6.
98. Schwilden, H., et al., *Testing and modelling the interaction of alfentanil and propofol on the EEG.* Eur J Anaesthesiol, 2003. **20**(5): p. 363-72.
99. Sakai, T., et al., *Use of an EEG-bispectral closed-loop delivery system for administering propofol.* Acta Anaesthesiol Scand, 2000. **44**(8): p. 1007-10.
100. Morley, A., et al., *Closed loop control of anaesthesia: an assessment of the bispectral index as the target of control.* Anaesthesia, 2000. **55**(10): p. 953-9.
101. Leslie, K., A. Absalom, and G.N. Kenny, *Closed loop control of sedation for colonoscopy using the Bispectral Index.* Anaesthesia, 2002. **57**(7): p. 693-7.
102. Mortier, E., et al., *Closed-loop controlled administration of propofol using bispectral analysis.* Anaesthesia, 1998. **53**(8): p. 749-54.
103. Locher, S., et al., *A new closed-loop control system for isoflurane using bispectral index outperforms manual control.* Anesthesiology, 2004. **101**(3): p. 591-602.
104. Gentilini, A., et al., *Modeling and closed-loop control of hypnosis by means of bispectral index (BIS) with isoflurane.* IEEE Trans Biomed Eng, 2001. **48**(8): p. 874-89.
105. Milne, S.E., G.N. Kenny, and S. Schraag, *Propofol sparing effect of remifentanil using closed-loop anaesthesia.* Br J Anaesth, 2003. **90**(5): p. 623-9.
106. Gentilini, A., et al., *Multitasked closed-loop control in anesthesia.* IEEE Eng Med Biol Mag, 2001. **20**(1): p. 39-53.
107. Glass, P.S.A. and I.J. Rampil, *Automated Anesthesia: Fact or Fantasy ?* Anesthesiology, 2001. **95**: p. 1-2.
108. Manberg, P.J., C.M. Vozella, and S.D. Kelley, *Regulatory challenges facing closed-loop anesthetic drug infusion devices.* Clin Pharmacol Ther, 2008. **84**(1): p. 166-9.
109. Soltero, D.E., A. Faulconer, Jr., and R.G. Bickford, *The clinical application of automatic anesthesia.* Anesthesiology, 1951. **12**(5): p. 574-82.
110. Bellville, J.W., J.F. Artusio, Jr., and M.W. Bulmer, *Continuous servo motor integration of the electrical activity of the brain and its application to the control of cyclopropane anesthesia.* Electroencephalogr Clin Neurophysiol, 1954. **6**(2): p. 317-20.
111. Bellville, J.W. and G.M. Attura, *Servo control of general anesthesia.* Science, 1957. **126**(3278): p. 827-30.
112. Suppan, P., *Feed-back monitoring in anaesthesia. II. Pulse rate control of halothane administration.* Br J Anaesth, 1972. **44**(12): p. 1263-71.
113. Suppan, P., *Feed-back monitoring in anaesthesia. IV. The indirect measurement of arterial pressure and its use for the control of halothane administration.* Br J Anaesth, 1977. **49**(2): p. 141-50.
114. Linkens, D.A., et al., *Identification and control of muscle-relaxant anaesthesia.* IEEE Proc, 1982. **129**: p. 136-141.

115. Rametti, L.B., H.S. Bradlow, and P.C. Uys, *Online parameter estimation and control of d-tubocurarine-induced muscle relaxation.* Med Biol Eng Comput, 1985. **23**(6): p. 556-64.
116. Ritchie, G., et al., *A microcomputer based controller for neuromuscular block during surgery.* Ann Biomed Eng, 1985. **13**(1): p. 3-15.
117. Lampard, D.G., et al., *Computer-controlled muscle paralysis with atracurium in the sheep.* Anaesth Intensive Care, 1986. **14**(1): p. 7-11.
118. de Vries, J.W., H.H. Ros, and L.H. Booij, *Infusion of vecuronium controlled by a closed-loop system.* Br J Anaesth, 1986. **58**(10): p. 1100-3.
119. Schils, G.F., F.J. Sasse, and V.C. Rideout, *Automatic control of anesthesia using two feedback variables.* Ann Biomed Eng, 1987. **15**(1): p. 19-34.
120. Webster, N.R. and A.T. Cohen, *Closed-loop administration of atracurium. Steady-state neuromuscular blockade during surgery using a computer controlled closed-loop atracurium infusion.* Anaesthesia, 1987. **42**(10): p. 1085-91.
121. Jaklitsch, R.R., et al., *A comparison of computer-controlled versus manual administration of vecuronium in humans.* J Clin Monit, 1987. **3**(4): p. 269-76.
122. Millard, R.K., C.P. Monk, and C. Prys-Roberts, *Self-tuning control of hypotension during ENT surgery using a volatile anaesthetic.* IEEE Proc, 1988. **135**: p. 95-105.
123. Monk, C.R., et al., *Automatic arterial pressure regulation using isoflurane: comparison with manual control.* Br J Anaesth, 1989. **63**(1): p. 22-30.
124. MacLeod, A.D., et al., *Automatic control of neuromuscular block with atracurium.* Br J Anaesth, 1989. **63**(1): p. 31-5.
125. Schwilden, H., H. Stoeckel, and J. Schuttler, *Closed-loop feedback control of propofol anaesthesia by quantitative EEG analysis in humans.* Br J Anaesth, 1989. **62**(3): p. 290-6.
126. O'Hara, D.A., et al., *Closed-loop infusion of atracurium with four different anesthetic techniques.* Anesthesiology, 1991. **74**(2): p. 258-63.
127. Olkkola, K.T. and H. Schwilden, *Adaptive closed-loop feedback control of vecuronium-induced neuromuscular relaxation.* Eur J Anaesthesiol, 1991. **8**(1): p. 7-12.
128. Olkkola, K.T., H. Schwilden, and C. Apffelstaedt, *Model-based adaptive closed-loop feedback control of atracurium-induced neuromuscular blockade.* Acta Anaesthesiol Scand, 1991. **35**(5): p. 420-3.
129. Schwilden, H. and H. Stoeckel, *Closed-loop feedback controlled administration of alfentanil during alfentanil-nitrous oxide anaesthesia.* Br J Anaesth, 1993. **70**(4): p. 389-93.
130. Edwards, N.D., D.G. Mason, and J.J. Ross, *A portable self-learning fuzzy logic control system for muscle relaxation.* Anaesthesia, 1998. **53**(2): p. 136-9.
131. Allen, R. and D. Smith, *Neuro-fuzzy closed-loop control of depth of anaesthesia.* Artif Intell Med, 2001. **21**(1-3): p. 185-91.
132. Gentilini, A., et al., *A new paradigm for the closed-loop intraoperative administration of analgesics in humans.* IEEE Trans Biomed Eng, 2002. **49**(4): p. 289-99.
133. Liu, N., et al., *Feasibility of closed-loop titration of propofol guided by the Bispectral Index for general anaesthesia induction: a prospective randomized study.* Eur J Anaesthesiol, 2006. **23**(6): p. 465-9.
134. Puri, G.D. and P.J. Mathew, *Closed-loop control of anesthesia using the bispectral index in open heart surgery.* Acta Anaesthesiol Taiwan, 2009. **47**(3): p. 123-7.
135. Hemmerling, T.M., et al., *A randomized controlled trial demonstrates that a novel closed-loop propofol system performs better hypnosis control than manual administration.* Can J Anaesth, 2010. **57**(8): p. 725-35.

136. Lockhart, S.H., et al., *Cerebral uptake and elimination of desflurane, isoflurane, and halothane from rabbit brain: an in vivo NMR study.* Anesthesiology, 1991. **74**(3): p. 575-80.
137. Lockhart, S.H., et al., *Absence of abundant binding sites for anesthetics in rabbit brain: an in vivo NMR study.* Anesthesiology, 1990. **73**(3): p. 455-60.
138. Gepts, E., et al., *Disposition of propofol administered as constant rate intravenous infusions in humans.* Anesth Analg, 1987. **66**(12): p. 1256-63.
139. Billard, V., et al., *A comparison of spectral edge, delta power, and bispectral index as EEG measures of alfentanil, propofol, and midazolam drug effect.* Clin Pharmacol Ther, 1997. **61**(1): p. 45-58.
140. James, W.P.T., *Research on obesity. .* London: Her Majesty's Stationery Office, 1976.
141. Abernethy, D.R., et al., *Alterations in drug distribution and clearance due to obesity.* J Pharmacol Exp Ther, 1981. **217**(3): p. 681-5.
142. Barvais, L., I. Rausin, and J.B. Glen, *Administration of propofol by target-controlled infusion in patients undergoing coronary artery surgery.* J. Cardiothorac Vasc Anesth 1996. **10**: p. 877-883.
143. Davidson, J.A., et al., *Effective concentration 50 for propofol with and without 67% nitrous oxide.* Acta Anaesthesiol Scand, 1993. **37**(5): p. 458-64.
144. Swinhoe, C.F., et al., *Evaluation of the predictive performance of a 'Diprifusor' TCI system.* Anaesthesia, 1998. **53 Suppl 1**: p. 61-7.
145. Servin, F., et al., *Propofol infusion for maintenance of anesthesia in morbidly obese patients receiving nitrous oxide. A clinical and pharmacokinetic study.* Anesthesiology, 1993. **78**(4): p. 657-65.
146. Lemmens, H.J., J.B. Brodsky, and B. D.P., *Estimating ideal body weight - a new formula.* Obes surg, 2005. **15**: p. 1082-1083.
147. Linkens, D.A. and S.S. Hacisalihzade, *Computer control systems and pharmacological drug administration: a survey.* J Med Eng Technol, 1990. **14**(2): p. 41-54.
148. Rampil, I.J., *A primer for EEG signal processing in anesthesia [see comments].* Anesthesiology, 1998. **89**(4): p. 980-1002.
149. Sigl, J.C. and N.G. Chamoun, *An introduction to bispectral analysis for the electroencephalogram.* J Clin Monit, 1994. **10**(6): p. 392-404.
150. Sheiner, L.B., et al., *Simultaneous modeling of pharmacokinetics and pharmacodynamics: application to d-tubocurarine.* Clin Pharmacol Ther, 1979. **25**(3): p. 358-71.
151. Schwilden, H., J. Schuttler, and H. Stoeckel, *Quantitation of the EEG and pharmacodynamic modelling of hypnotic drugs: etomidate as an example.* Eur J Anaesthesiol, 1985. **2**(2): p. 121-31.
152. Schuttler, J. and H. Schwilden, *Present state of closed-loop drug delivery in anesthesia and intensive care.* Acta Anaesthesiol Belg, 1999. **50**(4): p. 187-91.
153. Bailey, J.M. and S.L. Shafer, *A simple analytical solution to the three-compartment pharmacokinetic model suitable for computer-controlled infusion pumps.* IEEE Trans Biomed Eng, 1991. **38**(6): p. 522-5.
154. Holford, N.H. and L.B. Sheiner, *Understanding the dose-effect relationship: clinical application of pharmacokinetic-pharmacodynamic models.* Clin Pharmacokinet, 1981. **6**(6): p. 429-53.
155. Ausems, M.E., et al., *Comparison of a computer-assisted infusion versus intermittent bolus administration of alfentanil as a supplement to nitrous oxide for lower abdominal surgery.* Anesthesiology, 1988. **68**(6): p. 851-61.

156. Ludbrook, G.L., et al., *The effect of rate of administration on brain concentrations of propofol in sheep.* Anesth Analg, 1998. **86**(6): p. 1301-6.
157. Struys, M., et al., *Clinical usefulness of the bispectral index for titrating propofol target effect-site concentration.* Anaesthesia, 1998. **53**(1): p. 4-12.
158. Leslie, K., et al., *Propofol blood concentration and the Bispectral Index predict suppression of learning during propofol/epidural anesthesia in volunteers.* Anesth Analg, 1995. **81**(6): p. 1269-74.
159. Glass, P.S., et al., *Bispectral analysis measures sedation and memory effects of propofol, midazolam, isoflurane, and alfentanil in healthy volunteers.* Anesthesiology, 1997. **86**(4): p. 836-47.
160. Iselin-Chaves, I.A., et al., *The effect of the interaction of propofol and alfentanil on recall, loss of consciousness, and the Bispectral Index.* Anesth Analg, 1998. **87**(4): p. 949-55.
161. Struys, M., et al., *Comparison of spontaneous frontal EMG, EEG power spectrum and bispectral index to monitor propofol drug effect and emergence.* Acta Anaesthesiol Scand, 1998. **42**(6): p. 628-36.
162. Schwilden, H., J. Schuttler, and H. Stoeckel, *Closed-loop feedback control of methohexital anesthesia by quantitative EEG analysis in humans.* Anesthesiology, 1987. **67**(3): p. 341-7.
163. Jacobs, J.R., *Infusion rate control algorithms for pharmacokinetic model-driven drug infusion devices.* Int Anesthesiol Clin, 1995. **33**(3): p. 65-82.
164. Jacobs, J.R. and J.G. Reves, *Effect site equilibration time is a determinant of induction dose requirement [editorial; comment].* Anesth Analg, 1993. **76**(1): p. 1-6.
165. Bailey, J., *Pharmacodynamics as a research tool.* J Vlin Anesth, 1996. **8**: p. 48S-52S.
166. Mason, D.G., et al., *Development of a portable closed-loop atracurium infusion system: systems methodology and safety issues.* Int J Clin Monit Comput, 1996. **13**(4): p. 243-52.
167. Zbinden, A.M., S. Petersen-Felix, and D.A. Thomson, *Anesthetic depth defined using multiple noxious stimuli during isoflurane/oxygen anesthesia. II. Hemodynamic responses [see comments].* Anesthesiology, 1994. **80**(2): p. 261-7.
168. Kazama, T., et al., *Investigation of effective anesthesia induction doses using a wide range of infusion rates with undiluted and diluted propofol.* Anesthesiology, 2000. **92**(4): p. 1017-28.
169. Gobburu, J.V. and P.J. Marroum, *Utilisation of pharmacokinetic-pharmacodynamic modelling and simulation in regulatory decision-making.* Clin Pharmacokinet, 2001. **40**(12): p. 883-92.
170. Tullo, F., *Let's make better use of simulator time.* Aviation Week & Space Technology, 1999. **151**: p. 66.
171. Struys, M.M., et al., *Performance evaluation of two published closed-loop control systems using bispectral index monitoring: a simulation study.* Anesthesiology, 2004. **100**(3): p. 640-7.
172. Schnider, T.W., et al., *Population pharmacodynamic modeling and covariate detection for central neural blockade.* Anesthesiology, 1996. **85**(3): p. 502-12.
173. Press, W., et al., *Numerical Recipes in C, The Art of Scientific Computing*. 2nd edition ed, Cambridge, UK: Cambridge University Press.
174. Struys, M.M., et al., *Comparison of plasma compartment versus two methods for effect compartment--controlled target-controlled infusion for propofol.* Anesthesiology, 2000. **92**(2): p. 399-406.
175. Vereecke, H.E., et al., *New composite index based on midlatency auditory evoked potential and electroencephalographic parameters to optimize correlation with propofol effect site concentration: comparison with bispectral index and solitary used fast extracting auditory evoked potential index.* Anesthesiology, 2005. **103**(3): p. 500-7.

176. Liu, N., et al., *Titration of propofol for anesthetic induction and maintenance guided by the bispectral index: closed-loop versus manual control: a prospective, randomized, multicenter study.* Anesthesiology, 2006. **104**(4): p. 686-95.
177. Reves, J.G., et al., *Therapeutic uses of sodium nitroprusside and an automated method of administration.* Int Anesthesiol Clin, 1978. **16**(2): p. 51-88.
178. De Smet, T., et al., *Estimation of optimal modeling weights for a Bayesian-based closed loop system for propofol administration using the BIS as a controlled variable: A simulation study.* . Anesth Analg, 2007. **accepted for publication**.
179. Joint National Committee on the detection, e.a.t.h.b.p., *The sixth report of the joint National Committee on detection, evaluation and treatment of high blood pressure.* Archives of Internal Medicine, 1997. **157**: p. 2413-2446.
180. Bouillon, T.W., et al., *Pharmacodynamic interaction between propofol and remifentanil regarding hypnosis, tolerance of laryngoscopy, bispectral index, and electroencephalographic approximate entropy.* Anesthesiology, 2004. **100**(6): p. 1353-72.
181. Parker, S.D., et al., *Catecholamine and cortisol responses to lower extremity revascularization: correlation with outcome variables. Perioperative Ischemia Randomized Anesthesia Trial Study Group.* Crit Care Med, 1995. **23**(12): p. 1954-61.
182. Riles, T.S., et al., *Plasma catecholamine concentrations during abdominal aortic aneurysm surgery: the link to perioperative myocardial ischemia.* Ann Vasc Surg, 1993. **7**(3): p. 213-9.
183. Monk, T.G., Y. Ding, and P.F. White, *Total intravenous anesthesia: effects of opioid versus hypnotic supplementation on autonomic responses and recovery.* Anesth Analg, 1992. **75**(5): p. 798-804.
184. Rantanen, M., et al., *Novel multiparameter approach for measurement of nociception at skin incision during general anaesthesia.* Br J Anaesth, 2006. **96**(3): p. 367-76.
185. Lydic, R. and H.A. Baghdoyan, *Sleep, anesthesiology, and the neurobiology of arousal state control.* Anesthesiology, 2005. **103**(6): p. 1268-95.
186. Guignard, B., et al., *The effect of remifentanil on the bispectral index change and hemodynamic responses after orotracheal intubation.* Anesth Analg, 2000. **90**(1): p. 161-7.
187. Franks, N.P., *General anaesthesia: from molecular targets to neuronal pathways of sleep and arousal.* Nat Rev Neurosci, 2008. **9**(5): p. 370-86.
188. Shafer, S.L., *All models are wrong.* Anesthesiology, 2012. **116**(2): p. 240-1.
189. Mathews, D.M., et al., *Increases in electroencephalogram and electromyogram variability are associated with an increased incidence of intraoperative somatic response.* Anesth Analg, 2012. **114**(4): p. 759-70.
190. Ellerkmann, R.K., et al., *Response of the Composite Variability Index to a standardized noxious stimulus during propofolremifentanil*
anesthesia. Anesthesia&Analgesia, 2013. **116**(3): p. 580-8.
191. Short, T.G., et al., *Efficient Trial Design for Eliciting a Pharmacokinetic- Pharmacodynamic Model-based Response Surface Describing the Interaction between Two Intravenous Anesthetic Drugs.* Anesthesiology, 2002. **96**(2): p. 400-8.
192. Bouillon, T., et al., *Non-steady state analysis of the pharmacokinetic interaction between propofol and remifentanil.* Anesthesiology, 2002. **97**(6): p. 1350-62.
193. Chernik, D.A., et al., *Validity and reliability of the Observer's Assessment of Alertness/Sedation Scale: study with intravenous midazolam.* J Clin Psychopharmacol, 1990. **10**(4): p. 244-51.

194. Rantanen, M., et al., *Tetanic stimulus of the ulnar nerve as a predictor of heart rate response to skin incision in propofol-remifentanil anaesthesia.* Eur J Anaesthesiol, 2006. **23**((Suppl)): p. A-95.
195. Struys, M.M., et al., *Changes in a surgical stress index in response to standardized pain stimuli during propofol remifentanil infusion.* Br J Anaesth, 2007. **99**(3): p. 359-67.
196. Smith, W.D., R.C. Dutton, and N.T. Smith, *A measure of association for assessing prediction accuracy that is a generalization of non-parametric ROC area.* Stat Med, 1996. **15**(11): p. 1199-215.
197. Smith, W.D., R.C. Dutton, and N.T. Smith, *Measuring the performance of anesthetic depth indicators.* Anesthesiology, 1996. **84**(1): p. 38-51.
198. Struys, M.M., et al., *Performance of the ARX-derived auditory evoked potential index as an indicator of anesthetic depth: a comparison with bispectral index and hemodynamic measures during propofol administration.* Anesthesiology, 2002. **96**(4): p. 803-16.
199. Kalkman, C. and J. Drummond, *Monitors of Depth of Anesthesia, Quo Vadis? (Editorial).* Anesthesiology, 2002. **96**(4): p. 784-786.
200. Matthews, B.W., *Comparison of the predicted and observed secondary structure of T4 phage lysozyme.* Biochim Biophys Acta, 1975. **405**(2): p. 442-51.
201. von Dincklage, F., et al., *Monitoring of the responsiveness to noxious stimuli during anaesthesia with propofol and remifentanil by using RIII reflex threshold and bispectral index.* Br J Anaesth, 2009. **104**(2): p. 201-8.
202. Gruenewald, M., et al., *Influence of different remifentanil concentrations on the performance of the surgical stress index to detect a standardized painful stimulus during sevoflurane anaesthesia.* Br J Anaesth, 2009. **103**(4): p. 586-93.
203. Bergmann, I., et al., *Surgical pleth index-guided remifentanil administration reduces remifentanil and propofol consumption and shortens recovery times in outpatient anaesthesia.* Br J Anaesth, 2013. **110**(4): p. 622-8.
204. Mashour, G.A., *Neurophysiology and intraoperative nociception: new potentials?* Anesthesiology, 2013. **118**(2): p. 239-40.
205. Glass, P.S., *Anesthetic drug interactions: an insight into general anesthesia--its mechanism and dosing strategies [editorial; comment].* Anesthesiology, 1998. **88**(1): p. 5-6.
206. Eger, E.I., 2nd, et al., *Is a new paradigm needed to explain how inhaled anesthetics produce immobility?* Anesth Analg, 2008. **107**(3): p. 832-48.
207. Hendrickx, J.F., et al., *Is synergy the rule? A review of anesthetic interactions producing hypnosis and immobility.* Anesth Analg, 2008. **107**(2): p. 494-506.
208. Zbinden, A.M., et al., *Anesthetic depth defined using multiple noxious stimuli during isoflurane/oxygen anesthesia. I. Motor reactions [see comments].* Anesthesiology, 1994. **80**(2): p. 253-60.
209. Yli-Hankala, A., et al., *Auditory steady-state response, upper facial EMG, EEG and heart rate as predictors of movement during isoflurane-nitrous oxide anaesthesia.* Br J Anaesth, 1994. **73**(2): p. 174-9.
210. van Amsterdam, K., et al., *Visual metaphors on anaesthesia monitors do not improve anaesthetists' performance in the operating theatre.* Br J Anaesth, 2013. **110**(5): p. 816-22.
211. Kitano, H., *Systems biology: a brief overview.* Science, 2002. **295**(5560): p. 1662-4.
212. Niño, J., et al., *EPSAC-controlled anesthesia with online gain adaptation.* International Journal of Adaptive Control and Signal Processing., 2009. **23**: p. 455-471.

213. Crosby, G. and D.J. Culley, *Processed electroencephalogram and depth of anesthesia: window to nowhere or into the brain?* Anesthesiology, 2012. **116**(2): p. 235-7.
214. Avidan, M.S. and G.A. Mashour, *Prevention of intraoperative awareness with explicit recall: making sense of the evidence.* Anesthesiology, 2013. **118**(2): p. 449-56.
215. Heyse, B., et al., *Comparison of contemporary EEG derived depth of anesthesia monitors with a 5 step validation process.* Acta Anaesthesiol Belg, 2009. **60**(1): p. 19-33.
216. Coppens, M., et al., *Study of the time course of the clinical effect of propofol compared with the time course of the predicted effect-site concentration: Performance of three pharmacokinetic-dynamic models.* Br J Anaesth, 2010. **104**(4): p. 452-8.
217. Glass, P.S., *Automated control of anesthesia ten years later: futuristic novelty or present day reality.* Can J Anaesth, 2010. **57**(8): p. 715-719.
218. Bouillon, T.W., *Hypnotic and Opioid Anesthetic Drug Interactions on the CNS, Focus on Response Surface Modelling*, in *Modern Anesthetics, Handbook of Experimental Pharmacology 182*, J. Schuttler and H. Schwilden, Editors. 2008, Springer-Verlag: Berlin Heidelberg. p. 471-487.
219. Luginbuhl, M., et al., *Noxious stimulation response index: a novel anesthetic state index based on hypnotic-opioid interaction.* Anesthesiology, 2010. **112**(4): p. 872-80.
220. Struys, M.M., et al., *Optimizing intravenous drug administration by applying pharmacokinetic/pharmacodynamic concepts.* Br J Anaesth, 2011. **107**(1): p. 38-47.
221. Egan, T.D. and C.F. Minto, *Principles of drug action : Pharmacodynamic drug interactions in anesthesia.* , in *Anesthetic Pharmacology*, A.S. Evers, M. Maze, and E.D. Kharasch, Editors. 2011, Cambridge University Press: Cambridge. p. 147-165.
222. Heyse, B., et al., *Sevoflurane Remifentanil Interaction: Comparison of Different Response Surface Models.* Anesthesiology, 2012. **116**(2): p. 311-323.
223. Vereecke, H.E., et al., *Interaction between nitrous oxide, sevoflurane, and opioids: a response surface approach.* Anesthesiology, 2013. **118**(4): p. 894-902.
224. Heyse, B., et al., *A response surface model approach for continuous measures of hypnotic and analgesic effect during sevoflurane-remifentanil interaction: quantifying the pharmacodynamic shift evoked by stimulation.* Anesthesiology, 2014. **120**(6): p. 1390-9.
225. Avidan, M.S., et al., *Anesthesia awareness and the bispectral index.* N Engl J Med, 2008. **358**(11): p. 1097-108.
226. Kertai, M.D., et al., *Association of perioperative risk factors and cumulative duration of low bispectral index with intermediate-term mortality after cardiac surgery in the B-Unaware Trial.* Anesthesiology. **112**(5): p. 1116-27.
227. Sanders, R.D., A. Absalom, and J.W. Sleigh, *V. 'For now we see through a glass, darkly': the anaesthesia syndrome.* Br J Anaesth, 2014. **112**(5): p. 790-3.
228. Weber, F., M. Seidl, and T. Bein, *Impact of the AEP-Monitor/2-derived composite auditory-evoked potential index on propofol consumption and emergence times during total intravenous anaesthesia with propofol and remifentanil in children.* Acta Anaesthesiol Scand, 2005. **49**(3): p. 277-83.
229. Blusse van Oud-Alblas, H.J., et al., *Comparison of bispectral index and composite auditory evoked potential index for monitoring depth of hypnosis in children.* Anesthesiology, 2008. **108**(5): p. 851-7.
230. Sahinovic, M.M., et al., *Accuracy of the Composite Variability Index as a Measure of the Balance Between Nociception and Antinociception During Anesthesia.* Anesth Analg, 2014. **119**: p. 288-301.

231. Schneider, G., et al., *Monitoring depth of anesthesia utilizing a combination of electroencephalographic and standard measures.* Anesthesiology, 2014. **120**(4): p. 819-28.
232. Liu, N., et al., *Feasibility of closed-loop titration of propofol and remifentanil guided by the spectral M-Entropy monitor.* Anesthesiology, 2012. **116**(2): p. 286-95.
233. Mashour, G.A., *Consciousness and the 21st century operating room.* Anesthesiology, 2013. **119**(5): p. 1003-5.

Summary

The objective of any drug administration is to obtain and maintain a desired clinical and therapeutic level of drug effect as fast and accurate as possible while minimizing adverse drug effects. Optimizing drug administration during anesthesia and sedation has gained importance as essential part of higher standards in patient care and peri-operative management. Most drugs for general anesthesia control exhibit large inter-individual variability requiring the anesthesiologist to titrate drug administration continuously to reach and maintain the optimal anesthetic condition for that individual patient based on observation of clinical effects. Computer-based closed-loop systems may assist the clinician in this task by autonomously adapting the administered amount of drugs to reach and maintain directly the target effect carefully selected by the anesthesiologist. In closed-loop systems, measurements of the control variable (e.g. measure of the hypnotic or analgesic component of anesthesia) are made and the errors between the set point and the actual value are used to alter the input to the system. In closed-loop control, the anesthesiologist only enters the desired clinical-effect to be maintained.

In this thesis, we hypothesized that it is feasible to develop an automatic closed-loop system for the administration of intravenous hypnotic-anesthetic drugs during sedation and anesthesia and that this system does offer more accurate drug administration than manual control. We claimed that the incorporation of population-based pharmacological models and the implementation of Bayesian optimizing theories is beneficial.

We were able to develop an automatic closed-loop system for the administration of intravenous hypnotic-anesthetic drugs during sedation and anesthesia and we were able to prove that it offers more accurate drug administration than manual control under the studied conditions. By developing our system, we proved that the integration of pharmacological models in such a closed-loop system offers accurate control, even under extreme conditions. We were able to develop a technology that considers pre-existing population variability during control of intravenous anesthetic-hypnotic drugs administration with the application of Bayesian theories, and we showed that this technology is feasible to be used both in clinical practice and specific research conditions. We depicted that our closed-loop system is very helpful in offering stable research conditions to maintain a specific level of the hypnotic component of anesthesia.

Samenvatting

Het doel van de toediening van een geneesmiddel is een gewenst klinisch en therapeutisch niveau zo snel en nauwkeurig mogelijk en met minimale bijwerkingen te bereiken. De optimalisatie van de toediening van geneesmiddelen bij anesthesie en sedatie heeft aan belang gewonnen als essentieel onderdeel van kwalitatieve zorg voor de patiënt en geschikte heelkundige condities.

De meeste medicijnen die gebruikt worden om de anesthesie te controleren vertonen een zeer grote interindividuele variabiliteit. Daardoor moet de anesthesist de toediening van het medicijn voortdurend zorgvuldig titreren om de optimale anesthesie condities voor een individuele patiënt te bereiken en te behouden, op basis van de door hem waargenomen klinische effecten.
Computer-gestuurde *closed-loop* systemen kunnen de clinicus hierbij ondersteunen door autonoom de hoeveelheid toegediend medicijn continu aan te passen om een specifiek klinisch effect, zorgvuldig gekozen door de anesthesist, aan te houden. Bij het gebruik van *closed-loop* systemen wordt de waarde van de te controleren variabele (bijv. meten van de hypnotische of analgetische component van de anesthesie) gemeten en wordt de fout tussen de ingestelde en de actuele waarde gebruikt om de toediening van het medicijn aan te passen. Gedurende *closed-loop* controle zal de anesthesist enkel het gewenste te behouden klinisch effect ingeven.

In deze thesis stelden we als hypothese dat het mogelijk is om een automatisch *closed-loop* te ontwikkelen om intraveneuze hypnotica-anesthetica toe te dienen. We stelden dat dit systeem een meer accurate toediening van het medicijn toe laat tegenover manuele toediening. We beweerden hierbij dat de integratie van een op een populatie gebaseerd farmacologisch model en de implementatie van Bayesiaanse optimalisatie methode voordelen zou opleveren.
We zijn in staat geweest om een automatisch *closed-loop* te ontwikkelen om intraveneuze hypnotica-anesthetica toe te dienen tijdens anesthesie en sedatie en we hebben kunnen aantonen dat dit systeem onder de bestudeerde omstandigheden een meer nauwkeurige toediening van deze medicijnen toe laat ten opzichte van manueel gecontroleerde toediening. Tijdens de ontwikkeling van ons systeem hebben we bewezen dat farmacologische modellen kunnen gebruikt worden in deze closed-loop en accurate controle toelaten, zelfs onder extreme omstandigheden. De ontwikkelde technologie kan, door het toepassen van Bayesiaanse theorieën, rekening houden met vooraf

bepaalde modellen en hun populatie variabiliteit. We hebben bovendien aangetoond dat deze technologie klinisch uitvoerbaar is en de ideale assistentie levert om stabiele omstandigheden te creëren door een ingesteld niveau van de hypnotische component van de anesthesie aan te houden.

List of abbreviations

BET	bolus, elimination, transfer infusion scheme
BIS BIS A2000 Monitor BIS Vista Monitor	the Bispectral Index derived from the EEG and its generations of implementation devices (Aspect Medical, Norwood, MA, USA, now Covidien, Boulder, CO)
BIS_{LOC}	BIS at the moment of loss of consciousness
BIS_{PEAK}	observed BIS value at $t_{PEAK, BIS}$
BMI	body mass index
BP	blood pressure
C_{50}	sigmoid EMax model: concentration at 50% of drug effect
Ce_{CALC}	calculated effect-site concentration
Ce_{PROP}	propofol effect-site concentration
Ce_{REMI}	remifentanil effect-site concentration
Ce_T	targeted effect-site concentration
Cp_{CALC}	calculated plasma concentration
Cp_M	measured plasma concentration
Cp_{PROP}	propofol plasma concentration
Cp_{REMI}	remifentanil plasma concentration
Cp_T	targeted plasma concentration
CV	coefficient of variation
CVI	composite variability index (variability in the Bispectral Index)
Diprifusor®	the first commercially available TCI system (AstraZeneca, London, UK)
E_0	sigmoid EMax model covariate: effect value at no drug effect

EEG	electroencephalogram
E_{max}	sigmoid EMax model covariate: variation of effect value from none to maximum drug effect
EMG	electromyographic power
γ	sigmoid EMax model covariate: steepness of drug effect around 50%
HR	heartrate
k_{eO}	elimination rate constant in a mammilary compartmental model
k_{ij}	rate exchange constant between compartments i,j of a mammilary compartmental model
LBM	lean body mass
MAP	mean arterial pressure
MDAPE	median absolute prediction error
MDPE	median prediction error
MF	EEG median frequency
MLAEP	mid-latency auditory evoked potential
MPC	model predictive controller
NMT	neuromuscular transition monitoring
NONMEM	acronym for non-linear mixed effects modeling, a software package developed by Stuart L. Beal and Lewis B. Sheiner in the late 1970s at UCSF for population pharmacokinetic modeling. (http://www.iconplc.com/technology/products/nonmem)
OAAS	Observer Assessment of Alertness and Sedation
PD, pharmacodynamics	describes the relationship between blood or effect-organ concentration of a drug and its clinical effect
PE	prediction error

PID	proportional-integral-differential
PK, Pharmacokinetics	describes the relationship between administered dose of a drug and its plasma concentration
PK/PD	the coupling between pharmacokinetics and pharmacodynamics
Rugloop®, RugloopII©	general infusion pump control and data management system, available at http://www.demed.be
$Sample_{TO}$	sample timeout, represents the optimal number of samples to consider for model estimation
SD	standard deviation
sigmoid E_{max} model (Hill-curve)	mathematical model of the nonlinear dose-effect relationship
Stanpump	general infusion pump control system, available at http://opentci.org/doku.php?id=code:code
SYS	systolic blood pressure
SYS_{LOC}	SYS at the moment of loss of consciousness
SYS_{PEAK}	observed SYS value at $t_{PEAK, SYS}$
$t_{BIS\ TARGET}$	observed time required for reaching the target BIS value
TBW	total body weight
TCI	target-controlled infusion
t_{EQ}	time to steady-state: observed time to reach the target value of the controlled variable after the initial overshoot
t_{PEAK}, TTPE	peak time: observed time to reach maximal effect of the observed variable after unit input
$t_{PEAK, BIS}$	observed time to reach maximal drug effect (lowest BIS value) after unit input

$t_{PEAK, SYS}$	observed time to reach maximal drug effect (lowest SYS value) after unit input
V_1, V_d	central (initial) volume of distribution in a mammilary compartmental model
VAR_{C50}	Bayesian variance for squared deviation in C_{50}
VAR_{Delay}	Bayesian variance for the squared deviation in delay
VAR_{γ}	Bayesian variance for squared deviation in γ
VAR_{Sample}	Bayesian variance for the squared deviation in observed samples
Wobble	median $\{\lvert PE_{ij} - MDPE_i \rvert, j = 1,..., N_i\}$